frontiers | Research Topics

Antimicrobials alternatives for the prevention and treatment of veterinary infectious diseases

Edited by
Kun Li, Amjad Islam Aqib and Ambreen Ashar

Published in
Frontiers in Veterinary Science

ISSN 1664-8714
ISBN 978-2-83250-296-9
DOI 10.3389/978-2-83250-296-9

About Frontiers

Frontiers is more than just an open access publisher of scholarly articles: it is a pioneering approach to the world of academia, radically improving the way scholarly research is managed. The grand vision of Frontiers is a world where all people have an equal opportunity to seek, share and generate knowledge. Frontiers provides immediate and permanent online open access to all its publications, but this alone is not enough to realize our grand goals.

Frontiers journal series

The Frontiers journal series is a multi-tier and interdisciplinary set of open-access, online journals, promising a paradigm shift from the current review, selection and dissemination processes in academic publishing. All Frontiers journals are driven by researchers for researchers; therefore, they constitute a service to the scholarly community. At the same time, the *Frontiers journal series* operates on a revolutionary invention, the tiered publishing system, initially addressing specific communities of scholars, and gradually climbing up to broader public understanding, thus serving the interests of the lay society, too.

Dedication to quality

Each Frontiers article is a landmark of the highest quality, thanks to genuinely collaborative interactions between authors and review editors, who include some of the world's best academicians. Research must be certified by peers before entering a stream of knowledge that may eventually reach the public - and shape society; therefore, Frontiers only applies the most rigorous and unbiased reviews. Frontiers revolutionizes research publishing by freely delivering the most outstanding research, evaluated with no bias from both the academic and social point of view. By applying the most advanced information technologies, Frontiers is catapulting scholarly publishing into a new generation.

What are Frontiers Research Topics?

Frontiers Research Topics are very popular trademarks of the *Frontiers journals series*: they are collections of at least ten articles, all centered on a particular subject. With their unique mix of varied contributions from Original Research to Review Articles, Frontiers Research Topics unify the most influential researchers, the latest key findings and historical advances in a hot research area.

Find out more on how to host your own Frontiers Research Topic or contribute to one as an author by contacting the Frontiers editorial office: frontiersin.org/about/contact

Antimicrobials alternatives for the prevention and treatment of veterinary infectious diseases

Topic editors

Kun Li — Nanjing Agricultural University, China

Amjad Islam Aqib — Cholistan University of Veterinary and Animal Sciences, Pakistan

Ambreen Ashar — North Carolina State University, United States

Citation

Li, K., Aqib, A. I., Ashar, A., eds. (2022). *Antimicrobials alternatives for the prevention and treatment of veterinary infectious diseases*. Lausanne: Frontiers Media SA.

doi: 10.3389/978-2-83250-296-9

Table of contents

frontiers | Frontiers in Veterinary Science

TYPE Editorial
PUBLISHED 09 September 2022
DOI 10.3389/fvets.2022.1025150

OPEN ACCESS

EDITED AND REVIEWED BY
Michael Kogut,
United States Department of Agriculture, United States

*CORRESPONDENCE
Kun Li
lik2014@sina.com
Amjad Islam Aqib
amjadislamaqib@cuvas.edu.pk
Ambreen Ashar
ambreenashar@gcwuf.edu.pk

†These authors have contributed equally to this work and share first authorship

SPECIALTY SECTION
This article was submitted to Veterinary Infectious Diseases, a section of the journal Frontiers in Veterinary Science

RECEIVED 22 August 2022
ACCEPTED 23 August 2022
PUBLISHED 09 September 2022

CITATION
Kulyar MF-e-A, Chen X, Bhutta ZA, Boruah P, Shabbir S, Akhtar M, Aqib AI, Ashar A and Li K (2022) Editorial: Antimicrobials alternatives for the prevention and treatment of veterinary infectious diseases. *Front. Vet. Sci.* 9:1025150. doi: 10.3389/fvets.2022.1025150

Editorial: Antimicrobials alternatives for the prevention and treatment of veterinary infectious diseases

Muhammad Fakhar-e-Alam Kulyar[1,2†], Xiushuang Chen[1†], Zeeshan Ahmad Bhutta[3], Prerona Boruah[4], Samina Shabbir[5], Muhammad Akhtar[2], Amjad Islam Aqib[6*], Ambreen Ashar[7*] and Kun Li[1*]

[1]Institute of Traditional Chinese Veterinary Medicine, College of Veterinary Medicine, Nanjing Agricultural University, Nanjing, China, [2]College of Veterinary Medicine, Huazhong Agricultural University, Wuhan, China, [3]Laboratory of Biochemistry and Immunology, College of Veterinary Medicine, Chungbuk National University, Cheongju, South Korea, [4]DY Patil, Deemed to be University, Navi Mumbai, Maharastra, India, [5]Institute of Plant Protection, Guangdong Academy of Agricultural Sciences, Guangzhou, China, [6]Department of Medicine, Cholistan University of Veterinary and Animal Sciences, Bahawalpur, Pakistan, [7]Department of Chemistry, Government College Women University, Faisalabad, Pakistan

KEYWORDS

antimicrobials, antibiotics, antibiotic alternatives, veterinary, infectious diseases, veterinary infectious diseases, probiotics, antimicrobial peptides

Editorial on the Research Topic
Antimicrobials alternatives for the prevention and treatment of veterinary infectious diseases

Antibiotics have carried the promise of curing and managing infectious diseases throughout their discovery, resulting an enormous increase in antibiotic use in all sectors, including routine animal husbandry techniques (1). Laws against the extra-label use of antibiotics are uncommon, even in developed countries. So, the rate of rising in the prevalence of antimicrobial resistant infections is now inversely related to the rate at which new medications are being approved. Therefore, developing resistance to antimicrobials is one of the most pressing public health issue of the 21st century. When veterinary medicine is considered, the quantity of antibiotics utilized by animals is almost twice that used by humans (2). Long periods have been spent using such extensive antimicrobial medications to either increase feed conversion or avoid diseases. These non-therapeutic applications allow an extraordinary selection pressure on bacteria, resulting in novel survival strategies. These adaptation strategies are responsible for antibiotic resistance. According to the most recent findings in scientific research, this phenomenon seems to be wired, although it was only contextualized after the conclusion of World War II. Its goal was to enhance animal protein production *via* low-cost methods, a goal still relevant today in countries with low per capita incomes (3). In such countries, the use of antimicrobials in animal feeding as growth promoters is highly

linked with the development and spread of antimicrobial-resistant, which makes it difficult to cure infectious diseases.

Antibiotics are administered to many food-producing animals to reduce the risk of infections and compensate for the lack of sanitary conditions on commercial livestock farms (4). Therefore, livestock serves as a source that disperses resistant bacteria into the environment *via* the consumption of contaminated bio wastes, milk, or meat, as well as through direct contact with animals and people who work on animal farms. Similarly, zoonotic diseases may transfer their antibiotic resistance to humans. Because animals and commodities derived from livestock are carried throughout the globe. In same sense, animal and plant diseases that disrupt the food supply in one country might spread to other countries and cause problems elsewhere. In addition, germs may become resistant to antibiotics when they are subjected to low concentrations over extended periods. Feeding livestock antibiotics at low doses is a widespread technique used to increase animal body weight. These antibiotics are also administered arbitrarily to avoid diseases in herds or flocks that have restricted space. These kinds of behaviors help to foster the development of antibiotic resistance as well as its subsequent dissemination. The methods result a significant buildup of antibiotics in the environment and the development of antibiotic resistance in the microorganisms that come into contact with them (5). However, it is difficult to identify the route and capability of resistance elements from animals to people and to establish that animals serve as reservoirs of resistant genes since it is difficult to understand how resistance factors are passed between the species. The fact that there are naturally occurring resistance genes in the environment adds a layer of complexity to the situation. For instance, it was discovered that natural resistance to antibiotics occurred a very long time before the development of agriculture (6).

Several options other than traditional antibiotics have been developed to tackle antimicrobial resistance and manage bacterial infections. Some methods have taken a step while others are still in the research phase. However, the quick adoption of alternatives is hampered by several issues. Experts agree that a shortage of governmental and private funds for antibiotics' alternative research is the most pressing problem. The low level of interest in this field is often linked to the hope of confirming the efficacy of products that have already undergone preliminary testing. In addition to the product's qualities, its popularity may also be attributed to the openness of farmers and veterinarians to new possibilities. Since veterinarians play such a pivotal role in raising farmers' understanding of animal health and the principles of new treatments. Such novel options must have a clear mechanism of action, and their use must be simple and obvious to both the veterinarian and the farmer (7). As a result, there is a need for a multi-actor, cross-sectoral strategy to address animal diseases. Furthermore, the effectiveness, toxicity, and mechanism of these therapies should be investigated during pre-clinical trials to optimize their dose and formulation. The findings and a survey of veterinarians, farmers, and consumers' perceptions of antimicrobial alternatives should be used to identify treatments for large-scale farm trials, i.e., measuring clinical effectiveness and effects on antimicrobial usage. Furthermore, a portfolio of numerous options for treating or preventing infectious diseases, such as phage treatment, antimicrobial peptides, bacteriocins, probiotics, fecal transplant therapy, predatory bacteria, and antibodies, should be developed (Figure 1).

Meanwhile, we must remember that "prevention is better than cure." Antibiotics are still useful in preventing and managing animal infections in many underdeveloped countries due to the poor agricultural environment and high disease incidence. It is shown that the ban on growth promoters necessitates increased agricultural hygiene. When the number of "old" antibiotics used in feed decreases due to the ban, the frequency of bacterial infections is expected to grow unless the production environment is fundamentally improved. This

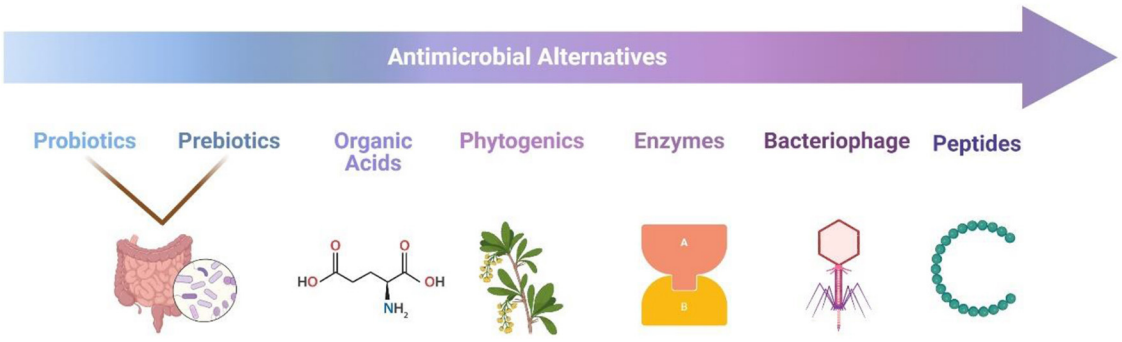

FIGURE 1
Various options for antimicrobial alternatives that are normally available all over the world.

may increase the therapeutic use of powerful antibiotics, which may have unforeseen repercussions for public health problems. Furthermore, there is no scientific evidence to distinguish the causal link between antibiotic therapy and preventative usage regarding resistance development. Before enacting such a strategy due to political/social pressure, the final benefit and danger should be examined since microorganisms may not always "listen" to politicians. As a result, the choice to administer in-feed antibiotics should be founded on scientific evidence. Antibiotic bans as growth promoters cannot be repeated in every country. Some "vintage" medicines may identify new bacterial targets and boost anti-infectious treatment for certain bacteria. Also, novel formulations may enable targeted drug administration, and increase the interaction of molecules through antibacterial activity (8). Hence, it is essential to switch to the most appropriate narrow-spectrum agent as soon as an infection has been brought under control and the culture and susceptibility testing results have been reported. Doing so reduces the potential for adverse drug reactions and the chance of developing antibiotic-induced resistance.

In summary, it is essential to find a suitable replacement for antibiotics with the improvement of animal feed administration, production, and hygiene. In addition to conducting research and developing new alternatives that are efficient and risk-free, we should investigate the possibility of combining the application of antibiotics and their alternatives in order to sustain a healthy agricultural economy and ensure their potential for use in the veterinary sector.

Author contributions

MK and XC wrote the first draft of the manuscript. All other authors have made a substantial, direct, and intellectual contribution to the work and approved it for publication.

Funding

This study was supported by the Start-up fund of Nanjing Agricultural University (804131) and the Start-up Fund for Distinguished Scholars of Nanjing Agricultural University (80900219).

Acknowledgments

We would like to show our appreciation to all authors who contributed to the Research Topic and have opened more doors in the study of antimicrobial alternatives by providing major insights into the prevention and treatment of veterinary infectious diseases.

Conflict of interest

The authors declare that the research was conducted in the absence of any commercial or financial relationships that could be construed as a potential conflict of interest.

Publisher's note

All claims expressed in this article are solely those of the authors and do not necessarily represent those of their affiliated organizations, or those of the publisher, the editors and the reviewers. Any product that may be evaluated in this article, or claim that may be made by its manufacturer, is not guaranteed or endorsed by the publisher.

References

1. Palma E, Tilocca B, Roncada P. Antimicrobial resistance in veterinary medicine: An overview. *Int J Mol Sci.* (2020) 21:1914. doi: 10.3390/ijms21061914

2. Silva KC, Knobl T, Moreno AM. Antimicrobial resistance in veterinary medicine: mechanisms and bacterial agents with the greatest impact on human health. *Braz J Vet Res Anim Sci.* (2013) 50:171–83. doi: 10.11606/issn.1678-4456.v50i3p171-183

3. Vercelli C, Gambino G, Amadori M, Re G. Implications of Veterinary Medicine in the comprehension and stewardship of antimicrobial resistance phenomenon. From the origin till nowadays. *Veter Animal Sci.* (2022) 16:100249. doi: 10.1016/j.vas.2022.100249

4. Kumar M, Sarma DK, Shubham S, Kumawat M, Verma V, Nina PB, et al. Futuristic non-antibiotic therapies to combat antibiotic resistance: A review. *Front Microbiol.* (2021) 12:609459. doi: 10.3389/fmicb.2021.609459

5. Allen HK. Antibiotic resistance gene discovery in food-producing animals. *Curr Opin Microbiol.* (2014) 19:25–9. doi: 10.1016/j.mib.2014.06.001

6. Bebrone C. Metallo-β-lactamases (classification, activity, genetic organization, structure, zinc coordination) and their superfamily. *Biochem Pharmacol.* (2007) 74:1686–701. doi: 10.1016/j.bcp.2007.05.021

7. Nowakiewicz A, Zieba P, Gnat S, Matuszewski Ł. Last call for replacement of antimicrobials in animal production: modern challenges, opportunities, and potential solutions. *Antibiotics.* (2020) 9:883. doi: 10.3390/antibiotics9120883

8. Bourlioux P. De quelles alternatives notre arsenal thérapeutique anti-infectieux dispose-t-il face aux bactéries multi-résistantes? In *Annales Pharmaceutiques Françaises.* (2013). vol. 71, p. 150–158. Elsevier Masson. doi: 10.1016/j.pharma.2013.02.005

frontiers | Frontiers in Veterinary Science

ORIGINAL RESEARCH
published: 08 April 2022
doi: 10.3389/fvets.2022.857183

Phytochemical Constituents of Propolis Flavonoid, Immunological Enhancement, and Anti-porcine Parvovirus Activities Isolated From Propolis

Xia Ma[1,2,3*†], *ZhenHuan Guo*[1,2,3†], *Yana Li*[2,3,4], *Kun Yang*[1,2,3], *Xianghui Li*[1,2,3], *Yonglu Liu*[1,2,3], *Zhiqiang Shen*[5], *Li Zhao*[1,2,3] *and Zhiqiang Zhang*[2,3,6*]

[1] *Medicinal Engineering Department, Henan University of Animal Husbandry and Economy, Zhengzhou, China,* [2] *Zhengzhou Key Laboratory of Veterinary Immunopharmacology, Henan University of Animal Husbandry and Economy, Zhengzhou, China,* [3] *Henan Research Center for Inheritance and Innovation Technology of Classical and Prescriptions of Chinese Veterinary, Zhengzhou, China,* [4] *School of Animal Science, Yangtze University, Jingzhou, China,* [5] *Binzhou Animal Science and Veterinary Medicine Academy of Shandong Province, Binzhou, China,* [6] *College of Pharmacy, Henan University of Chinese Medicine, Zhengzhou, China*

OPEN ACCESS

Edited by:
Kun Li,
Nanjing Agricultural University, China

Reviewed by:
Liwei Guo,
Yangtze University, China
Yi Wu,
Nanjing Agricultural University, China

***Correspondence:**
Xia Ma
maxia801010@126.com
Zhiqiang Zhang
392073683@qq.com

† These authors have contributed equally to this work

Specialty section:
This article was submitted to Veterinary Infectious Diseases, a section of the journal Frontiers in Veterinary Science

Received: *18 January 2022*
Accepted: *31 January 2022*
Published: *08 April 2022*

Citation:
Ma X, Guo Z, Li Y, Yang K, Li X, Liu Y, Shen Z, Zhao L and Zhang Z (2022) Phytochemical Constituents of Propolis Flavonoid, Immunological Enhancement, and Anti-porcine Parvovirus Activities Isolated From Propolis. Front. Vet. Sci. 9:857183. doi: 10.3389/fvets.2022.857183

Propolis is widely used in health preservation and disease healing; it contains many ingredients. The previous study had revealed that the ethanolic or water extracts of propolis have a wide range of efficacy, such as antiviral, immune enhancement, anti-inflammatory, and so on, but its antiviral components and underlying mechanism of action remain unknown. In this study, we investigated the chemical composition, anti-porcine parvovirus (PPV) effectiveness, and immunological enhancement of propolis flavone ethanolic extracts. The chemical composition of propolis flavone was distinguished by ultra-performance liquid chromatography-quadrupole/time-of-flight tandem mass spectrometry analysis. In this study, the presence and characterization of 26 major components were distinguished in negative ionization modes to evaluate the effects of propolis flavonoid used as an adjuvant on the immune response of Landrace–Yorkshire hybrid sows immunized with an inactivated vaccine of PPV. Thirty Landrace-Yorkshire hybrid sows were randomly assigned to one of three groups, and the sows in the adjuvant groups were intramuscularly injected with PPV vaccine with a 2.0-ml propolis flavonoid adjuvant (PA) and oil emulsion adjuvant. After that, serum hemagglutination inhibition antibody titers and specific immunoglobulin (Ig)M and IgG subclasses were measured to evaluate the adjuvant effects of propolis flavonoid on the humoral immune responses, as well as peripheral lymphocyte proliferation activity and serum concentrations of Th1 and Th2 cytokines for cellular immunity. Results indicated an enhancing effect of PA on IgM, interleukins 2 and 4, interferon-γ, and IgG subclass responses. Especially in the effect of improving cellular immune response, the PA was the best. These findings suggested that PA can significantly enhance the immune responses against the PPV vaccine and could be an alternative way to improve PPV vaccination in sows. Furthermore, we screened the PF chemical components to the effectiveness of anti-PPV. Ferulic acid has an excellent anti-PPV effect.

Keywords: phytochemical constituents, propolis flavonoid, UPLC-Q/TOF-MS/MS, ferulic acid, porcine parvovirus

INTRODUCTION

Nature products and natural product derivatives have drawn more attention due to their wide spectrum of biological and pharmaceutical properties. Propolis is a gelatinous solid substance with an aromatic smell, which is collected from plant trunks and flower bracts by bees and mixed with the secretions of their maxillary glands and beeswax (1, 2). The pharmaceutical industries have widely marketed propolis as alternative medicine and as a healthy food in various parts of the world (3). Bioactive constituents isolated from the propolis, flavonoids, terpenes, organic acids, fatty acids, amino acids, enzymes, vitamins, trace elements, and minerals have applications in treating diseases due to their anticancer, anti-inflammatory, antioxidant, antibacterial, antimycotic, antifungal, and immunomodulatory properties (4). So far, more than 500 chemical compounds have been isolated from propolis (5). Also, our previous studies revealed that propolis and its constituents exerted immunological enhancement *in vivo*, as well as the anti-porcine parvovirus (PPV) effect *in vitro*.

PPV is one of the main pathogens that cause swine reproductive disorder and increasing economic losses in the world (6–8). Several studies have pointed out that vaccination is an effective method for controlling this disease (9). The successful vaccination depends on their association with a potent adjuvant, which can increase vaccine immunogenicity. A better adjuvant can activate specific effectors of the immune system, such as cytotoxic or auxiliary T cells (Th1/Th2) and strengthen the humoral and/or cellular immune responses against that antigen (10, 11). On the other hand, a suitable adjuvant should have lower toxicity and adverse effects (12). However, there are some shortages in commonly used adjuvants; for example, oil emulsion adjuvant (OA) can cause inflammation, induration, or necrosis in the local and disseminated granulomas in lungs, liver, kidneys, heart, lymph nodes, and skeletal muscles in rabbits or rats (13). An aluminum salt adjuvant is a widely used adjuvant in human vaccines licensed by the US Food and Drug Administration (14), but it is a poor inducer of Th1 cellular immune response and easy to induce immunoglobulin E antibody response associated with some allergic reactions (15, 16). Thus, the natural product propolis as an immunologic adjuvant has attracted more and more attention due to its minor adverse effects and more pharmacological efficacy.

Most of the studies in the literature have investigated the anti-PPV and immunological enhancement effectiveness of propolis flavonoid (PF) isolated from propolis (17). PF, a kind of ingredient extracted from propolis, as a harmless natural adjuvant, has been used in chickens vaccinated with an activated vaccine, and the results showed that PF could improve the immune-enhancing activity in the humoral and cellular immune response (18). Because the major effectiveness of propolis is derived from the active ingredient, the anti-PPV and immunological enhancement effect are highly dependent on its extraction method and the content of the active ingredients of PF. Ethanol-extracted propolis is still the main method for PFs. However, still little is known regarding the anti-PPV effect of PF compounds, such as ferulic acid, quercetin, chrysin, and so on.

Thus, in this study, an ultra-performance liquid chromatography-quadrupole/time-of-flight mass spectrometry (UPLC-Q/TOF-MS) is used to distinguish and exhibit the standard chemical map of PF. In addition, this study aimed to evaluate the adjuvant effect and characteristics of PF on the humoral and cellular immune response of immunized pigs and screen out good anti-PPV PF compounds.

Abbreviations: BC, blank control group; CCK-8, cell counting kit-8; DMEM, Dulbecco's modified eagle medium; ELISA, enzyme-linked immunosorbent assay; HA, hemagglutination; HI, hemagglutination inhibition; IgA, immunoglobulin A; IgG, immunoglobulin G; IgM, immunoglobulin M; IL-2, interleukin 2; IL-4, interleukin 4; IL-6, interleukin 6; IL-10, interleukin 10; IL-12, interleukin 12; IFN-γ, interferon-γ; MTT, methyl thiazolyl tetrazolium; OA, oil emulsion adjuvant; PA, propolis flavonoid adjuvant; PBS, phosphate-buffered saline; PF, propolis flavonoid; PPV, porcine parvovirus; UPLC-Q/TOF-MS, ultra-performance liquid chromatography-quadrupole/time-of-flight mass spectrometry.

MATERIALS AND METHODS

Propolis Sample Collection, Extraction, and Processing

Propolis samples were collected in September of 2018 in Liaocheng Apiculture Research Institute, Shandong province, China. The ethanolic extract was prepared as reported by Almeida et al. (19). Ten grams of the powder was mixed with 100 ml of 75% ethanol in a sealed container protected from light (to avoid loss of volatile and photosensitive compounds) under agitation in a water bath at 70°C for 30 min. After extraction, the mixture was filtered. The filtrated liquid was combined with the original liquid. The ethanol was recovered by rotary evaporation and left overnight to obtain the crude propolis extract in the upper layer and the crude propolis extract in the lower layer.

Mass Spectrum Analysis and Verification of Methodology

Propolis flavone sample analysis was managed and consisted of SIL-30SD autosampler, Shimadzu UPLC (Kyoto, Japan), CTO-30A column oven, an LC-30AD Binary liquid pump, DGU-20A5R On-Line Solvent Degasser, AB SCIEX Triple TOF 5600+ system, and ESI source. Chromatographic conditions were as follows: performed on a C18 reversed-phase LC column (Agilent ZorBax SB-C18 50 × 2.1 mm, 1.8 mm), and the column temperature was maintained at 25°C. The mobile phase consisted of 0.1% (v/v) formic acid water (solvent A) and acetonitrile (solvent B) using a gradient program as follows. Gradient elution program was as follows: 5–25% B, 0–1 min; 25–30% B, 1–4 min; 30–55% B, 4–12 min; 55–70% B, 12–1 8min; 70–100% B, 18–25 min; 100–5% B, 25–28 min; flow rate: 0.3 ml/min; column temperature: 35°C; injection volume: 1 μl. Mass spectrometry conditions are as follows: ESI source and data collection in positive and negative ion modes. The source parameters were set as follows: ion spray voltage floating: +4,500/−4,500; declustering potential: +60/−60 V; source temperature: 550°C; the atomizing gas is N2, curtain gas: 35 psi; gas1 (nebulizer gas): 55 psi; gas2 (heater gas): 55 psi; collision energy: +35/−35 e V; using tandem mass spectrometry secondary mode: The

mass spectrometry ion scanning range was m/z 100–2,000. The tandem mass spectrometry ion scanning range was m/z 50–1,000; turn on dynamic background subtraction.

Identification of Chemical Constituents

The ultra-high-performance liquid chromatography (UHPLC)-Q/TOF-MS data of all of the studied samples were analyzed using MarkerView and PeakView software (AB Sciex, Massachusetts, USA) for the purpose of identifying PF chemical constituents.

Preparation of Adjuvant and Vaccine

PF was prepared in our laboratory in a final purity of 925 $mg{\cdot}g^{-1}$. The PA was prepared as previously described. The PF was dissolved in phosphate-buffered saline (PBS, pH 6.2), in a final concentration of 40 $mg{\cdot}ml^{-1}$. The China Institute of Veterinary Drug Control supplied PPV. After propagating *in vitro* in PK-15 cell cultures, the virus that contained 2,048 hemagglutination units (HAU)$\cdot ml^{-1}$ was inactivated with formaldehyde and stirred 24 h at 37°C. The inactivated virus that contained 512 HAU$\cdot ml^{-1}$ was used as a vaccine antigen. Three adjuvant vaccines containing PA or OA were prepared by Lvdu Veterinary Biologicals Co. Ltd., Binzhou, China. Their virus contents were the same.

Animals, Housing, and Treatment

Thirty Landrace-Yorkshire hybrid sows (aged from 198 to 204 days, and the average weight is 64.5 kg) were randomly assigned to one of three groups, receiving an intramuscular injection of PPV vaccine with 2.0-ml PA, OA, or physiological saline as the blank control group (BC). The animals were kept in 10 pigpens divided equally under standard conditions in the Experimental Animal Center of Binzhou Animal Science and Veterinary Medicine Academy, Shandong province [no. SYXK (lu) 20110066]. They were maintained in an air-conditioned room with light from 06:00 to 18:00 h. The room temperature (24 ± 3°C) and humidity were controlled automatically. They were fed with water and food *ad libitum*. All procedures related to the animals and their care conformed to the internationally accepted principles as found in the Guidelines for Keeping Experimental Animals issued by the government of China. The antibody against PPV was negative before the experiment.

Before vaccination and on days 7, 14, 21, 28, 35, and 49 after vaccination, the blood of six pigs randomly from each group was sampled for determination of serum hemagglutination inhibition (HI) antibody titer of PPV by micro-method dynamically and continuously. On days 7, 14, 21, and 35 after vaccination, the blood of four pigs randomly from each group was sampled for examination of lymphocyte proliferation by methyl thiazolyl tetrazolium (MTT) assay and analyzing specific immunoglobulin (Ig)M and IgG1, IgG2, IgG3, IgG4, interleukin (IL)-2, IL-4, and interferon-γ (IFN-γ) in serum by enzyme-linked immunosorbent assay (ELISA) kit.

Hemagglutination Inhibition Antibody Titer of Porcine Parvovirus Determination

Blood samples (1.0 ml per pig) from the ear vein were drawn into Eppendorf tubes and allowed to clot at 37°C for 1 h. Serum was separated by centrifugation for the determination of HI antibody. Briefly, twofold serial dilution of 50-μl serum, after inactivated at 56°C for 30 min, was made in a 96-well V-shaped bottom microtiter plate containing 50 μl of calcium/magnesium-free PBS in all wells, then 50 μl of PPV antigen (4 HA units) was added into all wells except for the last row, which served as the controls. Serum dilutions ranged from 1:2 to 1:2,048. The antigen–serum mixture was incubated at 37°C for 10 min. Fifty microlitres of 1% rooster erythrocytes suspension was added into each well and re-incubated for 30 min. A positive serum, a negative serum, erythrocytes, and antigens were also included. The highest dilution of serum causing complete inhibition was considered the endpoint. The geometric mean titer was expressed as reciprocal log2 values of the highest dilution that displayed HI antibody titer.

Peripheral Lymphocyte Proliferation Assay

The blood sample from the precaval vein was diluted in Hanks' solution. After centrifugation (800 × *g* at 4°C for 10 min), the cells were washed three times with PBS and resuspended in RPMI-1640. The cells were counted with a hemocytometer by trypan blue dye exclusion technique, and their viability exceeded 95%. Briefly, lymphocytes at 5.0 × 106 $cell{\cdot}ml^{-1}$ were seeded into a 96-well flat-bottom microtiter plate, 100 μl each well, then Con A (final concentration 5 $\mu g{\cdot}ml^{-1}$) or medium was added. The plates were incubated in a humid atmosphere with 5% CO_2 at 37°C for 48 h. All the tests were carried out in quadruplication. The cell proliferation was evaluated by MTT methods. Briefly, 30 μl of MTT solution (5 $mg{\cdot}ml^{-1}$) was added to each well at 4 h before the end of incubation. The plates were centrifuged (1,000×*g*, 5 min) at room temperature, and MTT was removed carefully. After 150-μl dimethyl sulfoxide was added into each well, the plates were shaken for 5 min to dissolve the formazan crystals completely, and the absorbance at 570 nm (A570 value) was determined by ELISA reader (BioTek Instruments Inc.) as the index of lymphocyte proliferation.

Cytokine and Immunoglobulin Determination

Serum concentrations of cytokines (including IL-2, IFN-γ, and IL-4) and specific IgM and IgG subclasses were assayed by ELISA according to the manufacturer's instructions. Briefly, a 96-well flat-bottom microtiter plate (Nunc, USA) was coated with a capture antibody specific for each cytokine. The plate was washed and blocked before 10 μl of the serum, and serially diluted specific standards were added to the respective wells. After a series of washing, the captured cytokine was detected using the specific conjugated detection antibody. The substrate reagent was added into each well, and, after color development, the plate was read at 450 nm using an ELISA reader (BioTek Instruments Inc.). Cytokine concentrations and IgM and IgG subclasses were accomplished by a standard curve plotting the A450 value against each dilution of the standard concentration.

Screening of Flavonoids in Propolis Against Porcine Parvovirus *in vitro*

PK-15 cells (presented by Binzhou Animal Husbandry and Veterinary Research Institute of Shandong province) were

cultured in DMEM medium containing 10% fetal calf serum (South American origin) in a 5% CO_2 cell incubator at 37°C, with 0.25% trypsin (0.02% ethylenediaminetetraacetic acid) digestion passage.

In PK-15 cells with trypsin digestion, 1×10^5/ml was vaccinated in 96 well plates, 100 μl per hole, under the condition of 37°C and 5% CO_2 training for 24 h; the supernatant was abandoned, and PBS washing was done, except for the blank

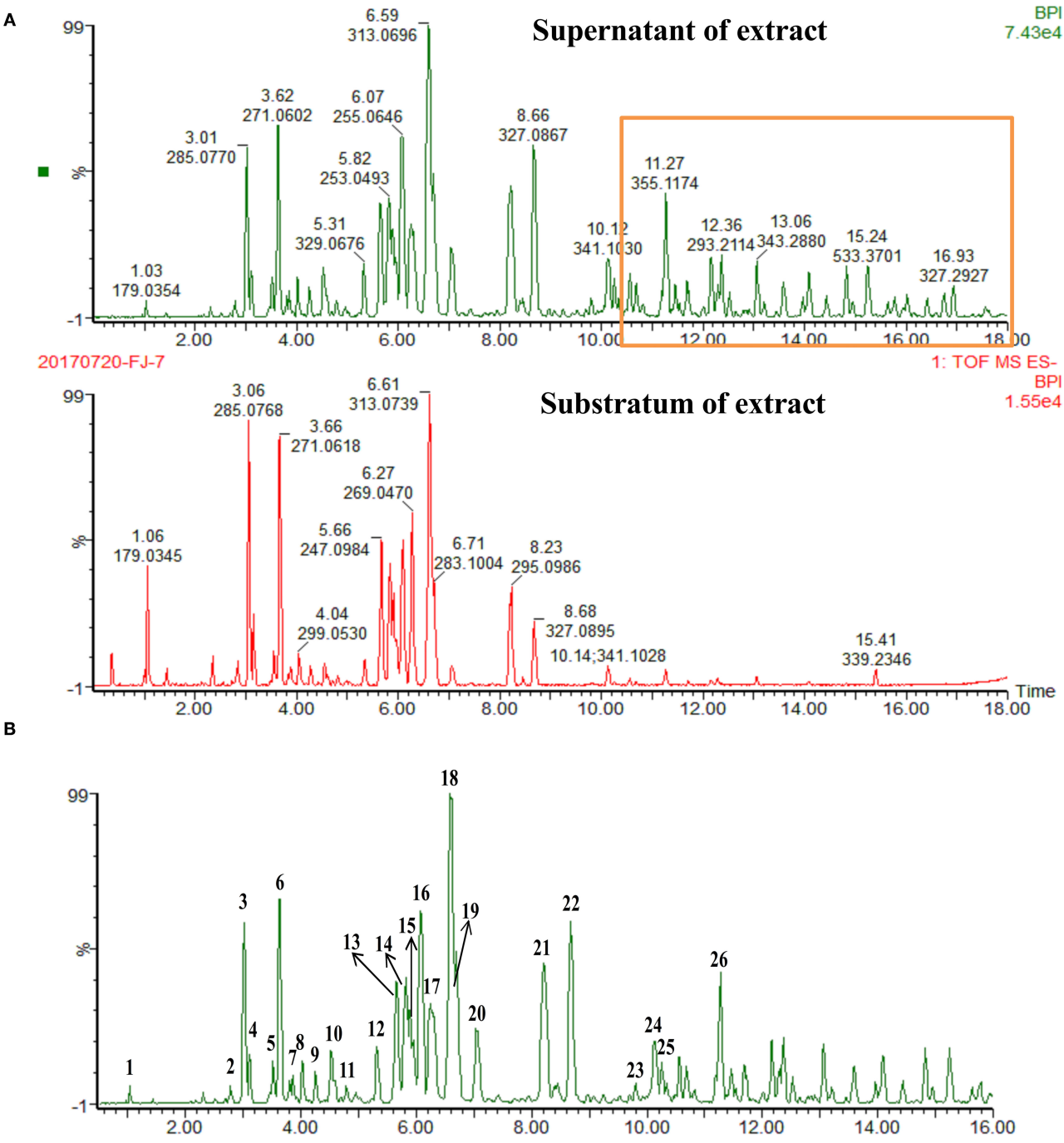

FIGURE 1 | UHPLC-Q/TOF-MS chemical fingerprints (TIC chromatography) of propolis extract. **(A)** Superstratum and substratum of propolis ethanol extract. **(B)** (1) Caffeic acid, (2) Quercetin, (3) 5-Methoxypinobanksin, (4) 3-Methoxyquercetin, (5) Apigenin, (6) Pinobanksin, (7) Isorhamnetin, (8) 5-Methoxyluteolin, (9) 5,7-Dimethoxyquercetin, (10) 5-Methoxygalangin, (11) 7-Methoxyquercetin, (12) 7-Methoxyquercetin-X-methyl ester, (13) Isoprene caffeic acid ester, (14) Chrysin, (15) Caffeic acid benzyl ester, (16) Pinocembrin, (17) Galangin, (18) 3-O-Acetylpinobanksin, (19) Caffeic acid phenethyl ester, (20). Methoxychrysin, (21) Cinnamate caffeic acid, (22) Pinobanksin-3-O- propanoate, (23) P-Cinnamyl coumarate, (24) Pinobanksin-3-O-butyrate, (25) Pinobanksin-3-O-pentenoic acid ester, (26) Pinobanksin-3-O-valerate.

group, which added DMEM, containing the rest of the holes to join with a multiplicity of infection = 1.0 PPV cultures of 100 μl, training after 4 h. Then, the supernatant was abandoned, except the blank group and model group with DMEM; in the remaining wells, the 100-μl medium was added with a 50-μM concentration of galangin, kaolin, quercetin, ferulic acid, aspen, and apigenin, and four replicates were set for each drug. After 48 h, the supernatant was discarded, and a 10-μl CCK-8 medium was added to a 100-μl DMEM medium per well for a 30-min culture, and the absorbance value of CCK-8 was detected.

Statistical Analysis

Data analysis was performed with SPSS 19.0 software (SPSS Inc., Chicago, IL, USA). Differences in mean values among the polysaccharide and control groups were analyzed by one-way analysis of variance. The data were expressed as mean ± standard error. Values of $P < 0.05$ were considered to be statistically significant.

RESULTS

Identification of Active Components of Alcohol Extract by Ultra-High-Performance Liquid Chromatography-Quadrupole/Time-of-Flight Mass Spectrometry

The crude total PFs were ∼80% in the alcohol extraction. According to the analytical results for the chemical constituents (as shown in **Figure 1A**), the different components in the supernatant and substratum of propolis extract are mainly small polar components. We analyzed the chemical fingerprint (UHPLC-Q/TOF-MS) of PF (**Figure 1B**). The analysis in negative ionization modes revealed the presence and characterization of 26 major components (**Table 1**).

Identification and Characterization of Propolis Flavonoids

Figure 2A results show that the molecular composition of the compound was C10H10O4. In the anion mode, m/z 194 [M-H]-,

TABLE 1 | Identification of compounds in ethanolic crude extract from propolis of Melipona quadrifasciata by UPLC-MS analysis.

Peak No.	Rt (min)	Tentative identification	Chemical formula	[M-H]- (m/z)		
				Mean measured mass (Da)	Theoretical exact mass (Da)	Mass accuracy (ppm)
1	1.03	Caffeic acid	C9H8O4	179.0345	179.0344	0.6
2	2.78	Quercetin	C15H10O7	301.0348	301.0350	0.7
3	3.01	5-Methoxypinobanksin	C16H14O5	285.0768	285.0763	1.8
4	3.10	3-Methoxyquercetin	C16H12O7	315.0507	315.0505	0.6
5	3.51	Apigenin	C15H10O5	269.0455	269.0450	1.9
6	3.62	Pinobanksin	C15H12O5	271.0602	271.0606	−1.5
7	3.86	Isorhamnetin	C16H12O7	315.0499	315.0505	−1.9
8	4.02	5-Methoxyluteolin	C16H12O6	299.0541	299.0556	−5.0
9	4.25	5,7-Dimethoxyquercetin	C17H14O7	329.0666	329.0661	1.5
10	4.52	5-Methoxygalangin	C16H12O5	283.0610	283.0606	1.4
11	4.78	7-Methoxyquercetin	C16H12O7	315.0497	315.0505	−2.5
12	5.31	7-Methoxyquercetin-X- methyl ester	C17H14O7	329.0653	329.0661	−2.4
13	5.63	Isoprene caffeic acid ester	C14H16O4	247.0974	247.0970	1.6
14	5.82	Chrysin	C15H10O4	253.0493	253.0501	−3.2
15	5.89	Caffeic acid benzyl ester	C16H14O4	269.0825	269.0814	4.1
16	6.07	Pinocembrin	C15H12O4	255.0646	255.0657	−4.3
17	6.24	Galangin	C15H10O5	269.0457	269.0450	2.6
18	6.59	3-O-Acetylpinobanksin	C17H14O6	313.0696	313.0712	−5.1
19	6.69	Caffeic acid phenethyl ester	C17H16O4	283.0966	283.0970	−1.4
20	7.04	Methoxychrysin	C16H12O5	283.0602	283.0606	−1.4
21	8.20	Cinnamate caffeic acid	C18H16O4	295.0970	295.0970	0.0
22	8.66	Pinobanksin-3-O- propanoate	C18H16O6	327.0867	327.0869	−0.6
23	9.80	P-Cinnamyl coumarate	C18H16O3	279.1031	279.1021	3.6
24	10.12	Pinobanksin-3-O-butyrate	C19H18O6	341.1030	341.1025	1.5
25	10.25	Pinobanksin-3-O- Pentenoic acid ester	C20H18O6	353.1035	353.1025	2.8
26	11.27	Pinobanksin-3-O-Valerate	C20H20O6	355.1174	355.1182	−2.3

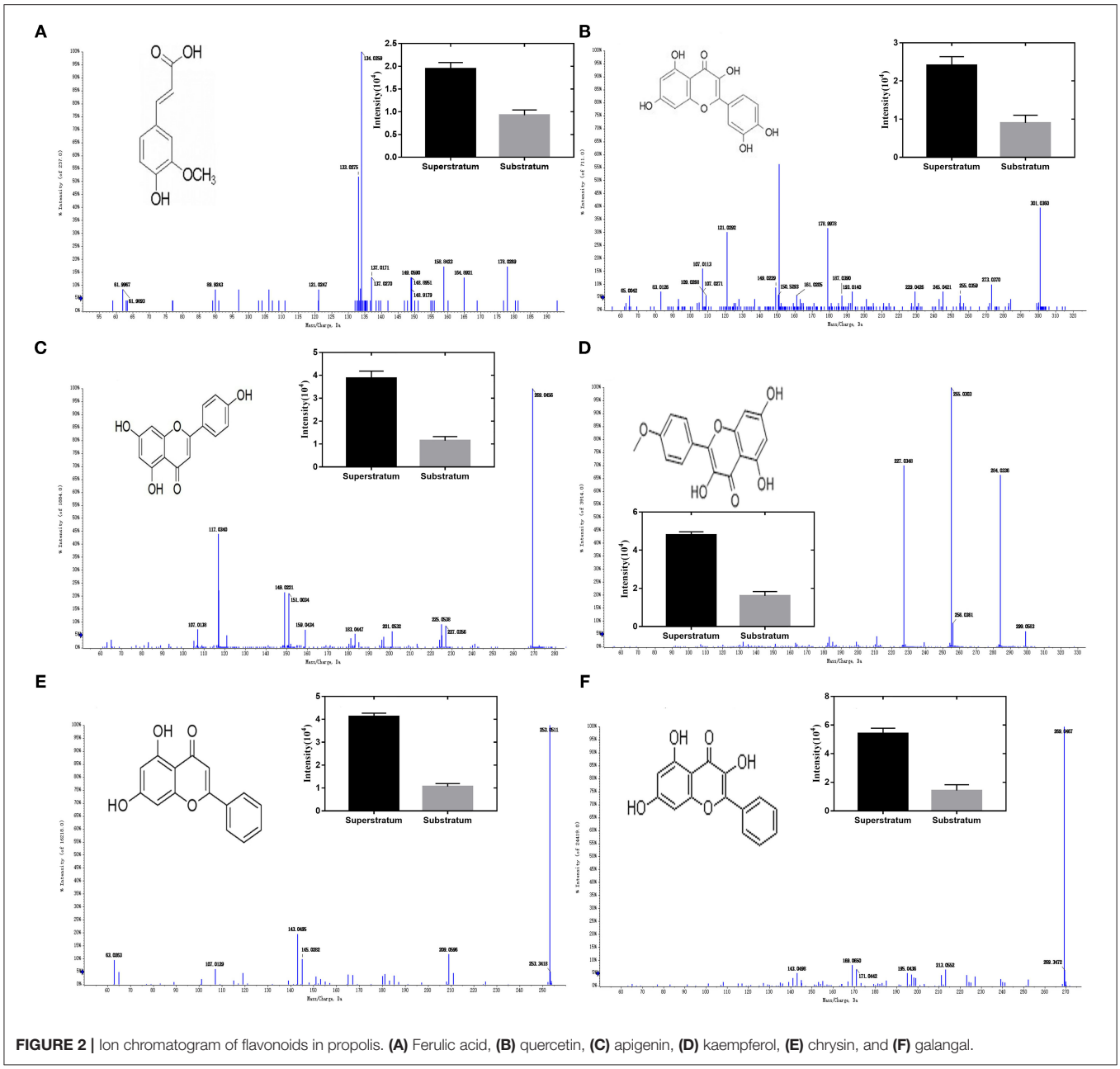

FIGURE 2 | Ion chromatogram of flavonoids in propolis. **(A)** Ferulic acid, **(B)** quercetin, **(C)** apigenin, **(D)** kaempferol, **(E)** chrysin, and **(F)** galangal.

typical fragment ion peaks such as 178 and 164 were found in the secondary mass spectrogram, and m/z 194 lost OCH3 to obtain m/z 178, which was speculated to be ferulic acid by comparing the mass spectrogram information with the reference substance.

Figure 2B results show that the molecular composition of the compound was C15H10O7. In the anion mode, m/z 301 [M-H]-, the secondary mass spectrogram showed typical fragment ion peaks such as 273, 179, 151, and 107, m/z 301 lost CO to obtain m/z 273, aglycone RDA reaction produced m/z179, 151, and 107, and compound B was speculated to be Quercetin by comparing the mass spectrogram information with the reference substance.

Figure 2C results show that the molecular composition of the compound was C15H10O5. In the anion mode, typical fragment ion peaks such as 151 and 117 were found in the secondary mass spectrogram of m/z 269[M-H]-, and compared with the mass spectrogram of the reference substance, compound C was speculated to be apigenin.

Figure 2D results show that the molecular composition of the compound was C15H10O6. In the anion mode, typical fragment ion peaks such as m/z 284 [M-H]- and 255 and 227 were found in the secondary mass spectrogram. m/z 284 lost COH to get m/z 255, whereas m/z 255 lost CO to get

m/z 227. By comparing the mass spectrogram information with the reference substance, compound D was speculated to be kaempferol.

Figure 2E results show that the molecular composition of the compound was C15H10O4. In the anion mode, m/z 253 [M-H]-, secondary mass spectrometry 143, 63, and other typical fragment

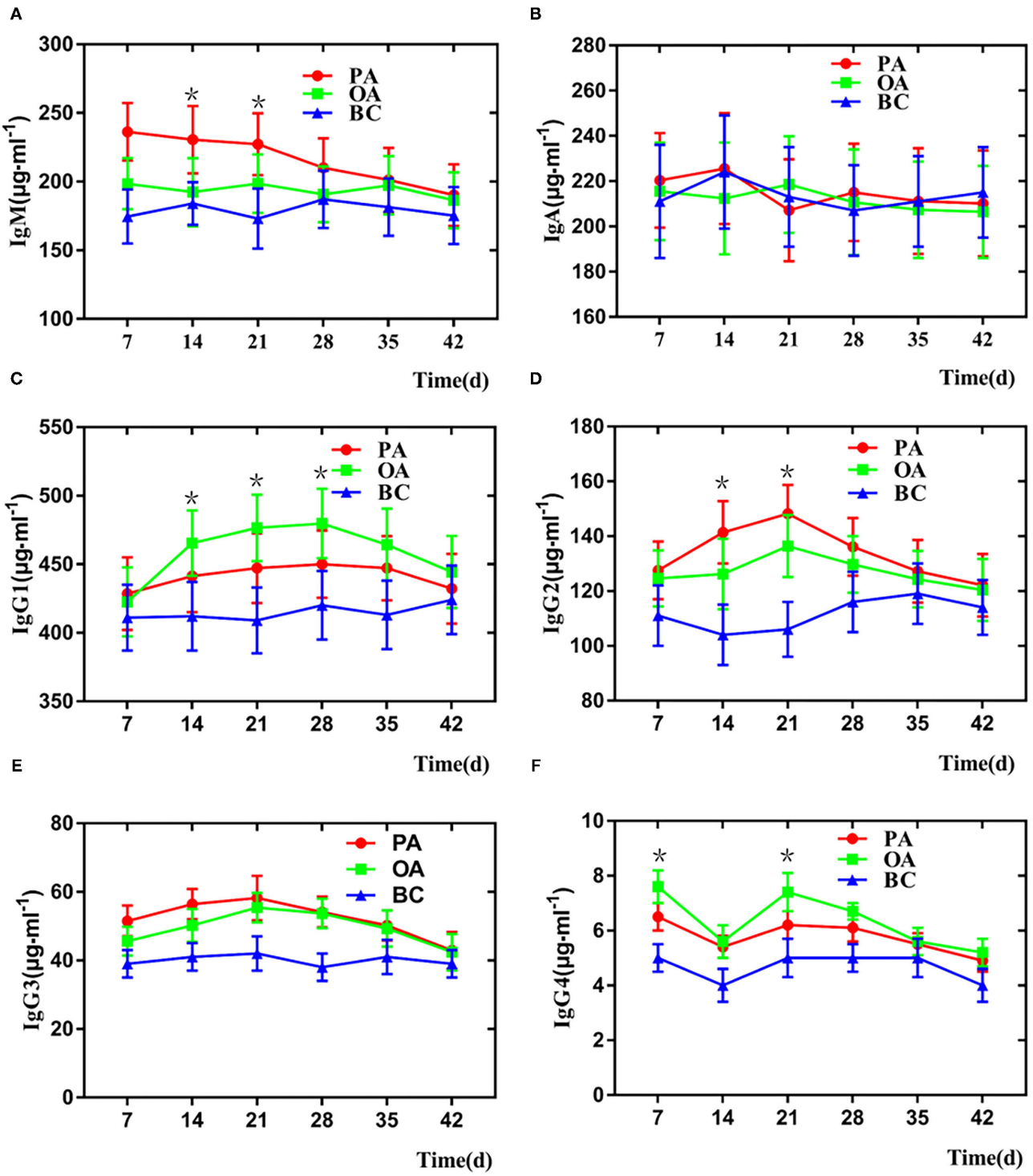

FIGURE 3 | Change of serum IgM and IgG in each group. **(A)** IgM, **(B)** IgA, **(C)** IgG1, **(D)** IgG2, **(E)** IgG3, and **(F)** IgG4. *There is a significant difference compared with BC group.

ion peaks were found. By comparing the mass spectrometry information with the reference substance, it was speculated that compound E was chrysin.

Figure 2F results show that the molecular composition of the compound was C15H10O5. In the anion mode, the ion peaks of typical fragments such as 213, 171, and 169 were found in the secondary mass spectrogram of m/z 269 [M-H]-, and the mass spectrogram information was compared with the reference substance, suggesting that compound E was galangal.

Serum Immunoglobulin M and G Subclasses Detected by Enzyme-Linked Immunosorbent Assay

As illustrated in **Figure 3A**, on days 7 and 35 after vaccination, the IgM level of the PA group was higher than those of other groups, whereas on days 14 and 21 after vaccination, the IgM level of the PA group only was numerically higher than the OA group and higher than that of the BC group. In addition, the IgA serotype is a monomer, and the immune function is weak. The IgA level of all groups has no significant difference due to the sample being the serum (**Figure 3B**). IgG1 levels in the two adjuvant groups were higher than that of the BC group when the samples were collected after immunization. On days 14, 21, and 28 after vaccination, the IgG1 levels of the PA group were significantly higher than those of the BC group (**Figure 3C**). PA triggered a stronger IgG2 level than the OA and BC groups on days 14 and 21, respectively (**Figure 3D**). The IgG3 level was higher in the pigs of the PA group than that of the pigs immunized with the OA group. However, no significant difference was observed for the responses of IgG3 between the OA and BC groups (**Figure 3E**). As illustrated in **Figure 3F**, on days 7 and 35 after vaccination, the IgG4 level of the PA group was higher than those of other groups, whereas on days 7 and 21 after vaccination, the IgG4 level of the PA group was only numerically higher than the OA group and higher than that of the BC group.

TABLE 2 | Changes in lymphocyte proliferation of blood (A570 value).

Group	D_7	D_{14}	D_{21}	D_{35}
PA	0.158 ± 0.015^a	0.140 ± 0.013^a	0.142 ± 0.009^a	0.133 ± 0.010^a
OA	0.120 ± 0.010^b	0.127 ± 0.015^b	0.137 ± 0.012^b	0.130 ± 0.027^a
BC	0.100 ± 0.021^c	0.108 ± 0.012^c	0.120 ± 0.013^c	0.112 ± 0.012^b

PA, propolis adjuvant; OA, oil emulsion adjuvant; BC, Blank control, the same as follows.
$^{a-c}$Data within a column without the same superscripts differ significantly ($p < 0.05$).

Propolis Flavonoid Promoted the Activity of Peripheral Lymphocyte Proliferation

The lymphocyte proliferation activities are shown in **Table 2**. In all adjuvant groups, the peak values of lymphocyte proliferation activity were on day 7 after vaccination. The A570 values in the PA group were significantly highest and significantly higher than the OA group from days 7 to 21. On day 35, the A570 values in the two adjuvant groups were significantly higher than that of the BC group.

Serum Antibody Titer

The serum HI antibody titers of each group are shown in **Table 3**. As compared with the BC group, the antibody titers in all vaccination groups increased ($p < 0.05$). On days 21, 28, 35, and 42, the antibody titers in the PA group were significantly lower than those in the OA group.

Serum Cytokine Level Detected by Enzyme-Linked Immunosorbent Assays

Serum cytokine levels are listed in **Figure 4**. On days 14, 21, and 28, the serum IL-2, IL-4, and IFN- γ levels in two adjuvant groups were significantly higher when compared with those in the BC group (**Figures 4A,B,F**). Interestingly, the serum IL-6, IL-10, IL-12 levels in the two groups are not significantly higher when compared with those in the BC group (**Figures 4C–E**). IL-6 and IL-12 could promote the expression level of tumor necrosis factor-α. In addition, despite this, we think PF could be an immune enhancement *in vivo*.

Screening of Flavonoids in Propolis Against Porcine Parvovirus *in vitro*

As shown in **Figures 5A,B**, ferulic acid, chrysin, kaempferol, and galangal had a good inhibitory effect on PPV-induced PK-15 cells, but ferulic acid and chrysin had the best effect.

DISCUSSION

Propolis is an important medicinal material with a variety of pharmacological activities. The chemical analysis of propolis alcohol extract revealed the presence of flavonoids compounds. The traditional method of extracting and purifying traditional Chinese medicine extract is done first, and then, identifying the structure by nuclear magnetic resonance after the monomer is obtained is complicated and requires a large amount of work. UPLC-MS techniques combined with HPLC rapid high

TABLE 3 | Dynamic variation of HI antibody titer after vaccination (log2).

Group	D_0	D_7	D_{14}	D_{21}	D_{28}	D_{35}	D_{49}
PA	0 ± 0^a	4.5 ± 0.4^a	7.4 ± 0.5^a	7.5 ± 0.4^b	7.8 ± 0.7^b	7.3 ± 0.5^b	6.5 ± 0.5^b
OA	0 ± 0^a	4.3 ± 0.5^a	7.3 ± 0.5^a	8.5 ± 0.6^a	8.8 ± 0.5^a	8.3 ± 0.7^a	7.5 ± 0.7^a
BC	0 ± 0^a	0 ± 0^c	0 ± 0^c	0 ± 0^c	0 ± 0^c	0 ± 0^c	0 ± 0^c

$^{a-c}$Data within a column without the same superscripts differ significantly ($p < 0.05$).

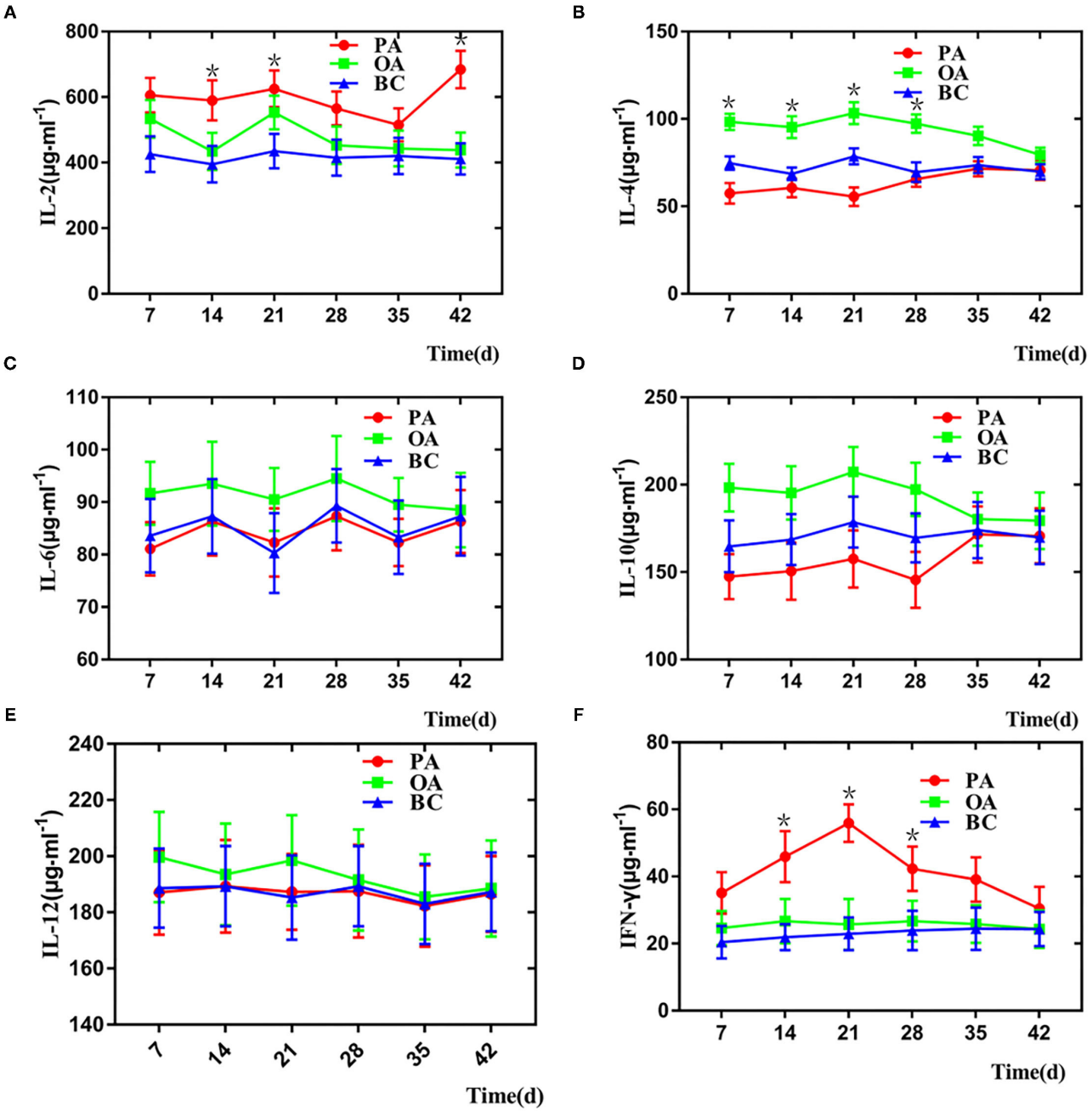

FIGURE 4 | Change of serum cytokine in each group. **(A)** IL-2, **(B)** IL-4, **(C)** IL-6, **(D)** IL-10, **(E)** IL-12, and **(F)** IFN-γ. *There is a significant difference compared with BC group.

separation ability and high sensitivity and high accuracy of high-resolution mass spectrometry, to avoid the disadvantages of traditional component separation analysis method, not only can do a fast qualitative analysis of complex components but also has the characteristics of simple operation, a large amount of information, and saving solvent, thus increasing in the study of Chinese herbal medicine composition.

The current study revealed that PF from propolis had antivirus activity and immune enhancement and antioxidant activity. PF enhances immune responses in various ways, such as the formation of the immunostimulating complex and activation of helper and cytotoxic T cells. In addition to stimulating the humoral immune response, PF also increased cellular immune responses (20, 21). In this study, PF was varied regarding their adjuvant effects on the immune responses that stimulated the immune system cells to produce cytokines. As shown in **Figure 4**, PF significantly increased the production of both Th2 cytokines IL-4 and Th1 cytokines IL-2 and IFN-γ, which suggested that PF

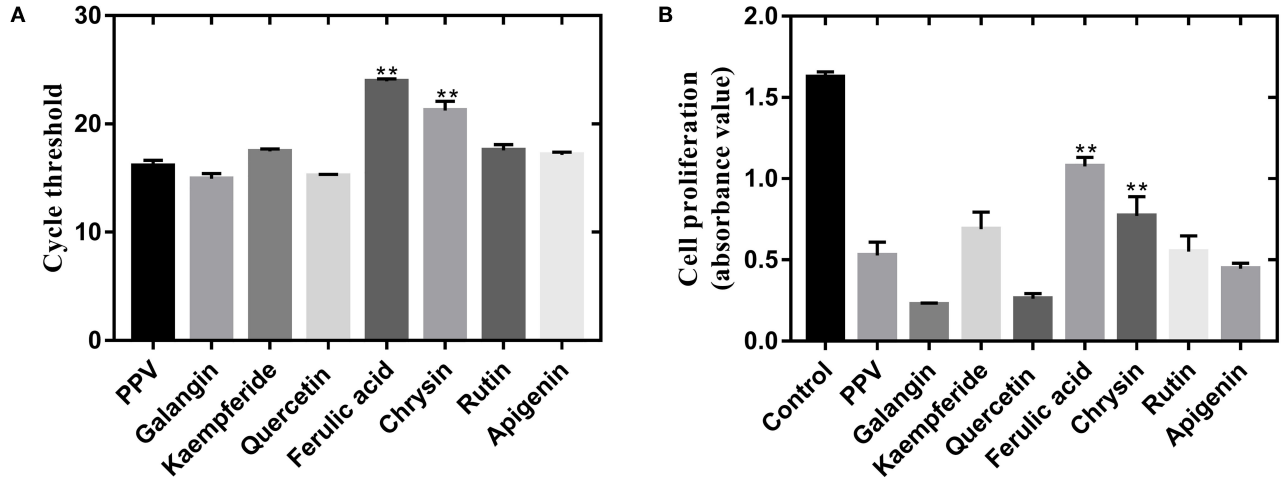

FIGURE 5 | PF isolated from propolis inhibited PPV-induced cell death of PK-15 cells. **(A)** Effect of PF treatment on PPV replication. Virus replication ability was detected by real-time polymerase chain reaction. **(B)** Cell proliferation of PPV-infected PK-15 cells after PF treatment. Cell proliferation was measured by CCK-8 assay. **There is a significant difference compared with PPV group.

simultaneously elicited a Th1 and Th2 immune response. These findings are consistent with Blonska's study, which demonstrated that PF could enhance the activity of T lymphocytes, promoting the secretion of some cytokines, such as IL-2 and tumor necrosis factor-α, thus improving the immune function of the organism (22).

Th1 activation contributes to cell-mediated immunity, whereas Th2 activation favors the humoral immune response (23). Th1/Th2 balance is a prerequisite for the functionality of the immune system against infections. PF immunomodulatory action has been widely investigated lately, both *in vitro* and *in vivo* (24). PF has been suggested to be a promising adjuvant substance in duck-inactivated vaccines (25). Important functional properties of immune cells are their capability to synthesize and secrete soluble polypeptide factors referred to as cytokines. Most cytokines are secreted and then bind to specific receptors on the surface of target cells. Upon binding, they act to regulate growth and/or differentiation and to optimize the immune response. Using a Polish sample, Ansorge (26) found that propolis has immunoregulatory effects that may be mediated by Erk2 MAP kinase signals that promote cellular growth. Orsolic suggested that propolis stimulated macrophages, thus influencing specific and nonspecific immune defense mechanisms. Activation of macrophages is important for the modulating property of tested compounds, as it leads to the production of factors regulating activities of B and T cells. During a T cell-dependent immune response, there is a progressive change in the predominant immunoglobulin class of the specific antibody produced. This change, isotype switch, is influenced by T cells and their cytokines. IL-4 preferentially switches activated B cells to the IgG1 isotype (Th2 type immune response); IFN-γ enhances IgG2 and IgG3 responses (Th1 type) (27, 28).

In summary, PF significantly increased the serum levels of IgG subclasses, as well as T lymphocyte proliferation, when administered in pigs with an inactivated vaccine against PPV. The enhanced IgG subclass levels paralleled the increased serum levels of IFN-γ and IL-2. This adjuvant activity was evident in the increase in both cellular and humoral immune responses. In addition, PF could inhibit PPV-induced apoptosis by immune enhancement. Interestingly, FA as a PF component's significance inhibited the PPV replication. Also, FA is a potential antiviral adjuvant, which could be widely used in veterinary clinics.

DATA AVAILABILITY STATEMENT

The original contributions presented in the study are included in the article/supplementary material, further inquiries can be directed to the corresponding authors.

ETHICS STATEMENT

The animal study was reviewed and approved by Binzhou Animal Science and Veterinary Medicine Academy, Shandong province (NO. SYXK (lu) 20110066). Written informed consent was obtained from the owners for the participation of their animals in this study.

AUTHOR CONTRIBUTIONS

XM and ZZ: research concept, methodology, data extraction, analysis, and draft writing. ZG, YLi, and LZ: resource searching, verification, formal analysis, supervision, and manuscript reviewing and editing. KY and XL: resources, methodology, project administration, supervision, and manuscript reviewing and editing. YLiu and ZS: resource searching and manuscript reviewing and editing. XM and ZZ: methodology and manuscript reviewing and editing. All authors contributed to the article and approved the submitted version.

FUNDING

The present work was funded by the National Natural Science Foundation of China (Grant nos. 31602098 and 32072906), the Scientific and Technological Project of Henan Province (Grant nos. 192102110188, 192102110184, and 212102110103), the Postgraduate Research and Practice Innovation Program of Jiangsu Province (KYCX20-1494), the veterinary drugs science subject in Henan University of Animal Husbandry and Economy (Grant no. 41000003), the scientific research and innovation team in the Henan University of Animal Husbandry and Economy (Grant no. 2018KYTD18), and the science and technology major project of Prevention and Treatment of Major Infectious Diseases such as AIDS and Viral Hepatitis: Research on new technology of integrated field rapid detection of important viruses (Grant no. ZX10711001-003-003).

REFERENCES

1. Bankova V, Bertelli D, Borba R, Conti BJ. Standard methods for Apis mellifera propolis research. J Apic Res. (2016) 1–49. doi: 10.1080/00218839.2016.1222661
2. Salatino A, Fernandessilva CC, Righi AA, Salatino MLF. Propolis research and the chemistry of plant products. *Nat Prod Rep.* (2011) 28:925–36. doi: 10.1039/c0np00072h
3. Zabaiou N, Fouache A, Trousson A, Baron S, Zellagui A, Lahouel M. Lobaccaro J. Biological properties of propolis extracts: Something new from an ancient product. *Chem Phys Lipids*. (2017) 207:214–22. doi: 10.1016/j.chemphyslip.2017.04.005
4. Watanabe MAE, Amarante MK, Conti BJ. Cytotoxic constituents of propolis inducing anticancer effects: a review. *J Pharm Pharmacol.* (2011) 63:1378–86. doi: 10.1111/j.2042-7158.2011.01331.x
5. Huang S, Zhang CP, Wang K, Li GQ, Hu FL. Recent advances in the chemical composition of propolis. *Molecules.* (2014) 19:19610–32. doi: 10.3390/molecules191219610
6. Zhang XJ, Xiong YL, Zhang J. Autophagy Promotes Porcine Parvovirus Replication and Induces Non-Apoptotic Cell Death in Porcine Placental Trophoblasts. *Viruses*. (2019) 12:15. doi: 10.3390/v12010015
7. Streck AF, Truyen U. Porcine Parvovirus. *Curr Issues Mol Biol.* (2020) 37:33–46. doi: 10.21775/cimb.037.033
8. Cao L, Xue M, Chen J. Porcine parvovirus replication is suppressed by activation of the PERK signaling pathway and endoplasmic reticulum stress-mediated apoptosis. *Virology.* (2019) 539:1–10. doi: 10.1016/j.virol.2019.09.012
9. Gardner IA, Carpenter TE, Leontides L. Financial evaluation of vaccination and testing alternatives for control of parvovirus-induced reproductive failure in swine. *J Am Vet Med Assoc.* (1996) 208:863–9.
10. Leclerc C. New approaches in vaccine development. *Comp Immunol Microbiol Infect Dis.* (2003) 26:329–41. doi: 10.1016/S0147-9571(03)00018-3
11. Barr TA, Carlring J, Heath AW. Co-stimulatory agonists as immunological adjuvants. *Vaccine.* (2006) 24:3399–407. doi: 10.1016/j.vaccine.2006.02.022
12. Aguilar JC, Rodríguez EG. Vaccine adjuvants revisited. *Vaccine.* (2007) 25:3752–62. doi: 10.1016/j.vaccine.2007.01.111
13. Holmdahl R, Lorentzen JC, Lu S. Arthritis induced in rats with nonimmunogenic adjuvants as models for rheumatoid arthritis. *Immunol Rev.* (2001) 184:184–202. doi: 10.1034/j.1600-065x.2001.1840117.x
14. Vrieling H, Kooijman S, De Ridder JW. Activation of Human Monocytes by Colloidal Aluminum Salts. *J Pharmac Sci*. (2020) 109:750–60. doi: 10.1016/j.xphs.2019.08.014
15. Hu Y, Smith D, Zhao Z. Alum as an adjuvant for nanoparticle based vaccines: A case study with a hybrid nanoparticle-based nicotine vaccine. *Nanomedicine.* (2019) 20:102023. doi: 10.1016/j.nano.2019.102023
16. Shi S, Zhu H, Xia X. Vaccine adjuvants: Understanding the structure and mechanism of adjuvanticity. *Vaccine.* (2019) 37:3167–78. doi: 10.1016/j.vaccine.2019.04.055
17. Torres AR, Sandjo LP, Friedemann MT. Chemical characterization, antioxidant and antimicrobial activity of propolis obtained from Melipona quadrifasciata quadrifasciata and Tetragonisca angustula stingless bees. *Braz J Med Biol Res.* (2018) 51:e7118. doi: 10.1590/1414-431x20187118
18. Fan Y, Ma L, Zhang W. Microemulsion can improve the immune-enhancing activity of propolis flavonoid on immunosuppression and immune response. *Int J Biol Macromol.* (2014) 63:126–32. doi: 10.1016/j.ijbiomac.2013.09.039
19. Almeida A, Sobrinho E, Pinho L. Toxicidade aguda dos extratos hidroalcoólicos das folhas de alecrim-pimenta, aroeira e barbatimo e do farelo da casca de pequi administrados por via intraperitoneal. *Ciencia Rural.* (2010) 40:200–3. doi: 10.1590/S0103-84782009005000230
20. Fischer G, Paulino N, Marcucci MC. Green propolis phenolic compounds act as vaccine adjuvants, improving humoral and cellular responses in mice inoculated with inactivated vaccines. *Mem Inst Oswaldo Cruz.* (2010) 105:908–13. doi: 10.1590/S0074-02762010000700012
21. Pagliarone AC, Missima F, Orsatti CL. Propolis effect on Th1/Th2 cytokines production by acutely stressed mice. *J Ethnopharmacol.* (2009) 125:0–233. doi: 10.1016/j.jep.2009.07.005
22. Blonska M, Bronikowska J, Pietsz G, Czuba ZP. Scheller S. Effects of ethanol extract of propolis (EEP) and its flavones on inducible gene expression in J774A1 macrophages. *J Ethnopharmacol.* (2004) 91:25–30. doi: 10.1016/j.jep.2003.11.011
23. Piskareva O, Lackington W, Lemass D. The Human L1 Element. A Potential Biomarker in Cancer Prognosis, Current Status and Future Directions. *Curr Mol Med.* (2011) 11:286–303. doi: 10.2174/156652411795677954
24. Fischer G, Cleff MB, Dummer LA. Adjuvant effect of green propolis on humoral immune response of bovines immunized with bovine herpesvirus type 5. Veterinary immunology and immunopathology. (2007) 116:79–84. doi: 10.1016/j.vetimm.2007.01.003
25. Zhou Y, Leng X, Luo X. Regulatory Dendritic Cells Induced by K313 Display Anti-Inflammatory Properties and Ameliorate Experimental Autoimmune Encephalitis in Mice. *Front Pharmacol.* (2019) 10:1579. doi: 10.3389/fphar.2019.01579
26. Ansorge S, Reinhold D, Lendeckel U. Propolis and some of its constituents down-regulate DNA synthesis and inflammatory cytokine production but induce TGF-beta1 production of human immune cells. *Z Naturforsch C J Biosci.* (2003) 58:580–9. doi: 10.1515/znc-2003-7-823
27. Orsolic N, Terzic S, Sver L. Polyphenolic compounds from propolis modulate immune responses and increase host resistance to tumor cells. *Food Agric Immunol.* (2005) 16:165–79. doi: 10.1080/09540100500258484
28. Shen ZQ, Liu JS, LI F. Study on the combined inactivated vaccine of avian cholera and escherichia coli polyvalent probee. *Chin J Prev Vet Med.* (2004) 4:51–8. doi: 10.3969/j.issn.1008-0589.2004.04.014

Conflict of Interest: The authors declare that the research was conducted in the absence of any commercial or financial relationships that could be construed as a potential conflict of interest.

frontiers | Frontiers in Veterinary Science

ORIGINAL RESEARCH
published: 11 April 2022
doi: 10.3389/fvets.2022.874679

Impacts of Colored Light-Emitting Diode Illumination on the Reproductive Performance and Bioactive Constituents and the Molecular Mechanism of Hypothalamus Gland in Zi-geese

Li Manyu[1,2], *Zhao Xiuhua*[2], *Liu Guojun*[2] *and Zhang Guixue*[1*]

[1] College of Animal Science and Technology, Northeast Agricultural University, Harbin, China, [2] Institute of Animal Husbandry, Heilongjiang Academy of Agricultural Sciences, Harbin, China

Goose is a seasonal breeding animal. Its reproduction is regulated by hypothalamus-pituitary-gonad axis and also affected by environmental factors such as light and location. Zi-goose is characterized with long egg-laying period and high egg-laying potential and belongs to the long-day type of seasonal breeding. In this study, the regulation mechanism of different lighting on reproductive performance of Zi-goose by using metabonomics analysis technology. In addition, 1,481 differential metabolites were screened out totally. 583 differential metabolites were identification in hypothalamus of Zi-goose. 196 differential metabolites were identification in pituitary of Zi-goose. 692 differential metabolites were identification in ovary of Zi-goose. Under red light condition for 12 h, expression of 433 differential metabolites were down-regulated and expression of 150 differential metabolites were up regulated in hypothalamus of Zi-goose, expression of 125 differential metabolites were down-regulated and expression of 71 differential metabolites were up-regulated in pituitary of Zi-goose, expression of 355 differential metabolites were down-regulated and expression of 337 differential metabolites were up-regulated in ovary of Zi-goose. 33 differential metabolites were closely associated with 1,264 transcripts and 400 homologous genes of related enzymes in hypothalamus of Zi-goose. 15 differential metabolites were closely associated with 163 transcripts and 47 homologous genes of related enzymes in pituitary of Zi-goose. 55 differential metabolites were closely associated with 1,255 transcripts and 360 homologous genes of related enzymes in ovary of Zi-goose. It was confirmed that four metabolic pathways were closely related to light regulation of reproductive performance of Zi-goose, namely GnRH signaling pathway, prolactin signaling pathway, thyroid hormone synthesis and ovarian steroidogenesis. Typical differential metabolites of arachidonic acid, glucose-6-phosphate, progesterone, glutathione, oxidized glutathione, testosterone, deoxyepiandrosterone and their related protein genes would play an important role in light regulation of reproductive performance of Zi-goose.

Keywords: Zi-goose, lighting, reproduction performance, metabolome, pathogenesis

OPEN ACCESS

Edited by:
Kun Li,
Nanjing Agricultural University, China

Reviewed by:
Muhammad Akhtar,
Huazhong Agricultural University, China
Huanmin Yang,
Heilongjiang Bayi Agricultural University, China

***Correspondence:**
Zhang Guixue
gxzhang@neau.edu.cn

Specialty section:
This article was submitted to Veterinary Infectious Diseases, a section of the journal Frontiers in Veterinary Science

Received: *12 February 2022*
Accepted: *02 March 2022*
Published: *11 April 2022*

Citation:
Manyu L, Xiuhua Z, Guojun L and Guixue Z (2022) Impacts of Colored Light-Emitting Diode Illumination on the Reproductive Performance and Bioactive Constituents and the Molecular Mechanism of Hypothalamus Gland in Zi-geese. Front. Vet. Sci. 9:874679. doi: 10.3389/fvets.2022.874679

INTRODUCTION

Metabonomics is an essential component of systems biology (1). Its research idea is to follow the example of genomics and proteomics, using high-throughput and high-sensitivity modern analysis technology to quantitatively analyze all metabolites in the organism as well as to find the corresponding relationship between metabolites and physiological and pathological changes (2, 3). Metabolomics is the study of all metabolites in a sample at a certain time by LC-MS/GC-MS. Metabonomics magnifies the slight variations of gene and protein expression reflecting the physiological and pathological state of the body system (4). Through metabonomics analysis, the different metabolites between the experimental group and the control group could be further clarified, which provides a linkage for revealing the material and energy metabolism activities between the experimental and the control groups (5, 6).

In the previous studies, it has been indicated that 12 h red light was beneficial to improve the reproductive performance of Zi-geese, and the differentially expressed candidate genes and possible regulatory pathways of Zi-geese under different light conditions were analyzed by transcriptome sequencing technology (7, 8). To further reveal the mechanism of the 12 h red light improving the reproductive performance of geese, the samples of the hypothalamus, ovaries, and pituitaries from the Zi-geese during the peak laying season were studied through this research and those samples processed through the metabolomics, transcriptomics, and metabolomics combined analysis. This study was aimed to find out the differential metabolites in response to light regulation, and to clarify the regulatory genes of the differential metabolites and their differences in the regulation mode of reproductive performance for the geese, as well as to further analyze the regulation mechanism of different light conditions on reproductive performance of the Zi-geese.

METHODS AND MATERIAL

The Experimental Materials

Fifty layings Zi-geese were purchased from the Yuanfang geese industry in Harbin.

Animals Experiment

The fifty geese were randomly separated into two groups with 25 geese in each group. Those geese were respectively treated with the white incandescent lamp and red LED lamp set 12 h long. The experimental groups were shown in **Table 1**. Conventional feeding management, mixed group feeding of male and female geese, as well as the experimental diet, were shown in **Table 2**. At the end of the experiment, 3 geese in each treatment were randomly slaughtered. Thalamus, pituitary, and ovary tissues were sampled and put into an enzyme-free aseptic cryopreservation tube and quickly frozen in liquid nitrogen. After that, they were taken back to the laboratory and stored at −80°C for transcriptome and metabonomic analysis.

TABLE 1 | Experimental grouping and sampling number.

Groups	Treatment	Sampling organ	Serial number
Experimental group	Red LED 12 h	Hypothalamus, hypophysis, oophoron	RH RP RO
Control group	White light 12 h	Hypothalamus, hypophysis, oophoron	WH WP WO

Preparation of the Detection Samples

In total, 60 mg of tissue samples were added to 600 uL of methanol, shaken for 30 s, and centrifuged at 4°C and 12,000 r/min for 10 min to obtain the sample, which was used for the UPLC-Q/TOF-MS detection.

Analyse of the Components by UPLC-Q/TOF-MS

The analysis of the drug-containing plasma samples was performed in an LC-30A UPLC (Shimadzu, Kyoto, Japan) coupled hybrid quadrupole time-of-flight tandem mass spectrometer (LC/MS-Triple TOFTM 5600+, AB Sciex, Concord, ON, Canada) equipped with an electrospray ionization (ESI) interface (9, 10). The chromatographic conditions were were consistent with those described in our previously published article.

Construction of the Component-Target-Disease Network

Cytoscape V3.7.2 is an open-source software used to visualize complicated networks and integrate different types of attribute data (11). The aforementioned data were imported into Cytoscape V3.7.2, which was used to construct an active component-target-disease interaction network. The nodes indicate components or targets, and the edges indicate their relationships. The topological parameters, including "Degree"e "Closeness Centrality" and "Betweenness Centrality"e which can be used to evaluate the importance of components and targets, were calculated by Network Analyzer. The core components were screened as ligands for molecular docking based on the degree values. The degree value of a molecule represents the number of connections between the molecule and targets in the core architecture of the network.

Construction of the Protein–Protein Interaction (PPI) Network

To analyze the interactions between the CR component targets and primary dysmenorrhea-related targets, the overlapping targets were imported to the STRING database (https://string-db.org/, ver. 11.0). The organism was programmed to be "*Anas*"n and the confidence level was set as "highest confidence (0.900)"0 The PPI network was obtained from the targets most strongly associated with the overlapping targets. Cytoscape V3.7.2 was used to construct and visualize the PPI network. The top 10 correlated targets were identified by calculating the correlation degree of the target proteins in the PPI network.

TABLE 2 | Joint analysis results of hypothalamic metabolites and transcripts in Zi-geese.

Metabolite ID	Metabolite name	Transcript no.	Homologous genes no.
C00003	Nicotinamide adenine dinucleotide	359	116
C00019	S-adenosine methionine	218	83
C00022	Pyruvic acid	55	18
C00025	L-glutamic acid	103	30
C00072	Ascorbic acid	71	5
C00092	6-phosphoglucose	27	8
C00188	L-threonine	25	11
C00219	Arachidonic acid	66	20
C00410	Progesterone	19	5
C00491	l-cystine	2	1
C00504	Folic acid	1	1
C00523	Androsterone	6	1
C00526	Deoxyuridine	31	6
C00530	Hydroquinone	47	13
C00576	Betaine aldehyde	9	2
C00584	Prostaglandin E2	8	4
C00669	γ-glutamate kinase	47	3
C00777	Retinoic acid	38	12
C01561	Ossification diol	8	3
C02470	Yellow urea acid	24	13
C03167	Phosphonyl acetaldehyde	24	13
C03205	Deoxycorticosterone	7	4
C04742	15-hydroxyeicosaptaenoic acid	7	1
C05290	19-hydroxyandrosteno-4-ene-3, 17-dione	1	1
C05490	11-dehydrocorticosterone	14	8
C05503	17β-estradiol 3-(β-D-glucuronide)	6	1
C06104	Adipic acid	20	6
C06426	Gamma linolenic acid	9	4
C06428	Eicosapentaenoic acid	6	3
C08362	Palmitic acid	2	1
C15572	Guaiacol	1	1
C16285	Thiobenzamide	1	1
C18060	N-acetyl-α-d-galactosamine 1-phosphate	2	1

GO and KEGG Enrichment Analyses

OmicShare (http://www.omicshare.com/tools) was used to visualize the results of Gene Ontology (GO) functional enrichment analysis and Kyoto Encyclopedia of Genes and Genomes (KEGG) pathway enrichment analysis (12). GO analysis included biological process (BP), molecular function (MF), and cellular component (CC) ontologies. The statistical significance threshold was set at $P<0.05$.

RESULTS

The LC-MS Analysis of the Organ Metabolites

Ultra-high performance liquid chromatography-tandem time of flight mass spectrometry (UPLC-Q-TOF/MS) of Waters was used for LC-MS analysis of samples, and quality control samples were used to test the performance of the method (13). According to the ion flow diagram of the base peak of the quality control sample in the positive and negative ion mode (**Figures 1A,B**), it can be known that the chromatographic peak was uniform, the number was large, the peak shape was good, there was no oversaturation tailing and other adverse phenomena, and the methodology and sample quality were qualified. PCA examination of the test results (**Figure 1C**) showed that all the points of the quality control sample (QC) were closely clustered, indicating that the whole experimental process has been well repeated and no abnormal data.

Identification of Metabolites and Screening of Differential Metabolites

As shown in **Figure 2**, 4,105 metabolites were identified based on the standard of Progenesis QI. On this basis, univariate statistical analysis was used to screen differential metabolites according to the difference multiple (FC > 2 or FC < 0.5) and *P*-value (*P*-value < 0.05, t-test). Through the experiment, 1481 differential metabolites were screened, among which 583 were screened from the hypothalamus of the candidate geese and 384 were unique; 196 differential metabolites and 117 unique differential metabolites were screened from the pituitaries of that; 692 differential metabolites and 513 unique differential metabolites were screened from the ovary of the Zi-geese. Additionally, 44 different metabolites were identification in the hypothalamus and pituitaries, 144 different metabolites were identification in the hypothalamus and ovary, 24 different metabolites were identification in pituitary and ovary, and 11 differential metabolites in the hypothalamus, pituitaries, and ovary.

Cluster Analysis of Differential Metabolites

According to the Cluster thermogram of differential metabolites, the accumulation of 125 differential metabolites in the pituitaries of the Zi-geese decreased under the 12 h red light, while the accumulation of 71 differential metabolites increased under the red light within 12 h (**Figure 3A**).The accumulation of 433 differential metabolites in the hypothalamus of the geese decreased under the light, while 150 differential metabolites increased under the same condition(**Figure 3B**). The accumulation of 355 differential metabolites in the ovary of the geese decreased under the 12 h red light, and 337 differential metabolites increased under the red light (**Figure 3C**). The accumulation of these differential metabolites

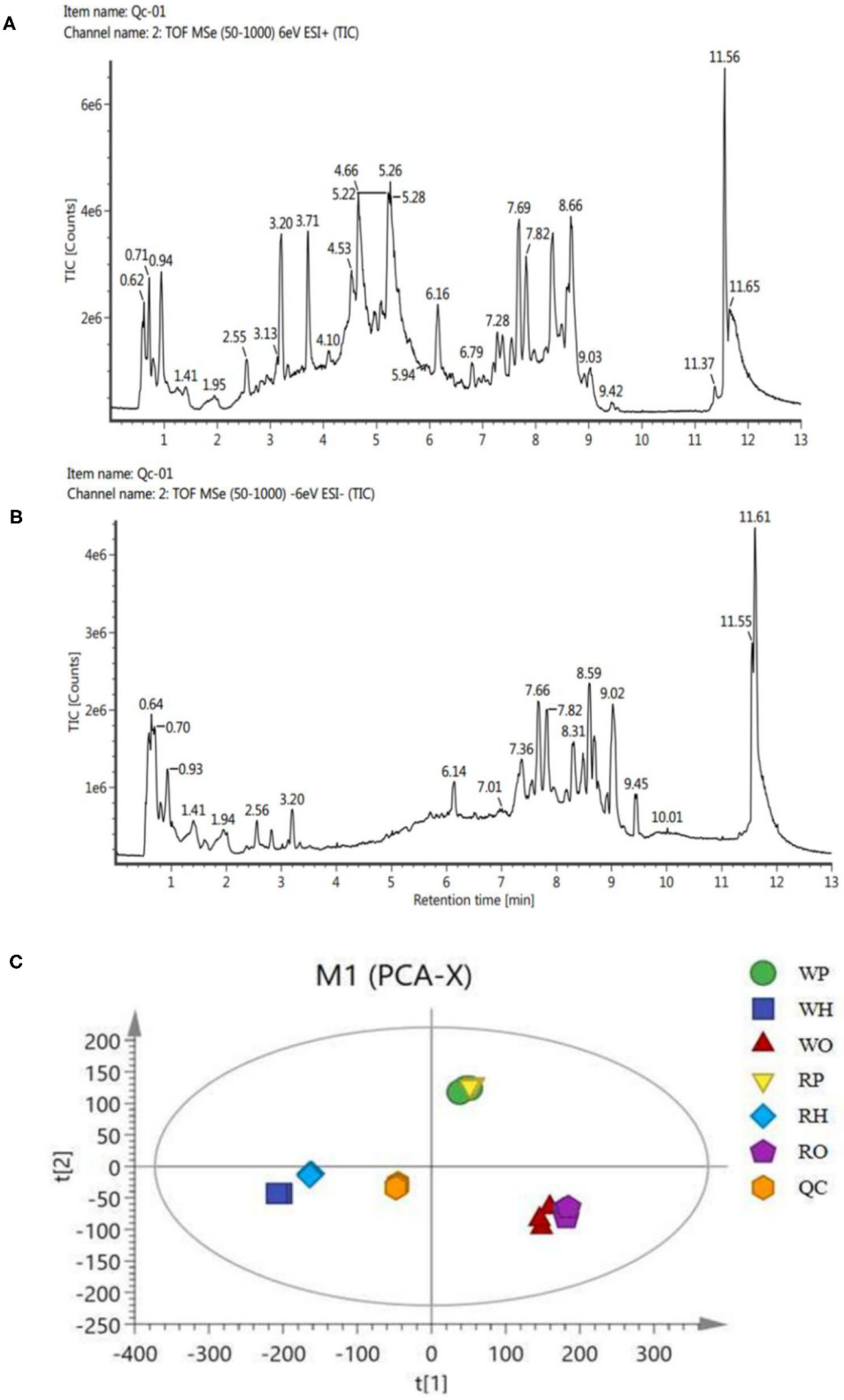

FIGURE 1 | (A) BPI(+) ion flow chart of control samples. **(B)** BPI(-) ion flow chart of control samples. **(C)** PCA plots for all samples.

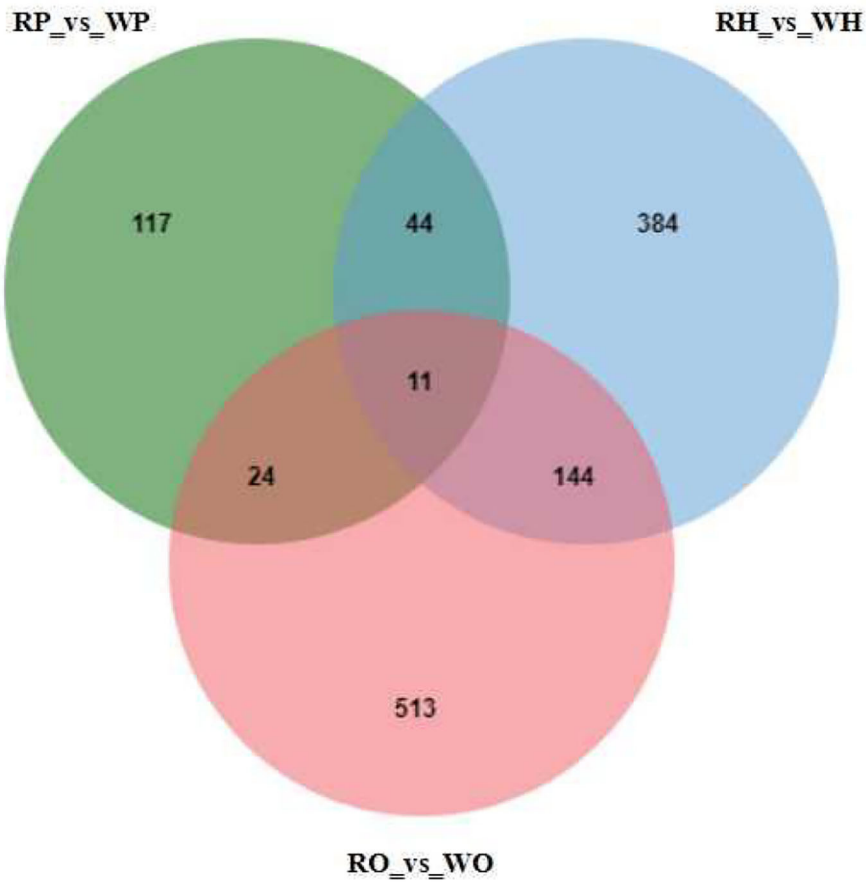

FIGURE 2 | Mutual and specific differential metabolites among the difference analysis of each group.

in different organs will be the main basis for the improvement of reproductive performance of the Zi-geese under red light for 12 h.

Combined Analysis of Metabolites and Transcripts

The results of the combined analysis showed that 33 differential metabolites were closely related to 1,264 transcripts and 400 homologous genes of related enzymes in the hypothalamus of the geese (**Table 2**); In the Zi-geese' pituitaries, 15 differential metabolites were closely related to 163 transcripts and 47 homologous genes of related enzymes (**Table 3**); There were 55 differential metabolites in Zi-geese' ovary, which were closely related to 1,255 transcripts and 360 homologous genes of related enzymes (**Table 4**).

According to the results of differential expression between metabolites and corresponding transcripts (log2 (FC) > 1), 15 pairs of metabolites were further screened in the hypothalamus of Zi-geese. The co-expression of transcripts significantly responded to the changes of light conditions (**Table 5**), and the marker metabolites were nicotinamide adenine dinucleotide, pyruvate, L-glutamic acid, ascorbic acid, 6-phosphate glucose ester, arachidonic acid, prostaglandin E2, glutamic acid γ-Glutamate kinase and hydroquinone. Three pairs of metabolites were further screened out from the pituitary gland of Zi-geese. The co-expression of transcripts significantly responded to the changes of light conditions, and the marker metabolites involved were vanillic acid and adipic acid (**Table 6**). 186 pairs of metabolites were further screened out in the ovary of Zi-geese. The co-expression of transcripts significantly responded to the changes of light conditions, involving marker metabolites including glycine, L-aspartic acid, glutathione, L-serine, ascorbic acid, L-methionine, phosphoenolpyruvate, L-cysteine, oxidized glutathione, 5,10-methylenetetrahydrofolate, nicotinamide, glycolic acid, gluconolactone, sarcosine, nicotinic acid, hypoxanthine Inosine, pyridoxine, thiamine, xanthine, carnosine, guanosine, L-cystine, hydroquinone, testosterone, betaine aldehyde, guanidino acetic acid, gentian acid, cortisol, deoxycytidine, thiamine monohydrate, hydroxyproline, dehydroepiandrosterone, ossifying diol, xanthine nucleoside, pyroglutamine, dihydrozeatin, phenyl glyoxylic acid, deoxyinosine, 2,5-dihydroxybenzaldehyde, canfel Adipic acid α- Linolenic acid, hydroquinone, 6-(α-

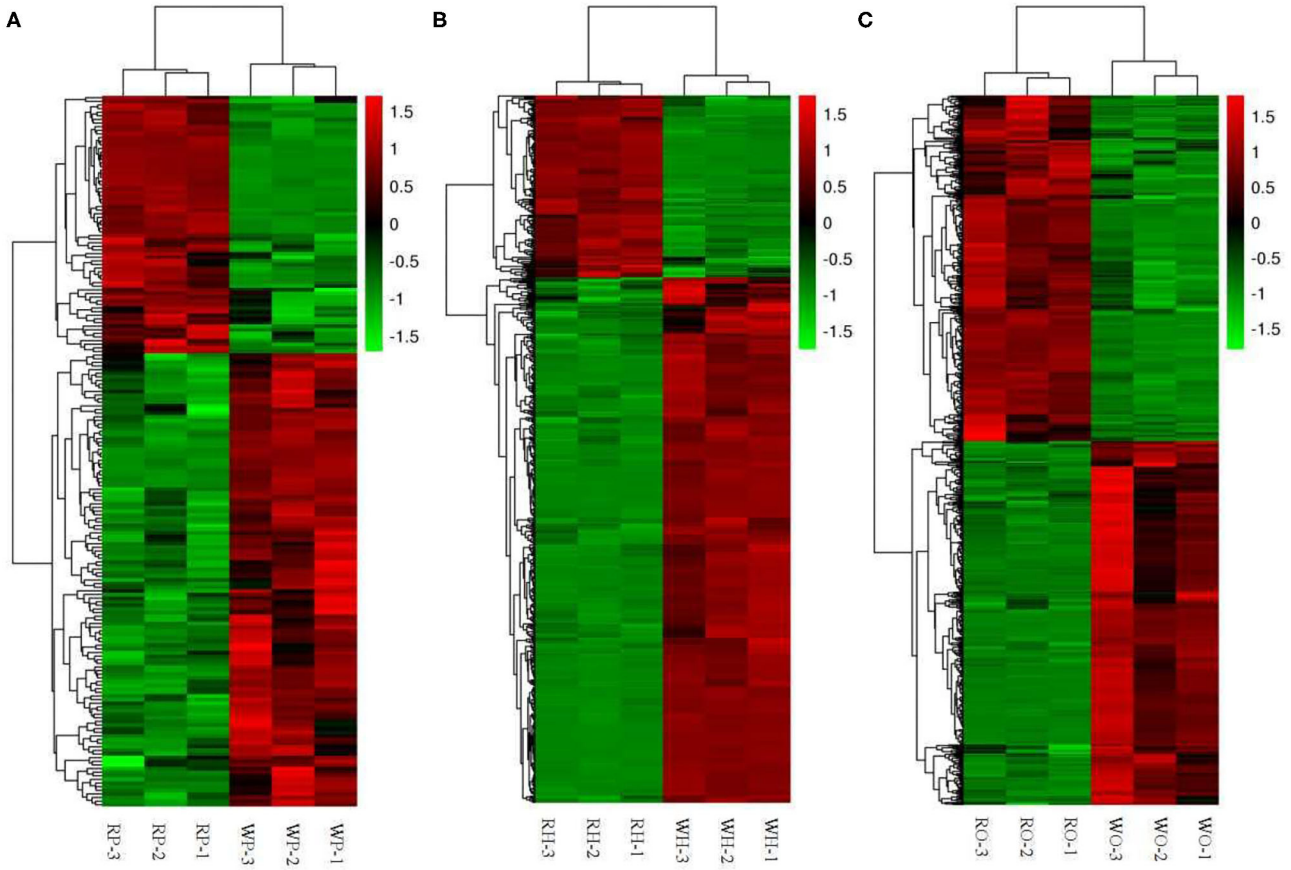

FIGURE 3 | Cluster thermogram of differential metabolites. **(A)** pituitaries, **(B)** hypothalamus, **(C)** ovary.

TABLE 3 | Joint analysis results of pituitary metabolites and transcripts in Zi-geese.

Metabolite ID	Metabolite name	Transcript no.	Homologous genes no.
C00036	Butanone diate	44	12
C00158	Citric acid	15	3
C00490	Itaconic acid	2	1
C00534	Pyridoxamine	9	4
C01561	Ossification diol	8	3
C02166	Leukotriene C4	2	1
C05422	Dehydroascorbic acid	8	3
C05584	Vanilla aldehyde acid	10	2
C05587	3-methoxytyramine	4	2
C06104	Adipic acid	20	6
C06427	Alpha linolenic acid	34	7
C15658	6-(α-D-glucose−1-D-inositol)	4	1
C16702	4 '-o-methyl norbornene	1	1
C16836	1, 4 '-piperidin-1' -carboxylic acid	2	1

D-glucose-1-d-inositol) and 2-oxo-10-methylthiodecanoic acid (**Table 7**).

According to the results of transcripts and metabolites pathway analysis, combined with transcripts and metabolites differential co-expression, there were four metabolic pathways closely relating to light regulation of reproductive performance of the geese has been selected, namely GnRH signaling pathway, prolactin signaling pathway, thyroxine synthesis pathway and ovarian steroid synthesis pathway (**Figure 4**). In the GnRH signaling pathway, arachidonic acid was a typical differential metabolite, and 36 genes and 112 proteins (transcripts) played corresponding roles in the pathway. The typical differential metabolites involved in the prolactin signaling pathway were glucose-6-phosphate and progesterone, and 15 genes and 67 proteins (transcripts) play corresponding roles in the pathway. In the thyroid hormone synthesis pathway, the typical differential metabolites involved in the hypothalamus were glucose-6-phosphate, while the typical differential metabolites involved in the ovary were glutathione and oxidized glutathione. Meanwhile, 20 genes and 77 proteins (transcripts) played the corresponding roles in the pathway. Arachidonic acid and progesterone were the typical differential metabolites in the hypothalamus, and 24 genes and 77 proteins (transcripts) played corresponding roles in the pathway; The typical differential metabolites involved in the ovary were testosterone and deoxyepiandrosterone, and 24 genes and 69 proteins (transcripts) played corresponding roles in the pathway.

TABLE 4 | Joint analysis results of ovarian metabolites and transcripts in Zi-geese.

Metabolite ID	Metabolite name	Transcript no.	Homologous genes no.
C00037	Glycine	56	21
C00049	L-aspartic acid	79	11
C00051	Glutathione	78	21
C00065	L-serine	20	7
C00072	Ascorbic acid	71	5
C00073	L-methionine	54	24
C00074	Phosphoenolpyruvate	16	4
C00097	L-cysteine	93	14
C00120	Biotin	15	5
C00127	Oxidized glutathione	15	4
C00143	5, 10-methylene–tetrahydrofolate	24	7
C00153	Nicotinamide	64	20
C00160	Glycolic acid	5	1
C00198	Gluconolactone	2	1
C00213	Creatine	8	3
C00248	Sulfur symplectic amide	7	1
C00253	Niacin	4	2
C00262	Hypoxanthine	7	3
C00294	Inosine	25	4
C00314	Pyridoxine	9	4
C00366	Uric acid	3	1
C00378	Thiamine	28	5
C00385	Xanthine	9	4
C00386	Carnosine	9	4
C00387	Guanosine	22	2
C00491	l-Cystine	2	1
C00530	Hydroquinone	47	13
C00535	Testosterone	43	14
C00576	Betaine aldehyde	9	2
C00581	Guanidine acetic acid	5	2
C00628	Gentisic acid	2	1
C00735	Cortisol	30	11
C00881	DNA cytidine	24	3
C00954	Indole acetic acid	24	8
C01081	Thiamine single	22	12
C01157	hydroxyproline	14	3
C01227	DHEa	23	11
C01561	Ossification diol	8	3
C01762	Xanthine nucleoside	25	3
C01879	The focal glutamate	43	3
C02029	Dihydrozealin	40	20
C02067	pseudouridine	1	1
C02137	Phenylglyoxylic acid	12	7
C05443	Vitamin D3	3	1
C05512	DNA inosine	7	4
C05582	Homovanillic acid	10	2
C05585	2, 5-dihydroxybenzaldehyde	2	1
C05903	As the alcohol	40	20
C06104	Adipic acid	20	6
C06427	Alpha linolenic acid	34	7
C06672	Vanillic acid	24	13
C15572	Guaiacol	1	1
C15658	6-(α-D-glucose−1-D-inositol)	4	1
C16285	Thiobenzamide	1	1
C17232	2-oxo-10-methyl thio-decanoic acid	12	7

TABLE 5 | Results of differential co-expression of hypothalamic metabolites and related transcripts in Zi-geese.

Metabolite_Transcript ID	Type	log2(FC)
C00003_TRINITY_DN136565_c0_g1	Metabolics	1.08
C00003_TRINITY_DN136565_c0_g1	mRNA	−1.79
C00003_TRINITY_DN127160_c0_g1	Metabolics	1.08
C00003_TRINITY_DN127160_c0_g1	mRNA	1.09
C00003_TRINITY_DN119684_c1_g3	Metabolics	1.08
C00003_TRINITY_DN119684_c1_g3	mRNA	−1.42
C00003_TRINITY_DN121542_c0_g4	Metabolics	1.08
C00003_TRINITY_DN121542_c0_g4	mRNA	1.22
C00003_TRINITY_DN134625_c3_g2	Metabolics	1.08
C00003_TRINITY_DN134625_c3_g2	mRNA	−2.14
C00022_TRINITY_DN119684_c1_g3	Metabolics	−1.26
C00022_TRINITY_DN119684_c1_g3	mRNA	−1.42
C00022_TRINITY_DN136565_c0_g1	Metabolics	−1.26
C00022_TRINITY_DN136565_c0_g1	mRNA	−1.79
C00025_TRINITY_DN129572_c3_g1	Metabolics	1.34
C00025_TRINITY_DN129572_c3_g1	mRNA	−2.56
C00072_TRINITY_DN133392_c0_g5	Metabolics	6.85
C00072_TRINITY_DN133392_c0_g5	mRNA	−4.66
C00092_TRINITY_DN126050_c0_g3	Metabolics	1.36
C00092_TRINITY_DN126050_c0_g3	mRNA	−2.15
C00219_TRINITY_DN122928_c1_g1	Metabolics	−1.23
C00219_TRINITY_DN122928_c1_g1	mRNA	−1.16
C00584_TRINITY_DN134625_c3_g2	Metabolics	−1.43
C00584_TRINITY_DN134625_c3_g2	mRNA	−2.14
C00669_TRINITY_DN113290_c0_g1	Metabolics	1.74
C00669_TRINITY_DN113290_c0_g1	mRNA	1.44
C15603_TRINITY_DN121542_c0_g4	Metabolics	−1.00
C15603_TRINITY_DN121542_c0_g4	mRNA	1.22

DISCUSSION

Currently, the widely applied metabonomics research methods include Nuclear Magnetic Resonance (NMR), GC-TOF/MS, and UPLCQ-TOF/MS (14, 15). In comparison, nuclear magnetic resonance (NMR) technology is widely used for its advantages of non-destructive, absolute quantitative, and outstanding repeatability (16). However, meanwhile, its disadvantages are very prominent, such as low detection sensitivity, unable to detect extremely trace and low concentration substances;

TABLE 6 | Results of differential co-expression of pituitary metabolites and related transcripts in Zi-geese.

Metabolite_Transcript ID	Type	log2(FC)
C05584_TRINITY_DN136141_c0_g1	Metabolics	−1.07
C05584_TRINITY_DN136141_c0_g1	mRNA	−4.10
C05584_TRINITY_DN130821_c0_g3	Metabolics	−1.07
C05584_TRINITY_DN130821_c0_g3	mRNA	−4.99
C06104_TRINITY_DN139541_c0_g1	Metabolics	−2.85
C06104_TRINITY_DN139541_c0_g1	mRNA	−1.40

Although GC-TOF/MS technology can identify more complex metabolites with low cost, the pretreatment is complicated which increases the possibility of errors (17); In recent years, UPLC-Q-TOF/MS technology has been widely used in biomedicine, food science, agricultural science and other research fields by its properties of "separation capability", "reliability", and "sensitivity" (18). Through this experiment, UPLC-Q-TOF/MS technology was used to study the metabonomics of the hypothalamus, pituitary, and ovary of Zi-geese under the different light conditions. 18 samples were analyzed, and a quality control sample (QC) was inserted into every 6 samples for quality control to investigate the repeatability of the whole analysis procedure. According to the ion flow diagram of the base peak under the positive and negative ion mode of the quality control sample, the chromatographic peaks were uniform, large in number, good in shape, without oversaturation, tailing, and other adverse phenomena. At the same time, the PCA examination of the test results also showed that all the points of the quality control sample (QC) were closely clustered, which indicated that the whole experimental process has outstanding repeatability and no abnormal data. The results showed that the quality of the test sample was qualified, and the analysis technology was practical and effective. Through the transcriptomic analysis, 1,481 differential metabolites were screened out, among which 583 were screened out from the hypothalamus of Zi-geese and 384 were unique; 196 differential metabolites and 117 unique differential metabolites were screened from the pituitaries of Zi-geese; 692 differential metabolites and 513 unique differential metabolites were screened from the ovary of the geese. The results showed that the changes in light conditions could significantly affect the metabolic processes related to the reproductive performance of Zi-geese.

To further understand the inner mechanism of light regulation on reproductive performance of Zi-geese, the transcriptomics and metabonomics combined analysis technology has been used to analyze the differentially expressed genes and differentially accumulated metabolite information of the test samples for gene-gene, gene-metabolite, metabolite-metabolite "co-expression" analysis, to identify the key metabolic pathway and figure out the main regulatory factors and structural genes. The regulation mechanism was analyzed and verified by physiological, biochemical, genetic, and molecular biology methods. Through transcriptomic and metabonomic analysis,

TABLE 7 | Results of differential co-expression of ovarian metabolites and related transcripts in Zi-geese.

Metabolite_Transcript ID	Type	log2(FC)
C00037_TRINITY_DN129582_c7_g1	Metabolics	−1.85
C00037_TRINITY_DN129582_c7_g1	mRNA	1.13
C00037_TRINITY_DN137486_c6_g2	Metabolics	−1.85
C00037_TRINITY_DN137486_c6_g2	mRNA	1.08
C00037_TRINITY_DN111806_c0_g1	Metabolics	−1.85
C00037_TRINITY_DN111806_c0_g1	mRNA	−8.97
C00037_TRINITY_DN118954_c0_g3	Metabolics	−1.85
C00037_TRINITY_DN118954_c0_g3	mRNA	4.58
C00037_TRINITY_DN125224_c0_g1	Metabolics	−1.85
C00037_TRINITY_DN125224_c0_g1	mRNA	2.14
C00037_TRINITY_DN123719_c0_g1	Metabolics	−1.85
C00037_TRINITY_DN123719_c0_g1	mRNA	6.49
C00037_TRINITY_DN124585_c0_g1	Metabolics	−1.85
C00037_TRINITY_DN124585_c0_g1	mRNA	1.44
C00037_TRINITY_DN118954_c0_g1	Metabolics	−1.85
C00037_TRINITY_DN118954_c0_g1	mRNA	3.22
C00037_TRINITY_DN68105_c0_g1	Metabolics	−1.85
C00037_TRINITY_DN68105_c0_g1	mRNA	2.85
C00037_TRINITY_DN126075_c1_g1	Metabolics	−1.85
C00037_TRINITY_DN126075_c1_g1	mRNA	1.67
C00049_TRINITY_DN122295_c3_g1	Metabolics	−1.21
C00049_TRINITY_DN122295_c3_g1	mRNA	1.86
C00049_TRINITY_DN124466_c2_g1	Metabolics	−1.21
C00049_TRINITY_DN124466_c2_g1	mRNA	3.28
C00049_TRINITY_DN133015_c5_g3	Metabolics	−1.21
C00049_TRINITY_DN133015_c5_g3	mRNA	−1.68
C00049_TRINITY_DN136189_c6_g8	Metabolics	−1.21
C00049_TRINITY_DN136189_c6_g8	mRNA	8.87
C00049_TRINITY_DN126078_c0_g2	Metabolics	−1.21
C00049_TRINITY_DN126078_c0_g2	mRNA	1.81
C00049_TRINITY_DN141027_c3_g1	Metabolics	−1.21
C00049_TRINITY_DN141027_c3_g1	mRNA	1.73
C00049_TRINITY_DN120188_c0_g1	Metabolics	−1.21
C00049_TRINITY_DN120188_c0_g1	mRNA	−1.26
C00049_TRINITY_DN136146_c4_g1	Metabolics	−1.21
C00049_TRINITY_DN136146_c4_g1	mRNA	1.12
C00049_TRINITY_DN133015_c5_g1	Metabolics	−1.21
C00049_TRINITY_DN133015_c5_g1	mRNA	−1.53
C00049_TRINITY_DN128440_c1_g1	Metabolics	−1.21
C00049_TRINITY_DN128440_c1_g1	mRNA	2.73
C00049_TRINITY_DN132073_c2_g3	Metabolics	−1.21
C00049_TRINITY_DN132073_c2_g3	mRNA	1.14
C00049_TRINITY_DN126544_c1_g1	Metabolics	−1.21
C00049_TRINITY_DN126544_c1_g1	mRNA	1.74
C00051_TRINITY_DN128264_c3_g1	Metabolics	−3.08
C00051_TRINITY_DN128264_c3_g1	mRNA	1.71
C00051_TRINITY_DN126607_c2_g2	Metabolics	−3.08
C00051_TRINITY_DN126607_c2_g2	mRNA	1.35
C00051_TRINITY_DN126075_c1_g1	Metabolics	−3.08

(Continued)

TABLE 7 | Continued

Metabolite_Transcript ID	Type	log2(FC)
C00051_TRINITY_DN126075_c1_g1	mRNA	1.67
C00051_TRINITY_DN137420_c3_g2	Metabolics	−3.08
C00051_TRINITY_DN137420_c3_g2	mRNA	−1.65
C00065_TRINITY_DN68105_c0_g1	Metabolics	−2.79
C00065_TRINITY_DN68105_c0_g1	mRNA	2.85
C00065_TRINITY_DN131715_c0_g1	Metabolics	−2.79
C00065_TRINITY_DN131715_c0_g1	mRNA	3.69
C00065_TRINITY_DN141180_c5_g1	Metabolics	−2.79
C00065_TRINITY_DN141180_c5_g1	mRNA	2.39
C00065_TRINITY_DN119556_c3_g3	Metabolics	−2.79
C00065_TRINITY_DN119556_c3_g3	mRNA	−1.19
C00072_TRINITY_DN130784_c0_g1	Metabolics	4.58
C00072_TRINITY_DN130784_c0_g1	mRNA	8.62
C00072_TRINITY_DN133392_c0_g5	Metabolics	4.58
C00072_TRINITY_DN133392_c0_g5	mRNA	−5.36
C00072_TRINITY_DN122008_c2_g1	Metabolics	4.58
C00072_TRINITY_DN122008_c2_g1	mRNA	−2.02
C00072_TRINITY_DN122360_c0_g1	Metabolics	4.58
C00072_TRINITY_DN122360_c0_g1	mRNA	−2.71
C00072_TRINITY_DN123314_c3_g1	Metabolics	4.58
C00072_TRINITY_DN123314_c3_g1	mRNA	1.28
C00072_TRINITY_DN133392_c0_g8	Metabolics	4.58
C00072_TRINITY_DN133392_c0_g8	mRNA	−10.88
C00072_TRINITY_DN120532_c0_g1	Metabolics	4.58
C00072_TRINITY_DN120532_c0_g1	mRNA	−4.28
C00072_TRINITY_DN112795_c0_g1	Metabolics	4.58
C00072_TRINITY_DN112795_c0_g1	mRNA	6.68
C00073_TRINITY_DN117575_c4_g8	Metabolics	−1.50
C00073_TRINITY_DN117575_c4_g8	mRNA	−4.78
C00073_TRINITY_DN133322_c1_g1	Metabolics	−1.50
C00073_TRINITY_DN133322_c1_g1	mRNA	1.90
C00073_TRINITY_DN117575_c4_g1	Metabolics	−1.50
C00073_TRINITY_DN117575_c4_g1	mRNA	−5.29
C00073_TRINITY_DN125846_c0_g1	Metabolics	−1.50
C00073_TRINITY_DN125846_c0_g1	mRNA	8.65
C00073_TRINITY_DN128420_c3_g1	Metabolics	−1.50
C00073_TRINITY_DN128420_c3_g1	mRNA	1.37
C00074_TRINITY_DN135685_c1_g2	Metabolics	−3.56
C00074_TRINITY_DN135685_c1_g2	mRNA	2.39
C00074_TRINITY_DN135685_c1_g1	Metabolics	−3.56
C00074_TRINITY_DN135685_c1_g1	mRNA	8.43
C00074_TRINITY_DN131703_c0_g1	Metabolics	−3.56
C00074_TRINITY_DN131703_c0_g1	mRNA	6.69
C00074_TRINITY_DN132519_c0_g3	Metabolics	−3.56
C00074_TRINITY_DN132519_c0_g3	mRNA	3.75
C00074_TRINITY_DN138024_c0_g1	Metabolics	−3.56
C00074_TRINITY_DN138024_c0_g1	mRNA	−1.54
C00097_TRINITY_DN139025_c5_g1	Metabolics	1.79
C00097_TRINITY_DN139025_c5_g1	mRNA	−2.28
C00097_TRINITY_DN141059_c4_g2	Metabolics	1.79

(Continued)

TABLE 7 | Continued

Metabolite_Transcript ID	Type	log2(FC)
C00097_TRINITY_DN141059_c4_g2	mRNA	−2.68
C00097_TRINITY_DN125224_c0_g1	Metabolics	1.79
C00097_TRINITY_DN125224_c0_g1	mRNA	2.14
C00097_TRINITY_DN122396_c1_g2	Metabolics	1.79
C00097_TRINITY_DN122396_c1_g2	mRNA	2.75
C00097_TRINITY_DN139749_c0_g1	Metabolics	1.79
C00097_TRINITY_DN139749_c0_g1	mRNA	1.50
C00127_TRINITY_DN126607_c2_g2	Metabolics	−9.13
C00127_TRINITY_DN126607_c2_g2	mRNA	1.35
C00143_TRINITY_DN124585_c0_g1	Metabolics	−1.03
C00143_TRINITY_DN124585_c0_g1	mRNA	1.44
C00143_TRINITY_DN115258_c0_g1	Metabolics	−1.03
C00143_TRINITY_DN115258_c0_g1	mRNA	1.67
C00143_TRINITY_DN111951_c0_g2	Metabolics	−1.03
C00143_TRINITY_DN111951_c0_g2	mRNA	1.57
C00143_TRINITY_DN68105_c0_g1	Metabolics	−1.03
C0043_TRINITY_DN68105_c0_g1	mRNA	2.85
C00143_TRINITY_DN111951_c0_g1	Metabolics	−1.03
C00143_TRINITY_DN111951_c0_g1	mRNA	−1.73
C00153_TRINITY_DN139949_c1_g2	Metabolics	−3.73
C00153_TRINITY_DN139949_c1_g2	mRNA	−2.04
C00153_TRINITY_DN125347_c0_g1	Metabolics	−3.73
C00153_TRINITY_DN125347_c0_g1	mRNA	1.79
C00153_TRINITY_DN130743_c0_g1	Metabolics	−3.73
C00153_TRINITY_DN130743_c0_g1	mRNA	2.43
C00153_TRINITY_DN116220_c0_g1	Metabolics	−3.73
C00153_TRINITY_DN116220_c0_g1	mRNA	−1.26
C00153_TRINITY_DN133137_c0_g1	Metabolics	−3.73
C00153_TRINITY_DN133137_c0_g1	mRNA	3.16
C00160_TRINITY_DN136176_c0_g1	Metabolics	1.04
C00160_TRINITY_DN136176_c0_g1	mRNA	1.06
C00160_TRINITY_DN110820_c0_g2	Metabolics	1.04
C00160_TRINITY_DN110820_c0_g2	mRNA	6.89
C00198_TRINITY_DN123462_c0_g2	Metabolics	−9.71
C00198_TRINITY_DN123462_c0_g2	mRNA	5.29
C00198_TRINITY_DN127850_c1_g1	Metabolics	−9.71
C00198_TRINITY_DN127850_c1_g1	mRNA	5.47
C00213_TRINITY_DN111806_c0_g1	Metabolics	−1.40
C00213_TRINITY_DN111806_c0_g1	mRNA	−8.97
C00213_TRINITY_DN111951_c0_g1	Metabolics	−1.40
C00213_TRINITY_DN111951_c0_g1	mRNA	−1.73
C00213_TRINITY_DN111951_c0_g2	Metabolics	−1.40
C00213_TRINITY_DN111951_c0_g2	mRNA	1.57
C00253_TRINITY_DN130743_c0_g1	Metabolics	6.06
C00253_TRINITY_DN130743_c0_g1	mRNA	2.43
C00262_TRINITY_DN130743_c0_g1	Metabolics	−1.95
C00262_TRINITY_DN130743_c0_g1	mRNA	2.43
C00262_TRINITY_DN125813_c1_g5	Metabolics	−1.95
C00262_TRINITY_DN125813_c1_g5	mRNA	5.81
C00262_TRINITY_DN129874_c1_g1	Metabolics	−1.95
C00262_TRINITY_DN129874_c1_g1	mRNA	5.01

(Continued)

TABLE 7 | Continued

Metabolite_Transcript ID	Type	log2(FC)
C00294_TRINITY_DN130743_c0_g1	Metabolics	−2.63
C00294_TRINITY_DN130743_c0_g1	mRNA	2.43
C00294_TRINITY_DN115131_c0_g1	Metabolics	−2.63
C00294_TRINITY_DN115131_c0_g1	mRNA	−1.78
C00294_TRINITY_DN137643_c0_g1	Metabolics	−2.63
C00294_TRINITY_DN137643_c0_g1	mRNA	1.24
C00294_TRINITY_DN135736_c0_g1	Metabolics	−2.63
C00294_TRINITY_DN135736_c0_g1	mRNA	4.02
C00314_TRINITY_DN141165_c7_g3	Metabolics	1.15
C00314_TRINITY_DN141165_c7_g3	mRNA	3.57
C00314_TRINITY_DN141165_c7_g1	Metabolics	1.15
C00314_TRINITY_DN141165_c7_g1	mRNA	1.63
C00378_TRINITY_DN117569_c9_g1	Metabolics	4.34
C00378_TRINITY_DN117569_c9_g1	mRNA	10.38
C00378_TRINITY_DN127457_c1_g1	Metabolics	4.34
C00378_TRINITY_DN127457_c1_g1	mRNA	1.39
C00378_TRINITY_DN127457_c1_g3	Metabolics	4.34
C00378_TRINITY_DN127457_c1_g3	mRNA	1.75
C00378_TRINITY_DN134236_c3_g1	Metabolics	4.34
C00378_TRINITY_DN134236_c3_g1	mRNA	1.13
C00385_TRINITY_DN130743_c0_g1	Metabolics	1.51
C00385_TRINITY_DN130743_c0_g1	mRNA	2.43
C00385_TRINITY_DN135376_c2_g1	Metabolics	1.51
C00385_TRINITY_DN135376_c2_g1	mRNA	1.52
C00386_TRINITY_DN139951_c1_g1	Metabolics	0.11
C00386_TRINITY_DN139951_c1_g1	mRNA	3.02
C00386_TRINITY_DN139951_c1_g4	Metabolics	1.11
C00386_TRINITY_DN139951_c1_g4	mRNA	3.12
C00387_TRINITY_DN135736_c0_g1	Metabolics	−1.83
C00387_TRINITY_DN135736_c0_g1	mRNA	4.02
C00387_TRINITY_DN130743_c0_g1	Metabolics	−1.83
C00387_TRINITY_DN130743_c0_g1	mRNA	2.43
C00387_TRINITY_DN137643_c0_g1	Metabolics	−1.83
C00387_TRINITY_DN137643_c0_g1	mRNA	1.24
C00387_TRINITY_DN115131_c0_g1	Metabolics	−1.83
C00387_TRINITY_DN115131_c0_g1	mRNA	−1.78
C00491_TRINITY_DN122396_c1_g2	Metabolics	2.80
C00491_TRINITY_DN122396_c1_g2	mRNA	2.75
C00530_TRINITY_DN138536_c1_g3	Metabolics	−7.99
C00530_TRINITY_DN138536_c1_g3	mRNA	−1.47
C00530_TRINITY_DN132747_c2_g3	Metabolics	−7.99
C00530_TRINITY_DN132747_c2_g3	mRNA	3.25
C00530_TRINITY_DN133363_c0_g1	Metabolics	−7.99
C00530_TRINITY_DN133363_c0_g1	mRNA	−2.00
C00530_TRINITY_DN137025_c2_g1	Metabolics	−7.99
C00530_TRINITY_DN137025_c2_g1	mRNA	−1.01
C00530_TRINITY_DN93937_c0_g2	Metabolics	−7.99
C00530_TRINITY_DN93937_c0_g2	mRNA	3.09
C00535_TRINITY_DN120919_c7_g2	Metabolics	1.04
C00535_TRINITY_DN120919_c7_g2	mRNA	7.52
C00535_TRINITY_DN129814_c0_g1	Metabolics	1.04
C00535_TRINITY_DN129814_c0_g1	mRNA	1.55
C00535_TRINITY_DN119253_c3_g1	Metabolics	1.04
C00535_TRINITY_DN119253_c3_g1	mRNA	5.13
C00535_TRINITY_DN129783_c0_g2	Metabolics	1.04
C00535_TRINITY_DN129783_c0_g2	mRNA	3.35
C00535_TRINITY_DN130231_c2_g1	Metabolics	1.04
C00535_TRINITY_DN130231_c2_g1	mRNA	6.55
C00535_TRINITY_DN134262_c1_g1	Metabolics	1.04
C00535_TRINITY_DN134262_c1_g1	mRNA	1.93
C00535_TRINITY_DN129783_c0_g3	Metabolics	1.04
C00535_TRINITY_DN129783_c0_g3	mRNA	2.51
C00535_TRINITY_DN134262_c0_g2	Metabolics	1.04
C00535_TRINITY_DN134262_c0_g2	mRNA	2.60
C00535_TRINITY_DN134262_c1_g2	Metabolics	1.04
C00535_TRINITY_DN134262_c1_g2	mRNA	2.24
C00535_TRINITY_DN129528_c2_g1	Metabolics	1.04
C00535_TRINITY_DN129528_c2_g1	mRNA	−3.03
C00535_TRINITY_DN133519_c0_g1	Metabolics	1.04
C00535_TRINITY_DN133519_c0_g1	mRNA	6.67
C00535_TRINITY_DN136732_c0_g3	Metabolics	1.04
C00535_TRINITY_DN136732_c0_g3	mRNA	2.44
C00535_TRINITY_DN120617_c0_g2	Metabolics	1.04
C00535_TRINITY_DN120617_c0_g2	mRNA	2.67
C00535_TRINITY_DN129783_c0_g1	Metabolics	1.04
C00535_TRINITY_DN129783_c0_g1	mRNA	2.23
C00576_TRINITY_DN126727_c0_g2	Metabolics	1.04
C00576_TRINITY_DN126727_c0_g2	mRNA	2.24
C00576_TRINITY_DN117587_c2_g1	Metabolics	1.04
C00576_TRINITY_DN117587_c2_g1	mRNA	1.90
C00576_TRINITY_DN126727_c0_g1	Metabolics	1.04
C00576_TRINITY_DN126727_c0_g1	mRNA	7.77
C00581_TRINITY_DN137240_c0_g1	Metabolics	−7.01
C00581_TRINITY_DN137240_c0_g1	mRNA	1.78
C00581_TRINITY_DN118954_c0_g1	Metabolics	−7.01
C00581_TRINITY_DN118954_c0_g1	mRNA	3.22
C00581_TRINITY_DN118954_c0_g3	Metabolics	−7.01
C00581_TRINITY_DN118954_c0_g3	mRNA	4.58
C00581_TRINITY_DN137240_c0_g2	Metabolics	−7.01
C00581_TRINITY_DN137240_c0_g2	mRNA	2.17
C00628_TRINITY_DN128233_c1_g1	Metabolics	−8.05
C00628_TRINITY_DN128233_c1_g1	mRNA	3.13
C00628_TRINITY_DN137617_c1_g1	Metabolics	−8.05
C00628_TRINITY_DN137617_c1_g1	mRNA	2.75
C00735_TRINITY_DN137011_c1_g3	Metabolics	−4.23
C00735_TRINITY_DN137011_c1_g3	mRNA	−10.07
C00735_TRINITY_DN136353_c1_g1	Metabolics	−4.23
C00735_TRINITY_DN136353_c1_g1	mRNA	3.71
C00735_TRINITY_DN139698_c2_g1	Metabolics	−4.23
C00735_TRINITY_DN139698_c2_g1	mRNA	−6.86
C00735_TRINITY_DN124132_c0_g1	Metabolics	−4.23
C00735_TRINITY_DN124132_c0_g1	mRNA	1.46

(Continued)

TABLE 7 | Continued

Metabolite_Transcript ID	Type	log2(FC)
C00735_TRINITY_DN121491_c0_g1	Metabolics	−4.23
C00735_TRINITY_DN121491_c0_g1	mRNA	−1.17
C00735_TRINITY_DN132364_c1_g1	Metabolics	−4.23
C00735_TRINITY_DN132364_c1_g1	mRNA	−9.68
C00735_TRINITY_DN129390_c5_g2	Metabolics	−4.23
C00735_TRINITY_DN129390_c5_g2	mRNA	−6.67
C00735_TRINITY_DN135404_c0_g1	Metabolics	−4.23
C00735_TRINITY_DN135404_c0_g1	mRNA	6.51
C00881_TRINITY_DN115131_c0_g1	Metabolics	−1.76
C00881_TRINITY_DN115131_c0_g1	mRNA	−1.78
C00881_TRINITY_DN137643_c0_g1	Metabolics	−1.76
C00881_TRINITY_DN137643_c0_g1	mRNA	1.24
C00881_TRINITY_DN135736_c0_g1	Metabolics	−1.76
C00881_TRINITY_DN135736_c0_g1	mRNA	4.02
C01081_TRINITY_DN127457_c1_g1	Metabolics	1.94
C01081_TRINITY_DN127457_c1_g1	mRNA	1.39
C00881_TRINITY_DN126571_c1_g1	Metabolics	−1.76
C00881_TRINITY_DN126571_c1_g1	mRNA	2.59
C01081_TRINITY_DN134733_c0_g2	Metabolics	1.94
C01081_TRINITY_DN134733_c0_g2	mRNA	1.01
C01081_TRINITY_DN127457_c1_g3	Metabolics	1.94
C01081_TRINITY_DN127457_c1_g3	mRNA	1.75
C01081_TRINITY_DN134236_c3_g1	Metabolics	1.94
C01081_TRINITY_DN134236_c3_g1	mRNA	1.13
C01157_TRINITY_DN138437_c1_g1	Metabolics	−1.50
C01157_TRINITY_DN138437_c1_g1	mRNA	5.49
C01157_TRINITY_DN138437_c1_g2	Metabolics	−1.50
C01157_TRINITY_DN138437_c1_g2	mRNA	10.32
C01227_TRINITY_DN133519_c0_g1	Metabolics	−1.11
C01227_TRINITY_DN133519_c0_g1	mRNA	6.67
C01227_TRINITY_DN129783_c0_g3	Metabolics	−1.11
C01227_TRINITY_DN129783_c0_g3	mRNA	2.51
C01227_TRINITY_DN134262_c0_g2	Metabolics	−1.11
C01227_TRINITY_DN134262_c0_g2	mRNA	2.60
C01227_TRINITY_DN134262_c1_g1	Metabolics	−1.11
C01227_TRINITY_DN134262_c1_g1	mRNA	1.93
C01227_TRINITY_DN119253_c3_g1	Metabolics	−1.11
C01227_TRINITY_DN119253_c3_g1	mRNA	5.13
C01227_TRINITY_DN129783_c0_g2	Metabolics	−1.11
C01227_TRINITY_DN129783_c0_g2	mRNA	3.35
C01227_TRINITY_DN134262_c1_g2	Metabolics	−1.11
C01227_TRINITY_DN134262_c1_g2	mRNA	2.24
C01227_TRINITY_DN129528_c2_g1	Metabolics	−1.11
C01227_TRINITY_DN129528_c2_g1	mRNA	−3.03
C01227_TRINITY_DN129783_c0_g1	Metabolics	−1.11
C01227_TRINITY_DN129783_c0_g1	mRNA	2.23
C01227_TRINITY_DN130965_c1_g2	Metabolics	−1.11
C01227_TRINITY_DN130965_c1_g2	mRNA	2.69
C01561_TRINITY_DN122647_c3_g2	Metabolics	1.16
C01561_TRINITY_DN122647_c3_g2	mRNA	10.78
C01561_TRINITY_DN122647_c3_g1	Metabolics	1.16
C01561_TRINITY_DN122647_c3_g1	mRNA	4.93
C01762_TRINITY_DN137643_c0_g1	Metabolics	1.89
C01762_TRINITY_DN137643_c0_g1	mRNA	1.24
C01762_TRINITY_DN135736_c0_g1	Metabolics	1.89
C01762_TRINITY_DN135736_c0_g1	mRNA	4.02
C01762_TRINITY_DN130743_c0_g1	Metabolics	1.89
C01762_TRINITY_DN130743_c0_g1	mRNA	2.43
C01762_TRINITY_DN115131_c0_g1	Metabolics	1.89
C01762_TRINITY_DN115131_c0_g1	mRNA	−1.78
C01879_TRINITY_DN139025_c5_g1	Metabolics	−1.23
C01879_TRINITY_DN139025_c5_g1	mRNA	−2.28
C02029_TRINITY_DN111850_c0_g1	Metabolics	4.18
C02029_TRINITY_DN111850_c0_g1	mRNA	−1.15
C02029_TRINITY_DN128988_c2_g1	Metabolics	4.18
C02029_TRINITY_DN128988_c2_g1	mRNA	1.02
C02137_TRINITY_DN121491_c0_g1	Metabolics	−3.99
C02137_TRINITY_DN121491_c0_g1	mRNA	−1.17
C02137_TRINITY_DN124132_c0_g1	Metabolics	−3.99
C02137_TRINITY_DN124132_c0_g1	mRNA	1.46
C02137_TRINITY_DN135404_c0_g1	Metabolics	−3.99
C02137_TRINITY_DN135404_c0_g1	mRNA	6.51
C05512_TRINITY_DN129874_c1_g1	Metabolics	−2.83
C05512_TRINITY_DN129874_c1_g1	mRNA	5.01
C05512_TRINITY_DN130743_c0_g1	Metabolics	−2.83
C05512_TRINITY_DN130743_c0_g1	mRNA	2.43
C05512_TRINITY_DN125813_c1_g5	Metabolics	−2.83
C05512_TRINITY_DN125813_c1_g5	mRNA	5.81
C05585_TRINITY_DN128233_c1_g1	Metabolics	−5.55
C05585_TRINITY_DN128233_c1_g1	mRNA	3.13
C05585_TRINITY_DN137617_c1_g1	Metabolics	−5.55
C05585_TRINITY_DN137617_c1_g1	mRNA	2.75
C05903_TRINITY_DN111850_c0_g1	Metabolics	1.66
C05903_TRINITY_DN111850_c0_g1	mRNA	−1.15
C05903_TRINITY_DN128988_c2_g1	Metabolics	1.66
C05903_TRINITY_DN128988_c2_g1	mRNA	1.02
C06104_TRINITY_DN139541_c0_g1	Metabolics	−1.12
C06104_TRINITY_DN139541_c0_g1	mRNA	1.53
C06427_TRINITY_DN127483_c1_g1	Metabolics	−2.03
C06427_TRINITY_DN127483_c1_g1	mRNA	2.28
C06427_TRINITY_DN139240_c0_g1	Metabolics	−2.03
C06427_TRINITY_DN139240_c0_g1	mRNA	2.22
C06427_TRINITY_DN119196_c1_g1	Metabolics	−2.03
C06427_TRINITY_DN119196_c1_g1	mRNA	1.04
C06427_TRINITY_DN122469_c1_g1	Metabolics	−2.03
C06427_TRINITY_DN122469_c1_g1	mRNA	1.18
C06427_TRINITY_DN112767_c0_g3	Metabolics	−2.03
C06427_TRINITY_DN112767_c0_g3	mRNA	2.81
C06427_TRINITY_DN137047_c2_g1	Metabolics	−2.03
C06427_TRINITY_DN137047_c2_g1	mRNA	−3.40
C06427_TRINITY_DN110387_c0_g1	Metabolics	−2.03
C06427_TRINITY_DN110387_c0_g1	mRNA	−2.68

(Continued)

TABLE 7 | Continued

Metabolite_Transcript ID	Type	log2(FC)
C06427_TRINITY_DN119122_c0_g1	Metabolics	−2.03
C06427_TRINITY_DN119122_c0_g1	mRNA	1.97
C15603_TRINITY_DN138437_c1_g1	Metabolics	−7.99
C15603_TRINITY_DN138437_c1_g1	mRNA	5.49
C15603_TRINITY_DN138437_c1_g2	Metabolics	−7.99
C15603_TRINITY_DN138437_c1_g2	mRNA	10.32
C15603_TRINITY_DN123475_c1_g3	Metabolics	−7.99
C15603_TRINITY_DN123475_c1_g3	mRNA	1.15
C15603_TRINITY_DN121542_c0_g4	Metabolics	−7.99
C15603_TRINITY_DN121542_c0_g4	mRNA	3.90
C15658_TRINITY_DN139332_c5_g2	Metabolics	4.40
C15658_TRINITY_DN139332_c5_g2	mRNA	3.29
C17232_TRINITY_DN135404_c0_g1	Metabolics	1.77
C17232_TRINITY_DN135404_c0_g1	mRNA	6.51
C17232_TRINITY_DN121491_c0_g1	Metabolics	1.77
C17232_TRINITY_DN121491_c0_g1	mRNA	−1.17
C17232_TRINITY_DN124132_c0_g1	Metabolics	1.77
C17232_TRINITY_DN124132_c0_g1	mRNA	1.46

204 pairs of metabolites were found. The co-expression of transcripts identified four metabolic pathways closely related to the reproductive performance of Zi-geese, which pointed out the direction and goal for understanding the internal mechanism of light regulation of reproductive performance of Zi-geese.

Since the change of light conditions can affect the reproductive performance of poultry and the expression of related genes, the change of light conditions would inevitably lead to the change of metabolites related to reproductive performance. To further reveal the possible mechanism of red light for 12 h improving reproductive performance of Zi-geese, the metabonomics of hypothalamus, pituitary, and ovary samples of Zi-geese were studied. The results showed that 583 differential metabolites were found in the hypothalamus of the geese, and 384 were unique; 196 differential metabolites and 117 unique differential metabolites were screened from the pituitaries of the geese; 692 differential metabolites and 513 unique differential metabolites were screened from the ovaries of Zi Goose. This confirmed that there were significant differences in material metabolism between red light and white light at the peak laying period. Further analysis showed that 433 differentially expressed metabolites were down-regulated and 150 differentially expressed metabolites were u*P*-regulated in the hypothalamus of Zi-geese under red light for 12 h; 125 differential metabolites were down-regulated and 71 differential metabolites were up-regulated; 355 differentially expressed metabolites were down-regulated and 337 differentially expressed metabolites were up-regulated. The amount of these different metabolites might be the main substances that affect the reproductive performance of Zi-geese, and it is also the main object that needs to be focused on in the future. Co-expression of differentially expressed genes and metabolites was confirmed by transcriptome and metabolomic analysis, which provided the guarantee for mining core metabolic pathways and typical metabolites. The results showed that there were 15, 3, and 186 pairs of metabolites in the hypothalamus, pituitaries, and ovaries of Zi-geese. Four metabolic pathways were closely related to the light regulation of reproductive performance in the geese, including the GnRH signaling pathway, prolactin signaling pathway, thyroxine synthesis pathway, and ovarian steroid synthesis pathway. The differential metabolites involved in these metabolic pathways are arachidonic acid, glucose-6-phosphate, progesterone, glutathione, oxidized glutathione, testosterone, and deoxyepiandrosterone, which would play an essential role in the light regulation of the reproductive performance of Zi geese.

CONCLUSION

This study was found out the differential metabolites in response to light regulation, and to clarify the regulatory genes of the differential metabolites and their differences in the regulation mode of reproductive performance for the geese. In this study,1,481 differential metabolites were screened, among which 583 differential metabolites were screened from the hypothalamus of seeded goose, and 384 differential metabolites were endemic to the hypothalamus of seeded goose. A total of 196 differential metabolites were screened out from the pituitary gland of the goose, and 117 unique differential metabolites were found. 692 differential metabolites were screened from seed goose egg nests, and 513 differential metabolites were endemic. The accumulation of 433 differential metabolites in the hypothalamus of seed geese decreased under 12 h red light, while the accumulation of 150 differential metabolites increased under 12 h red light. The accumulation of 125 differential metabolites in pituitary gland decreased under 12 h red light condition, while the accumulation of 71 differential metabolites increased under 12 h red light condition. The accumulation of 355 differential metabolites in the nest of seed goose eggs decreased under 12 h red light, while the accumulation of 337 differential metabolites increased under 12 h red light. The results of joint analysis showed that 33 differential metabolites were closely related to the homologous genes of 1,264 transcripts and 400 related enzymes in the hypothalamus of Seed Geese. There were 15 differential metabolites closely related to 163 transcripts and 47 homologous genes of related enzymes in pituitary gland. There were 55 differential metabolites associated with 1,255 transcripts and 360 homologous genes of related enzymes in the nest of seed goose egg. In the hypothalamus, pituitary and ovary of seed geese, 15, 3 and 186 metabolite transcripts were screened out in response to the change of light conditions. Four metabolic pathways were determined to be closely related to light regulation of reproductive performance of seed geese, namely GnRH signaling pathway, prolactin signaling pathway, thyroxine synthesis pathway and ovarian steroid synthesis pathway. Canonical differential metabolites such as arachidonic acid, glucose 6-phosphate, progesterone, glutathione, glutathione oxidase, testosterone and deoxyepandrosterone, as well as their

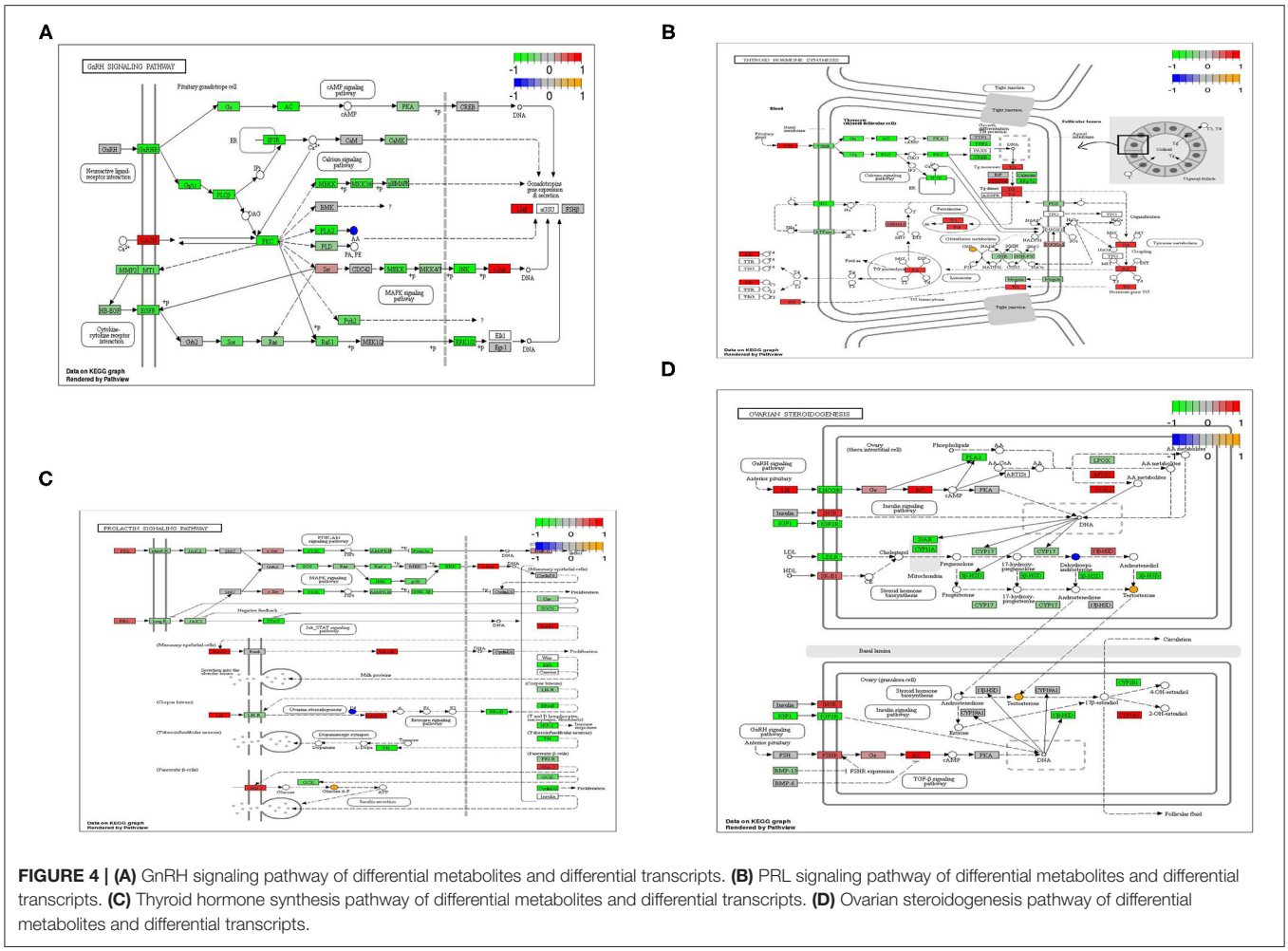

FIGURE 4 | (A) GnRH signaling pathway of differential metabolites and differential transcripts. **(B)** PRL signaling pathway of differential metabolites and differential transcripts. **(C)** Thyroid hormone synthesis pathway of differential metabolites and differential transcripts. **(D)** Ovarian steroidogenesis pathway of differential metabolites and differential transcripts.

related genes and protein genes, will play an important role in light regulation of reproductive performance of seed geese.

DATA AVAILABILITY STATEMENT

The original contributions presented in the study are included in the article/supplementary material, further inquiries can be directed to the corresponding author/s.

AUTHOR CONTRIBUTIONS

LM: research concept, methodology, data extraction, analysis, and draft writing. ZX: resource searching, verification, formal analysis, supervision, and manuscript reviewing and editing. LG: resources, methodology, project administration, supervision, and manuscript reviewing and editing. ZG: resource searching, manuscript reviewing and editing, and methodology. All authors contributed to the article and approved the submitted version.

FUNDING

The research was supported by the research business expenses of the Scientific Research Institutes of Heilongjiang Province (No. CZKYF2021B003) and National Modern Waterfowl Industry Technical System Special Project (No. CARS-42-24).

REFERENCES

1. Ma L, Wang X, Chai J. Application and research progress of metabonomics in the diagnosis and treatment of burn injury. *Chin J Injury Repair and Wound Healing (Chinese)*. (2017) 12:212–5.
2. Ghaderi A, Mojtahedi Z. Proteomics studies in oncology towards personalized medicine in public health: Opportunities and challenges for OMICS research in Iran. *Curr Pharmacogen Pers Med.* (2012) 10:265–70. doi: 10.2174/187569212803901747
3. Guo X, Hao Y, Kamilijiang M, Hasimu A, Yuan J, Wu G, et al. Potential predictive plasma biomarkers for cervical cancer by 2D-DIGE proteomics and ingenuity pathway analysis. *Tumour Biol.* (2015) 36:11–20. doi: 10.1007/s13277-014-2772-5
4. Akdeniz M, Yener I, Ertas A, Firat M, Resitoglu B, Hasimi N, et al. Biological and chemical comparison of natural and cultivated samples of satureja macrantha. *Rec Nat Prod.* (2021) 15:568–84. doi: 10.25135/rnp.237.21.02.1957

5. Lu X, Zhao X, Bai C, Zhao C, Lu G, Xu G. LC-MS-based metabonomics analysis. *J chromatogr B.* (2008) 866:64–76. doi: 10.1016/j.jchromb.2007.10.022
6. Griffin JL. Metabonomics: NMR spectroscopy and pattern recognition analysis of body fluids and tissues for characterisation of xenobiotic toxicity and disease diagnosis. *Curr Opin Chem Biol.* (2003) 7:648–54. doi: 10.1016/j.cbpa.2003.08.008
7. Kang B, Jiang D, Liu B, Yang H. Quantitative studies on expression level of FTH and eight ESTs mRNA in the ovaries of Zi Geese. *Chin J Anim Husbandry (Chinese).* (2011) 47:16–9.
8. Chang S, Zhuang Z, Lin M, Cheng C, Lin T, Jea Y, et al. Effects of monochromatic light sources on sex hormone levels in serum and on semen quality of ganders. *Anim Reprod Sc.* (2016) 167:96–102. doi: 10.1016/j.anireprosci.2016.02.012
9. Yu C, Xu T, Zhang X, Dong M, Niu Y. Differential mechanism of toxicity in normal and blood-stasis mice following Rhizoma Curcumae exposure based on "YOU-GU-WU-YUN" theory. *Acta Pharm Sin (Chinese).* (2019) 54:329–34.
10. Xu Y, Zhao R, Hu Q. Effect of Curcumae Rhizoma on the pharmacokinetics of methotrexate in normal and blood stasis rats. *J Guangdong Pharm Univ (Chinese).* (2016) 32:403–5.
11. Baumbach J, Apeltsin L. Linking Cytoscape and the corynebacterial reference database CoryneRegNet. *BMC Genomics.* (2008) 9:184. doi: 10.1186/1471-2164-9-184
12. Jiang X, Lu H, Xu Z, Zhang Y, Zhao Q. Network pharmacology-based research uncovers cold resistance and thermogenesis mechanism of Cinnamomum cassia. *Fitoterapia.* (2020) 149:104824. doi: 10.1016/j.fitote.2020.104824
13. Singh J, Jayaprakasha GK, Patil BS. Rapid ultra-high-performance liquid chromatography/quadrupole time-of-flight tandem mass spectrometry and selected reaction monitoring strategy for the identification and quantification of minor spinacetin derivatives in spinach. *Rapid Commu Mass Spectrom.* (2017) 31:1803–12. doi: 10.1002/rcm.7967
14. Powers R, Siegel MM. 5-Applications of nuclear magnetic resonance and mass spectrometry to anticncer drug discovery. In: Adjei AA, Buolamwini JK. The strategies for discovery and clinical testing—novel anticancer agents. Cambridge: Academic Press (2006). p. 107–90. doi: 10.1016/B978-012088561-9/50006-5
15. Lalwani S, Venditto VJ, Chouai A, Rivera GE, Shaunak S, Simanek EE. Electrophoretic behavior of anionic triazine and PAMAM dendrimers: methods for improving resolution and assessing purity using capillary electrophoresis. *Macromolecules.* (2009) 42:3152–61. doi: 10.1021/ma802250c
16. Li P, Chen A, Fu Y, Han W. Study on determining Nuclear Magnetic Resonance (NMR) T_2 cutoff combined with the oil displacing water experiments. *Prog Geophys (Chinese).* (2019). 34:1050–4.
17. Libardoni M, Hasselbrink E, Waite JH, Sacks R. At-column heating and a resistively heated, liquid-cooled thermal modulator for a low-resource benchtop GC×GC. *J Sep Sci.* (2015) 29: 1001–8. doi: 10.1002/jssc.200500298
18. Huang Q, Zhang F, Liu S, Jiang Y, Ouyang D. Systematic investigation of the pharmacological mechanism for renal protection by the leaves of *Eucommia ulmoides* Oliver using UPLC-Q-TOF/MS combined with network pharmacology analysis. *Biomed Pharmacother.* (2021) 140:111735. doi: 10.1016/j.biopha.2021.111735

Conflict of Interest: The authors declare that the research was conducted in the absence of any commercial or financial relationships that could be construed as a potential conflict of interest.

Publisher's Note: All claims expressed in this article are solely those of the authors and do not necessarily represent those of their affiliated organizations, or those of the publisher, the editors and the reviewers. Any product that may be evaluated in this article, or claim that may be made by its manufacturer, is not guaranteed or endorsed by the publisher.

frontiers | Frontiers in Veterinary Science

ORIGINAL RESEARCH
published: 18 April 2022
doi: 10.3389/fvets.2022.877066

Trans-anethole Ameliorates Intestinal Injury Through Activation of Nrf2 Signaling Pathway in Subclinical Necrotic Enteritis-Induced Broilers

Caiyun Yu[1], *Yichun Tong*[1], *Qiming Li*[1], *Tian Wang*[1]* *and Zaibin Yang*[2]*

[1] College of Animal Sciences and Technology, Nanjing Agricultural University, Nanjing, China, [2] College of Animal Sciences and Technology, Shandong Agricultural University, Tai'an, China

OPEN ACCESS

Edited by:
Amjad Islam Aqib,
Cholistan University of Veterinary and Animal Sciences, Pakistan

Reviewed by:
Mughees Aizaz Alvi,
Lanzhou Veterinary Research Institute (CAAS), China
Hafiz Iftikhar Hussain,
Huazhong Agricultural University, China
Awais Ihsan,
COMSATS University Islamabad, Sahiwal Campus, Pakistan

***Correspondence:**
Tian Wang
tianwangnjau@163.com
Zaibin Yang
yangzb@sdau.edu.cn

Specialty section:
This article was submitted to Veterinary Infectious Diseases, a section of the journal Frontiers in Veterinary Science

Received: 16 February 2022
Accepted: 21 March 2022
Published: 18 April 2022

Citation:
Yu C, Tong Y, Li Q, Wang T and Yang Z (2022) Trans-anethole Ameliorates Intestinal Injury Through Activation of Nrf2 Signaling Pathway in Subclinical Necrotic Enteritis-Induced Broilers. Front. Vet. Sci. 9:877066. doi: 10.3389/fvets.2022.877066

This study was conducted to investigate the alleviative effects of *trans*-anethole (TA) on intestinal oxidative stress by enhancing the activities of intestinal antioxidant enzymes and activating the Nrf2 signaling pathway in subclinical necrotic enteritis (NE) infected broilers. A total of 192 1-day-old male Arbor Acres broilers were randomly allocated into three treatment groups: (1) control (CON); (2) subclinical NE challenge (NE); (3) NE challenge + 600 mg/kg TA (NE+TA600). Subclinical NE was induced by oral administration of live coccidiosis vaccine containing 2×10^4 oocysts at 10 days of age and 2 ml of *Clostridium perfringens* type A solution (3×10^8 CFU/ml) daily from days 14 to 19. The results showed that NE infection led to a severe decline ($p < 0.05$) in the final body weight (BW) and average daily gain (ADG), but an increase ($p < 0.05$) in feed/gain (F/G) of broilers at day 10–21 and day 1–21 compared with the control group. TA administration improved ($p < 0.05$) the growth performance of NE birds. The intestinal villus height (VH) and villus height/crypt depth (VH/CD) were reduced ($p < 0.05$) by NE challenge as compared with those of the control group, which was elevated by TA administration. Subclinical NE infection decreased ($p < 0.05$) serum activities of total superoxide dismutase (T-SOD), total antioxidant capacity (T-AOC), and jejunal and ileal glutathione peroxidase (GSH-PX), and T-SOD activity as well as T-AOC in the jejunum, while TA interventions positively elevated that ($p < 0.05$). Administration of TA protected the intestine against oxidative stress through up-regulation of intestinal nuclear factor erythroid 2-related factor 2 (Nrf2) signaling pathway as compared with the NE group ($p < 0.05$). In addition, dietary inclusion of TA elevated ($p < 0.05$) mRNA abundance of c-mesenchymal-epithelial transition factor (c-Met), jejunal epidermal growth factor receptor (EGFR), and transforming growth factor-beta 1 (TGF-β1) in the jejunum and ileum of birds after subclinical NE challenge. In conclusion, 600 mg/kg of TA may be a promising tool to prevent and control subclinical NE by increasing intestinal antioxidant status in broilers.

Keywords: *Trans*-anethole, broiler, subclinical necrotic enteritis, intestinal oxidative stress, intestinal mucosal repair factor

INTRODUCTION

Necrotic enteritis (NE) is a worldwide high incidence of intestinal disease in poultry induced by *Clostridium perfringens* type A and C, or Net B (1, 2) and annually results in a global economic loss of 6 billion dollars (3). This infectious disease has been well-controlled for many years by the traditional use of antibiotics. Currently, the use of antibiotics has been banned due to the development of bacterial resistance and the production of antibiotic residues in poultry products (4). Therefore, there has been an increasing concern in exploring new strategies for prevention and treatment of NE other than the use of antibiotics.

Necrotic enteritis infection could result in intestinal lesions, intestinal inflammation, and intestinal oxidative stress (4, 5). Oxidative stress leads to the release of intracellular cytokines and further causes systemic and chronic inflammation (6). Oxidative stress is accompanied by increasing the production of reactive oxygen species (ROS) and is thought to be a trigger for intestinal injury (7, 8). Enhancement of endogenous antioxidant enzymes activities, such as superoxide dismutase (SOD), catalase (CAT), and glutathione peroxidase (GSH-PX), could eliminate the excessive production of ROS, and further ameliorate oxidative stress (9). Accordingly, fortifying the intestinal antioxidant status may be a promising strategy for preventing or treating NE in broilers.

Trans-anethole [TA, 1-methoxy-4-(prop-1-enyl) benzene], a major component (higher than 80%) of the essential oil extracted from the plant of anise and fennel, has been used as a flavoring agent in foods, cosmetics, alcoholic beverage, and perfumes and herbal medicine (10–12). It is a volatile terpenoid with anise flavor, poor water solubility, and easy to be deteriorated when exposed to light and high temperature. It is worth noting that TA is non-toxic with no genotoxic activity recognized by the United States Food and Drug Administration. Several recent studies have confirmed the antioxidant capacity of TA. It was demonstrated that TA sachets improved overall freshness and odor of organic ready-to-eat iceberg lettuce packages due to their antimicrobial and antioxidant activities (13). TA could prevent hydrogen peroxide-induced collagen metabolism alterations and apoptosis in human skin fibroblasts, proving that TA may be beneficial against oxidative stress (10). Moreover, our previous study found that star anise oil enhanced antioxidant status in laying hens (14). However, the mechanism by which the inclusion of TA enhanced antioxidant status of broilers has not been elucidated yet. Nuclear factor E2-related factor 2 (Nrf2), which is a member of the NF-E2 family of the basic leucine zipper of redox-sensitive transcription factors, is well known for scavenging free radicals and preventing oxidative stress (15, 16). It is a classic antioxidant signaling pathway that regulates the expression of phase II antioxidant enzyme genes against oxidative stress. Therefore, the present study aimed to investigate whether TA had alleviative potential on intestinal oxidative stress of subclinical NE challenged broilers through activating the Nrf2 signaling pathway.

MATERIALS AND METHODS

Ethics Approval

This study was reviewed and approved by the Institutional Animal Care and Use Committee of Nanjing Agricultural University (Permit No. SYXK-2017-0027).

Preparation of *Trans*-anethole

Trans-anethole was purchased from Nanjing Dilger Medical Technology Co., Ltd (D105737, Nanjing, China). The analyzed purity of TA was 98.35%. The TA was stored in the dark and at 4°C until use.

Preparation of Bacterial Strain

Freeze-dried bacteria powder of *C. perfringens* type A strain (125404) was obtained from BeNa Culture Collection (Xinyang, China). It was cultured anaerobically with fluid thioglycollate (FT) medium (HB5190; Hopebio Biotechnology Co., Ltd, Qingdao, China) in panel for 24 h at 37°C, then aseptically picked single colony into 2 L conical flask with FT medium and anaerobically incubated by shaker for 13 h at 37°C.

Animals, Diets, and Experimental Design

A total of 192 1-day-old male Arbor Acres broilers (42.43 ± 0.88 g) were purchased from Yantai Land Animal Husbandry (Shandong, China). On arrival, all birds were weighed and randomly allocated into three groups, with 8 replicates of 8 birds in each group. The basal diets were formulated to meet the bird's nutritional requirements according to NY/T 33-2004 [(17); **Supplementary Table 1**]. TA was blended with soybean oil and then mixed with other ingredients. All of the diets were pelleted and crumbled. All birds were reared in wire cages and had free access to diet and water throughout the entire experimental period. Room temperature was maintained at 33°C during the first 5 days and then gradually decreased by 0.5°C daily until 22°C. The treatment groups were as follows: (1) CON group (basal diet); (2) NE group (subclinical NE challenge); and (3) NE + TA600 group (subclinical NE challenge + 600 mg/kg of TA). The procedure of subclinical NE challenge was performed with minor modifications by Liu et al. (18) and Zhang et al. (19). Briefly, all chicks in the subclinical NE infected groups were each orally gavaged with live coccidiosis vaccine (Foshan Standard Biotechnology Co., Ltd, Guangdong, China) containing 2×10^4 oocysts suspended in 500 μl of normal saline with coccidia suspension agent at 10 days of age and then with 2 ml of *C. perfringens* type A solution (3×10^8 CFU/mL) daily from days 14 to 19. Birds in the CON group were orally gavaged with the same amount of normal saline at 10 days of age and sterile FT medium solution during days 14–19. TA was supplemented throughout the whole experimental period.

Sample Collection

On the morning of day 22, 8 birds per group with average body weight (BW) of its replicate were selected for sampling. The serum samples were collected from peripheral blood, which was centrifuged at 3,500 × g for 10 min at 4°C, then were stored at −80°C until analysis. After blood sampling,

TABLE 1 | Effect of dietary TA supplementation on the growth performance of broilers challenged with subclinical necrotic enteritis[1].

Items[2]	CON	NE	NE + TA600	*p*-value
Initial BW, kg	42.03 ± 0.22	42.00 ± 0.54	42.07 ± 0.81	0.232
Final BW, kg	873.18 ± 24.42[a]	826.13 ± 24.34[b]	835.71 ± 38.99[ab]	0.004
Pre-Challenge (0–9 d)				
ADFI, g/d	27.79 ± 1.30	27.89 ± 0.80	27.81 ± 1.31	0.984
ADG, g/d	23.07 ± 0.71	23.32 ± 0.62	23.50 ± 1.31	0.689
F/G, g/g	1.20 ± 0.03	1.20 ± 0.04	1.19 ± 0.07	0.773
Post-Challenge (10–21 d)				
ADFI, g/d	68.19 ± 1.32	65.40 ± 2.42	67.65 ± 2.77	0.074
ADG, g/d	56.79 ± 0.47[a]	48.78 ± 1.86[c]	53.86 ± 2.22[b]	<0.001
F/G, g/g	1.20 ± 0.02[b]	1.34 ± 0.09[a]	1.26 ± 0.05[ab]	0.002
Overall (1–21 d)				
ADFI, g/d	50.79 ± 2.95	49.27 ± 2.92	50.36 ± 2.37	0.579
ADG, g/d	41.56 ± 0.42[a]	37.36 ± 1.09[c]	39.68 ± 1.51[b]	<0.001
F/G, g/g	1.22 ± 0.06[b]	1.32 ± 0.10[a]	1.27 ± 0.06[ab]	0.024

[a–c]*Means within a row with different letters differ significantly ($p < 0.05$).*

[1]*Data are means for 8 replicates of 6 birds per replicate. No birds died during the experimental period. The data in each group was expressed as mean with their standard errors ($n = 8$).*

[2]*ADFI, average daily feed intake; ADG, average daily gain; F/G, feed/gain; BW, body weight.*

the birds were stunned and sacrificed by cervical dislocation. Approximately 1 cm of middle segments of jejunum and ileum were cut off carefully and fixed in 4% paraformaldehyde solution for histomorphology analysis. Approximately 3 cm of middle jejunum and ileum segments of each bird were dissected and washed with ice-cold sterile saline, then frozen in liquid nitrogen and stored at −80°C for subsequent analysis.

Growth Performance

The BW and feed intake of birds of each replicate were recorded weekly to calculate the average daily feed intake (ADFI), average daily gain (ADG), and feed/gain (F/G).

Intestinal Morphology

The fixed jejunum and ileum segments were dehydrated, transparentized, and embedded in paraffin. Each sample was sliced into 5–μm cross-sections, deparaffinized in xylene, graded rehydrated, and finally stained with hematoxylin-eosin. With reference to Ekim et al. (20), 10 well-oriented villi and crypts per sample were selected for measuring the villus height (VH) and crypt depth (CD) using light microscope (Olympus CX31, Tokyo, Japan) and Image-Pro Plus 6.0 software (Media Cybernetics, Inc., Rockville, MD, USA).

Determination of Antioxidant Capacity

Frozen jejunum and ileum were weighed, and homogenized (3 min) with ice-cold physiologic saline in the ratio of 1:4 (wt/vol). The homogenates were then centrifuged at 4,000 × g for 10 min at 4°C. The supernatants were then diluted into the optimal content for examining the activities of total SOD (A001-1-1), total antioxidant capacity (T-AOC; A015-1-2), and GSH-PX (A005-1-2), and the concentration of malondialdehyde (MDA; A003-1-2) using the assay kits (Nanjing Jiancheng Bioengineering Institute, Nanjing, China). The total protein concentration of supernatants was detected by bicinchoninic acid (BCA) protein assay kit (P0010; Beyotime Institute of Biotechnology, Nanjing, China). The results were expressed as activities of antioxidant enzyme and concentration of MDA in per mg of protein in the intestinal tissues of broilers. Additionally, the serum activities of T-SOD, T-AOC, GSH-PX, and concentration of MDA were also detected using the same assay kits and presented as that in per ml of serum.

Quantitative Real-Time PCR Assay

Extraction of total RNA in the jejunum and ileum was performed using Trizol reagent (9108; TaKaRa Biotechnology, Dalian, Liaoning, China). The quality and concentration of total RNA were detected using a NanoDrop-1000 microspectrophotometer (Thermo Fisher Scientific, Waltham, MA, USA), and the integrity of extracted RNA was evaluated with 2.0% agarose gel electrophoresis. Subsequently, the reverse transcription polymerase chain reaction (PCR) was conducted to produce the complementary DNA using the PrimeScriptTMRT reagent Kit (RR036A; TaKaRa Biotechnology Co., Ltd, Dalian, China) by two steps: 37°C for 15 min and 85°C for 5 s. qRT-PCR reactions were conducted to determine the relative mRNA abundance of Nrf2, NAD(P)H quinone dehydrogenase 1 (NQO1), heme oxygenase 1 (HO1), superoxide dismutase 1 (SOD1), glutathione peroxidase (GSH-PX), epidermal growth factor receptor (EGFR), c-mesenchymal epithelial transition factor (c-Met), transforming growth factor-alpha (TGF-α), transforming growth factor-beta 1 (TGF-β1), and beta-actin (β-actin) ChamQ SYBR® qPCR Master Mix Kit (Q311-02; Vazyme Biotechnology, Nanjing, China) based on Applied Biosystems 7500 Real–time PCR System (Life Technologies, CA, USA). The primers were commercially synthesized by Sangon Biotechnology Co., Ltd (Shanghai, China), which are shown in **Supplementary Table 2**. The amplification program consists of an initial denaturation step at 95°C for 30 s,

followed by 40 cycles of 95°C for 10 s and 60°C for 30 s, then 15 s at 95°C, and 60 s at 60°C, with a final step at 95°C for 15 s. The relative mRNA abundance of target genes were analyzed using the $2^{-\Delta\Delta Ct}$ method and normalized against the reference gene (β-actin) expression level.

Western Blot Assay

Total protein extracted from the jejunum and ileum tissues was performed by radioimmunoprecipitation assay lysis buffer and protease inhibitor (P0013B and ST506; Beyotime Institute of Biotechnology, Nanjing, China). Nuclear protein was isolated by Nuclear and Cytoplasmic Protein Extraction Kit (P0027; Beyotime Institute of Biotechnology, Nanjing, China) for detection of Nrf2 protein expression. The concentrations of total cellular protein and nuclear protein were detected by the BCA assay kit (P0010; Beyotime Institute of Biotechnology, Nanjing, China). Equal amounts of protein were separated through sodium dodecylsulfate polyacrylamide gel electrophoresis (SDS-PAGE), transferred onto polyvinylidene difluoride (PVDF) membranes. Subsequently, the membranes were blocked with 5% skimmed milk (w/v) in tris-buffered saline with 0.1% tween (TBST) buffer for 2 h at room temperature, and then incubated with primary antibodies against Nrf2 (16396-1-AP; Proteintech Group, Inc., Wuhan, China), HO1 (10701-1-AP; Proteintech), SOD1 (10269-1-AP; Proteintech), and β-actin (20536-1-AP; Proteintech) overnight at 4°C, and then incubated with secondary goat anti-rabbit IgG horseradish peroxidase-conjugated antibody for 1.5 h at room temperature. The expression of target proteins was determined using ECL chemiluminescence reagents (E412-01; Vazyme Biotechnology) and images were captured by Imager-Bio-Rad (Bio-Rad Laboratories, Inc., Hercules, CA, USA). The band intensities were quantified using Image J software.

Statistical Analysis

All data were presented as mean ± standard error of mean. The Shapiro–Wilk test was used to determine the dataset normality and homogeneity of variances. Data sets were analyzed using one-way analysis of variance (ANOVA), followed by Tukey's HSD test (SAS Institute, 2001). Results were regarded statistically significant with a $p < 0.05$.

RESULTS

Growth Performance

No mortality was observed in the prevention groups during the experimental period. NE infection led to a severe decline ($p < 0.05$) in the final BW and ADG, but an increase ($p < 0.05$) in F/G of broilers at day 10–21 and 1–21 compared with control groups (**Table 1**), but TA administration reversely altered ($P < 0.05$) those of NE birds. No remarkable difference was found with regards to initial BW, and ADFI at day 0–9 and 1–21 among groups ($p > 0.05$), but the ADFI at day 10–21 tended to be decreased ($p = 0.074$) by NE infection. Moreover, the ADG and F/G were not altered ($p > 0.05$) by TA supplementation before NE infection.

Intestinal Morphology

Figure 1A revealed that there was some damage to jejunal and ileal villi development after NE infection, as found by broken and shortened villi. Consistent with the histological observations of tissue sections, NE infection significantly reduced the VH and VH/CD in jejunal and ileal tissues as compared with those of control (**Figure 1B**), which was elevated by TA supplementation ($p < 0.05$). In addition, the intestinal CD was not affected by NE challenge ($p > 0.05$).

Activities of Antioxidant Enzymes

As revealed by **Figure 2**, these data indicated that the serum activities of T-SOD, T-AOC, and GSH-PX were decreased ($p < 0.05$) by subclinical NE infection, but TA interventions elevated that (**Figures 2A–D**). Although no significant difference was shown with regards to ileal MDA concentration and T-AOC activity among the four groups, the inclusion of TA increased ($p < 0.05$) the T-SOD activity in the jejunum and ileum as well as T-AOC activity in the jejunum in comparison with subclinical NE group (**Figures 2E–G**). In addition, the GSH-PX activity in the jejunum ($p = 0.068$) and ileum ($p = 0.062$) was tended to be reduced after subclinical NE infection, but elevated by TA administration.

Expression of Nrf2 Signaling Pathway

As exhibited in **Figure 3**, the results showed that subclinical NE challenge downregulated the jejunal and ileal mRNA expression of Nrf2, HO1, NQO1, SOD1, and GSH-PX as compared with control group, while the inclusion of TA upregulated ($p < 0.05$) the mRNA abundance of these genes.

Western blot results revealed that the jejunal and ileal nuclear translocation level of Nrf2, and protein abundance of HO1, and SOD1 of subclinical NE infected birds fed with TA was higher ($p < 0.05$) than those in the NE group (**Figure 4**).

Expression of Genes Related to Mucosal Repair Factors

Figure 5 presents the results of jejunal and ileal mucosal repair factors gene expression. Dietary inclusion of TA elevated downregulated ($p < 0.05$) mRNA abundance of jejunal and ileal c-Met, and jejunal EGFR and TGF-β1 in subclinical NE infected birds. The ileal EGFR and TGF-β1, and jejunal and ileal TGF-α did not differ ($p > 0.05$) among the groups.

DISCUSSION

Necrotic enteritis caused by *C. perfringens* destroys the intestinal barrier integrity and leads to intestinal dysfunction in chickens, resulting in a decrease in growth performance (21). NE annually costs up to six billion dollars in the poultry industry (3). Previous studies reported that subclinical NE infection could cause more serious economic loss than clinical NE infection due to mild intestinal damage, poor digestion, and further poor growth performance (22, 23). The results of our study revealed that NE infection led to a severe decline in the final BW and ADG, but an increase in F/G of broilers compared with controls, while TA administration at 600 mg/kg reversely

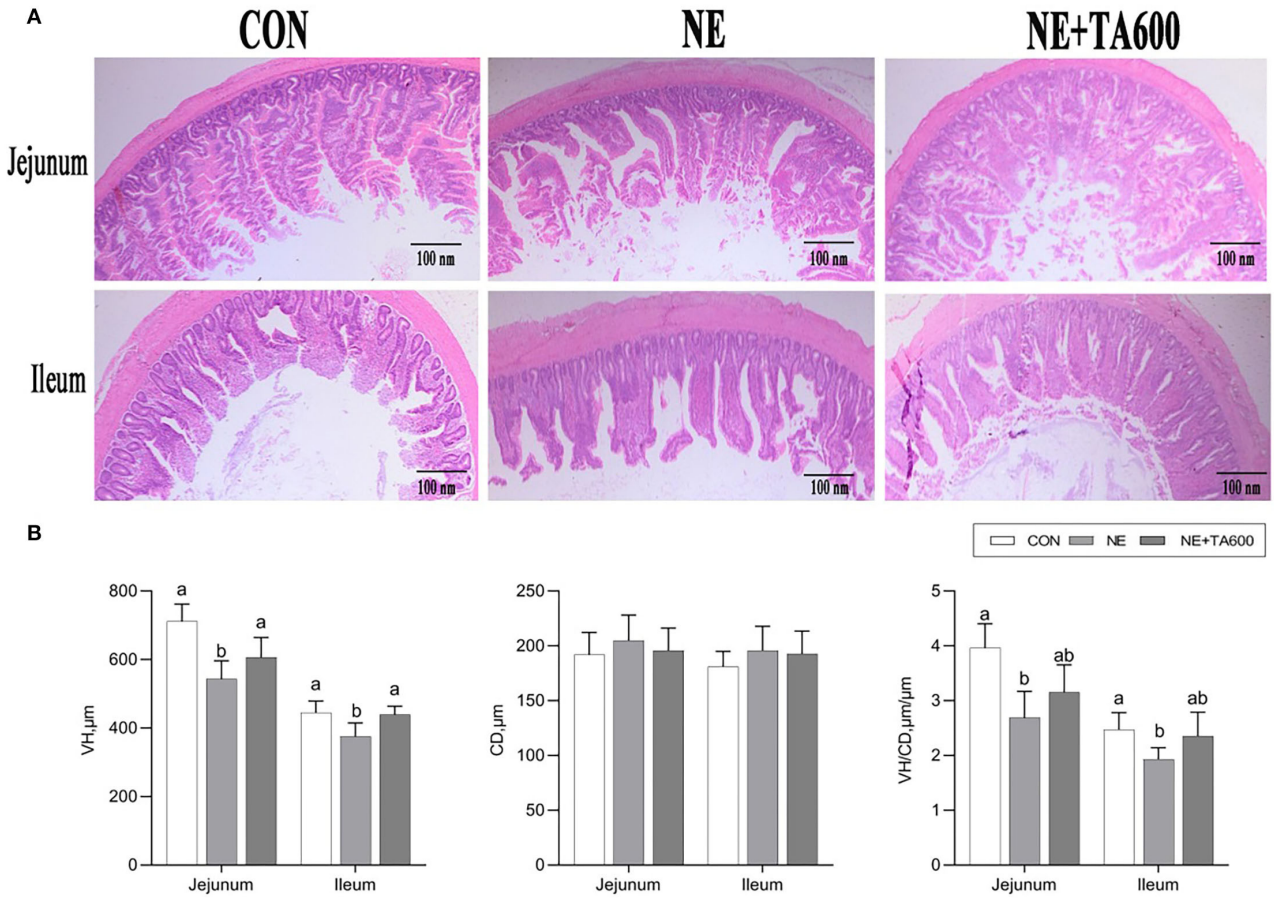

FIGURE 1 | Effects of TA on intestinal morphology of subclinical NE broilers. **(A)** Hematoxylin and eosin staining, **(B)** VH, CD, and VH/CD of the intestine. Values were expressed as mean with standard error represented by vertical bars. [a,b]Means with different letters differ significantly among the groups ($p < 0.05$). VH, villus height; CD, crypt depth.

improved the growth performance of NE birds. Accordingly, the VH and VH/CD were improved by TA during the NE challenge. This may be attributed to the previously reported beneficial effects of TA in increasing nutrient digestibility (24), gastroprotector activity (25), antimicrobial (13, 26), and anti-inflammatory (27–29) activities. However, the results of this study revealed that ADG and F/G were not altered by TA supplementation before NE infection. Similar with that, a recent study investigated the effects of different concentrations of TA on the growth performance of broilers and observed that TA inclusion had no distinct effect on ADG, BW, and F/G (17). It was reported that the growth performance of broilers was not affected by the inclusion of essential oils consisting of menthol and anethole (30). Additionally, the experimental conditions, hygiene, animal age, diet type, and altered microbiota may also affect the performance response of broilers to TA (31, 32). Taken together, the effects of TA on growth performance of broilers under normal feeding conditions and subclinical NE challenge require to be further characterized.

Necrotic enteritis infection is usually accompanied by intestinal lesions, intestinal inflammation, and intestinal oxidative stress (4, 5). Rochat et al. (33) also indicated that bacterial infection could cause gastrointestinal inflammation and further lead to oxidative stress. Therefore, we conducted the current study to investigate whether TA could ameliorate subclinical NE in broilers by enhancing the intestinal antioxidant status and intestinal mucous repair factor expression.

The anti-inflammatory activity of *Foeniculum vulgare* essential oil (81.08% TA) against acetic acid-induced colitis in rats has been reported (27). TA, one of the main active constituents present in essential oils of plants, such as *Syzygium anisatum*, *F. vulgare*, *Coriandrum sativum*, and star anise, has been shown the anti-inflammatory activity by regulation of Th17/Treg function in the mouse model of lipopolysaccharide-induced acute lung injury (28). In another study, TA showed a hepatoprotective effect against hepatic ischemia/reperfusion injury *via* inhibition of toll-like receptor activation (34). Additionally, treatment with TA exerted a protective effect

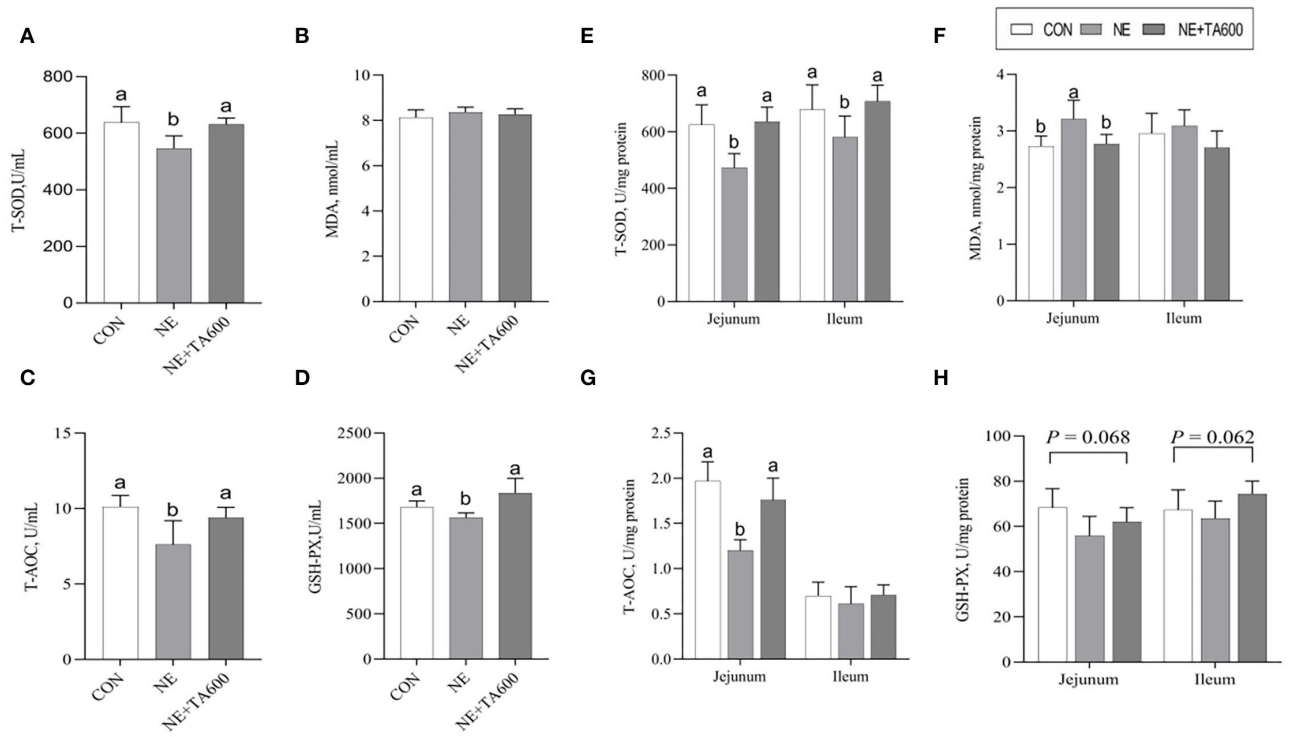

FIGURE 2 | Effects of TA on the activities of antioxidant enzymes in the serum and intestine of subclinical NE broilers. **(A–D)** The activities of T-SOD, MDA, T-AOC, and GSH-PX of serum; **(E–H)** The activities of T-SOD, MDA, T-AOC, and GSH-PX in the jejunum and ileum. Values are means with their standard errors represented by vertical bars. ^{a,b}Means within a row with different letters differ significantly ($p < 0.05$). T-SOD, total superoxide dismutase; MDA, malondialdehyde; T-AOC, total antioxidant capacity; GSH-PX, glutathione peroxidase.

on the hepatotoxicity induced by acetaminophen *via* down-regulating the pro-inflammatory mediators (35). These data indicated that TA may ameliorate intestinal injury due to its anti-inflammatory activity. The present study shows that TA inclusion reduces intestinal damage induced by *C. perfringens* in the experimental model of subclinical NE through the increase of serum and intestinal antioxidant enzymes activities. Previously, TA was reported to play an crucial role in the maintenance of the redox balance through either decreasing ROS levels (36) or enhancing the activities of cellular antioxidant enzymes, such as SOD and GSH-PX (37). Oxidative stress leads to the release of intracellular cytokines and further causes systemic and chronic inflammation (6, 38). Changes in antioxidant enzyme activities can result in oxidative stress. It is well-known that the levels of antioxidant defense can be reflected by the determination of antioxidant activities of T-SOD, T-AOC GSH-PX, and MDA concentration. SOD and GSH-PX are vital intracellular antioxidant enzymes responsible for the antioxidant defense system *via* converting oxygen radicals to hydrogen peroxide (39). Overall antioxidant defense capacity can be determined by T-AOC. In this study, TA inclusion enhanced serum and intestinal SOD activities as well as the jejunal mRNA and protein levels of SOD1 in subclinical NE-infected birds. Furthermore, TA interventions reversely elevated the serum and jejunal activities of T-AOC and GSH-PX, and mRNA abundance of GSH-PX in the jejunum and ileum of birds infected with subclinical NE. These results indicated that the increased expression and activities of antioxidant enzymes may be the mechanism of action by which TA alleviates the intestinal damage caused by subclinical NE. Similarly, Chaudhari et al. (40) observed that TA exhibited the *in vitro* free radicals scavenging activity and the inhibiting capacity of lipid oxidation in stored maize samples, confirming the antioxidant activity of TA in preserving maize samples. TA reduced oxidative stress of *in vitro* primordial follicles and bovine embryos development *by* decreasing the production of ROS and regulating the redox balance (8, 41). TA also prevented hydrogen peroxide-induced collagen metabolism alterations and apoptosis in human skin fibroblasts, proving that TA may be an effective therapeutic agent for oxidative stress-related skin diseases (10). Besides that, the antioxidant potential of TA has been widely reported (25, 42, 43). The antioxidant activity of TA may be attributed to the conjugated double bonds and phenol group in its chemical structure, which has high reactivity with peroxyl radicals (10, 25, 44, 45). On the other hand, TA increased jejunal and ileal mRNA and protein expression of Nrf2, and downstream target molecules. Nrf2 is a principal transcription factor exerting an antioxidant role and maintaining cellular redox balance (46). Upon activation, Nrf2 moves into cell nucleus after releasing from Keap 1,

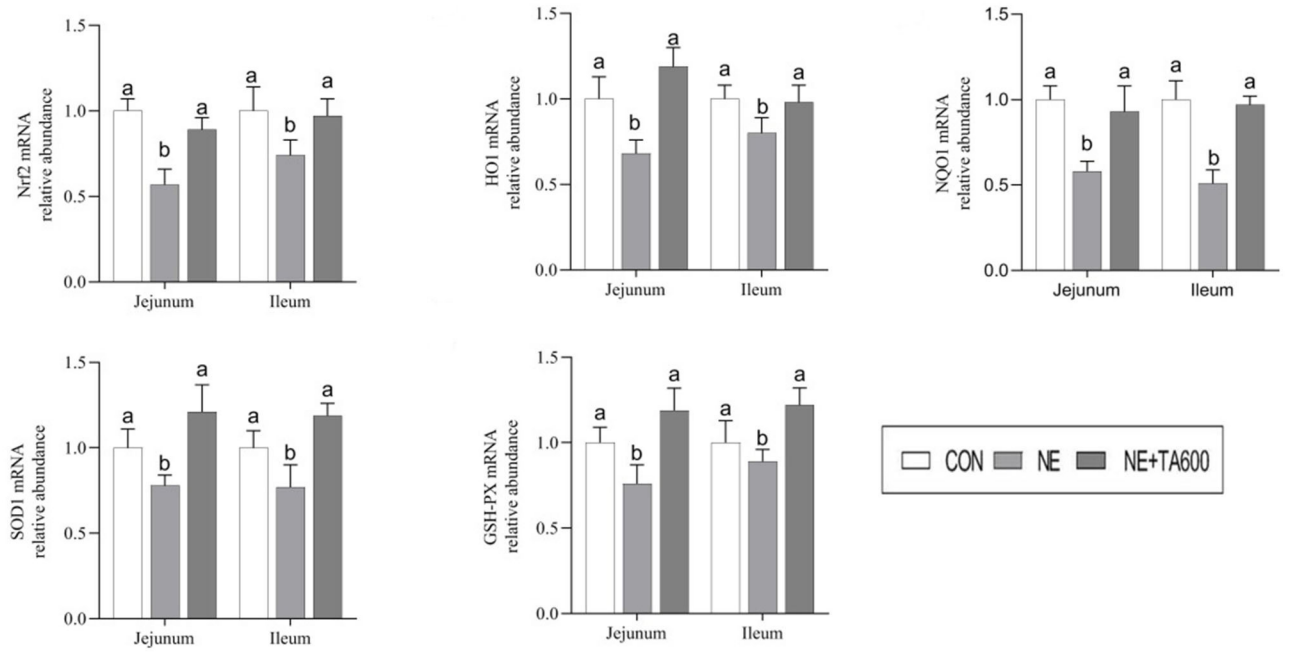

FIGURE 3 | Effects of TA on the mRNA abundance of Nrf2 pathway and antioxidant enzymes in the jejunum and ileum of subclinical NE broilers. Values are means with their standard errors represented by vertical bars. [a,b]Means within a row with different letters differ significantly ($p < 0.05$). Nrf2, nuclear factor erythroid 2-related factor 2; NQO1, NAD(P)H quinone dehydrogenase 1; HO1, heme oxygenase 1; SOD1, superoxide dismutase 1; GSH-PX, glutathione peroxidase.

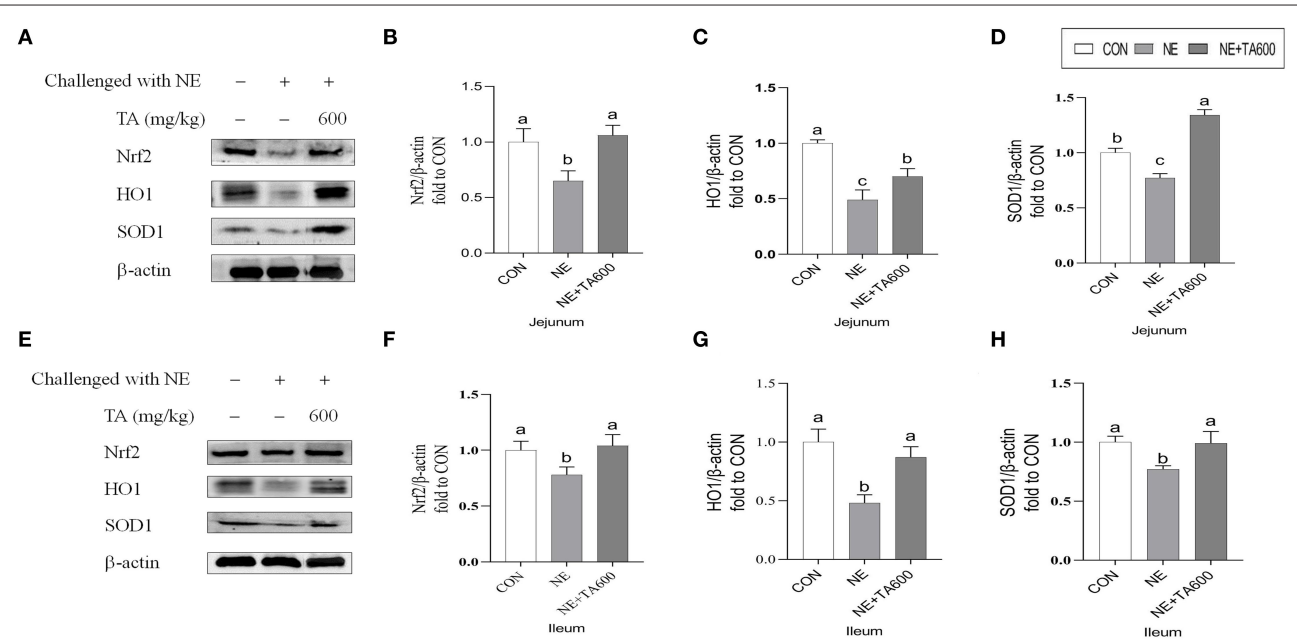

FIGURE 4 | Effects of TA on the relative protein abundance of Nrf2 and SOD1 in the jejunum and ileum of subclinical NE broilers. **(A–D)** The protein abundance of Nrf2, HO1, and SOD1 in the jejunum; **(E–H)** The protein abundance of Nrf2, HO1, and SOD1 in the ileum. Values are means with their standard errors represented by vertical bars. [a–c]Means within a row with different letters differ significantly ($p < 0.05$). Nrf2, nuclear factor erythroid 2-related factor 2; HO1, hemeoxygenase 1; SOD1, superoxide dismutase 1.

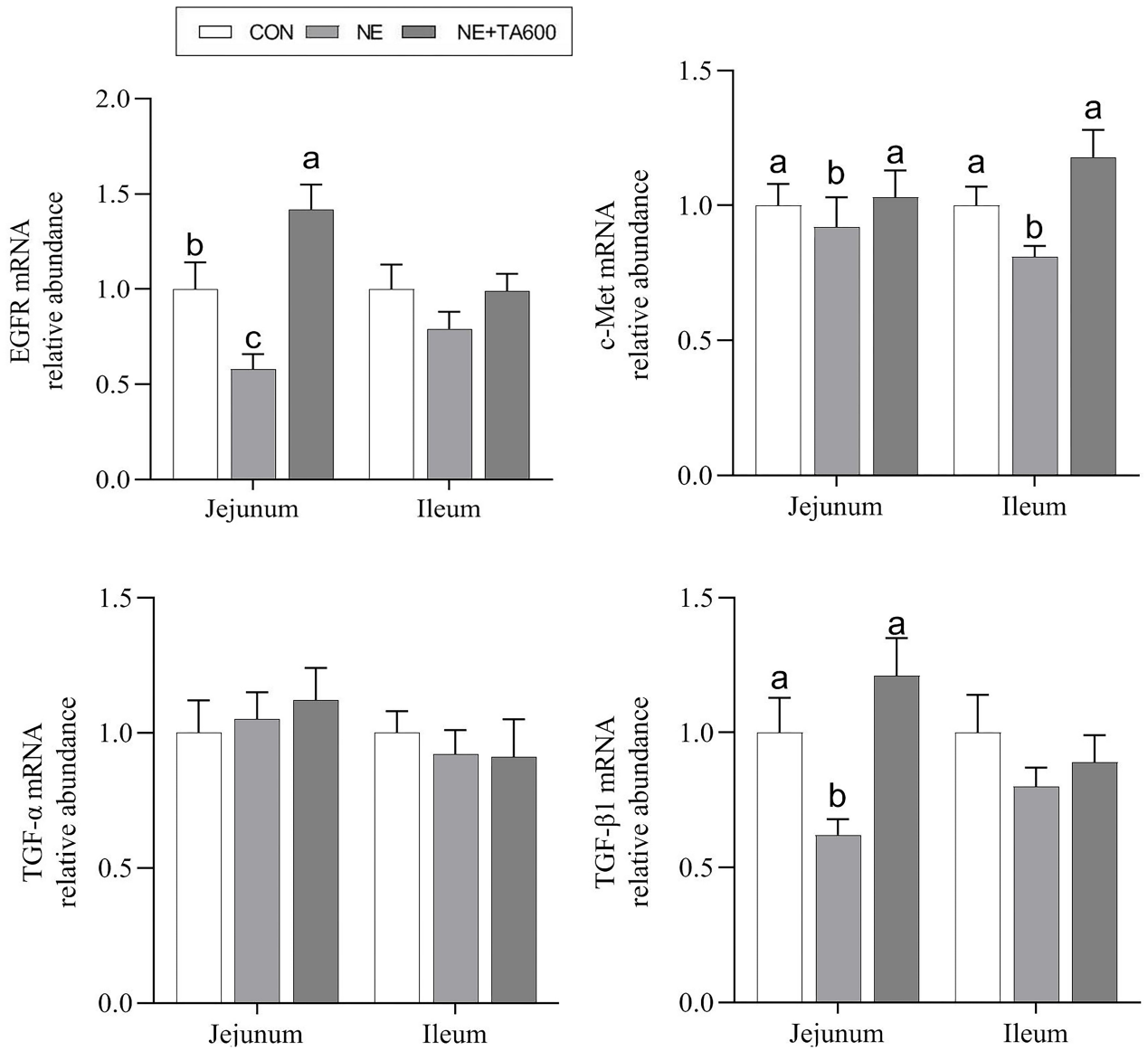

FIGURE 5 | Effects of TA on the mRNA abundance of intestinal mucosal repair factor of subclinical NE broilers. Values are means with their standard errors represented by vertical bars. $^{a-c}$Means within a row with different letters differ significantly ($p < 0.05$). EGFR, epidermal growth factor receptor; c-Met, c-mesenchymal epithelial transition factor; TGF-α, transforming growth factor-alpha; TGF-β1, transforming growth factor-beta 1.

where it is combined to the antioxidant response element to activate transcription of antioxidant genes. Similarly, it has been demonstrated that star anise oil could reduce the oxidative stress of birds during subclinical *Escherichia coli* challenges through upregulation of the Nrf2 signaling pathway (47). In addition, we found that NE infection resulted in vacuolization and swelling in the mitochondria, while TA administration improved that. Many lines of evidence indicate that mitochondria play a key role in preventing oxidative damage (48). Therefore, further research on the protective effects of TA on the subclinical NE-induced mitochondria dysfunction requires to be characterized.

Previous studies have widely reported that growth factors, including EGFR, TGF-β, and TGF-α, had positive impacts on epidermal repair and regeneration, inflammation, and proliferation (49–51). Alterations in the endogenous growth factors status are also correlated with poor clinical prognosis (52). In addition, the hepatocyte growth factor (HGF)/c-MeT signaling system may contribute to cell mobilization, tissue regeneration, and repair (53). Our results showed that dietary inclusion of TA elevated down-regulated mRNA abundance of jejunal and ileal c-Met, and jejunal EGFR and TGF-β1 in subclinical NE-infected birds. These data indicated that TA may have substantial repair effects on the damaged intestinal mucosa

induced by subclinical NE infection. The specific mechanism requires to be further characterized.

This study indicated that TA has promising potential treatment in subclinical NE in broilers. Prior to that, TA has been proven effective in animal and cell experimental models of a variety of diseases. Therefore, it may be worthwhile to further explore the pharmacological effects of TA in intestinal diseases of humans and animals.

CONCLUSION

The inclusion of 600 mg/kg of TA may be a promising tool to prevent and control subclinical NE by increasing intestinal antioxidant status and intestinal mucosal repair factor expression in broilers. The mechanisms by which TA exerts its antioxidant activity may be attributed to the activation of Nrf2 signaling pathway. Taken together, TA may be an effective agent to prevent and treat NE in poultry industry.

DATA AVAILABILITY STATEMENT

The original contributions presented in the study are included in the article/**Supplementary Material**, further inquiries can be directed to the corresponding author/s.

AUTHOR CONTRIBUTIONS

CY contributed to conceptualization, methodology, and writing—original draft. YT and QL contributed to investigation and supervision. TW contributed to supervision, project administration, and funding acquisition. ZY contributed to visualization, funding acquisition, writing, reviewing, and editing the manuscript. All authors contributed to the article and approved the submitted version.

FUNDING

This work was supported by the National Key Research and Development Program of China (Grant No. 2018YFD0501101).

SUPPLEMENTARY MATERIAL

The Supplementary Material for this article can be found online at: https://www.frontiersin.org/articles/10.3389/fvets.2022.877066/full#supplementary-material

REFERENCES

1. Engström BE, Fermér C, Lindberg A, Saarinen E, Båverud V, Gunnarsson A. Molecular typing of isolates of *Clostridium perfringens* from healthy and diseased poultry. *Vet Microbiol.* (2003) 94:225–35. doi: 10.1016/S0378-1135(03)00106-8
2. Prescott JF, Smyth JA, Shojadoost B, Vince A. Experimental reproduction of necrotic enteritis in chickens: a review. *Avian Pathol.* (2016) 45:317–22. doi: 10.1080/03079457.2016.1141345
3. Wade B, Keyburn A. The true cost of necrotic enteritis. *World Poult Sci J.* (2015) 31:16–7.
4. Cao L, Wu XH, Bai YL, Wu XY, Gu SB. Anti-inflammatory and antioxidant activities of probiotic powder containing *Lactobacillus plantarum* 1.2567 in necrotic enteritis model of broiler chickens. *Livest Sci.* (2019) 223:157–63. doi: 10.1016/j.livsci.2019.03.009
5. Park SS, Lillehoj HS, Allen PC, Park DW, FitzCoy S, Bautista DA, et al. Immunopathology and cytokine responses in broiler chickens coinfected with *Eimeria maxima* and *Clostridium perfringens* with the use of an animal model of necrotic enteritis. *Avian Dis.* (2008) 52:14–22. doi: 10.1637/7997-041707-Reg
6. Mitra S, Natarajan R, Ziedonis D, Fan XD. Antioxidant and anti-inflammatory nutrient status, supplementation, and mechanisms in patients with schizophrenia. *Prog Neuro Psychopharmacol Biol Psychiatry.* (2017) 78:1–11. doi: 10.1016/j.pnpbp.2017.05.005
7. Su WP, Zhang H, Ying ZX, Li Y, Zhou L, Wang F, et al. Effects of dietary L-methionine supplementation on intestinal integrity and oxidative status in intrauterine growth-retarded weanling piglets. *Eur J Nutr.* (2018) 57:2735–45. doi: 10.1007/s00394-017-1539-3
8. Sá NAR, Vieira LA, Ferreira ACA, Cadenas J, Bruno JB, Maside C, et al. Anethole supplementation during oocyte maturation improves *in vitro* production of bovine embryos. *Reprod Sci.* (2020) 27:1602–8. doi: 10.1007/s43032-020-00190-x
9. He L, He T, Farrar S, Ji LB, Liu TY, Ma X. Antioxidants maintain cellular redox homeostasis by elimination of reactive oxygen species. *Cell Physiol Biochem.* (2017) 44:532–53. doi: 10.1159/000485089
10. Galicka A, Kretowski R, Nazaruk J, Cechowska-Pasko M. Anethole prevents hydrogen peroxide-induced apoptosis and collagen metabolism alterations in human skin fibroblasts. *Mol Cell Biochem.* (2014) 394:217–24. doi: 10.1007/s11010-014-2097-0
11. Sheikh B, Pari L, Ayyasamy R, Ramasamy C. Trans-anethole, a terpenoid ameliorates hyperglycemia by regulating key enzymes of carbohydrate metabolism in streptozotocin induced diabetic rats. *Biochimie.* (2015) 112:57–65. doi: 10.1016/j.biochi.2015.02.008
12. Aprotosoaie AC, Costache II, Miron A. Anethole and its role in chronic diseases. *Adv Exp Med Biol.* (2016) 929:247–67. doi: 10.1007/978-3-319-41342-6_11
13. Wieczyńska J, Cavoski I. Antimicrobial, antioxidant and sensory features of eugenol, carvacrol and trans-anethole in active packaging for organic ready-to-eat iceberg lettuce. *Food Chem.* (2018) 259:251–60. doi: 10.1016/j.foodchem.2018.03.137
14. Yu CY, Wei JD, Yang CW, Yang ZB, Yang WR, Jiang SZ. Effects of star anise (*Illicium verum* Hook.f.) essential oil on laying performance and antioxidant status of laying hens. *Poult Sci.* (2018) 97:3957–66. doi: 10.3382/ps/pey263
15. Lee MS, Lee B, Park KE, Utsuki T, Shin T, Oh CW, et al. Dieckol enhances the expression of antioxidant and detoxifying enzymes by the activation of Nrf2-MAPK signaling pathway in HepG2 cells. *Food Chem.* (2015) 174:538–46. doi: 10.1016/j.foodchem.2014.11.090
16. Zhang H, Wang J, Liu Y, Sun B. Wheat bran feruloyl oligosaccharides modulate the phase II detoxifying/antioxidant enzymes via Nrf2 signaling. *Int J Biol Macromol.* (2015) 74:150–4. doi: 10.1016/j.ijbiomac.2014.12.011
17. Yu CY, Zhang JF, Zhang H, Chen YN, Wang C, Zhang LL, et al. Influence of trans-anethole on the nutrient digestibility and intestinal barrier function in broilers. *Poult Sci.* (2021) 100:101489. doi: 10.1016/j.psj.2021.101489
18. Liu D, Guo YM, Wang Z, Yuan JM. Exogenous lysozyme influences *Clostridium perfringens* colonization and intestinal barrier function in broiler chickens. *Avian Pathol.* (2010) 39:17–24. doi: 10.1080/03079450903447404
19. Zhang BB, Lv ZP, Li HX, Guo SS, Liu D, Guo YM. Dietary larginine inhibits intestinal *Clostridium perfringens* colonization and attenuates intestinal mucosal injury in broiler chickens. *Br J Nutr.* (2017) 118:321–32. doi: 10.1017/S0007114517002094
20. Ekim B, Calik A, Ceylan A, Saçakli P. Effects of *Paenibacillus xylanexedens* on growth performance, intestinal histomorphology, intestinal microflora, and immune response in broiler chickens challenged with *Escherichia coli* K88. *Poult Sci.* (2020) 99:214–23. doi: 10.3382/ps/pez460
21. Abudabos AM, Alyemni AH, Dafalla YM, Khan RU. The effect of phytogenics on growth traits, blood biochemical and intestinal histology in broiler chickens exposed to *Clostridium perfringens* challenge. *J Appl Anim Res.* (2018) 46:691–5. doi: 10.1080/09712119.2017.1383258

22. Kan LG, Guo FS, Liu Y, Pham VH, Guo YM, Wang Z. Probiotics *Bacillus licheniformis* improves intestinal health of subclinical necrotic enteritis-challenged broilers. *Front Microbiol.* (2021) 12:623739. doi: 10.3389/fmicb.2021.623739
23. Emami NK, Dalloul RA. Centennial review: recent developments in host-pathogen interactions during necrotic enteritis in poultry. *Poult Sci.* (2021) 100:101330. doi: 10.1016/j.psj.2021.101330
24. Jamroz D, Kamel C. Plant extracts enhance broiler performance. In non-ruminant nutrition: antimicrobial agents and plant extracts on immunity, health and performance. *J Anim Sci.* (2002) 80:41–6.
25. Freire RS, Morais SM, Catunda-Junior FEA, Pinheiro DCSN. Synthesis and antioxidant, anti-inflammatory and gastroprotector activities of anethole and related compounds. *Bioorgan Med Chem.* (2005) 13:4353–8. doi: 10.1016/j.bmc.2005.03.058
26. Kwiatkowski P, Grygorcewicz B, Pruss A, Wojciuk B, Dołęgowska B, Giedrys-Kalemba S, et al. The effect of subinhibitory concentrations of trans-anethole on antibacterial and antibiofilm activity of mupirocin against mupirocin-resistant *Staphylococcus aureus* strains. *Microb Drug Resist.* (2019) 25:1424–9. doi: 10.1089/mdr.2019.0101
27. Rezayat SM, Dehpour, A-R., Motamed SM, Yazdanparast M, Chamanara M, et al. Foeniculum vulgare essential oil ameliorates acetic acid-induced colitis in rats through the inhibition of NF-κB pathway. *Inflammopharmacol.* (2018) 26:851–9. doi: 10.1007/s10787-017-0409-1
28. Zhang S, Chen X, Devshilt I, Yun Q, Huang C, An LJ, et al. Fennel main constituent, trans-anethole treatment against LPS-induced acute lung injury by regulation of Th17/Treg function. *Mol Med Rep.* (2018) 18:1369–76. doi: 10.3892/mmr.2018.9149
29. Yi QY, Liu JX, Zhang YF, Qiao HZ, Chen F, Zhang SH, et al. Anethole attenuates enterotoxigenic *escherichia coli*-induced intestinal barrier disruption and intestinal inflammation via modification of TLR signaling and intestinal microbiota. *Front Microbiol.* (2021) 12:647242. doi: 10.3389/fmicb.2021.647242
30. Hafeez A, Männer K, Schieder C, Zentek J. Effect of supplementation of phytogenic feed additives (powdered vs. encapsulated) on performance and nutrient digestibility in broiler chickens. *Poult Sci.* (2016) 95:622–9. doi: 10.3382/ps/pev368
31. Goel G, Makkar HP, Becker K. Changes in microbial community structure, methanogenesis and rumen fermentation in response to saponin-rich fractions from different plant materials. *J Appl Microbiol.* (2008) 105:770–7. doi: 10.1111/j.1365-2672.2008.03818.x
32. Attia Y, Al-Harthi M, El-Kelawy M. Utilisation of essential oils as a natural growth promoter for broiler chickens. *Italian J Anim Sci.* (2019) 18:1005–12. doi: 10.1080/1828051X.2019.1607574
33. Rochat T, Bermúdez-Humarán L, Gratadoux JJ, Fourage C, Hoebler C, Corthier G, et al. Anti-inflammatory effects of Lactobacillus casei BL23 producing or not a manganese-dependant catalase on DSS-induced colitis in mice. *Microb. Cell. Fact*. (2007) 6, 22. doi: 10.1186/1475-2859-6-22
34. Cho HI, Kim, K-M., Kwak JH, Lee SK, Lee, et al. Protective mechanism of anethole on hepatic ischemia/reperfusion injury in mice. *J Nat Prod.* (2013) 76:1717–23. doi: 10.1021/np4004323
35. da Rocha BA, Ritter AMV, Ames FQ, Gonçalves OH, Leimann FV, Bracht L, et al. Acetaminophen-induced hepatotoxicity: preventive effect of trans-anethole. *Biomed Pharmacother.* (2017) 86:213–20. doi: 10.1016/j.biopha.2016.12.014
36. Rhee Y, Moon JH, Mo J, Pham T, Chung P. mTOR and ROS regulation by anethole on adipogenic differentiation in human mesenchymal stem cells. *BMC Cell Biol.* (2018) 19:12. doi: 10.1186/s12860-018-0163-2
37. Dongare V, Kulkarni C, Kondawar M, Magdum C, Haldavnekar V, Arvindekar A. Inhibition of aldose reductase and anti-cataract action of trans-anethole isolated from *Foeniculum vulgare* mill fruits. *Food Chem.* (2012) 132:385–90. doi: 10.1016/j.foodchem.2011.11.005
38. Yu ZW, Bao ZJ, Ruan QW, Ma YX. Oxi-inflamm-aging and its association with the polymorphism of ApoE genes. *Acta Physiol Sin.* (2013) 65:338–46.
39. Fattman CL, Chang LY, Termin TA, Petersen L, Enghild JJ, Oury TD. Enhanced bleomycin-induced pulmonary damage in mice lacking extracellular superoxide dismutase. *Free Radic Biol Med.* (2003) 35:763–71. doi: 10.1016/S0891-5849(03)00402-7
40. Chaudhari AK, Singh VK, Das S, Deepika SBK, Dubey NK. Antimicrobial, aflatoxin B_1 inhibitory and lipid oxidation suppressing potential of anethole-based chitosan nanoemulsion as novel preservative for protection of stored maize. *Food Bioprocess Tech.* (2020) 13:1462–77. doi: 10.1007/s11947-020-02479-w
41. Sá NAR, Bruno JB, Guerreiro DD, Cadenas J, Alves BG, Cibin FWS, et al. Anethole reduces oxidative stress and improves *in vitro* survival and activation of primordial follicles. *Braz J Med Biol Res.* (2018) 51:e7129. doi: 10.1590/1414-431x20187129
42. Singh G, Kapoor IPS, Singh P, de Heluani CS, Catalan CAN. Chemical composition and antioxidant potential of essential oil and oleoresins from anise seeds (*Pimpinella anisum* L.). *Int J Essent Oil Ther.* (2008) 2:122–30.
43. Senatore F, Oliviero F, Scandolera E, Taglialatela-Scafati O, Roscigno G, Zaccardelli M, et al. Chemical composition, antimicrobial and antioxidant activities of anethole-rich oil from leaves of selected varieties of fennel [*Foeniculum vulgare* Mill. ssp. vulgare var. azoricum (Mill.) Thell]. *Fitoterapia.* (2013) 90:214–9. doi: 10.1016/j.fitote.2013.07.021
44. Chainy GBN, Manna SK, Chaturvedi MM, Aggarwal BB. Anethole blocks both early and late cellular responses transduced by tumor necrosis factor: effect on NF-κB, AP-1, JNK. MAPK and apoptosis. *Oncogene.* (2000) 19:2943–50. doi: 10.1038/sj.onc.1203614
45. Amorati R, Foti MC, Valgimigli L. Antioxidant activity of essential oils. *J Agri Food Chem.* (2013) 61:10835–47. doi: 10.1021/jf403496k
46. Johnson JA, Johnson DA, Kraft AD, Calkins MJ, Jakel RJ, Vargas MR, et al. The Nrf2-ARE pathway: an indicator and modulator of oxidative stress in neurodegeneration. *Ann N Y Acad Sci.* (2008) 1147:61–9. doi: 10.1196/annals.1427.036
47. Ding X, Yang CW, Yang ZB, Ren XJ, Wang PP. Effects of star anise (*Illicium verum* Hook.f) oil on the nuclear factor E2-related factor 2 signaling pathway of chickens during subclinical *Escherichia coli* challenge. *Poult Sci.* (2020) 6:3092–101. doi: 10.1016/j.psj.2019.10.004
48. Lin MT, Beal MF. Mitochondrial dysfunction and oxidative stress in neurodegenerative diseases. *Nature.* (2006) 443:787–95. doi: 10.1038/nature05292
49. Zieske JD, Takahashi H, Hutcheon AE, Dalbone AC. Activation of epidermal growth factor receptor during corneal epithelial migration. *Invest Ophthalmol Vis Sci.* (2000) 41:1346–55. doi: 10.1007/s004170050379
50. Repertinger SK, Campagnaro E, Fuhrman J, El-Abaseri T, Yuspa SH, Hansen LA. EGFR enhances early healing after cutaneous incisional wounding. *J Invest Dermatol.* (2004) 123:982–9. doi: 10.1111/j.0022-202X.2004.23478.x
51. Lorente AF, Brooks SA, Vinageras EN, Alvarez MCB, Brito BW, Concepcion MT, et al. Effect of blockade of the EGF system on wound healing in patients vaccinated with CIMAvax® EGF. *World J Surg Oncol.* (2013) 11:275. doi: 10.1186/1477-7819-11-275
52. Arteaga CL. The epidermal growth factor receptor: from mutant oncogene in nonhuman cancers to therapeutic target in human neoplasia. *J Clin Oncol.* (2001) 19:32S—40S. doi: 10.1002/ijc.1442
53. Neuss S, Becher E, Wöltje M, Tietze L, Jahnen-Dechent W. Functional expression of HGF and HGF receptor/c-met in adult human mesenchymal stem cells suggests a role in cell mobilization, tissue repair, wound healing. *Stem Cells.* (2004) 22:405–14. doi: 10.1634/stemcells.22-3-405

Conflict of Interest: The authors declare that the research was conducted in the absence of any commercial or financial relationships that could be construed as a potential conflict of interest.

frontiers | Frontiers in Veterinary Science

ORIGINAL RESEARCH
published: 28 April 2022
doi: 10.3389/fvets.2022.880152

Assessment of the Endophytic Fungal Composition of *Lactobacillus plantarum* and *Enterococcus faecalis*-Fermented *Astragalus membranaceus* Using Single-Molecule, Real-Time Sequencing Technology

Liheng Zhang[1,2], *Xianghui Li*[2], *Xinghui Song*[1], *Chuanzhou Bian*[2], *Xiangtao Kang*[3], *Junqiang Zhao*[4], *Hongxing Qiao*[2*] and *Yanzhang Gong*[1*]

[1] Key Laboratory of Agricultural Animal Genetics, Breeding and Reproduction of Ministry of Education, College of Animal Science and Technology, Huazhong Agricultural University, Wuhan, China, [2] College of Veterinary Medicine, Henan University of Animal Husbandry and Economy, Zhengzhou, China, [3] College of Animal Science and Technology HAU, Henan Agricultural University, Zhengzhou, China, [4] Henan Tianhao Hongfa Biotechnology Co., Ltd., Zhengzhou, China

Endophytic fungus represents microorganisms existing within the healthy plant organs, which can significantly influence metabolic product production in plants, a process with great research value and broad prospects for development. To investigate the effect of fermentation with probiotic cultures on the endophytic fungal diversity and composition of *Astragalus membranaceus*, we used single-molecular, real-time sequencing (Pacific Biosciences) for 18S ribosomal RNA (rRNA) sequencing. The results showed that the endophytic fungi of *A. membranaceus* mainly belonged to *Aspergillus*, *Penicillium*, *Cystofilobasidium*, *Candida*, *Guehomyces,* and *Wallemia*. Furthermore, the endophytic fungal diversity and abundance of *A. membranaceus* were more variable after fermentation with *Enterococcus faecium and/or Lactobacillus plantarum*. Our data lays a solid and comprehensive foundation for further exploration of endophytic fungi from *A. membranaceus* as potential sources of functional compounds.

Keywords: *Astragalus membranaceus*, fermentation, endophytic fungi, SMRT sequencing, 18S rRNA

OPEN ACCESS

Edited by:
Kun Li,
Nanjing Agricultural University, China

Reviewed by:
Junqing Guo,
Henan Academy of Agricultural Sciences (HNAAS), China
Hua Zhang,
Guangdong Medical University, China
Zeeshan Ahmad Bhutta,
Chungbuk National University, South Korea

***Correspondence:**
Hongxing Qiao
zzmzqhx@163.com
Yanzhang Gong
poultry@mail.hzau.edu.cn

Specialty section:
This article was submitted to Veterinary Infectious Diseases, a section of the journal Frontiers in Veterinary Science

Received: *21 February 2022*
Accepted: *03 March 2022*
Published: *28 April 2022*

Citation:
Zhang L, Li X, Song X, Bian C, Kang X, Zhao J, Qiao H and Gong Y (2022) Assessment of the Endophytic Fungal Composition of Lactobacillus plantarum and Enterococcus faecalis-Fermented Astragalus membranaceus Using Single-Molecule, Real-Time Sequencing Technology. Front. Vet. Sci. 9:880152. doi: 10.3389/fvets.2022.880152

INTRODUCTION

Astragalus membranaceus (Fisch.)Bge. as part of one of the largest genera in the *Leguminosae* family, has been used as a traditional tonic for promoting digestion and metabolism, enhancing immunity, and accelerating injury/wound healing (1, 2).

Astragalus is a traditional Chinese herbal medicine that has been widely used by humans for hundreds of years. There are few studies on the use of *A. membranaceus* in livestock. With the rapid development of intensive livestock production, there is an urgent need for sustainable and environmentally friendly practices in this area. *A. membranaceus* is also utilized to be the supplementary agent in anti-tumor treatment, which exhibits diverse effects like anti-bacterium,

anti-virus, antioxidation, anti-inflammation, and hidroschesis. However, the extraction of *A. membranaceus*' functional ingredients is limited because of plant cell wall recalcitrance, while microbial fermentation offers a possibility to improve *A. membranaceus* utilization efficiency. Previous studies show that *A. membranaceus* fermentation by *Lactobacillus plantarum* (*L. plantarum*) and/or *Enterococcus faecium* (*E. faecium*) can increase *Astragalus* polysaccharides, flavonoids, and saponins contents, whereas *A. membranaceus* after fermentation has high microbial abundance and diversity (3). It can be speculated that the fermentation of *A. membranaceus* elevates the content of active components by affecting its endophytic fungi.

Microorganisms exist in almost all living and non-living niches on the earth, like in thermal vents, deep rocks, sediments, or under extreme conditions like marine habitats and deserts (4). Endophytes are microorganisms (mostly bacteria and fungi) that reside in plants during one part or the entire life cycle with no instigation of distinct infection symptoms or visible manifestation of diseases in their hosts (5, 6). Endophytic fungi are meiosporic or mitosporic ascomycetes and present great biological diversity, and at least one species exists in every plant (7). In addition, microorganisms also produce metabolites to promote development, repellents for pests and insects, protectors, and antibacterial agents to resist plant pathogens under conditions like stress (8, 9). Moreover, investigations have clearly demonstrated that plant survival and health are strongly dependent on their endophytes (10, 11). Endophytic fungi may generate specific secondary metabolites, and these may be utilized in fields like pharmaceutics and agriculture (8). Paclitaxel (Taxol), a commonly used antitumor agent, can be generated by *Taxus brevifolia* and subsequently *via Taxomyces andreanae* (also an endophytic fungus), which accounts for a distinct example for the production of endophyte-plant metabolites (4).

Recently, research mainly aimed to isolate endophytic fungi from *A. membranaceus* in China and examine their antimicrobial activities. Several reports have stated that *A. membranaceus* endophytic fungal species can generate diverse secondary metabolites with bioactivity (12). However, endophytic fungal species in fermented *A. membranaceus* have never been studied. Here, we aimed to detect and compare endophytic fungi in *A. membranaceus* under fermentation *via L. plantarum* and *E. faecium* by' single-molecular, real-time (SMRT) sequencing (Pacific Biosciences), the third next-generation sequencing platform.

MATERIALS AND METHODS

Fermented *Astragalus* Synthesis

Astragalus membranaceus dried roots were provided by Gansu Huisen Pharmaceutical Co., Ltd. (Minxian County, Gansu Province), whereas the isolation and preservation of *E. faecium* (CGMCC 1.130) and *L. plantarum* (CGMCC 1.557) were completed at the China General Microbial Species Preservation Center (CGMCC, Beijing, China). The preparation of fermented *A. membranaceus* was as previously reported (3). In short, *A. membranaceus* was first ground into powder and passed through the 100-mesh filter. Thereafter, we classified 10,000 g dried *A. membranaceus* powders into 4 groups: A, B, C, and D. This work inoculated group A by 10^6 colony-forming units (CFU)/g *E. faecium*, group B by 10^6 CFU/g *L. plantarum*, group C with 10^6 CFU/g *E. faecium* combined with *L. plantarum*, and group D by lactobacillus selector (agar) medium as a blank control. Each group had three replicates. Then, fermentation was carried out in plastic bags (35 × 45 mm, Zhejiang Jinhu Company, China), followed by vacuum pumping and sealing by vacuum packaging of the bags. Thereafter, the mixture was fermented under 37°C and anaerobic situation for a 6-day period for producing the fermented *A. membranaceus*. On the 6th day of fermentation, the four groups were sampled. Three repetitive samples were collected in each group and mixed into one sample for sequencing. This study labeled the samples as A, B, C, and D.

DNA Extraction

Four samples were collected from each group (200 mg each) after fermentation, followed by immediate freezing under −196°C to extract the DNA subsequently. Afterward, this study utilized the Qubit 2.0 fluorometer (Invitrogen, Carlsbad, CA, USA) for quantifying the DNA samples. We evaluated the quality of the extracted DNA through 0.8% agarose gel as well as 260/280 mm spectrophotometry. Before further analysis, the DNA extracted was preserved under −20°C. PCR was performed to amplify 18S ribosomal RNA (rRNA) of fungi, followed by being sequenced by SMRT barcodes using the primers below, 27F (5′-CCGTGTTTCAAGACGG-3′, forward) and 1492R (5′-CTTGGTCATATA GAGTAA-3′, reverse). The 25-μl amplification volume was prepared, containing 5 μl of 5 × GC buffer, 5 μl of 5 × reaction buffer, 2 μl of 2.5 mm dNTP, 2 μl DNA template, 1 μl of 10 μm reverse primer, 1 μl of 10 μm forward primer, 0.25 μl Q5 DNA polymerase, and 8.75 μLddH_2O. The PCR was implemented as follows: 2-min predenaturation step under 98°C; followed by 15-s under 98°C, 10-s under 55°C and 30-s under 72°C for 30 cycles; and eventual 5-min elongation under 72°C. The whole 18S rRNA length was sequenced by the Shanghai Passenger Company.

TABLE 1 | Estimated alpha-diversity indices of 18S ribosomal RNA (rRNA) gene libraries for four samples used for sequencing.

Sample	ACE	Chao 1	Shannon	Simpson
A	229.00	229.00	4.73	0.92
B	303.00	303.00	5.18	0.93
C	227.00	227.00	5.09	0.94
D	243.00	243.00	4.80	0.91

Astragalus membranaceus samples under fermentation with Enterococcus faecium (A), Lactobacillus plantarum (B), E. faecium + L. plantarum (C), and LBS (D) on day 6.

Abbreviations: *A. membranaceus*, *Astragalus membranaceus*; *L. plantarum*, *Lactobacillus plantarum*; *E. faecium*, *Enterococcus faecium*; SMRT, single-molecule, real-time; CFU, colony forming units; OTUs, operational taxonomic units; PCA, Principal component analysis.

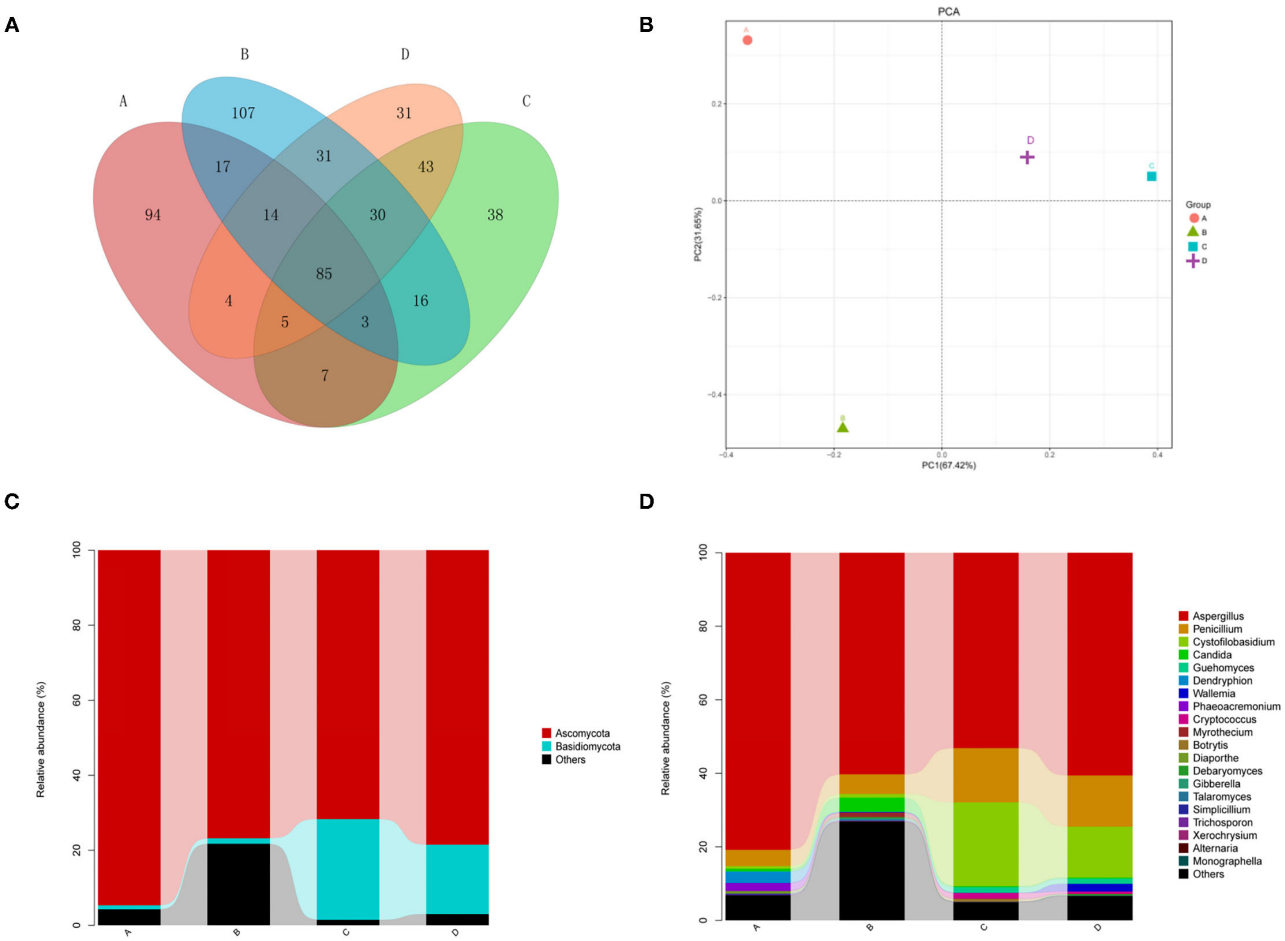

FIGURE 1 | (A) Venn diagram showing the distributions of operational taxonomic units (OTUs) across 4 groups. Astragalus membranaceus samples under fermentation with Enterococcus faecium. E. faecium (A), Lactobacillus plantarum (B), E. faecium + L. plantarum (C), and LBS (D) on day 6. **(B)** Two-dimensional principal component analysis plot of the samples. *A. membranaceus* samples under fermentation with *E. faecium* (A), *L. plantarum* (B), *E. faecium* + *L. plantarum* (C), and LBS (D) on day 6. **(C)** Phylum levels in samples. *A. membranaceus* samples under fermentation with *E. faecium* (A), *L. plantarum* (B), *E. faecium* + *L. plantarum* (C), and LBS (D) on day 6. **(D)** Genus levels in samples. *membranaceus* samples under fermentation with *E. faecium* (A), *L. plantarum* (B), *E. faecium* + *L. plantarum* (C), and LBS (D) on day 6.

Data Analysis

The original reads generated by cyclic consensus sequencing were used to render the accuracy of prediction up to 90%. We extracted high-quality sequences using the QIIME (Shanghai Personalbio Technology Co., Ltd, Shanghai, China) package (Quantitative Insights into Microbial Ecology, v1.8, https://docs.qiime2.org/2019.4/tutorials/) (13). In addition, we utilized USEARCH (Shanghai Personalbio Technology Co., Ltd, Shanghai, China) (v5.2.236, http://www.drive5.com/usearch/) for excluding chimeras and clustering the clean sequence data into operational taxonomic units (OTUs) at the similarity degree of 97% (14). Later, this work adopted UNITE fungal ITS database (https://unite.ut.ee/) for sequence comparison through blast search (15).

Moreover, ACE, Chao 1, Simpson, and Shannon indicators were utilized to estimate the alpha-diversity. The R software (Bell Lab, Lucent Technologies, Beijing, China) was also employed to classify data from 50 species with the highest abundances, later, the heat map was generated. This study also carried out principal component analysis (PCA) with R software (16).

The original sequence readings were imported into the National Center for Biotechnology Information Sequence Read Archive with accession No. SAMN07411593-SAMN07411601.

RESULTS

Diversity of Endophytic Fungal Species Originating From Fermented *A. membranaceus*

Full-length 18S rRNA gene was subject to SMRT sequencing for obtaining the precise fungal profiles from all four samples. We acquired altogether 99,923 sequence readings in the four samples, resulting in 24,980 readings per sample on average. Thereafter,

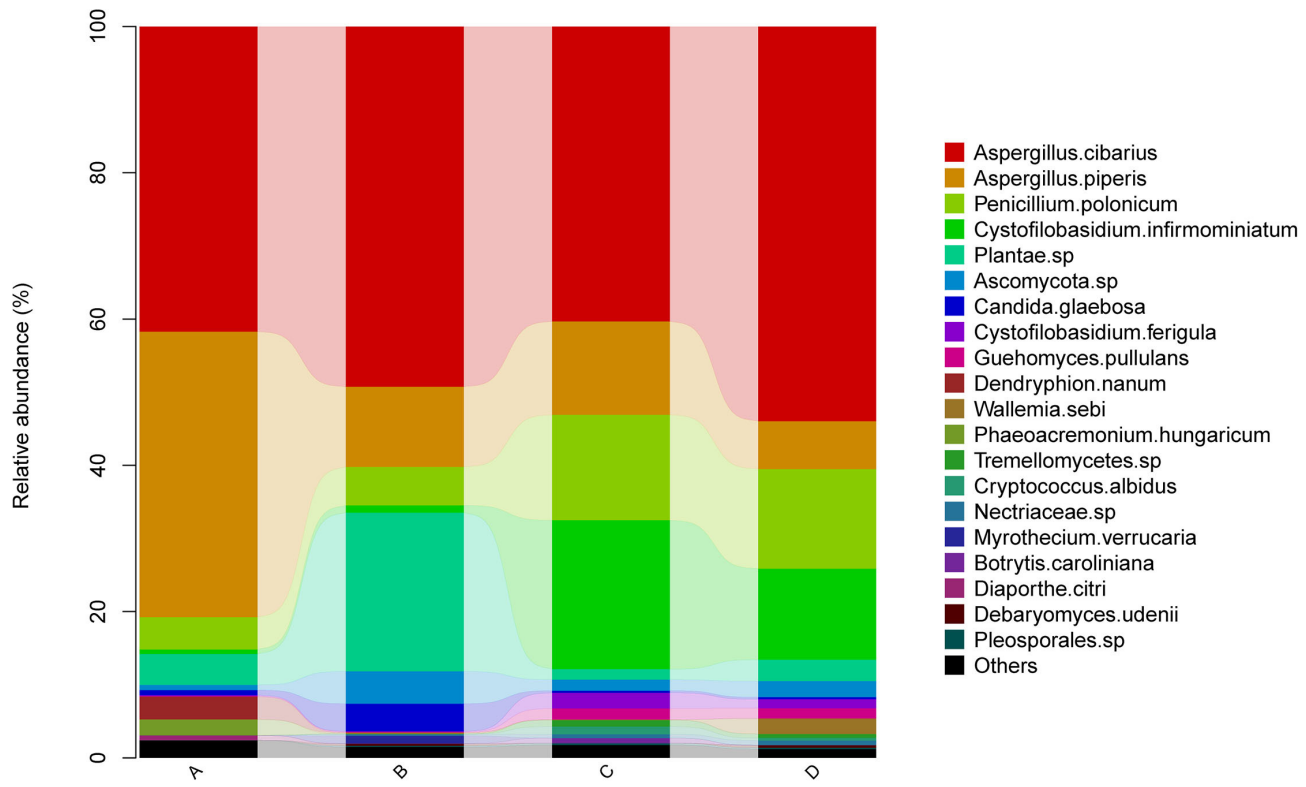

FIGURE 2 | Species levels in samples. *membranaceus* samples under fermentation with *E. faecium* (A), *L. plantarum* (B), *E. faecium* + *L. plantarum* (C), and LBS (D) on day 6.

this study determined Chao 1, ACE, Simpson, and Shannon indicators, together with the diversity of fungal species in each group is shown in **Table 1**. According to **Table 1**, Chao1, ACE, and Shannon indicators of group B were the highest, while the Simpson index showed little difference among the four groups.

Comparative Analysis

The comparative analysis of the total OTUs of groups A, B, C, and D was carried out (**Figure 1**). Altogether, 1,002 OTU types were detected from all groups, and 85 OTU types were common across them. Eighty-eight OTUs were common among groups A, B, and C, whereas 107, 160, and 163 OTU types of group D were specifically associated with groups A, B, and C, respectively.

Principal Component Analysis (PCA)

Two-dimensional PCA at the genus level was carried out for evaluating different fungal community structures among 4 groups (**Figure 1**). PC1/PC2 of the PCA at the genus level explained 67.42 and 31.65% of the total variation, separately. As revealed by PCA, all four groups were grouped separated, and groups C and D were closer than the others, indicating that the fungal communities of groups C and D were similar.

Phylum-Level Composition of the Endophytic Fungal Community

Our results showed that the dominant fungal phyla of *A. membranaceus* were *Ascomycota* and *Basidiomycota* (**Figure 1**). The abundances of *Ascomycota* in 4 groups were 94.7, 76.8, 71.7, and 78.5%. The abundances of *Basidiomycota* in the 4 groups were 1.1, 1.5, 26.9, and 18.5%. The abundances of unclassified phyla in the 4 groups were 4.2, 21.7, 1.4, and 2.9%. These results indicated that the fermentation of *A. membranaceus* by *L. plantarum* or *E. faecium* had a greater impact on endophytic fungi of *A. membranaceus*, with a significantly decreased abundance of *Basidiomycota*. Furthermore, *L. plantarum*-fermented *A. membranaceus* significantly increased the abundance of unclassified phyla.

Genus Level Compositions of the Endophytic Fungal Communities

According to **Figure 1**, the dominant fungal genera of *A. membranaceus* were *Aspergillus*, *Penicillium*, *Cystofilobasidium*, *Candida*, *Guehomyces*, and *Wallemia*. The abundances of *Aspergillus* in 4 groups were 80.8, 60.3, 53.1, and 60.6%. The abundances of *Penicillium* in the 4 groups were 4.4, 5.3, 14.7, and 13.9%. The abundances of *Cystofilobasidium* were.7, 1.0, 22.8, and 13.8%. The abundances of *Candida* were 0.7, 3.8, 0.3, and 0.3%. The abundances of *Guehomyces* were 0.1, 0.1, 1.5, and 1.4%. The abundances of *Wallemia* were 0.0, 0.2, 0.1, and 2.1%. The abundances of unclassified genera were 4.9, 26.1, 2.9, and 5.1%. The above results suggested that the fermentation of *A. membranaceus* by *E. faecium* increased the abundance of *Aspergillus*, while the fermentation of *A. membranaceus* by *E. faecium* or *L. plantarum* reduced the abundance of *Penicillium*

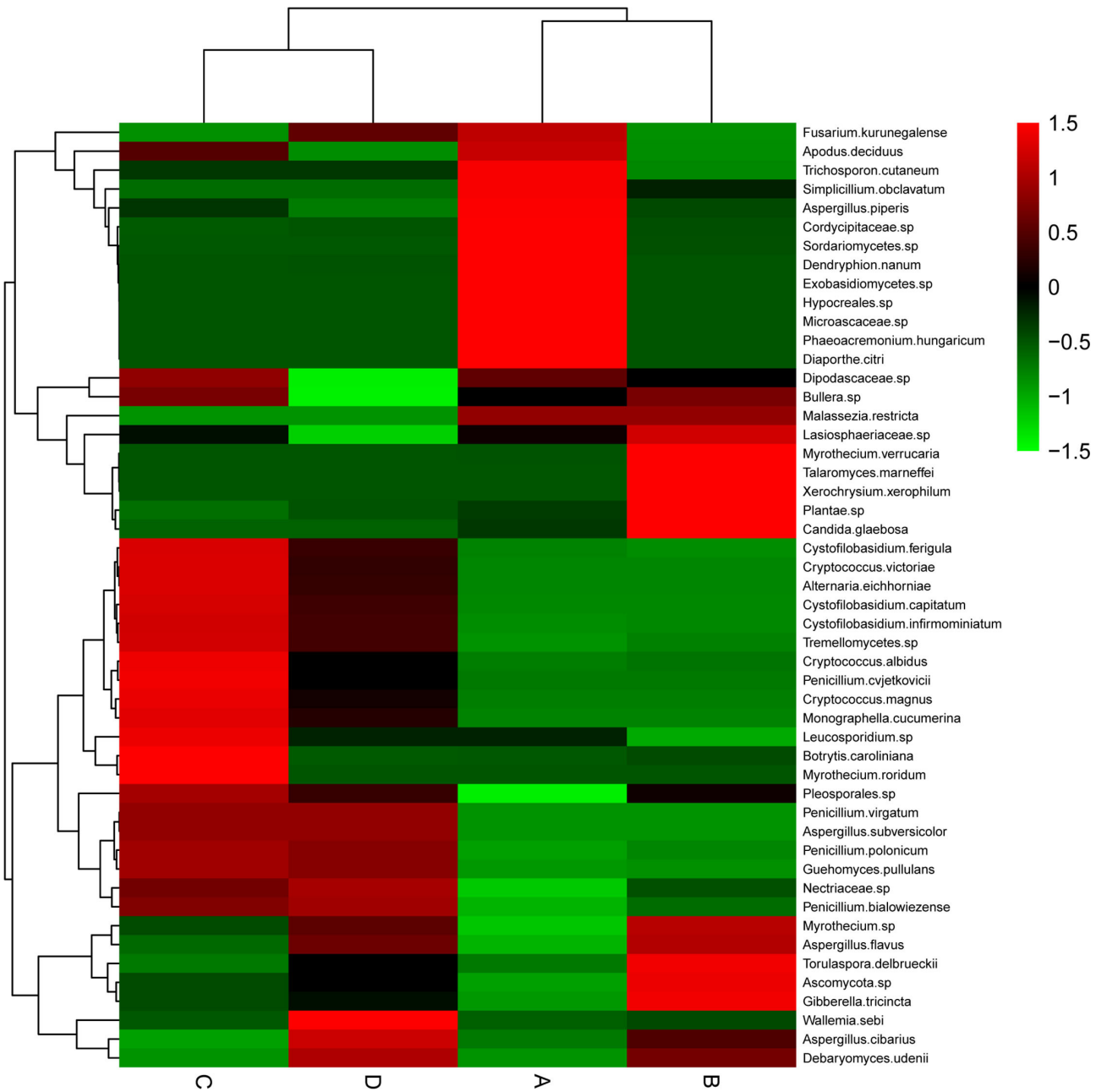

FIGURE 3 | Heat map of endophytic fungal community composition with cluster analysis. *A. membranaceus* samples under fermentation with *E. faecium* (A), *L. plantarum* (B), *E. faecium* + *L. plantarum* (C), and LBS (D) on day 6. Green and red colors stand for low and high abundances, respectively.

and *Cystofilobasidium*. Moreover, *L. plantarum*-fermentation of *A. membranaceus* significantly increased the abundance of unclassified genera.

Species-Level Compositions of the Endophytic Fungal Communities

Endophytic fungal species in *A. membranaceus* were mainly *Aspergillus cibarius*, *Aspergillus piperis*, *Penicillium polonicum*, *Cystofilobasidium infirmominiatum,* and *Plantae* sp (**Figure 2**). The abundances of *Aspergillus cibarius* in the 4 groups were 41.7, 49.3, 40.3, and 54.0%. The abundances of *Aspergillus piperis* were 39.1, 11.0, 12.8, and 6.5%. The abundances of *Penicillium polonicum* were 4.4, 5.3, 14.4, and 13.6%. The abundances of *Cystofilobasidium infirmominiatum* were 0.6, 1.0, 20.4, and 12.5%. The abundances of *Plantae* were 4.2, 21.7, 1.4, and 2.9%, respectively. The above results show that the fermentation of *A. membranaceus* by *E. faecium* mainly increased the abundance of *Aspergillus piperis* and reduced that of *Penicillium polonicum* and *Cystofilobasidium infirmominiatum*. Meanwhile, fermentation of *A. membranaceus* by *L. plantarum* reduced the abundance of

Penicillium polonicum and *Cystofilobasidium infirmominiatum* but increased that of *Plantae*.

Cluster Analysis

This study clustered those 50 species with the highest abundances by R software. As revealed by the heat map (**Figure 3**), the highly abundant species of fungi in groups A, B, and C were much better than those in group D. Group A had a higher abundance of *Trichosporon cutaneum*, *Simplicillium obclavatum*, *Aspergillus.piperis*, *Cordycipitaceae sp.*, *Sordariomycetes sp.*, *Dendryphion nanum*, *Exobasidiomycetes sp.*, *Hypocreales sp.*, *Microascaceae sp.*, *Phaeoacremonium hungaricum*, and *Diaporthe citri*. Group B had a higher abundance of *Myrothecium verrucaria*, *Talaromyces marneffei*, *Xerochrysium xerophilum*, *Plantae sp.*, *Candida glaebosa*, *Torulaspora delbrueckii*, *Ascomycota sp.*, and *Gibberella tricincta*. In group C, *Cryptococcus albidus*, *Penicillium cvjetkovicii*, *Cryptococcus magnus*, *Monographella cucumerina*, *Leucosporidium sp.*, *Botrytis caroliniana,* and *Myrothecium roridum* were the most abundant species. However, only *Wallemia sebiand* and *Aspergillus cibarius* were particularly abundant species in group D. The above results demonstrated that the endophytic fungal abundance of *A. membranaceus* can be changed by fermentation, and the change was closely related to the bacteria used for fermentation.

DISCUSSION

Endophytic fungi are extensively distributed within healthy plant organs, which are the critical parts in the plant micro-ecosystems during the long-term evolution, significantly influencing plant metabolite production and affecting medicinal plants-derived crude medicine quantity and quality (7). At present, the cultivation method is primarily adopted for investigating endophytic fungal diversity, but this method is limited by the low authenticity of endophytic fungal community composition. With the rapid development of sequencing technology, SMRT sequencing can more accurately describe microbial diversity (17). Previously, 16S rRNA gene-SMRT sequencing was conducted for analyzing *A. membranaceus* diversity fermented by *L. plantarum* and *E. faecium*. As a result, it was appropriate to assess fermented *A. membranaceus* quality using the SMRT sequencing system (3). For exploring how *E. faecium* and *L. plantarum* fermentation affected the endophytic fungi of *A. membranaceus*, 18S rRNA gene-SMRT sequencing was used for analyzing *A. membranaceus* fermented endophytic fungal composition and diversity.

Based on the ACE, Chao, and Shannon indices, *A. membranaceus* fermented by *L. plantarum* possessed the highest fungal community diversity. Furthermore, *A. membranaceus* fermented by *L. plantarum* exhibited the highest number of OTUs by sequencing, suggesting that *L. plantarum* fermentation increased the abundance of endophytic fungal diversity of *A. membranaceus*. In general, the endophytic fungal diversity of *A. membranaceus* was relatively low, independent of fermentation. Composition analysis of the endophytic fungal community showed that the dominant fungal phyla of *A. membranaceus* were *Ascomycota* and *Basidiomycota*, and the abundance of *Ascomycota* was increased by *E. faecium* fermentation and decreased by *E. faecium and L. plantarum* fermentation. However, *E. faecium and L. plantarum* fermentation increased the abundance of *Basidiomycota*. *Aspergillus* was the genus with the greatest relative abundance among the endophytic fungi of *A. membranaceus*. In Asian cuisines, *Aspergilli* represent the critical microorganisms that can enhance the flavors, nutrients, and textures of fermented foods (18). Moreover, the use of *Aspergillus* fungus for fermenting the native *A. membranaceus* significantly elevated phenolic levels of *A. membranaceus*; besides, *A. membranaceus* after fermentation displayed significantly increased antioxidation capacity (19). According to our results, the fermented *E. faecium* had markedly increased *Aspergillus* abundance. Overall, the results showed that fermentation can change the proportions of endophytic fungi of *A. membranaceus*, which might change the metabolite contents of *A. membranaceus* processed by fermentation.

A recent study on the saponins of *Dipsacus asperoides* showed that endophytic fungi from taproots generated metabolites with bioactivity close to plant hosts, and their quantity showed positive relation to *Dipsacus* saponin content (20).

Some studies used high-throughput sequencing technology to analyze and identify the endophytic fungal community of *A. membranaceus*, explored the diversity information of endophytic fungi of *A. membranaceus*, solved the limitations of non-culturable and low-abundance fungi that could not be detected in traditional methods, and provided a reference for the use of endophytic fungi in *A. mongholicus* for pure fermentation or mixed fermentation to transform glycosides in *Astragalus*.

High-throughput sequencing in this study may provide a partial answer to previous research demonstrating that the active substances of *A. membranaceus*, such as *Astragalus* polysaccharides, flavonoids, saponins, and organic acids, are changed by *L. plantarum and E. faecium* fermentation (3). Recently, endophytic fungi originating from *Astragalus* species have been used for the biotransformation of *Astragalus* sapogenins (21). *A. chinensis*-derived endophytic fungi are verified to be bactericides and fungicides (22). It is exciting to speculate that *Astragalus* polysaccharides or flavonoids may be obtained from the endophytic fungi that colonize *A. membranaceus*. Our findings provide evidence for this possibility.

In summary, 18S rRNA gene-SMRT sequencing was used for analyzing endophytic fungal composition and diversity from fermented *A. membranaceus*. Our study presents the most comprehensive data for a more extensive follow-up study.

DATA AVAILABILITY STATEMENT

The original contributions presented in the study are included in the article/supplementary material, further inquiries can be directed to the corresponding author/s.

AUTHOR CONTRIBUTIONS

YG and XK shouldered the responsibility of studying conception and design. LZ and XL were in charge of experiment implementation. XS and HQ were responsible for statistical analysis and were in charge of manuscript writing. JZ and CB isolated and preserved microbial strains. All authors revised the study and approved the final version for submission.

FUNDING

This work was supported by the Natural Science Foundation of Henan Province of China (202300410189), the Research and Innovation Team of Henan University of Animal Husbandry and Economy (2018KYTD13), and the Key Discipline of Preventive Veterinary Medicine of Henan University of Animal Husbandry and Economy (mxk2016102 and 2021HNUAHEDF004).

REFERENCES

1. Kim YB, Thwe AA Li X, Tuan PA, Lee S, Lee JW, et al. Accumulation of astragalosides and related gene expression in different organs of astragalus membranaceus Bge. var Mongholicus (Bge). *Molecules.* (2014) 19:10922–35. doi: 10.3390/molecules190810922
2. Wang X, Li Y, Shen J, Wang S, Yao J, Yang X. Effect of Astragalus polysaccharide and its sulfated derivative on growth performance and immune condition of lipopolysaccharide-treated broilers. *Int J Biol Macromol.* (2015) 76:188–94. doi: 10.1016/j.ijbiomac.2015.02.040
3. Qiao H, Zhang X, Shi H, Song Y, Bian C, Guo A. Assessment of the physicochemical properties and bacterial composition of Lactobacillus plantarum and Enterococcus faecium-fermented Astragalus membranaceus using single molecule, real-time sequencing technology. *Sci Rep.* (2018) 8:11862. doi: 10.1038/s41598-018-30288-x
4. Tanvir R, Javeed A, Bajwa AG. Endophyte bioprospecting in South Asian medicinal plants: an attractive resource for biopharmaceuticals. *Appl Microbiol Biotechnol.* (2017) 101:1831–44. doi: 10.1007/s00253-017-8115-x
5. Kouipou Toghueo RM, Boyom FF. Endophytic fungi from terminalia species: a comprehensive review. *J Fungi.* (2019) 5:43. doi: 10.3390/jof5020043
6. Strobel Gary A. Endophytes as sources of bioactive products. *Microbes and Infection.* (2003) 5:535–44. doi: 10.1016/S1286-4579(03)00073-X
7. Min J, Ling C, Hai-Liang X, Cheng-Jian Z, Khalid R, Ting H, et al. A friendly relationship between endophytic fungi and medicinal plants: a systematic review. *Front Microbiol.* (2016) 7:906. doi: 10.3389/fmicb.2016.00906
8. Golinska P, Wypij M, Agarkar G, Rathod D, Dahm H, Rai M. Endophytic actinobacteria of medicinal plants: diversity and bioactivity. *Antonie Van Leeuwenhoek.* (2015) 108:267–89. doi: 10.1007/s10482-015-0502-7
9. Ryan RP, Germaine K, Franks A, Ryan DJ. Dowling DNBacterial endophytes: recent developments and applications. *FEMS Microbiol Lett.* (2008) 278:1–9. doi: 10.1111/j.1574-6968.2007.00918.x
10. Hardoim PR, Van Overbeek LS, Berg G, Pirttilä AM, Compant S, Campisano A, et al. The hidden world within plants: ecological and evolutionary considerations for defining functioning of microbial endophytes. *Microbiol Molec Biol Rev.* (2015) 79:293–320. doi: 10.1128/MMBR.00050-14
11. Potshangbam M, Devi SI, Sahoo D, Strobel GA. Functional Characterization of Endophytic Fungal Community Associated with Oryza sativa L. and Zea mays L. *Front Microbiol.* (2017) 8:325. doi: 10.3389/fmicb.2017.00325
12. Xu YM, Espinosa-Artiles P, Liu MX, Arnold AE, Gunatilaka AL, Secoemestrin D. A Cytotoxic Epitetrathiodioxopiperizine and Emericellenes A–E, Five Sesterterpenoids from Emericella sp. AST0036, a Fungal Endophyte of Astragalus lentiginosus. *J Nat Prod.* (2013) 76:2330–2336. doi: 10.1021/np400762k
13. Caporaso JG, Kuczynski J, Stombaugh J, Bittinger K, Bushman FD, Costello EK, et al. QIIME allows analysis of high-throughput community sequencing data. *Nat Methods.* (2010) 7:335–6. doi: 10.1038/nmeth.f.303
14. Edgar RC. Search and clustering orders of magnitude faster than BLAST. *Bioinformatics.* (2010) 26:2460–1. doi: 10.1093/bioinformatics/btq461
15. Spouge JL. Towards a unified paradigm for sequence-based identification of fungi. *Molec Ecol.* (2013) 22:5271–7. doi: 10.1111/mec.12481
16. Lozupone C, Knight RJ. UniFrac: a new phylogenetic method for comparing microbial communities. *Appl Environ Microbiol.* (2005) 71:8228–35. doi: 10.1128/AEM.71.12.8228-8235.2005
17. Hestand MS, Ameur AJ. The versatility of SMRT sequencing. *Genes.* (2019) 10:24. doi: 10.3390/genes10010024
18. Park HS, Jun SC, Han KH, Hong SB Yu JH. Diversity, application, and synthetic biology of industrially important aspergillus fungi. *Adv Appl Microbiol.* (2017) 100:161–202. doi: 10.1016/bs.aambs.2017.03.001
19. Sheih IC, Fang TJ, Wu TK, Chang CH, Chen RY. Purification and properties of a novel phenolic antioxidant from radix astragali fermented by aspergillus oryzae M29. *J Agric Food Chem.* (2011) 59:6520–5. doi: 10.1021/jf2011547
20. Gong A, Zhou T, Xiao C, Jiang W, Zhou Y, Zhang J, et al. Association between dipsacus saponin VI level and diversity of endophytic fungi in roots of Dipsacus asperoides. *J Microbiol Biotechn.* (2019) 35:42. doi: 10.1007/s11274-019-2616-y
21. Ekiz G, Yilmaz S, Yusufoglu H, Ballar P, Bedir E. Microbial transformation of cycloastragenol and astragenol by endophytic fungi isolated from astragalus species. *Natural Products.* (2019) 82:2979–85. doi: 10.1021/acs.jnatprod.9b00336
22. Jahangir M, ILYAS S, Mazhar F, Abbasi MA, Usman MF, Rehman J, et al. Antimicrobial and Antioxidant Potential of Astragalus psilocentros Antimicrobial and Antioxidant Potential of Astragalus psilocentros. *Asian J Chem.* (2013) 25:175–80. doi: 10.14233/ajchem.2013.12859

Conflict of Interest: The authors declare that the research was conducted in the absence of any commercial or financial relationships that could be construed as a potential conflict of interest.

Publisher's Note: All claims expressed in this article are solely those of the authors and do not necessarily represent those of their affiliated organizations, or those of the publisher, the editors and the reviewers. Any product that may be evaluated in this article, or claim that may be made by its manufacturer, is not guaranteed or endorsed by the publisher.

frontiers | Frontiers in Veterinary Science

ORIGINAL RESEARCH
published: 29 April 2022
doi: 10.3389/fvets.2022.879857

Cangpu Oral Liquid as a Possible Alternative to Antibiotics for the Control of Undifferentiated Calf Diarrhea

Shengyi Wang, Dongan Cui, Yanan Lv, Zuoting Yan and Jiyu Zhang**

Key Laboratory of Veterinary Pharmaceutical Development of Ministry of Agriculture and Rural Affairs, Lanzhou Institute of Husbandry and Pharmaceutical Sciences of Chinese Academy of Agricultural Science, Lanzhou, China

Antibiotics are essential in the prevention of calf diarrhea epidemics. As more antibiotics become ineffective due to drug-resistant bacteria, attention must be directed toward alternative treatments for calf diarrhea. Natural antibiotic alternatives, such as Chinese herbal medicine, have become a research hotspot in the clinical treatment of diseases such as calf diarrhea due to their characteristics of fewer side effects, low cost, little residue, and no drug resistance. The Cangpu Oral Liquid (CP) was modified from a traditional herbal formula that had been widely used in ancient China to treat gastrointestinal diseases in animals. In order to evaluate the treatment effect of CP on neonatal calf diarrhea, a randomized controlled field trial was performed. Two hundred and forty-six diarrheal Holstein calves of 2–15 days old were selected and randomly divided into two treatment groups receiving either apramycin or CP. 101 out of 123 calves recovered from diarrhea in the CP group, whereas 77 out of 123 calves showed recovery after antibiotic therapy. There were no differences in initial weight between both groups, while the final weight was significantly different ($P = 0.892$, $P = 0.025$, respectively). The mean average daily gain (ADG) of calves (211.45 gram/day) in the CP group was significantly higher compared to the antibiotic group (164.56 gram/day) ($P = 0.001$). The CP group also showed a shorter recovery time from diarrhea (3.90 days vs. 6.62 days, $P = 0.001$). The current results indicate that the CP has a beneficial clinical effect on the treatment of diarrhea in neonatal calves and is an effective alternative treatment option.

Keywords: calf diarrhea, cangpu oral liquid, Chinese herbal medicine, randomized controlled trial, antibiotic alternative

OPEN ACCESS

Edited by:
Kun Li,
Nanjing Agricultural University, China

Reviewed by:
Khalid Mehmood,
Islamia University of Bahawalpur, Pakistan
Chenghong Xing,
Jiangxi Agricultural University, China
Jinli Wang,
Nanjing Agricultural University, China

****Correspondence:***
Shengyi Wang
wangshengyi@caas.cn
Jiyu Zhang
infzjy@sina.com

Specialty section:
This article was submitted to Veterinary Infectious Diseases, a section of the journal Frontiers in Veterinary Science

Received: *20 February 2022*
Accepted: *08 April 2022*
Published: *29 April 2022*

Citation:
Wang S, Cui D, Lv Y, Yan Z and Zhang J (2022) Cangpu Oral Liquid as a Possible Alternative to Antibiotics for the Control of Undifferentiated Calf Diarrhea. Front. Vet. Sci. 9:879857. doi: 10.3389/fvets.2022.879857

INTRODUCTION

The yearly survival calf ratio always measures the proliferation and development of cattle industries (1). However, the earlier onset of diarrhea in neonatal calf has been detrimental to the industry and affected their products worldwide. Neonatal calf diarrhea is a serious disease with a complex etiopathogenesis, high morbidity, and mortality, causing huge economic loss in beef or dairy farms (2). According to the literature, diarrhea or other digestive problem almost accounted for 14% of death in calf under 3 weeks and 23% of deaths in calf over 3 weeks (3). Environmental stress, management style, nutritional state, immune status, and enteric pathogens are major risk factors of calf diarrhea (4). The mostly reported

enteric pathogens were bovine rotavirus (BRV), bovine coronavirus (BCoV), *Escherichia (E.) coli* and *Cryptosporidium (C.) parvum* (5). Other infectious agent such as bovine viral diarrhea virus (BVDV), *Salmonella (S.) enteric, Clostridium (C.) perfringens*also were detected in fecal samples (6). Harsh weather conditions such as uncomfortable temperatures, rain, wind, and poor hygiene conditions could increase the susceptibility of calves to diarrhea (7). The quality and quantity of colostrum are also associated with the occurrence of calf diarrhea (8).

Antibiotics is a major way to prevent calf diarrhea outbreaks and have been used without being guided most of the time (9). Due to the widespread use of antimicrobials in animal husbandry, the possibility of cross-resistance between human and animal pathogens has aroused much public concern (10). Thus, the use of antibiotics is in a dilemma situation due to the occurrence of antimicrobial resistance. Antibiotic susceptibility testing is the main strategy to guide clinical antibiotic use (11). However, fecal bacterial species do not accurately mirror the intestinal bacterial species, and the breakpoints of susceptibility test results have not been reproducible (12). Therefore, it is urgent to develop alternative strategies to address this disease in calves. Some alternative treatments for diarrhea have been studied recently, including zinc, crofelemer, lactoferrin, cinnamaldehyde, and bacteriophages targeting enteropathogens (13–17). Ethnoveterinary or Chinese herbal medicine has become a research hotspot in the clinical treatment of diseases such as calf diarrhea due to its characteristics of fewer side effects, low cost, almost no residue, and no drug resistance (18–20).

Ethnoveterinary medicines play a pivotal role in animal health care worldwide, and medicinal plants are always used to treat calf diarrhea (21–25). Traditional Chinese Veterinary Medicine (TCVM), which has also been used to treat all kinds of animal diseases for centuries, may also be an ideal option for an antibiotic alternative for neonatal diarrhea. Cangpu oral liquid (CP) was a modified preparation from the classic TCVM formula of pingwei powder, which was first documented in the Yuan-heng-liao-ma-ji and widely employed to treat gastrointestinal diseases in animals. According to TCVM theory, CP was used to treat diarrhea with the syndrome of cold-dampness encumbering the spleen, and the function of which was warming the interior to dissipate cold, astringing the intestines and check diarrhea. A preliminary experiment indicated that the CP had a good therapeutic effect on calf diarrhea. This study evaluates the efficacy and potential as an antibiotic alternative of the CP in field cases of undifferentiated calf diarrhea.

MATERIALS AND METHODS

CP Preparations

The formula of CP is composed of five herbs (80 g of *Atractylodis Rhizoma*, 60 g of *Magnoliae Officinalis Cortex*, 50 g of *Coptidis Rhizoma*, 50 g of *Psoraleae Fructus*, 60 g of *Mume Fructus*), and all these herbs were purchased from Hui Ren Tang Chinese Medicine Co., Ltd. (Lanzhou, China). The quality of the herbs meets the Veterinary Pharmacopeia of the People's Republic of China (Chinese Veterinary Pharmacopoeia Commission, 2015). After pre-processing with washing, drying, and chopping, the mixed herbs were boiled three times for 1.5 h each time with 10 times purified water of the total herbal weight. The extract was collected and concentrated to 300 mL by boiling, resulting in a final concentration of 1.0 g crude herb/mL for the experiment.

Study Population

All experiment procedures were approved by the Ethics Committee of Lanzhou Institute of Husbandry and Pharmaceutical Sciences of the Chinese Academy of Agricultural Sciences (Approval No. LZMY 20021-0015). The clinical trial was conducted from May to July 2021 in the Reproduction and Breeding Demonstration Center of Chinese Holstein Dairy Cow of Gansu Province (36°19′N, 103°18′E), where reared approximately 5000 Holstein calves, 2000 of which were of pre-weaning age. Within 4h after birth, all calves were fed 4 L of colostrum with optimum quality by suckling or via the oro-esophageal feeder. The colostrum was collected within 1 to 2 h after calving and all calves were moved to individual outdoor hutches within 24 h of birth.

The study was devised to provide sufficient statistical power to achieve a difference in diarrhea resolution between groups. Based on the preliminary results, a 63% cure rate in the antibiotic group and a 80% cure rate in the CP group, 110 animals per group would provide sufficient power (0.80) to detect a significant difference at $\alpha = 0.05$. Allowing for a 10% loss to follow-up, more than 244 calves should be included and assigned to the two groups in this trial.

Enrollment/Exclusion Criteria

All calves were visually observed each morning by one of the co-authors during the first 15 days of life. The fecal consistency scores and dehydration scores were recorded according to previously described methods. Briefly, fecal scores were graded as follows: 1 (formed), 2 (semi-formed pasty), 3 (loose but stays on top of the bedding), or 4 (watery diarrhea that sifts through the bedding). Dehydration scores were recorded as 1 (no signs of dehydration), 2 (mild depression, skin tent in the neck region of 2–6 s, recessed eyes), 3 (skin tent >6 s, very recessed eyes, and the calf disinclined or reluctant to get up), or 4 (calf will not stand, skin does not flatten when tented) (26). Pre-weaning calves were enrolled if they developed diarrhea (fecal scores of 3 or 4) for the first time. Calves were rejected from the study if they had serious dehydration (dehydration score >2) or symptoms of disease other than diarrhea, such as an umbilical abscess, pneumonia, or meningitis, or if they needed immediate antibiotic therapy.

Study Design and Treatment Protocol

This study was devised as a randomized controlled trial. After enrollment, calves were sequentially randomized to one of two treatment groups in bulks that ranged from 2 to 15 calves according to the number of calves qualified at each enrollment day by using random-number generated by Microsoft Excel (Microsoft Crop., Redmond, WA). To limit the awareness of the investigator to assessment assignment, treatment allocation, administration was performed by one co-author and the data recording and treatment assessment were carried out by another co-author who was blinded for the treatment until the

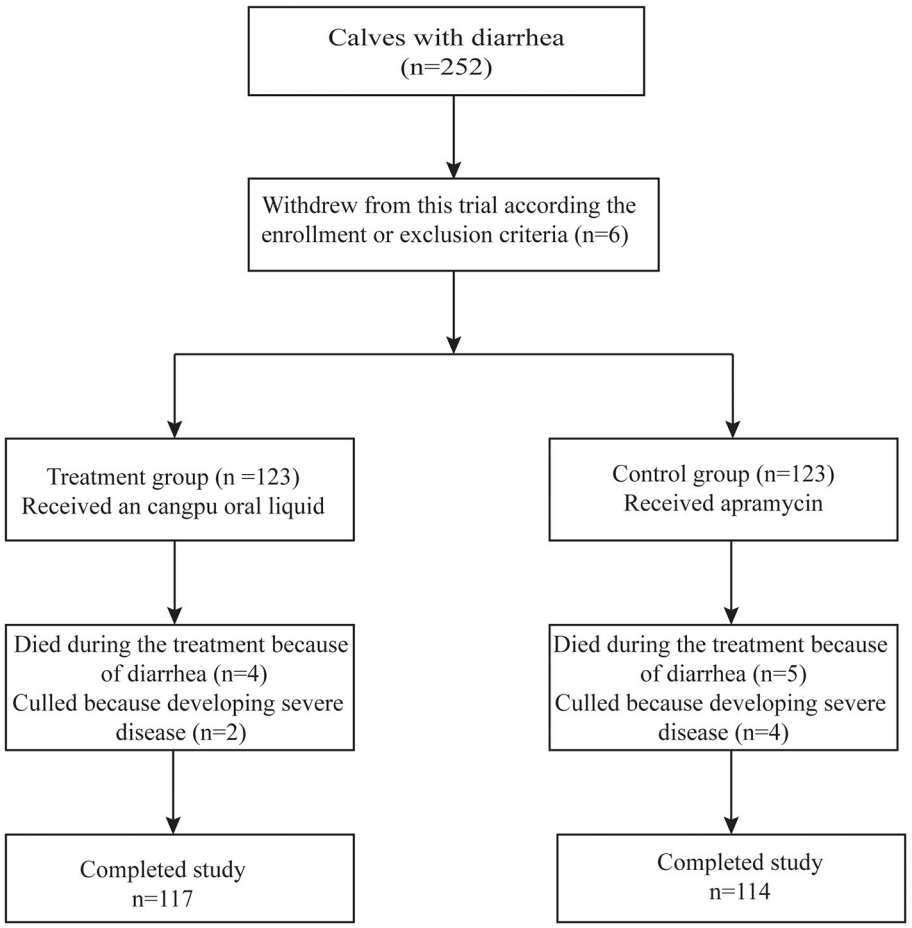

FIGURE 1 | Flow diagram showing the calves affected with diarrhea, randomization of calf with diarrhea, reasons for excluding calf from analyses, and completed study for statistical analysis.

completion of the trial. Calves received twice daily an oral dose of 100 mL of CP or twice daily an oral dose of 12 mg/kg of apramycin for four consecutive days. When calves had a fecal score of 1 or 2, a dehydration score of 1 in 2 consecutive days, they were regard as clinically cured.

Data Collection

Upon enrollment, the baseline characteristics of each calf were recorded including age, fecal scores, and dehydration scores. Calves were weighed respectively using a digital scale at enrollment and exit (day 10). Scale weights were not available for the first 10d of the study, and these calves were excluded from the analysis portion. Each calf received a complete physical examination each day and a maximum of 10 d following enrollment, or until calves had normal clinical parameters for two consecutive days. The fecal scores, dehydration scores, suck reflex, and other clinical abnormalities were recorded during the physical examination Disease duration was described as the number of days between enrollment and the first day when the calf was defined as clinically cured. Calves were culled if farm staff regarded that the severity of the disease needed other treatment.

Statistical Analysis

Means, proportions, and standard errors were displayed for baseline characteristics of calf diarrhea cases. General Linear Model (GLM) was used to testfor differences between treatment groups in weight at enrollment, final weight, and average daily gain (ADG). The differences in the proportion of calves with a fecal score of 4 or a dehydration score of 2 were tested by a chi-squared test. A nonparametric ANOVA (Kruskal-Wallis test) was used to compare age at enrollment between groups. Kaplan–Meier analysis was used to determine differences between groups in disease duration. Calves were right-censored if they died, culled, or had a fecal score >2 at exit (day 10). A Cox Proportional Hazard (PH) regression analysis estimated the hazard ratio for treatment. The proportional hazard assumption that clinical cure hazard is independent of time was assessed using each treatment group's log-minus-log (LML) survival plots. Statistical significance of the model parameters was tested using the Wald Chi-Square test.

TABLE 1 | The characteristics of calves in a randomized clinical trial on the effect of CP and apramycin on the treatment of calves for diarrhea.

Item	CP	apramycin	SE	*P*-value
Mean age (*d*)	5.80	6.20	0.310	0.192
Calves with fecal score = 4[% (*n*)]	46.3	41.5	/	0.779
Calves with dehydration score = 2[% (*n*)]	61.8	59.3	/	0.755
Day 1 weight (kg)	43.14	43.17	0.177	0.892
Day 10 weight (kg)	45.26	44.81	0.198	0.025
10-d ADG (g/d)	211.45	164.56	5.23	0.001

RESULTS

Enrollment

Two hundred and fifty two (252) calves were enrolled according to the inclusion criteria (126 calves in each group). Six calves were excluded from the trial including three calves in the CP group (two died immediately after enrollment and another one was enrolled with pneumonia) and three calves in the control group (all were enrolled with serious systemic disease and were unable to drink milk). All of the 246 calves included in this study, 15 died or were culled in the following 10 d: four died and two were culled in the CP group while five died and four were culled in the control group. **Figure 1** shows the disposition of the enrolled calves.

Baseline Comparison

The result of baseline comparisons showed that there were no significant differences in age ($P = 0.192$), initial weight ($P = 0.892$), percent with an initial fecal score of 4 ($P = 0.779$), and percent with an initial dehydration score of 2 ($P = 0.755$) between the two treatment groups at enrollment (**Table 1**).

Weight Measurements

Body weight at exit was weighed for 117 and 114 calves in the CP and control treatment groups, respectively (**Table 1**). The final body weight of the CP group was significantly better than that of the control group ($P = 0.002$), and the mean ADG of calves in the CP group (211.45 g/d) was significantly ($P = 0.001$) better than the control group (164.56 g/d) (**Figure 2**).

Clinical Cure

In the present study, 101 of 123 calves recovered from diarrhea following the treatment with CP, whereas 77 of 123 calves showed recovery after apramycin therapy. The mean days to recovery from diarrhea of calves between the two group were significant differences ($P = 0.001$) (**Figure 3**). The CP group showed a shorter recovery time from diarrhea (3.90 days vs.6.62 days, $P = 0.001$).

Based on the Cox Proportional Hazard (PH) regression analysis, the interaction between the two groups and initial fecal score, age, and weight was not significant ($P > 0.05$). Cox Proportional Hazard (PH) regression analysis also suggests that the initial fecal score of 3 or 4 had no significant interaction with the calf recovery from diarrhea (HR=1.116). Calves treated with CP had 2.923 times higher of a clinical cure at exitcompared to calves in the control group ($P = 0.002$).

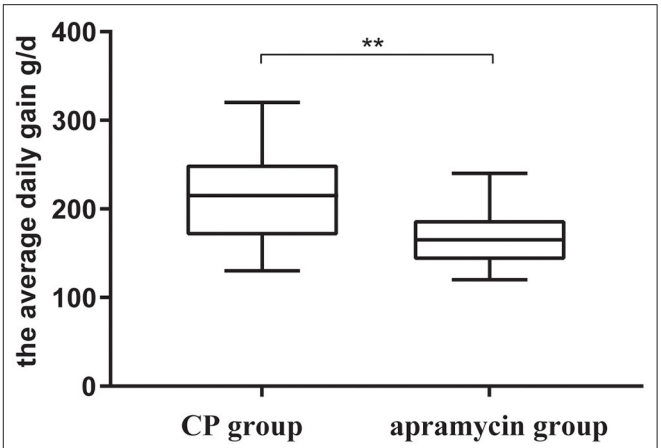

FIGURE 2 | The average daily gain of the calves at enrollment and exit received a twice daily oral dose of 100 ml per time of CP or a twice daily oral dose of 12 mg/kg per time of apramycin, $^{**}p < 0.01$.

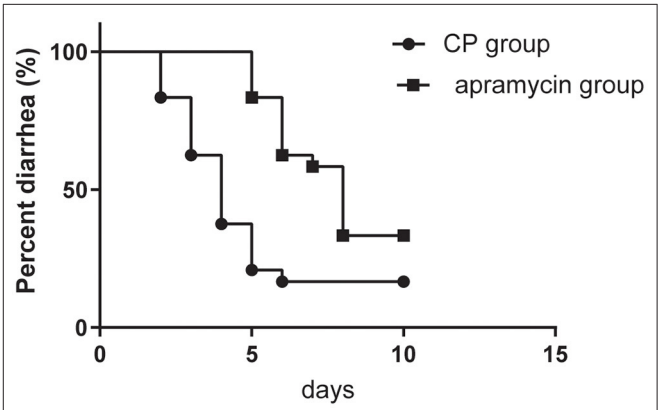

FIGURE 3 | Kaplan-Meier survival curve describing the time needed for recovery after the onset of diarrhea at the 123 diarrheal calves in the group of calves receiving CP and at the 123 diarrheic calves receiving apramycin treatment.

DISCUSSION

Randomized controlled trials are necessary to evaluate the effectiveness of alternatives to conventional therapies with antibiotics (15). Due to the misuse of antibiotics in the livestock industry, the possible cross-resistance between human and animal pathogens has attracted wide public concern. Antimicrobials have been reported to alter intestinal flora and function by depletion of the lumen down to the layer of the organism (27). The adoption of rapid antibiotic susceptibility testing is often used to guide clinical antibiotic usage (28). However, reports indicated that fecal bacterial culture and antimicrobial susceptibility testing were not recommended in calves with diarrhea because fecal bacterial populations do not accurately reflect small intestinal or blood bacterial populations (29). In addition, the breakpoints for susceptibility test results have not been validated (12). Therefore, alternative treatments

to antimicrobial have been investigated for many years. The CP used in this study was modified from a traditional herbal formula that had been widely used in ancient China. Medical literature suggests that apramycin significantly decreased the mortality rate in calves treated at 20 mg/kg PO q24h for 5 days (mortality 9%, $P < 0.01$) or 40 mg/kg PO q24h (mortality 6%, $P < 0.01$) when compared with untreated controls (mortality 30%) (11). In this trial, calves treated with CP had a higher clinical cure at exit compared to the controls and the CP could improve short-term outcomes of the diarrheal calves in weight gain and disease duration. It suggested that the CP had a beneficial effect on calf diarrhea as a treatment option under field conditions.

Calf diarrhea severely affects calf growth and subsequent production performance. The loss of water content and disease duration could aggravate the loss of water of the calf suffering from diarrhea to some extent. Hartmann and Reder described that calves suffering from watery diarrhea can lose up to 21% of their body weight (30). Oral electrolyte administration is the main way to prevent severe dehydration induced by secretory diarrhea. These results suggest the CP may be a better option for calves with more watery diarrhea (fecal score=4) and could reduce disease duration. Nonetheless, additional studies are necessary to validate the findings and explore potential mechanisms for the effect of CP on calf diarrhea.

In addition to promoting the selection of antimicrobial resistance in enteric bacteria, many antimicrobial agents produce adverse effects on small intestinal absorption function and normal intestinal flora, which affects the growth of animals (31, 32). Therefore, growth performance is an important indicator to evaluate the efficacy of drug therapy. In the current study, the average daily gain was significantly higher in the CP group (211.45 g/d) when compared with the control group (164.56 g/d). This difference in average daily weight gain may be associated with a shorter duration of disease.

CONCLUSION

This randomized clinical trial indicates that CP has a beneficial clinical effect for treatment of diarrhea in neonatal calves compared to apramycin treatment based on (1) a higher clinical cure rate, (2) a shorter duration of disease, and (3) A superior weight gain. Therefore, CP might represent a potentially effective alternative treatment option for calf diarrhea having several other advantages over antibiotic treatment.

DATA AVAILABILITY STATEMENT

The original contributions presented in the study are included in the article/**Supplementary Material**, further inquiries can be directed to the corresponding author/s.

ETHICS STATEMENT

The animal study was reviewed and approved by the Institutional Animal Care and Use Committee of Lanzhou Institute of Husbandry and Pharmaceutical Sciences of the Chinese Academy of Agricultural Sciences.

AUTHOR CONTRIBUTIONS

SW and JZ: conceptualization. DC: methodology, investigation, and data curation. YL: formal analysis. SW: writing—original draft preparation and funding acquisition. ZY: writing—review and editing. JZ: supervision and project administration. All authors have read and agreed to the published version of the manuscript.

FUNDING

This research was funded by National Natural Science Foundation of China (32172902); Key Research and Development Program of Gansu Province (20YF8NA028) and Innovation and Entrepreneurship Talent Project of Lanzhou (2018-RC-91).

ACKNOWLEDGMENTS

The authors would like to thank the Key Laboratory of Veterinary Pharmaceutical Development of Ministry of Agriculture and Rural Affairs, Key Laboratory of New Animal Drug Project of Gansu Province and Engineering and the Technology Research Center of Traditional Chinese Veterinary Medicine of Gansu Province personnel for their contribution to the project.

SUPPLEMENTARY MATERIAL

The Supplementary Material for this article can be found online at: https://www.frontiersin.org/articles/10.3389/fvets.2022.879857/full#supplementary-material

REFERENCES

1. Cooke RF, Daigle CL, Moriel P, Smith SB, Tedeschi LO, Vendramini JMB. Cattle adapted to tropical and subtropical environments: social, nutritional, and carcass quality considerations. *J Anim Sci.* (2020) 98:20. doi: 10.1093/jas/ska a014
2. Li XZ, Yan CG, Zan LS. Current situation and future prospects for beef production in China—a review. *Asian Australas J Anim Sci.* (2018) 31:984–91. doi: 10.5713/ajas.18.0212
3. Maier GU, Breitenbuecher J, Gomez JP, Samah F, Fausak E, Van Noord M. Vaccination for the prevention of neonatal calf diarrhea in cow-calf operations: a scoping review. *Vet Anim Sci.* (2022) 15:12. doi: 10.1016/j.vas.2022.100238
4. Al Mawly J, Grinberg A, Prattley D, Moffat J, Marshall J, French N. Risk factors for neonatal calf diarrhoea and enteropathogen shedding in New Zealand dairy farms. *Vet J.* (2015) 203:155–60. doi: 10.1016/j.tvjl.2015.01.010
5. Wei XJ, Wang WW, Dong Z, Cheng FS, Zhou XZ Li B, et al. Detection of infectious agents causing neonatal calf diarrhea on two large dairy farms in Yangxin County, Shandong Province, China. *Front Vet Sci.* (2021) 7:7. doi: 10.3389/fvets.2020.589126
6. Cho YI, Yoon KJ. An Overview of calf diarrhea—infectious etiology, diagnosis, and intervention. *J Vet Sci.* (2014) 15:1–17. doi: 10.4142/jvs.2014.15.1.1

7. Larson RL, Tyler JW. Reducing calf losses in beef herds. *Vet Clin N Am-Food Anim Pract*. (2005) 21:569. doi: 10.1016/j.cvfa.2005.02.009
8. Meganck V, Hoflack G, Opsomer G. Advances in prevention and therapy of neonatal dairy calf diarrhoea: a systematical review with emphasis on colostrum management and fluid therapy. *Acta Vet Scand.* (2014) 56:8. doi: 10.1186/s13028-014-0075-x
9. Eibl C, Bexiga R, Viora L, Guyot H, Felix J, Wilms J, et al. The antibiotic treatment of calf diarrhea in four European Countries: a survey. *Antibiotics-Basel.* (2021) 10:17. doi: 10.3390/antibiotics10080910
10. Ali A, Liaqat S, Tariq H, Abbas S, Arshad M, Li WJ, et al. Neonatal calf diarrhea: a potent reservoir of multi-drug resistant bacteria, environmental contamination and public health hazard in Pakistan. *Sci Total Environ.* (2021) 799:9. doi: 10.1016/j.scitotenv.2021.149450
11. Smith G. Antimicrobial decision making for enteric diseases of cattle. *Vet Clin N Am-Food Anim Pract*. (2015) 31:47. doi: 10.1016/j.cvfa.2014.11.004
12. Constable PD. Antimicrobial use in the treatment of calf diarrhea. *J Vet Intern Med.* (2004) 18:8–17. doi: 10.1111/j.1939-1676.2004.tb00129.x
13. Glover AD, Puschner B, Rossow HA, Lehenbauer TW, Champagne JD, Blanchard PC, et al. A double-blind block randomized clinical trial on the effect of zinc as a treatment for diarrhea in neonatal holstein calves under natural challenge conditions. *Prev Vet Med.* (2013) 112:338–47. doi: 10.1016/j.prevetmed.2013.09.001
14. Teixeira AGV, Stephens L, Divers TJ, Stokol T, Bicalho RC. Effect of crofelemer extract on severity and consistency of experimentally induced enterotoxigenic *Escherichia coli* diarrhea in newborn holstein calves. *J Dairy Sci.* (2015) 98:8035–43. doi: 10.3168/jds.2015-9513
15. Habing G, Djordjevic C, Schuenemann GM, Lakritz J. Understanding antimicrobial stewardship: disease severity treatment thresholds and antimicrobial alternatives among organic and conventional calf producers. *Prev Vet Med.* (2016) 130:77–85. doi: 10.1016/j.prevetmed.2016.06.004
16. Pempek JA, Holder E, Proudfoot KL, Masterson M, Habing G. Short communication: investigation of antibiotic alternatives to improve health and growth of veal calves. *J Dairy Sci.* (2018) 101:4473–8. doi: 10.3168/jds.2017-14055
17. Bicalho MLS, Machado VS, Nydam DV, Santos TMA, Bicalho RC. Evaluation of oral administration of bacteriophages to neonatal calves: phage survival and impact on fecal *Escherichia coli*. *Livest Sci.* (2012) 144:294–9. doi: 10.1016/j.livsci.2011.12.007
18. Teixeira AGV, Ribeiro BL, Junior PRM, Korzec HC, Bicalho RC. Prophylactic use of a standardized botanical extract for the prevention of naturally occurring diarrhea in newborn holstein calves. *J Dairy Sci.* (2017) 100:3019–30. doi: 10.3168/jds.2016-12139
19. Katsoulos PD, Karatzia MA, Dovas CI, Filioussis G, Papadopoulos E, Kiossis E, et al. Evaluation of the in-field efficacy of oregano essential oil administration on the control of neonatal diarrhea syndrome in calves. *Res Vet Sci.* (2017) 115:478–83. doi: 10.1016/j.rvsc.2017.07.029
20. Bonelli F, Turini L, Sarri G, Serra A, Buccioni A, Mele M. Oral administration of chestnut tannins to reduce the duration of neonatal calf diarrhea. *BMC Vet Res.* (2018) 14:6. doi: 10.1186/s12917-018-1549-2
21. van der Merwe D, Swan GE, Botha CJ. Use of Ethnoveterinary medicinal plants in cattle by setswana-speaking people in the madikwe area of the north west province of South Africa. *J S Afr Vet Assoc-Tydskr Suid-Afr Vet Ver.* (2001) 72:189–96. doi: 10.4102/jsava.v72i4.651
22. Lans C, Turner N, Khan T, Brauer G, Boepple W. Ethnoveterinary medicines used for ruminants in British Columbia, Canada. *J Ethnobiol Ethnomed.* (2007) 3:22. doi: 10.1186/1746-4269-3-11
23. McGaw LJ, Eloff JN. Ethnoveterinary Use of Southern African Plants and Scientific Evaluation of Their Medicinal Properties. *J Ethnopharmacol.* (2008) 119:559–74. doi: 10.1016/j.jep.2008.06.013
24. Mayer M, Vogl CR, Amorena M, Hamburger M, Walkenhorst M. Treatment of organic livestock with medicinal plants: a systematic review of european ethnoveterinary research. *Forsch Komplementmed.* (2014) 21:12. doi: 10.1159/000370216
25. Ayrle H, Mevissen M, Kaske M, Nathues H, Gruetzner N, Melzig M, et al. Medicinal plants—prophylactic and therapeutic options for gastrointestinal and respiratory diseases in calves and piglets? *A Systematic Review Bmc Veterinary Research.* (2016) 12:31. doi: 10.1186/s12917-016-0714-8
26. McGuirk SM. Disease management of dairy calves and heifers. *Vet Clin N Am-Food Anim Pract*. (2008) 24:139. doi: 10.1016/j.cvfa.2007.10.003
27. Zhu Z, Cao MZ, Wang WW, Zhang LW, Ma TH, Liu GH, et al. Exploring the prevalence and distribution patterns of antibiotic resistance genes in bovine gut microbiota using a metagenomic approach. *Microb Drug Resist.* (2021) 27:980–90. doi: 10.1089/mdr.2020.0271
28. Gebeyehu A, Taye M, Abebe R. Isolation, molecular detection and antimicrobial susceptibility profile of salmonella from raw cow milk collected from dairy farms and households in Southern Ethiopia. *BMC Microbiol.* (2022) 22:84. doi: 10.1186/s12866-022-02504-2
29. Wu YY, Wang LL, Luo RQ, Chen HL, Nie CX, Niu JL, et al. Effect of a multispecies probiotic mixture on the growth and incidence of diarrhea, immune function, and fecal microbiota of pre-weaning dairy calves. *Front Microbiol.* (2021) 12:15. doi: 10.3389/fmicb.2021.681014
30. Do NT, Cu HP, Nguyen NN, Nguyen XH, Au XT, Van TH, et al. Antimicrobial resistance phenotypes of etec isolates from piglets with diarrhea in North Vietnam. In: Blouin EF, Maillard JC, editors. *Impact of Emerging Zoonotic Diseases on Animal Health. Annals of the New York Academy of Sciences. 1081*. Malden: Wiley-Blackwell (2006). p. 543–5. doi: 10.1196/annals.1373.082
31. O'Brien S, Baumgartner M, Hall AR. Species interactions drive the spread of ampicillin resistance in human-associated gut microbiota. *Evol Med Public Health.* (2021) 9:256–66. doi: 10.1093/emph/eoab020
32. Srivani M, Reddy YN, Subramanyam KV, Reddy MR, Rao TS. Prevalence and antimicrobial resistance pattern of shiga toxigenic escherichia coli in diarrheic buffalo calves. *Veterinary World.* (2017) 10:774–8. doi: 10.14202/vetworld.2017.774-778

Conflict of Interest: The authors declare that the research was conducted in the absence of any commercial or financial relationships that could be construed as a potential conflict of interest.

Publisher's Note: All claims expressed in this article are solely those of the authors and do not necessarily represent those of their affiliated organizations, or those of the publisher, the editors and the reviewers. Any product that may be evaluated in this article, or claim that may be made by its manufacturer, is not guaranteed or endorsed by the publisher.

frontiers | Frontiers in Veterinary Science

ORIGINAL RESEARCH
published: 12 May 2022
doi: 10.3389/fvets.2022.877685

Construction of the waaF Subunit and DNA Vaccine Against *Escherichia coli* in Cow Mastitis and Preliminary Study on Their Immunogenicity

Hua Wang, Ligang Yuan, Tao Wang, Lu Cao, Fukang Liu, Juanjuan Song and Yong Zhang*

Gansu Key Laboratory of Animal Generational Physiology and Reproductive Regulation, College of Veterinary Medicine, Gansu Agricultural University, Lanzhou, China

OPEN ACCESS

Edited by:
Kun Li,
Nanjing Agricultural University, China

Reviewed by:
Gang Liu,
China Agricultural University, China
Zeeshan Ahmad Bhutta,
Chungbuk National University, South Korea
Muhammad Fakhar-e-Alam Kulyar,
Huazhong Agricultural University, China
Zhuo-Ma Luoreng,
Ningxia University, China

***Correspondence:**
Ligang Yuan
yuan2918@126.com

Specialty section:
This article was submitted to Veterinary Infectious Diseases, a section of the journal Frontiers in Veterinary Science

Received: *17 February 2022*
Accepted: *05 April 2022*
Published: *12 May 2022*

Citation:
Wang H, Yuan L, Wang T, Cao L, Liu F, Song J and Zhang Y (2022) Construction of the waaF Subunit and DNA Vaccine Against Escherichia coli in Cow Mastitis and Preliminary Study on Their Immunogenicity. Front. Vet. Sci. 9:877685. doi: 10.3389/fvets.2022.877685

Escherichia coli (*E. coli*) is one of the major pathogenic bacteria in bovine mastitis, which usually triggers systemic symptoms by releasing lipopolysaccharide (LPS). waaF is the core in LPS pathogenicity. In this study, a new waaF vaccine candidate was identified, constructed with the pcDNA3.1 (+)HisB-waaF plasmid to create to a DNA vaccine (pcwaaF), and transfected into MCF-7 cells to produce recombinant waaF subunit vaccine (rwaaF). After that, the safety of the two vaccine candidates was evaluated in mouse model. Immunogenicity and mortality of challenged mice were compared in 20 and 40 μg per dose, respectively. The results showed that rwaaF and pcwaaF were successfully constructed and the complete blood count and serum biochemical indicated that both of the vaccine candidates were safe ($p > 0.05$). In addition, histopathological staining showed no obvious pathological changes. The immune response induced by rwaaF was significantly higher than that of pcwaaF ($p < 0.01$), indicated by levels of serum concentration of IgG IL-2, IL-4, and IFN-γ, and feces concentration of sIgA. Survival rates of mice in rwaaF groups (both 80%) were also higher than in the pcwaaF groups (40 and 50%, respectively). Comparing the safety, immunogenicity, and *E. coli* challenge of two vaccine candidates, rwaaF had the better effect and 20 μg rwaaF was more economical. In conclusion, this study demonstrates the utility of a new *E. coli* vaccine and provides a rationale for further investigation of bovine mastitis therapy and management.

Keywords: *Escherichia coli*, waaF, pcDNA3.1-waaF, waaF recombined protein, immunogenicity

INTRODUCTION

Coliform mastitis is one of the most common diseases in the dairy industry worldwide. It can cause severe acute inflammation with toxemia, high fever, and decreased milk production (1, 2) and lead to serious economic losses (3, 4). In addition, the incidence of coliform mastitis has increased in the past few decades (5). It is among the environmental pathogens that occur wherever there are cows, such as the bovine digestive system (5). Therefore, ruminant feces are an important infectious source of *Escherichia coli* (*E. coli*) that can disseminate directly into the surrounding environment (5).

The virulence factors of the pathogenic *E. coli* include lipopolysaccharide (LPS) (6) and flagella (7) among others. LPS is the key to the cause of mastitis. When *E. coli* infects and proliferates in the mammary duct system, it releases LPS that causes breast infection (8) and activates the host's immune system (9). Although LPS can be engulfed and destroyed by immune cells, a large amount of LPS is released and causes systemic symptoms in the host.

LPS comprises the outer cell-wall constituents of Gram-negative bacteria. It is composed of three regions: an O-antigen of repeating oligosaccharide units, lipid A, and a core oligosaccharide. Among them, bacteria can be classified into smooth (S-) and rough (R-) types according to the presence of O-antigen (10). Lipid A is the most conserved part of LPS and is connected by lipid glucosamine disaccharide and phosphate through pyrophosphate bonds (11). The core oligosaccharide is separated into an outer and inner core; the outer core has a different composition and configuration in diverse strains, whereas the inner core is composed of heptose residues and 2-keto-3-deoxyoctanoic acid, which is highly conserved and is a common structure in all strains of *E. coli* (12). With the catalysis of heptosyltransferse (waa), lipid A is linked to the Kdo disaccharide of oligosaccharide forming the Kdo2-lipid A group, which is the most conserved in LPS and is called a toxic center (12). waaF is a heptosyltransferse II gene, which is the second Hep to Kdo2-lipid A (13). The loss of waaF results in a severely truncated LOS structure (14). Compared with other genes in waa family, the waaF mutant showed stronger hydrophobicity, autoaggregation, and outer membrane permeability. Furthermore, the effect on the flagella assembly, chemotaxis, and pro-inflammatory responses of bacteria is more significant (13, 15). Therefore, waaF is not only related to the adhesion of pathogenic bacteria, but also involved in the host-pathogen interaction. Therefore, waaF is an ideal gene as a target antigen for a vaccine feasibility study.

Among newly developed vaccines, DNA and subunit vaccines have been a focus of research. In DNA vaccines, a recombinant eukaryotic expression vector encoding a certain protein antigen is directly injected and expressed into the animal, and the resulting antigen activates the immune system, thus inducing specific humoral and cellular immune responses (16); the subunit vaccine is a recombinant protein vaccine that combines the main protective immunogen of pathogenic bacteria. Both of them not only have the advantages of being simple, effective, and more targeted, but also of being effective against a wide variety of pathogens simultaneously, or against a single pathogen by multilocus antigen (17). Many DNA and subunit vaccines have been developed against *E. coli* mastitis in dairy cows (18), but there are no reports on a waaF vaccine.

In this study, waaF of *E. coli* that was separated from milk was cloned and expressed in eukaryotic vector pcDNA3.1 (+)-HisB to construct the pcDNA-waaF vaccine (pcwaaF). Afterwards, it was transfected into MCF-7 cells to purify the waaF recombinant protein (rwaaF). Furthermore, we compared the safety, immunogenicity, and immune protection of waaF in two different vaccines that were used in a murine model.

MATERIALS AND METHODS

Animals and Institutional Approval

We purchased 110 lactating BALB/c female mice (6–8 weeks old) from the Institute of Veterinary Medicine, Chinese Academy of Agricultural Sciences (Lanzhou, China). This study was approved by the Academic Committee of Gansu Agricultural University and the National Natural Foundation of China (Grant No. 202009264), and researchers followed the guidelines for the protection and use of experimental animals of the Institute of Experimental Animal Resources of the National Research Council.

Methods

All molecular tests are performed according to the Molecular Cloning: A Laboratory manual (Fourth Edition) (19) specifications and Vaccine Technology (20).

Construction of PcDNA3.1–waaF (pcwaaF) and waaF Recombinant Protein (rwaaF)

Cloning of the waaF Gene

The waaF primers (Shanghai Bioengineering Co., Shanghai, China) (waaF-F-*KpnI*, 5′TGGGTACCAAGATGGGATGAAAATAC3′; waaF-R-*BamHI*; 5′CACACTGGATCCTCAGGCTTCC3′, the restriction sites are underlined) were added to *E. coli* NC-00913.3 (3794929-3795975). The standard PCR (BIO-RAD, USA) conditions were as follows: initial denaturation at 95°C for 5 min, followed by 35 cycles of 94°C for 60 s and annealing at 60°C for 45 s and then 72°C for 60 s, and final extension for 10 min at 72°C. PCR products were resolved by 1.0% agarose gel containing 0.1 μg/ml Golden View^{TM} and recovered with a Star Prep Gel Extraction Kit (TransGen Biotech Co., Beijing, China). Part of an amplified waaF gene was sent to Shanghai Bioengineering Co., Ltd for sequencing and the remainder stored at −20°C.

The PCR products of waaF was cloned into the *KpnI–BamHI* site of the pGEM-T-easy vector (Promega, USA) after digestion by two restriction endonucleases (TransGen Biotech Co., Beijing, China), transformed into *E. coli* DH5α (TransGen Biotech Co., Beijing, China), and then proliferated in Luria-Bertani (LB; Solarbio, Beijing, China) broth agar medium containing X-gal 40 μl (20 mg/ml) and IPTG 4 μl (200 mg/ml), (Solarbio, Beijing, China) for 4 h. The white plaque was removed and cultured in LB broth with anti-ampicillin for 8 h. Then extracted plasmid DNA was extracted and sent to Shanghai Bioengineering Co., Ltd. for sequencing.

Construction of pcwaaF

pcDNA3.1 V5-HisB (pc DNA 3.1), (Invitrogen, Shanghai, China), and the positive plasmid was split with *KpnI* and *BamHI* (Promega, USA) at 37°C and ligated at 16°C for 12 h by T4 DNA ligase (Promega, USA).

The resultant ligated pcDNA3.1-waaF (pcwaaF) was cloned into *E. coli* DH5α (For details, see Section Cloning of the waaF Gene). The positive plasmid DNA was extracted and purified by the minibest DNA purification Kit (TaKaRa, Dalian, China), digested with *Kpn*I and *BamHI*, and sent to Shanghai

TABLE 1 | Primers for qRT-PCR.

Gene name	Primers sequence	Tm (°C)
GAPDH	GGTACCAGGGCTGCTTT	60
	CTGTGCCGTTGAACTTGC	
waaF	GCCTTCCCACGACTGTGTAT	58
	GGAAAAGCTGTTGCCAGAAG	

TABLE 2 | Vaccine safety assessment procedures.

The vaccine type	Inoculum		
	0 d	7 d	14 d
PBS (μg)	80	80	80
rwaaF (μg)	60	60	60
rwaaF (μg)	80	80	80
pcwaaF (μg)	60	60	60
pcwaaF (μg)	80	80	80

Bioengineering Co., Ltd for sequencing again. The purity was measured by spectrophotometry using the A260/280 absorbances (Quawell, America).

Construction of rwaaF

Transfection. The pcwaaF plasmid DNA was extracted and quantitated as 1 μg/μl, and then digested with *KpnI* and *BamHI* and linearized. MCF-7 cells (Institute of Bioengineering, Fudan University, Shanghai, China) were grown on Dulbecco's modified Eagle's medium supplemented with 10 % fetal bovine serum (Sigma, Australia). Every 2 days, 2.5 ml fresh medium was added to the culture. Cells (1×10^5) were seeded in a 24 well plate (TransGen Biotech Co., Beijing, China) and transfected 24 h later. Furthermore, 90% of the wells were filled with cells and the medium used in the step was without any antibody. Lipofectamine 2000 (TransGen Biotech Co., Beijing, China) was used for transfection. The ratio of linearized plasmid DNA (1 μg) and lipofectamine (μl) was 1: 2. After 48 h incubation, the transfection products were selected by medium with G418 in a 96-well plate (TransGen Biotech Co., Beijing, China). The concentrations of G418 were 500, 600, 700, 800, 900, and 1,000 μg/μl. After 15 d, the suspected positive cells were harvested and assayed for the result of transfection.

Quantitative RT-PCR. RNA was extracted by Trizol when waaF positive cells were about 90% in six flasks. Then the concentration and OD 260/280 values was analyzed by spectrophotometer and samples diluted to 200 mg/μl. All RNA samples underwent RT-PCR as well as real-time quantitative reverse transcriptase-polymerase chain reaction (qRT-PCR) studies. The concentration of single-strand cDNA (TransGen Biotech Co., Beijing, China) was diluted to 200 mg/μl. RT-PCR analysis was performed on a LightCycler 96® system (Roche, Basle, Switzerland). All reactions were run in triplicate. The cycle threshold (ct) method was used to calculate values and the GAPDH were used to normalize the level of mRNA.

The GAPDH gene (Qinke, Xi'an, China) was designed by Primer 6.0 and the sequences were shown in **Table 1**. The reaction and the subsequent melting curve protocol were performed in a final volume of qRT-PCR assay with 25 μl, containing 0.5 μl cDNA, 1 μl (10 mM) of each primer, 12.5 μl SYBR premix EX TaqTM II (2×) (TransGen Biotech Co., Beijing, China), and 0.5 μl ROX Reference Dye II (50×) (TransGen Biotech Co., Beijing, China). Conditions for qRT-PCR included 95°C for 30 s, and 40 cycles at 95°C for 10 s, 60°C for 30 s, and an extension time for the melt curve from 60 to 95°C. The cooling step was performed at 40°C for 10 s (ramp rate of 1.5°C/s).

Purification of Recombinant Protein and Western Blot (WB).

The total protein formed by the cultured transfected cells with the highest expression was screened by qRT-PCR and other two vials of positive cells were extracted using a total protein extraction kit (TransGen Biotech Co., Beijing, China) separated by polyacrylamide gel electro phoresis (SDS-PAGE), and the target band cut down and transferred to polyvinylidene fluoride (PVDF, TransGen Biotech Co., Beijing, China) using anti-His Tag monoclonal antibody (AbM59012-18-PU, 1:2,000), (Beijing Protein Innovation, Beijing, China) at 4°C for 12 h. After washing for 3 × 10 min by tris-buffered saline with Tween 20 (TBST) (Solarbio, Beijing, China), PVDF was incubated in Rabbit Anti-Mouse IgG [ab 6728, H&L (HRP)], (Abcam, USA) secondary antibody at 37°C for 2 h, and washed for 1.5 h, as well as exposed by to chemiluminescence detection.

After that, the most highly expressed protein was purified by Ni-NTA affinity chromatography (TransGen Biotech Co., Beijing, China) according to the manufacturer's directions. The purified protein was dialyzed against PBS for 32 h at 4°C and concentrated with renaturation solution (0.1 M Tris, 1 mM glutathione, and urea at concentrations of 1, 2, 4, and 8 M).Protein was determined by HPLC C18 column (Thermo, America); the concentration of the sample was 250 μg/ml, and the volume of loading was 20 μl. Then the protein was quantified by the Protein Quantitative Kit (TransGen Biotech Co., Beijing, China), adjusted to 900 μg/ml, and stored at −80°C.

Vaccine Safety Assessments

We randomly divided 50 female lactation BALB/c mice (8–10 weeks old) into five groups with 10 mice in each group. The treatments are shown in **Table 2**. The pcwaaF or rwaaF was injected subcutaneously, whereas 10 control mice were inoculated with PBS.

During the immunization period, the energy, appetite, and death of mice were observed and recorded.

At 7 days after the last vaccination, intraperitoneal 1% pentobarbital sodium at a dose of 0.5 mg/10 g was used for anesthesia, and then two tubes of heart blood samples were collected, one with anticoagulant added for routine blood work and the other isolated from the other sample. The following parameters were evaluated: red blood cell count (RBC), hemoglobin concentration (HB), hematocrit (HCT), mean corpuscular volume (MCV), mean corpuscular hemoglobin (MCH), mean corpuscular hemoglobin concentration (MCHC),

TABLE 3 | Vaccine immunogenicity and *E. coli* challenge.

The vaccine type	Inoculum			*E. coli* challenge(CFU)
	1 d	7 d	14 d	
C1	20	20	20	4×10^6
C2	40	40	40	4×10^6
G1	20^a+20^b	20^a+20^d	20^a	4×10^6
G2	40^a+40^b	40^a+40^d	40^a	4×10^6
G3	20^c+20^b	20^c+20^d	20^a	4×10^6
G4	40^c+40^b	40^c+40^d	40^a	4×10^6

[a]*rwaaF.*
[b]*Complete Freund's adjuvant (CFA).*
[c]*pcwaaF.*
[d]*Incomplete Freund's adjuvant (IFA).*
The toxicity or adverse effects of vaccinated rwaaF (60 and 80 μg), pcwaaF (60 and 80 μg), and PBS against BALB/c mice were evaluated by complete blood count and serum biochemical profile. ANOVA test was used for the comparison of blood parameters between vaccinated and non-vaccinated group. $P < 0.05$ were considered significant.

platelet count (PLT), white blood cell count (WBC), and red blood cell volume distribution width (RDW). Blood biochemical indexes were as follows: alanine transaminase (ALT), aspartate aminotransferase (AST), alkaline phosphoesterase (ALP), total bilirubin (T-BIL), blood urea nitrogen (BUN), creatinine (CR), total protein (TP), albumin (ALB), and glucose (GLU).

The mice were sacrificed by cervical dislocation and the mammary glands, liver, kidney, and spleen were removed and stained to observe the pathological changes.

Immunogenicity Analysis

As shown in **Table 3**, 60 identical mice were randomly divided into six groups with 10 mice in each group and vaccinated three times in total, once a week. The dose and varieties of injections were as follows: rwaaF 20 μg (Goup1, G1), rwaaF 40 μg (Goup2, G2), pcwaaF 20 μg (Goup3, G3), pcwaaF 40 μg (Goup4, G4), PBS 20 μg (Control group 1, C1), and PBS 40 μg (Control group 2, C2).

Over the next 4 weeks, the blood samples were collected from the tail tip and feces of mice every week after immunization and serum IgG (Abcam, USA) and fecal sIgA (Abcam, USA) was determined by ELISA. After the last immunization, heart blood was collected with a disposable needle and IL-2, IL-4, and IFN-γ (Abcam, USA) were detected, determined by ELISA.

E. coli Challenge in Mice

At 7 days after cardiac blood collection, each mouse was subcutaneously injected with an *E. coli* dose of 4×10^6 CFU and the death rate of mice was recorded.

Measurement and Statistical Analyses

All assays in this study were performed in three independent biological experiments with at least three replicates.

PCR data was imported by the LightCycler 96® software (Roche, Basle, Switzerland) to perform analysis according to the instructions listed in the system. These data were copied in Office Excel 2007 (Microsoft Corporation, Redmond, WA, USA) and the Efficiency values, R^2, and Cq standard deviations were analyzed.

The sections were photographed by a NIKON ECLIPSE 80i mi croscope camera system and five non-repetitive fields (bar = 20 μm for the mammary gland, liver, and kidney and 10 μm for the spleen) were randomly selected for each section.

The gray curve of the Western blot expression band was analyzed by using Image J 1.48. The area under the peak was calculated as the band density value.

All data were analyzed with SPSS 20.0 software (SPSS Inc., Chicgo, IL, USA), and the statistical significance of differences between two groups was evaluated by Student's *t*-test; one-way ANOVA was used for more than two groups. The difference was considered to be significant at $p < 0.01$(difference between different capital letters is extremely significant) and $p < 0.05$(differences between different lowercase letters); the data was expressed as mean ± SD.

RESULTS

Development of pcwaaF and rwaaF

Cloning the waaF Gene

In previous research, we had isolated the wild-type *E. coli* from mastitis milk and extracted total DNA to use as templates. The 1,046 bp waaF gene was successfully amplified (**Figure 1A**) and inserted into pGEM-T-Easy vector and a new recombinant pGEM-T-waaF constructed. After that, it was digested with *BamHI* and *Kpn*I (**Figure 1B**) and a specific band found near 1,000 bp. Sequencing showed that the target fragment was 1,036 bp. Compared with the NCBI database (basic local alignment search tool), the waaF gene that had been mutated was digested in pGEM-T-waaF, and the homology was 99.7% with the reported sequence of *E. coli*. The result of comparison showed the 442–450, 1,046, and 10 genes were deleted, and no other point metamorphosis or frameshift was found. In order to analyze the effect of mutations on transcripts and evaluate the biological activity of cloned gene sequences, we predictively translated the sequencing genes and constructed the protein by the SWISS-MODEL, which was used to compare the difference of the three-dimensional structure and the two-dimensional structure of the mutations. The three-dimensional structure of the mutant waaF is shown in **Figures 1C,C'**. Its folding quantity, angle, stretching trend, and other structures are the same as that of the template. As shown in **Figure 1C** (a, b, and c), they were sites of amino acids with the corresponding gene deletion, ACAAAGGCA. After that, we analyzed the secondary structure of the waaF mutation. **Figure 1D** (a) shows the lack of 142–150 expressing the alanine (A), glutamine (Q), and aspartic acid (D), whereas, compared with the template sequence shown in **Figure 1D** (b), there is no conserved sequence (In Query Conservation, thicker gray lines indicate high conservatism, while thinner gray lines indicate moderate conservatism. Correspondingly, the red line is confidence). As shown in **Figure 1E**, the A, Q, and D in S4 does not participate in extracellular membrane activities directly, so, they were meaningless mutations.

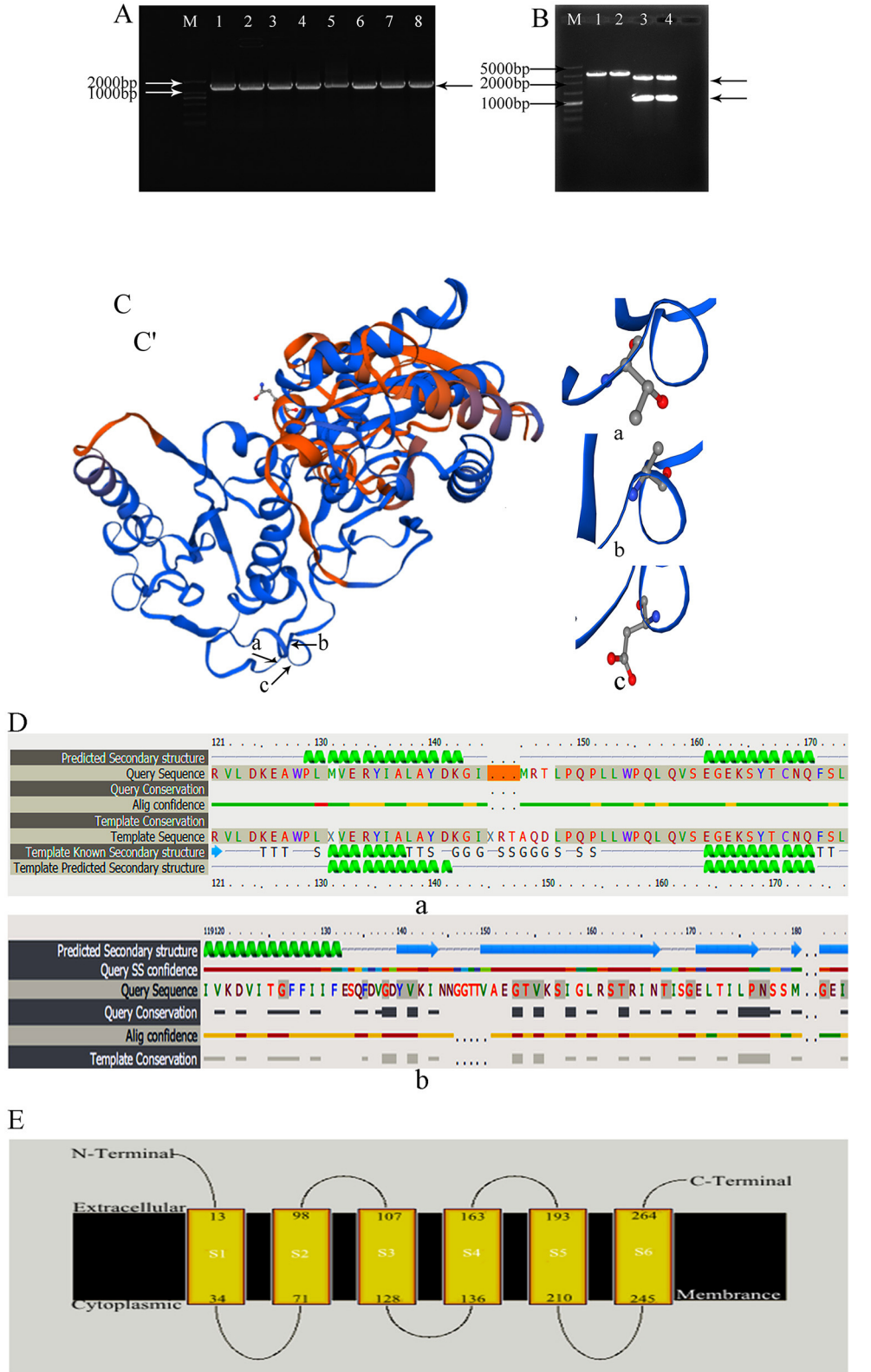

FIGURE 1 | (A) waaF gene amplification by PCR; M: 2,000 bp Marker. 1–8: amplified the waaF gene band which appeared near the 1,000 marker's band. **(B)** Plasmid vector PGEM-T-waaF enzyme digestion; M: 5,000 bp Marker. 1, 2: pGEM-T-waaF plasmid; 3, 4: pGEM-T-waaF plasmid was digested by *BamH* and *Kpn* I, the waaF

(Continued)

FIGURE 1 | genes was near 1,000 marker's band, and the other was pGEM. **(C,C')** the three-dimensional structure of the mutant waaF. (a–c) Are sites of amino acid which are corresponding gene deletion; (a) the missing amino acid Alanine corresponding to ACA genes; (b) the missing amino acid Glutamine corresponding to AAG genes; (c) the missing amino acid Aspartic corresponding to GCA genes. **(D)** The amplified sequence translation protein was analyzed by Phyre2. (a) The lack of 142–150 genes are expressed the Alanine (A), Glutamine (Q), and Aspartic acid (D), (the orange band); (b) template sequence; Thicker gray lines indicate high conservatism, thinner gray lines indicate moderate conservatism. Correspondingly, in Alig confidence, the red line is confidence. **(E)** The A, Q, and D in S4 did not participate in extracellular membrane activities directly.

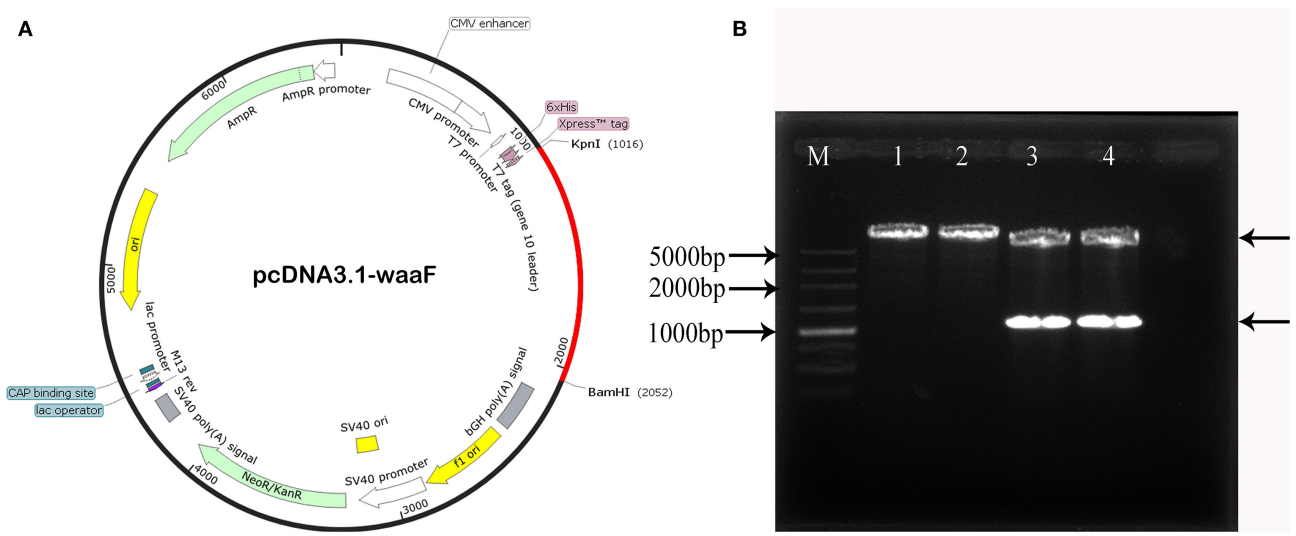

FIGURE 2 | (A) The new recombinant eukaryotic pcwaaF plasmid. The red part is the sequence of waaF genes inserted into the vector. **(B)** *BamHI* and *Kpn*I were digested the pcwaaF. Lane 1, 2 pcDNA 3.1-*waaF* plasmid; Lanes 3, 4 pcDNA 3. 1-waaF plasmid digested with *BamH* and *Kpn* I, and the band near 1,000 marker was waaF gene and the above band was pcDNA 3.1 plasmid; Lane M, 5,000 markers.

Construction of pcwaaF

The new constructed recombinant eukaryotic pcDNA3.1-waaF plasmid is shown in **Figure 2A**. The red part is the sequence of waaF genes inserted into the vector. The *BamHI* and *Kpn*I were digested with pcDNA3.1-waaF to 5,000 and 1,000 bp (**Figure 2B**). The results of sequence analysis showed that the pcwaaF was successfully constructed and OD (A260/280) was 1.867.

Construction of rwaaF

Transfection and Expression

With a screening concentration of G418 at 800 μg/ml, the mRNA expression of transfected cells was determined by qRT-PCR. As shown in **Figure 3A**, the expression of the No.2 cell is significantly higher than others ($p < 0.01$), and the Cq of all qPCR data were <30; the melting curve had one only one specific peak.

We chose the No.3 and No.4 cell as control with No.2 in western blotting.

Western blotting verified that the waaF expression protein of the No.2 cell was significantly higher than that of No.3 and No.4 ($p < 0.01$), as shown in **Figures 3B** and **C**. The molecular weight of waaF was ∼40 kDa, very similar to the expected size of 36.67 kDa.

The purification rate was about 91.3% by HPLC C18 column, and the rwaaF was successfully constructed.

Safety Assessments

We administered the amount of 3- and 4-times dosage of pcwaaF/rwaaF injection to mice and evaluated the safety level. Within 1 h after injection, the mice immunized with 60 and 80 μg pcwaaF showed torpor, especially those injected with 80 μg. After 1.5 h, the symptoms of the mice improved, and 2 h later, they ate and drank water normally. Furthermore, as shown in **Tables 4**, **5**, there were no significant differences between all the vaccine groups and the control group in complete blood count and blood biochemical profiles ($p > 0.05$). Beyond that, we observed the mammary glands, liver, kidney, and spleen of pathological sections in each group. The results are shown in **Figure 4**; there were no obvious pathological changes observed in each tissue. Under the microscope, the lactating breast epithelial cell was rich in lipid droplets and obvious secretions in the glandular cavity of the control group (**Figure 4a1**); in comparison, there were no obvious pathological damages in all vaccine groups (**Figures 4a2–a5**), but the breast glandular secretory structure was not obvious in 80 μg pcwaaF group. In the liver sections, the hepatic cord was clearly distributed surrounding the central vein (**Figure 4b1**). The hepatic cords in the 60 μg rwaaF and pcwaaF groups (**Figures 4b2,b4**) did not have obvious pathological changes, whereas the hepatic cords were slightly swollen in the 80 μg rwaaF and pcwaaF group (**Figures 4b3,b5**). In the kidney sections, the glomerular structure of the control group was clear (**Figure 4c1**), and there were no obvious pathological changes in

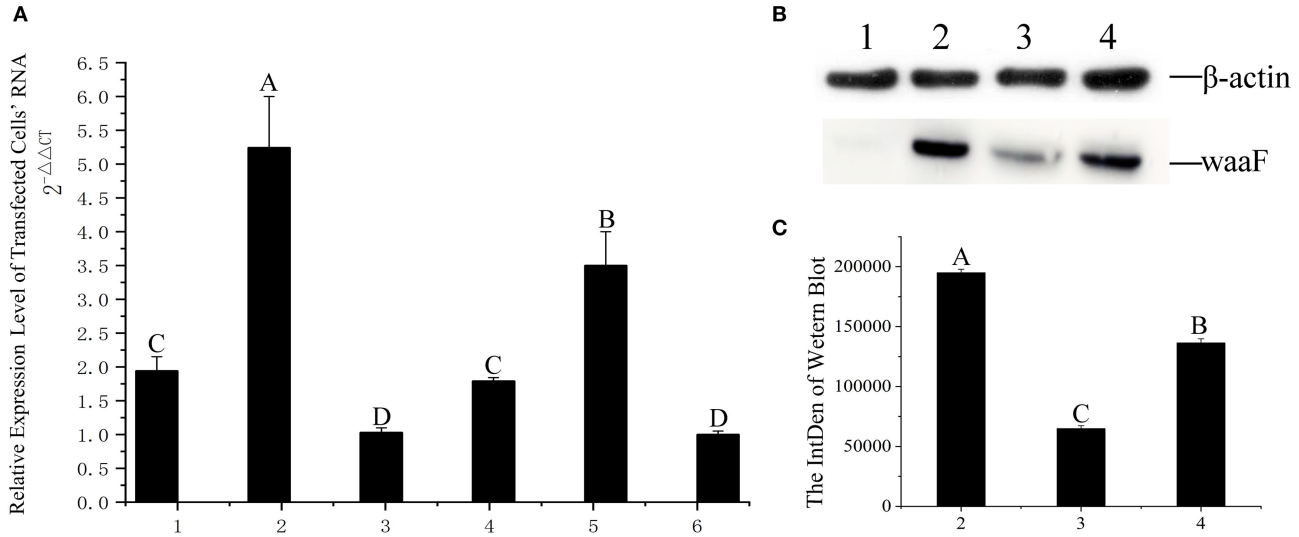

FIGURE 3 | (A) qRT-PCR was applied for assaying the level of expression at RNA level, 1–6: The same positive cells were cultured in six vials, their RNA extracted, and numbered 1–6, respectively; the difference between different capital letters is extremely significant ($p < 0.01$). **(B)** The expression of waaF protein. Lane 1, protein of MCF-7 cells. Lane 2–4, the waaF expression was observed in No. 2, No. 3, and No. 4 cells. **(C)** The curve of the western blot expression band; the difference between different capital letters is extremely significant ($p < 0.01$).

TABLE 4 | The results of hematologic about vaccinated BALB/c mice which were vaccinated rwaaF (60 and 80 μg), pcwaaF (60 and 80 μg), and PBS, respectively.

Group	PBS	rwaaF 60 μg	rwaaF 80 μg	pcwaaF 60 μg	pcwaaF 80 μg	*p*-value
RBC ($\times 10^{12} \cdot L^{-1}$)	10.35 ± 0.36	10.65 ± 0.37	10.61 ± 0.49	10.64 ± 0.32	10.18 ± 0.24	>0.05
HGB ($\times g \cdot dL^{-1}$)	14.27 ± 3.64	14.41 ± 2.68	14.5 ± 2.93	14.0 ± 2.83	14.0 ± 3.72	>0.05
WBC ($\times 10^{9} \cdot L^{-1}$)	8.3 ± 2.54	8.52 ± 2.15	8.50 ± 2.40	8.74 ± 3.09	8.48 ± 1.96	>0.05
HCT (%)	44.13 ± 7.76	42.98 ± 7.35	43.48 ± 7.13	40.38 ± 13.9	43.44 ± 9.46	>0.05
MCH (pg)	13.51 ± 2.03	13.25 ± 2.71	13.43 ± 2.14	13.79 ± 2.44	13.14 ± 2.35	>0.05
MCHC ($g \cdot L^{-1}$)	33.6 ± 2.06	33.27 ± 2.83	31.13 ± 6.80	33.35 ± 2.85	31.99 ± 3.88	>0.05
RDW (CV/fL)	18.50 ± 4.09	18.23 ± 2.85	18.22 ± 1.47	18.18 ± 1.82	18.36 ± 2.25	>0.05
PLT (×103/μl)	748.5 ± 176.23	757.31 ± 113.60	749.87 ± 119.64	751.03 ± 61.18	755.25 ± 175.52	>0.05

TABLE 5 | The results of Serum biochemical in vaccinated BALB/c mice which were vaccinated rwaaF (60 and 80 μg), pcwaaF (60 and 80 μg), and PBS, respectively.

Group	PBS	rwaaF 60 μg	rwaaF 80 μg	pcwaaF 60 μg	pcwaaF 80 μg	*p*-value
ALT ($U \cdot L^{-1}$)	32.12 ± 12.52	32.50 ± 7.69	31.98 ± 7.98	32.56 ± 7.92	35.08 ± 11.93	>0.05
AST ($U \cdot L^{-1}$)	111.42 ± 22.40	111.2 ± 19.93	111.40 ± 21.56	113.79 ± 19.38	112.26 ± 16.21	>0.05
ALP ($U \cdot L^{-1}$)	84.99 ± 9.77	86.23 ± 13.98	85.23 ± 11.79	82.89 ± 13.83	81.75 ± 10.73	>0.05
CR ($\mu mol \cdot L^{-1}$)	84.43 ± 14.04	82.29 ± 19.42	84.36 ± 16.18	85.80 ± 17.37	84.14 ± 13.99	>0.05
ALB ($g \cdot L^{-1}$)	30.21 ± 5.21	30.36 ± 5.10	29.64 ± 5.18	31.34 ± 5.30	32.06 ± 5.46	>0.05
GLU ($mmol \cdot L^{-1}$)	4.32 ± 1.66	4.03 ± 0.45	3.46 ± 0.59	3.12 ± 0.87	3.20 ± 1.43	>0.05
BUN ($mmol \cdot L^{-1}$)	9.39 ± 2.55	9.05 ± 1.51	9.15 ± 0.98	9.22 ± 1.68	6.20 ± 2.30	>0.05
TBIL ($\mu mol \cdot L^{-1}$)	1.92 ± 0.87	1.93 ± 1.53	1.96 ± 0.78	2.02 ± 1.26	1.9 ± 0.95	> 0.05
TP ($g \cdot L^{-1}$)	71.12 ± 9.35	72.10 ± 6.97	72.02 ± 7.24	72.38 ± 6.69	73.02 ± 5.56	>0.05

(n = 10). RBC, total number of red blood cells; HGB, hemoglobin; WBC, white blood cells; HCT, hematocrit; MCH, mean corpusular hemoglobin; MCHC, mean corpusular hemoglobin concentration; RDW, red blood cell distribution width; PLT, platelet count; ALT, alanine aminotransferase; AST, aspartate aminotransferase; ALP, alkaline phosphatase; CR, creatinine; ALB, albumin; GLU, glucose; BUN, blood urea nitrogen; TBIL, total bilirubin; TP, total protein.

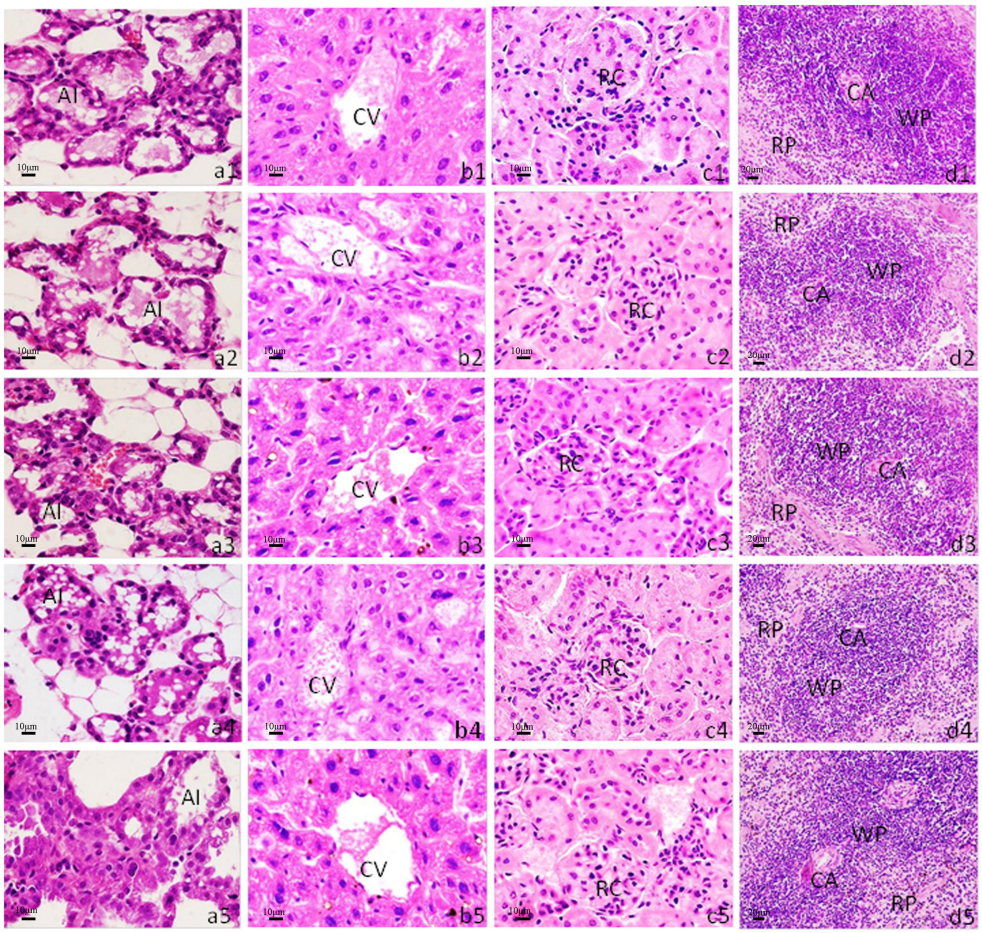

FIGURE 4 | Histological analysis of mouse mammary gland, liver, kidney, and spleen. H&E staining. The scale bar indicated as 10 μm for mammary gland, liver, kidney, and 20 μm for spleen. **(a1–a5)** Histological sections of mice mammary gland; **(b1–b5)** liver; **(c1–c5)** kidney; **(d1–d5)** spleen. **(a1–d1)** The tissues from control group which were inoculated the 80 μg PBS; **(a2–d2)** inoculated the 60 μg rwaaF; **(a3–d3)** inoculated the 80 μg rwaaF; **(a4–d4)** inoculated the 60 μg pcwaaF; **(a5–d5)** inoculated the 80 μg pcwaaF. AI, acinus; CA, central artery; CV, central vein; RC, renal corpuscle; RP, red pulp; WP, white pulp.

the other vaccine groups. In the spleen sections, the white and red pulp around the central artery of the spleen was distinct (**Figure 4d1**); the central artery was clear in the 60 and 80 μg rwaaF groups. Meanwhile, there was an obvious boundary between white pulp and red pulp (**Figures 4d2,d3**), but in the 60 and 80 μg pcwaaF groups, the number of white pulp lymphocytes were significantly decreased, the center artery was swollen, and there was no significant change in the red pulp (**Figures 4d4,d5**).

Immunogenicity—IgG, sIgA, IL-2, IL-4, and IFN-γ Were Detected by ELISA

We analyzed IgG in serum and sIgA in feces the 7th, 14th, 21st, and 28th days atter injection. We also analyzed IL-2, IL-4, and IFN-γ in serum on the 28th day. Among the groups, the levels of IgG, sIgA, IL-2, and IFN-γ in G1 and G2 were significantly higher than in G3 and G4 ($p < 0.01$); the levels of IL-4 in G1 and G2 were higher than in G3 and G4 ($p < 0.05$). There were no differences in IgG, IL-2, and IL-4 between G1 and G2 ($p > 0.05$); however, the level of sIgA in G1 was significantly higher than in G2 ($p < 0.01$), but the level of IL-4 in G2 was significantly higher than in G1 ($p < 0.01$).

Challenge Test

After being injected 4 times with an *E. coli* dose of 4×10^6 CFU, the mice in G1 and G2 were good mentally and emaciation was not obvious. Among them, a mouse died on the 2nd and 4th days in G1 and a mouse died on the 2nd and 6th days in G2; the overall survival rate was 80%, whereas the weight loss of mice in G3 and G4 was more obvious than that in G1 and G2. At the same time, the fur was rough, they were depressed, and the feed intake was less; after the 3rd day, they recovered gradually. In G3, two mice each died on the 3rd, 4th, and 5th day, and the survival rate was 40%. Meanwhile, in G4, two died on the 2nd and 4th days, and 1 died on the 6th day, and the survival rate was 50%. Compared with vaccine groups, the weight loss, rough fur, lack of eating, and somnolence of the mice in the C1 and C2 were more obvious. In C1, three died on the 2nd day, two on the 3rd day, four on the 4th day, and the reminder on the 5th day, while in C2, four died

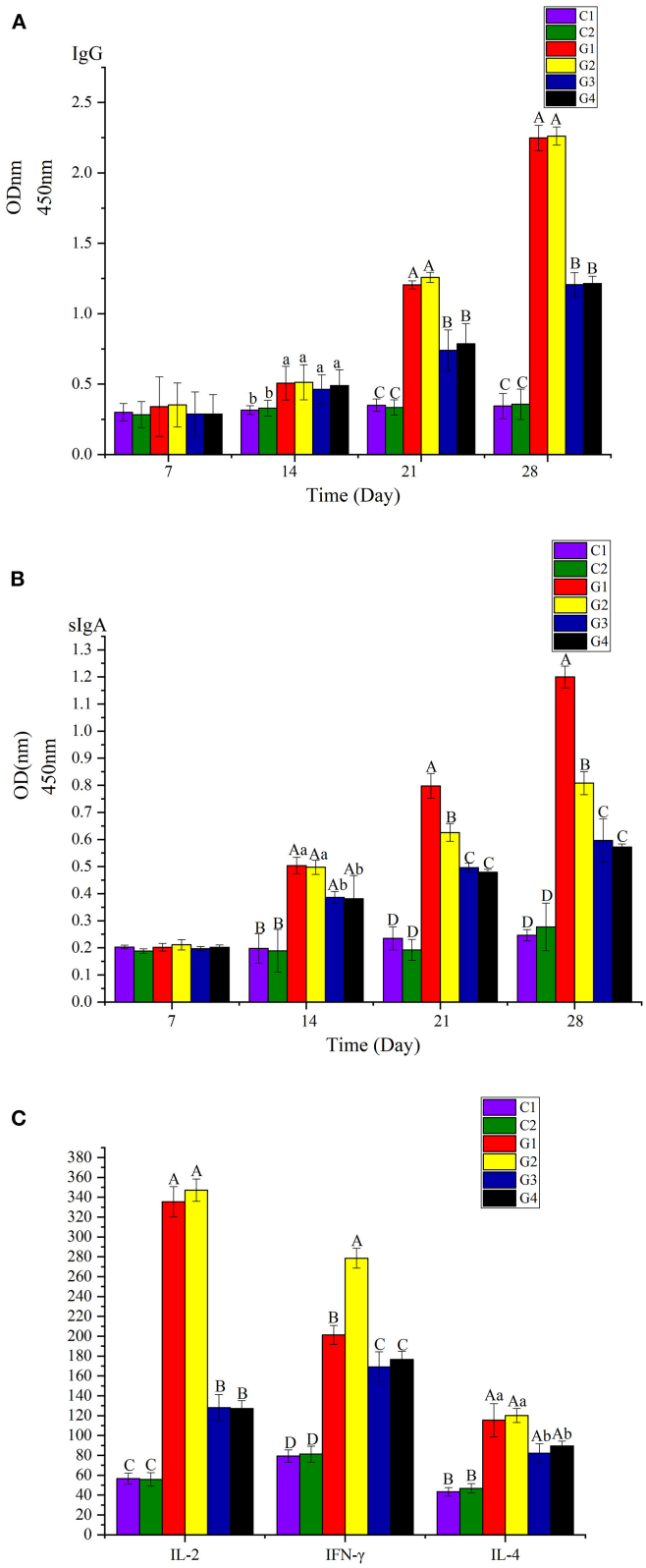

FIGURE 5 | (A) Analyzed the IgG on the 7th, 14th, 21th, and 28th days. **(B)** Analyzed the sIgA of feces on the 7th, 14th, 21th, and 28th days. **(C)** Analyzed the IL-2, IL-4, and IFN-γ of serum on the 28th day. The difference between different capital letters is extremely significant ($p < 0.01$), and the significant differences between different lowercase letters ($p < 0.05$).

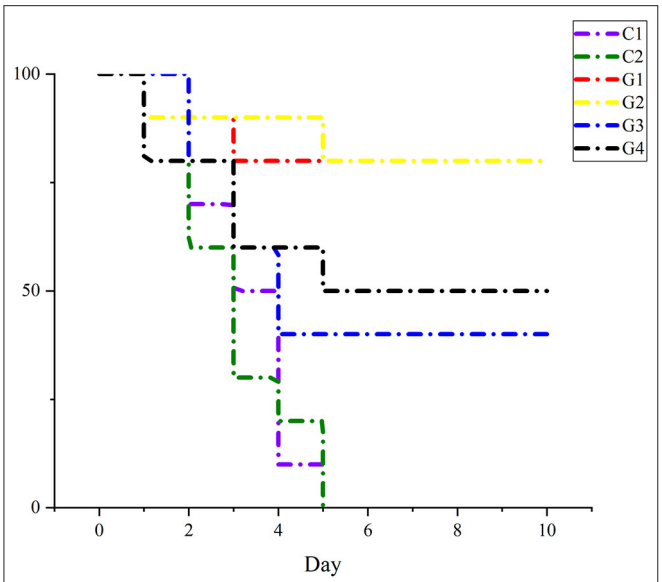

FIGURE 6 | The percent of survival rate of mice after being challenged with *E. coli* to each group.

on the 2nd day, three on the 3rd day, one on the 4th day, and the reminder died on the 5th day. Details are in **Figure 6**.

DISCUSSION

In a previous study, the research team collected 380 milk samples from dairy cows with clinical mastitis from dairy farms in Gansu, Ningxia, and Qinghai. The detection rate of *E. coli* was as high as 83.9% (21); therefore, a more cost-effective vaccine needs be developed to prevent *E. coli* mastitis in cows (22, 23). LPS is the key pathogenic factor in *E. coli* (24), and waaF is the core component with a highly conserved O-antigen gene in LPS that catalyzes the transfer of the second L-glycero-D-manno-heptose residue to the core oligosaccharide moiety of LPS (25). It not only affects the colonization, adhesion, and invasiveness of the pathogen (14), but it is also related to pro-inflammatory factors in the host (15). In addition, the gene of waaF is highly specific and highly consistent with the phenotype of other Gram-negative bacteria (25–28). Oldfield (25) and Chandan (29) added the waaF gene of *campylobacter* and *Helicobacter pylori* to the mutant *Salmonella typhimurium* lacking waaF, respectively, which not only restored the structure of core oligosaccharides, but also improved the adhesion and invasion of mutants. In this study, waaF was selected as the amplifying gene to construct the subunit and DNA vaccines for fundamentally inhibiting the binding of LPS to the target site. In addition, the immunogenicity and potential of two different forms of vaccines were compared and analyzed.

The eukaryotic vector is the main body of the DNA vaccine. The stronger the ability of the vector to express the antigen protein, the stronger the immune response induced in the host is (30). Some studies indicated that the waaF gene of *Bordetella pertussis* expressed in pBluescriptII (31) and *Vibrio parahaemolyticus* waaF cloned into pBBR1MCS2 (32) have prokaryotic expression. At present, there is no report on the construction of a eukaryotic vector of the waaF gene. In this study, the target gene was first cloned into pEGM-T, cut by *KpnI* and *BamH*, linearized by pcDNA3.1, and then the subcloned gene was expressed in the eukaryotic vector pcDNA3.1 and the pcwaaF was constructed. The successful development of pcwaaF was verified by sequencing.

The waaF gene sequence was transferred into MCF-7 cells in this study. There are many methods of transfection, and electroporation and liposome transfection are routinely used. Among them, electroporation has the highest transfection efficiency, which can reach more than 90% (33), but it can interfere with the key biological properties of cells, such as proliferation, metabolism, and gene expression (34). If the conditions of liposome transfection are optimized, the effect of liposome transfection is better than that of electroporation (35). Therefore, we selected G418 for transfection and concluded that 800 μg/mL was the lowest lethal dose. The WB results showed that the protein size was about 36 KDa, which was like the predicted results, and the rwaaF was successfully constructed.

The subunit vaccine is one of the most promising vaccines at present (36). Subunit vaccines for of hepatitis B, influenza, and pertussis (37) have been licensed for human use. Studies have been reported that the EspA subunit vaccine may become the first marketed vaccine against *E. coli* O157:H7 (38).

In vaccine research, low production cost, low price, and easy storage are key factors; however, safety is an important index for the utilization and promotion of the vaccine (39). At present, the universal vaccine for the prevention and treatment of coliform cow mastitis is the J5 vaccine which is inactivated *E. coli* vaccine with an incomplete O-antigen (39), and there are still some safety problems. It was found that the intraperitoneal injection of J5 inactivated vaccine could cause obvious toxic reactions in mice, such as rough coat, depression, hepatocyte enlargement, and inflammatory infiltration (39). Rainard reported that the J5 immune serum was not an improvement on the already high efficiency of naturally acquired antibodies to *E. coli* (40). However, the safety and effectiveness of the J5 vaccine in dairy cows has not been reported clearly (41). In this research, BALB/c mice were used to evaluate the safety at three to four times the immunization dose. The experimental mice did not have a poor mental state, and their hematological and blood biochemical indicators were within the normal range; beyond that, the mammary glands, liver, kidneys, and spleen of the mice did not show obvious pathological changes. This demonstrates that the DNA and subunit vaccines are safer than the J5 vaccine. The mice injected with the pcwaaF showed less energy and moved slowly, and the performance effects of a high dose were more obvious. The damage to mice in the rwaaF group was less severe than in the pcwaaF group. Therefore, rwaaF is safer than pcwaaF. The results of this study provide a very valuable basis for the promotion and application of the vaccine.

To compare the immunogenicity of rwaaF and pcwaaF, this study analyzed the IgG in serum and sIgA of feces on the

7th, 14th, 21st, and 28th days after injection, and detected IL-2, IL-4, and IFN-γ in serum on the 28th day. The results of ELISA showed that all the factors in the vaccine groups were significantly higher than in the control groups, and the levels of IgG in the 20 and 40 μg rwaaF groups were significantly higher than in the 20 and 40 μg pcwaaF groups. Beyond that, the effect of humoral immunity had nothing to do with the dose. This is consistent with comparison of the rwaaF and pcwaaF of *Corynebacterium pseudotuberculosis* acid phosphatase CP01850 (42); sIgA exists in the secretions of the nasal cavity, bronchus, and gastrointestinal juice, and it is the main antibody produced by mucosal immunity and an important indicator of mucosal immunity (43). The vaccine activated humoral immunity as well as mucosal immunity (44). The detection results of sIgA in feces were similar to those of IgG. However, the sIgA of the 20 μg rwaaF group was significantly higher than that of the 40 μg rwaaF group, further indicating that the effect of mucosal immunity is also dose independent. After immunization of mice with rwaaF/pcwaaF, because of the effect of TI and T2 (45), the levels of IL-2, IFN-γ, and IL-4 all increased and stimulated T and B lymphocytes to differentiate in different directions (46). Although both the rwaaF and pcwaaF stimulated cellular immunity, the detection of IL-2, IFN-γ, and IL-4 has further confirmed that the rwaaF is more effective than the pcwaaF. Among all the factors tested, only the 40 μg rwaaF group was IFN-γ-extremely significantly higher than in the 20 μg rwaaF group. In the challenge test, the survival rates of the 20 and 40 μg rwaaF groups were both 80%, and the survival rates of the 20 and 40 μg pcwaaF groups were 40 and 50%, respectively, while all the mice in the control group died. This shows that both rwaaF and pcwaaF produced immune protection in mice, and the rwaaF gave better protection. In summary, rwaaF is more immunogenic and has a better inoculation effect than pcwaaF; the analysis of this study proves that 20 μg rwaaF is more economical and practical than 40 μg, which provides a reference for subsequent clinical applications.

However, while waaF DNA vaccine and subunit vaccine could induce the humoral and cellular immunity in mice and show ideal immune protection effects, they have not been evaluated in dairy cows. In addition, DNA vaccine may be integrated with the chromosomal genome of the host cells (47–50), leading to cell transformation, canceration, etc. Further, the complex pathogenesis of bovine mastitis is closely related with pathogens, host immunity, internal environment, and other factors. So, there is still a gap in the research regarding enhancing immunity between waaF DNA vaccine and subunit vaccine, adapting to the internal environment of dairy cows, and synergizing host immunity. In conclusion, waaF DNA vaccine and subunit vaccine will be candidates for *E. coli* mastitis vaccine, and bring a new opportunity for prevention and treatment of *E. coli* mastitis.

CONCLUSION

This study demonstrates that waaF is a potential virulence factor in *E. coli,* and induced different immune responses as a purified recombinant subunit vaccine and DNA vaccine. The immune response elicited by waaF as a subunit vaccine is much stronger than DNA vaccine in murine model. These results suggest the utility of a new *E. coli* vaccine and provide a rationale for further investigation of bovine mastitis therapy and management.

DATA AVAILABILITY STATEMENT

The datasets presented in this study can be found in online repositories. The names of the repository/repositories and accession number(s) can be found in the article/supplementary material.

ETHICS STATEMENT

The animal study was reviewed and approved by the Academic Committee of Gansu Agricultural University.

AUTHOR CONTRIBUTIONS

HW put forward the research concept and design. TW, LC, and FL performed the data analysis and drafting the article. JS and YZ carried out the experiment and provided part of the test results for the manuscript. HW edited the manuscript for approval for submission. LY agreed to be accountable for all aspects of the work in ensuring that questions related to the accuracy or integrity of any part of the work are appropriately investigated and resolved. All the authors have approved the final version of the manuscript.

FUNDING

This work was supported by the fund of Gansu Key Laboratory of Animal Generational Physiology and Reproductive Regulation [Grant No. 20JR10RA563]; College of Veterinary Medicine, Gansu Agricultural University [Grant No. GAU XKJS 2018 056] and the fund of Innovation Star project of excellent postgraduates in Gansu Province [Grant No. 2021CXZX 358].

REFERENCES

1. Health EA, Animals BUF, Moretuslei P. Short communication : J-5 *Escherichia coli* vaccination does not influence severity of an *Escherichia coli* intramammary challenge in primiparous cows. *J Dairy Sci.* (2020) 103:6692–7. doi: 10.3168/jds.2019-17799
2. Turk R, Rošić N, Kuleš J, Horvatić A, Gelemanovic A, Galen A, et al. Milk and serum proteomes in subclinical and clinical mastitis in Simmental cows. *J Proteomics.* (2021) 244:104277. doi: 10.1016/j.jprot.2021.104277
3. Yang G, Yue Y, Li D, Duan C, Qiu X, Zou Y, et al. International immunopharmacology antibacterial and immunomodulatory effects of pheromonicin-NM on *Escherichia coli*-challenged bovine mammary epithelial cells. *Int Immunopharmacol.* (2020) 84:106569. doi: 10.1016/j.intimp.2020.106569
4. Toquet M, Gómez-Martín Á, Bataller E. Review of the bacterial composition of healthy milk, mastitis milk and colostrum in small ruminants. *Res Vet Sci.* (2021) 140:1–5. doi: 10.1016/j.rvsc.2021.07.022

5. Zadoks RN. An update on environmental mastitis : challenging perceptions. *Transbound Emerg Dis.* (2018) 65:166–85. doi: 10.1111/tbed.12704
6. Goldstone RJ, Harris S, Smith DGE. Genomic content typifying a prevalent clade of bovine mastitis- associated *Escherichia coli*. *Nat Publ Gr.* (2016) 1–15. doi: 10.1038/srep30115
7. Viguier C, Arora S, Gilmartin N, Welbeck K, Kennedy RO. Mastitis detection : current trends and future perspectives. *Sci Rep.* (2009) 6:30115. doi: 10.1016/j.tibtech.2009.05.004
8. Zhao X, Lacasse P, Zhao X, Lacasse P. Mammary tissue damage during bovine mastitis : causes and control. *J Anim Sci.* (2014) 86(13 Suppl.):57–65. doi: 10.2527/jas.2007-0302
9. Tran AX, Whitfield C. Lipopolysaccharides (endotoxins). In: *Encyclopedia of Microbiology*. Elsevier (2009). doi: 10.1016/B9780123739445.001966
10. Ledov VA, Golovina ME, Markina AA, Knirel YA, Vyacheslav LL, Kovalchuk AL, Aparin PG. Highly homogenous tri-acylated S-LPS acts as a novel clinically applicable vaccine against Shigella flexneri 2a infection. *Vaccine.* (2019) 37:1062–72. doi: 10.1016/j.vaccine.2018.12.067
11. Molinaro A. Chemistry of lipid A : at the heart of innate immunity. *Chemistry.* (2015) 21:500–19. doi: 10.1002/chem.201405771
12. Cote JM, Taylor EA. The glycosyltransferases of LPS core : a review of four heptosyltransferase enzymes in context. *Int J Mol Sci.* (2017) 18:2256. doi: 10.3390/ijms18112256
13. Wang Z, Wang J, Ren G, Li Y, Wang X. Deletion of the genes waaC, waaF, or waaG in *Escherichia coli* W3110 disables the fl agella biosynthesis. *J Basic Microbiol.* (2016) 56:1021–35. doi: 10.1002/jobm.201600065
14. Xu C, Zhang L, Zhang B, Feng S, Zhou S, Li J, et al. Involvement of lipooligosaccharide heptose residues of Haemophilus parasuis SC096 strain in serum resistance, adhesion and invasion. *Vet J.* (2013) 195:200–4. doi: 10.1016/j.tvjl.2012.06.017
15. Zeng Z, Chen X, Yue H, He H, Ren Y, Tang C, et al. The effect of rfaD and rfaF of Haemophilus parasuis on lipooligosaccharide induced inflammation by NF-κB/MAPKs signaling in porcine alveolar macrophages. *J Vet Med Sci.* (2018) 80:842–5. doi: 10.1292/jvms.16-0586
16. Chen Y, Yang Z, Dong Y, Chen Y. Recombinant PAL/PilE/FlaA DNA vaccine provides protective immunity against *Legionella pneumophila* in BALB/c mice. *BMC Biotechnol.* (2020) 20:28. doi: 10.1186/s12896-020-00620-3
17. Wang X, Guan Q, Wang X, Teng D, Mao R, Yao J, et al. Paving the way to construct a new vaccine against *Escherichia coli* from its recombinant outer membrane protein C via a murine model. *Process Biochem.* (2015) 50:1194–201. doi: 10.1016/j.procbio.2015.05.001
18. Chen W, Liu Y, Yin J, Deng Y, Ali T, Zhang J, et al. Cloning, expression, and immunogenicity of fimbrial-F17A subunit vaccine against *Escherichia coli* isolated from bovine mastitis. *Biomed Res Int.* (2017) 2017:3248483. doi: 10.1155/2017/3248483
19. Green MR, Sambrook J. *Molecular Cloning. A Laboratory Manual (Fourth Edition)*. New York (2012).
20. Josefsberg JO, Buckland B. Vaccine process technology. *Biotechnol Bioeng.* (2012) 109:1443–60. doi: 10.1002/bit.24493
21. Wu X. Establishment of eukaryotic expression system of dairy cow mastitis etiology gene ClfA, LPS and hlb and primary evaluation of immune protection of recombinant Clf A. Doctoral dissertation, Gansu Agri. Univ. (2016). p. 14–20.
22. Rainard P, Gilbert FB, Germon P, Foucras G. Invited review: a critical appraisal of mastitis vaccines for dairy cows. *J Dairy Sci.* (2021) 104:10427–48. doi: 10.3168/jds.2021-20434
23. Cunha AF, Andrade HM, Souza FN. Comparison of antibody repertories against *Staphylococcus aureus* in healthy and infected dairy cows with a distinct mastitis history and vaccinated with a polyvalent mastitis vaccine. *J Dairy Sci.* (2020) 103:4588–605. doi: 10.3168/jds.2019-17084
24. Steele NM, Swartz TH, Enger KM, Schramm H, Cockrum RR, et al. The effect of J5 bacterins on clinical, behavioral, and antibody response following an *Escherichia coli* intramammary challenge in dairy cows at peak lactation. *J Dairy Sci.* (2019) 102:11233–49. doi: 10.3168/jds.2019-16549
25. Oldfield NJ, Moran AP, Millar LA, Prendergast MM, Ketley JM. Characterization of the *Campylobacter jejuni* heptosyltransferase II gene, waaF, provides genetic evidence that extracellular polysaccharide is lipid A core independent. *J Bacteriol.* (2002) 184:2100–7. doi: 10.1128/JB.184.8.2100
26. Zeng Z, Fei L, He H, Chen X. Effect of lgtF,rfaF and rfaD genes in Haemophilus parasuis LOS induced pro-inflammatory cytokine expression in BALB/c mice. *J Southwest Univ Natl.* (2016) 42:281–4. doi: 10.11920/xnmdzk.2016.03.007
27. Nesper J, Kraiß A, Schild S, Bla J, Klose KE, Bockemühl J, et al. Comparative and genetic analyses of the putative *Vibrio cholerae* lipopolysaccharide core oligosaccharide biosynthesis (wav) gene cluster. *Infect Immun.* (2002) 70:2419–33. doi: 10.1128/IAI.70.5.2419
28. Gronow S, Brabetz W, Brade H. Comparative functional characterization *in vitro* of heptosyltransferase I (WaaC) and II (WaaF) from *Escherichia coli*. *Eur J Biochem.* (2000) 267:6602–11. doi: 10.1046/j.1432-1327.2000.01754.x
29. Chandan V, Logan SM, Harrison BA, Vinogradov E, Aubry A, Stupak J, et al. Characterization of a waaF mutant of *Helicobacter pylori* strain 26695 provides evidence that an extended lipopolysaccharide structure has a limited role in the invasion of gastric cancer cells. *Biochem Cell Biol.* (2007) 590:582–90. doi: 10.1139/O07-056
30. Peiris JSM, Yu WC, Leung CW, Cheung CY, Ng WF, Nicholls JM, et al. Re-emergence of fatal human influenza A subtype H5N1 disease. *Lancet.* (2004) 363:617–9. doi: 10.1016/S0140-6736(04)15595-5
31. Allen AG, Isobe T, Maskell DJ, Al AET, Acteriol JB. Identification and cloning of waaF (rfaF) from *Bordetella pertussis* and use to generate mutants of *Bordetella* spp. with deep rough lipopolysaccharide. *J Bacteriol.* (1998) 180:35–40.
32. Zhao F, Meng S, Zhou D. Construction and function of heptosyltransferase II gene deletion strain in O antigen gene cluster of *Vibrio parahaemolyticus*. *J Microbiol.* (2016) 56:291–300. doi: 10.13343/j.cnki.wsxb.20150258
33. Zu Y, Liu X, Chang A, Wang S. Bioelectrochemistry flow micropillar array electroporation to enhance size specific transfection to a large population of cells. *Bioelectrochemistry.* (2020) 132:107417. doi: 10.1016/j.bioelechem.2019.107417
34. Kumar ARK, Shou Y, Chan B, Krishaa L, Tay A. Materials for improving immune cell transfection. *Adv Mater.* (2021) 33:e2007421. doi: 10.1002/adma.202007421
35. Gladys G, Loretta P, Robert B, Rob S. Selection of an optimal RNA transfection reagent and comparison to electroporation for the delivery of viral RNA. *J Virol Methods.* (2009) 145:14–21. doi: 10.1016/j.jviromet.2007.04.013.Selection
36. Lin R, Zhu B, Zhang Y, Bai Y, Zhi F, Long B, et al. Microbial pathogenesis intranasal immunization with novel EspA-Tir-M fusion protein induces protective immunity against enterohemorrhagic *Escherichia coli* O157 : H7 challenge in mice. *Microb Pathog.* (2017) 105:19–24. doi: 10.1016/j.micpath.2017.01.062
37. Lee S, Nguyen MT. Recent advances of vaccine adjuvants for infectious diseases. *Immune Netw.* (2015) 15:51–7. doi: 10.4110/in.2015.15.2.51
38. Vande K, Vanrompay D, Cox E. Veterinary immunology and immunopathology bovine innate and adaptive immune responses against *Escherichia coli* O157 : H7 and vaccination strategies to reduce faecal shedding in ruminants. *Vet Immunol Immunopathol.* (2013) 152:109–20. doi: 10.1016/j.vetimm.2012.09.028
39. Xu Y, Zhou M, Zhu C, Ma W. Construction of recombinant strain of low toxic lipopolysaccharide-producing *Escherichia coli* J5 Gene. *Jiangsu Agric Sci.* (2020) 48:60–64. doi: 10.15889/j.issn.10021302.2020.17.009
40. Rainard P, Repérant-Ferter M, CGitton H, Germon P. Shielding effect of *Escherichia coli* O-antigen polysaccharide on J5-induced cross-reactive antibodies. *mSphere.* (2021) 6:1–15. doi: 10.1128/mSphere.01227-20
41. Zaatout N. An overview on mastitis-associated *Escherichia coli :* pathogenicity, host immunity and the use of alternative therapies. *Microbiol Res.* (2022) 256:126960. doi: 10.1016/j.micres.2021.126960
42. Brum AA, Braite DC, Thurow HS, Seixas FK, Portela RW, Borsuk S. Assessment of the acid phosphatase CP01850 from *Corynebacterium pseudotuberculosis* in DNA and subunit vaccine formulations against caseous lymphadenitis. *Arq Bras Med Vet Zootec.* (2020) 72:199–207. doi: 10.1590/1678416210790
43. Martinez FO, Helming L, Gordon S. Alternative activation of macrophages: an immunologic functional perspective. *Annu Rev Immunol.* (2009) 27:451–83. doi: 10.1146/annurev.immunol.021908.132532
44. Xu Z, Wang C, Yu R, Ding C. Efficacy analysis of severe acute respiratory syndrome coronavirus 2 DNA vaccine and recombinant subunit vaccine

inducing neutralizing antibodies in mice. *Acad J Second Mil Med Univ.* (2020) 41:474–48. doi: 10.16781/j.0258-879x.2020.05.0474
45. Wang T, Hu Y, Wangkahart E, Liu F, Wang A, Wang T. Interleukin (IL)-2 is a key regulator of T helper 1 and T helper 2 cytokine expression in fish: functional characterization of two divergent IL2 paralogs in salmonids. *Front. Immunol.* (2018) 9:1683. doi: 10.3389/fimmu.2018.01683
46. Xing J, Zhang Z, Luo K, Tang X, Sheng X, Zhan W. T and B lymphocytes immune responses in flounder (*Paralichthys olivaceus*) induced by two forms of outer membrane protein K from *Vibrio anguillarum* : subunit vaccine and DNA vaccine. *Mol Immunol.* (2020) 118:40–51. doi: 10.1016/j.molimm.2019.12.002
47. Nichols WW, Ledwith BJ, Manam SV, Troilo PJ. Potential DNA vaccine integration into host cell genome. *Ann N Y Acad Sci.* (1995) 772:30–9. doi: 10.1111/j.1749-6632.1995.tb44729.x
48. Manam S, Ledwith BJ, Barnum AB, Troilo PJ, Pauley CJ, Harper LB, et al. Plasmid DNA vaccines: tissue distribution and effects of DNA sequence, adjuvants and delivery method on integration into host DNA. *Intervirology.* (2000) 43:273–81. doi: 10.1159/000053994
49. Houston R, Moxon S, Nogué F, Papadopoulou N, Ramon M, Waigmann E. Assessment of the potential integration of the DNA plasmid vaccine CLYNAV into the salmon genome. *EFSA J.* (2017) 15:4689. doi: 10.2903/j.efsa.2017.4689
50. Doerfler W. Adenoviral vector DNA- and SARS-CoV-2 mRNA-based Covid-19 vaccines: possible integration into the human genome - are adenoviral genes expressed in vector-based vaccines? *Virus Res.* (2021) 302:198466. doi: 10.1016/j.virusres.2021.198466

Conflict of Interest: The authors declare that the research was conducted in the absence of any commercial or financial relationships that could be construed as a potential conflict of interest.

Publisher's Note: All claims expressed in this article are solely those of the authors and do not necessarily represent those of their affiliated organizations, or those of the publisher, the editors and the reviewers. Any product that may be evaluated in this article, or claim that may be made by its manufacturer, is not guaranteed or endorsed by the publisher.

frontiers | Frontiers in Veterinary Science

ORIGINAL RESEARCH
published: 12 May 2022
doi: 10.3389/fvets.2022.884425

Short Communication: Efficacy of Two Commercial Disinfectants on *Paenibacillus larvae* Spores

Joseph Kiriamburi[1], *Jamleck Muturi*[1], *Julius Mugweru*[1†], *Eva Forsgren*[2†] *and Anna Nilsson*[2*†]

[1] Department of Biological Sciences, University of Embu, Embu, Kenya, [2] Department of Ecology, Swedish University of Agricultural Sciences, Uppsala, Sweden

Paenibacillus larvae is a spore-forming bacterium causing American foulbrood (AFB) in honey bee larvae. The remains of a diseased larva contains billions of extremely resilient *P. larvae* spores viable for decades. Burning clinically symptomatic colonies is widely considered the only workable strategy to prevent further spread of the disease, and the management practices used for decontamination requires high concentrations of chemicals or special equipment. The aim of this study was to test and compare the biocidal effect of two commercially available disinfectants, "Disinfection for beekeeping" and Virkon S on *P. larvae*. The two products were applied to *P. larvae* spores in suspension as well as inoculated on two common beehive materials, wood and Styrofoam. "Disinfection for beekeeping" had a 100 % biocidal effect on *P. larvae* spores in suspension compared to 87.0–88.6% for Virkon S which, however, had a significantly better effect on *P. larvae* on Styrofoam. The two disinfectants had similar effect on infected wood material.

Keywords: *Paenibacillus larvae*, American foulbrood, disinfectants, apis mellifera, spores

OPEN ACCESS

Edited by:
Kun Li,
Nanjing Agricultural University, China

Reviewed by:
Giovanni Cilia,
Council for Agricultural and Economics Research (CREA), Italy
Milica Ljaljevic Grbic,
University of Belgrade, Serbia

***Correspondence:**
Anna Nilsson
anna.nilsson@slu.se

***ORCID:**
Eva Forsgren
orcid.org/0000-0002-8244-7265
Anna Nilsson
orcid.org/0000-0001-9219-2385
Julius Mugweru
orcid.org/0000-0002-8799-660X

Specialty section:
This article was submitted to Veterinary Infectious Diseases, a section of the journal Frontiers in Veterinary Science

Received: *26 February 2022*
Accepted: *04 April 2022*
Published: *12 May 2022*

Citation:
Kiriamburi J, Muturi J, Mugweru J, Forsgren E and Nilsson A (2022) Short Communication: Efficacy of Two Commercial Disinfectants on Paenibacillus larvae Spores. Front. Vet. Sci. 9:884425. doi: 10.3389/fvets.2022.884425

INTRODUCTION

Paenibacillus larvae is a spore-forming, Gram-positive bacterium causing the severe disease American foulbrood (AFB) in honey bee larvae. Honey bee larvae become infected from ingesting food contaminated with *P. larvae* spores that germinate in the midgut and eventually kills the larvae. The remains of the larvae contains billions of spores and serves as sources for new infections. The *P. larvae* spores are resilient and can remain viable in the environment for decades (1–3). A common way to control AFB is by burning the contaminated hives and bees, although the latter can sometimes be saved as an artificial swarm, housed on new or disinfected material (4). Hive material can be decontaminated using chemical disinfectants or heat. Chemical disinfectants have been shown to have a high efficacy on spores in suspension, but less effective on wood-based equipment (3, 5). There are several methods using heat for decontamination of hive material, for example dipping in hot paraffin, scorching, dry heat and autoclaving (3). These methods are effective (3, 6), but requires access to advanced equipment.

Our aim was to test and compare the biocidal effect of 2 disinfectants, "Disinfection for beekeeping" (DFB) (Swienty, Denmark) and Virkon S (Lanxess, Germany) on *P. larvae* spores. DFB is developed for disinfection of hive material, gloves and tools and, according to the manufacturer (www.swienty.com, viewed October 9 2019), have a 99.99% biocidal effect on all viruses, bacteria, spores and fungi. Virkon S is a common disinfectant that have been on the market for over

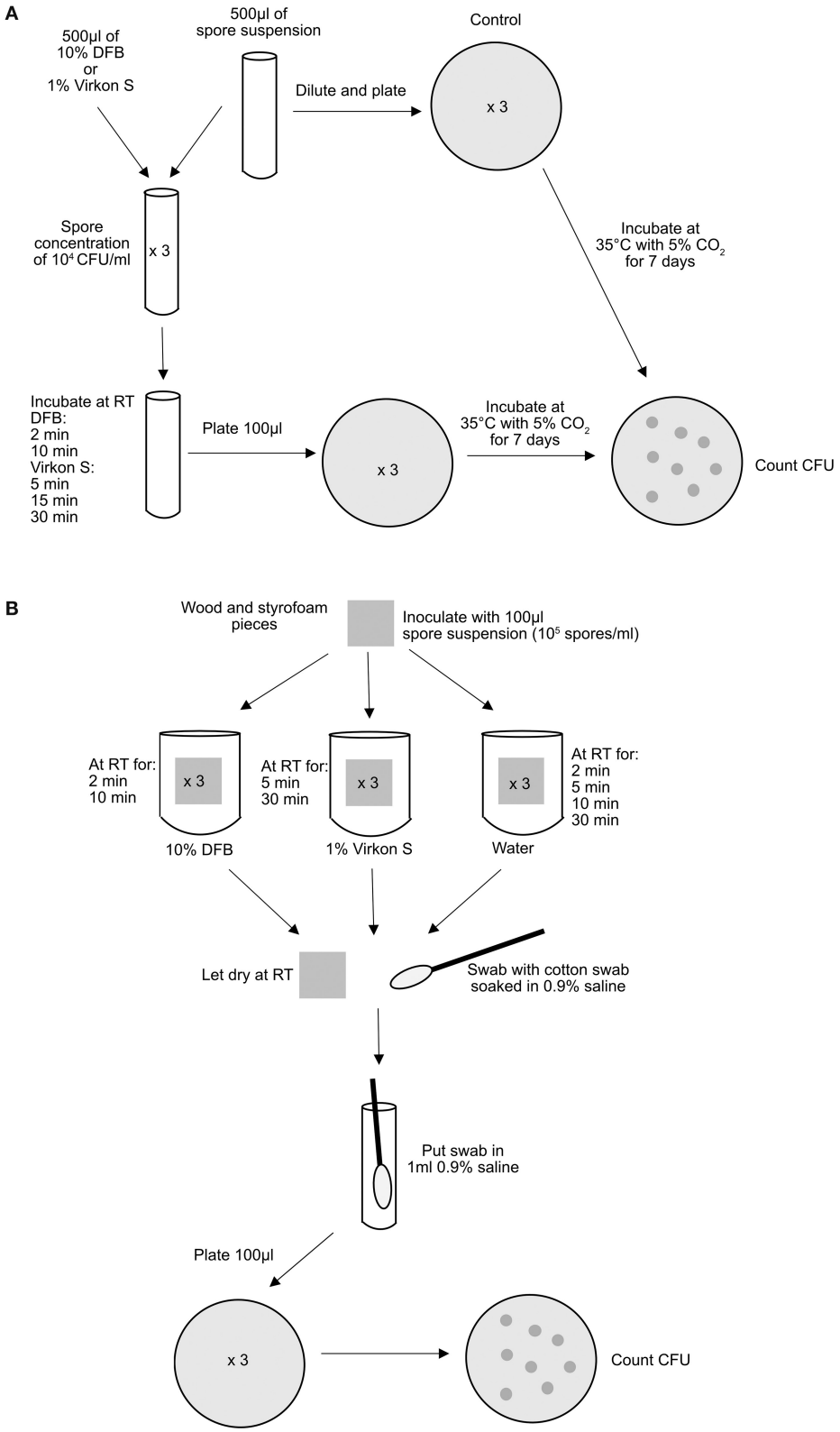

FIGURE 1 | Schematic description of the experimental setup. **(A)** in spore suspension and **(B)** on wood and Styrofoam. RT, room temperature.

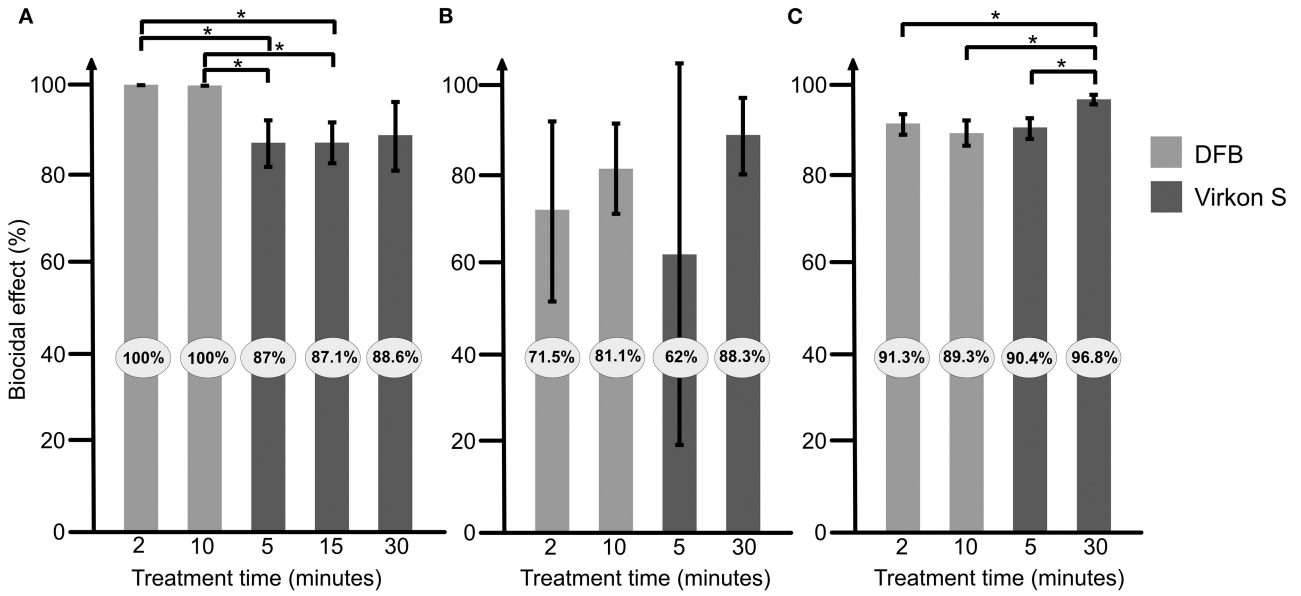

FIGURE 2 | Efficacy of the 2 disinfectants "Disinfection for beekeeping" (DFB) and Virkon S on *Paenibacillus larvae* spores in suspension **(A)**, on wood **(B)**, and on Styrofoam **(C)**. Light gray bars shows results for DFB and darker gray Virkon S. The result is presented as an average from at least 3 repeats, with error bars indicating standard deviation. Significant differences are indicated. *P <0.05.

30 years, originally developed for farm and livestock production (7) (www.virkons.se, viewed October 8 2019).

MATERIALS AND METHODS

A spore suspension was prepared from *P. larvae* cultures on agarplates (14 days to obtain sporulation) in sterile 0.9% saline solution. The spore suspension was stored at 4°C, heat shocked at 85°C for 10 min and diluted to the desired concentrations before the start of each experiment.

The experiments were performed as described in **Figure 1** and repeated at least 3 times. *P. larvae* were cultured according to standard cultivation methods (8).

The biocidal effect of the disinfectants was calculated by comparing the number of CFUs from the treated samples and the untreated spore suspension or the mock treated wood and Styrofoam pieces.

Student's t test (unpaired, 2-tailed) was used to identify statistically significant differences, with a $P \leq 0.05$ considered significant.

RESULTS

DFB had the highest biocidal effect (100% already after 2 min) on spores in suspension and was significantly more efficient than the 5 and 15 min Virkon S treatments (all $P = 0.01$, **Figure 2A**).

On wood, no significant differences could be seen between DFB and Virkon S, or the between the different treatment times (**Figure 2B**).

On Styrofoam, a significantly higher biocidal effect was observed after 30 min treatment with Virkon S compared to 2 and 10 min treatment with DFB (both $P = 0.02$, **Figure 2C**). The 30 min treatment with Virkon S had also a significantly higher biocidal effect than the 5 min treatment ($P = 0.01$, **Figure 2C**).

DISCUSSION

This study compares the biocidal effect of 2 disinfectants on *P. larvae* spores. Both disinfectants had an effect on the bacterial spores in suspension and on wood and Styrofoam. DFB had the best effect on the bacterial spores in suspension where all *P. larvae* spores were killed. These results are in line with the information from the manufacturer saying that DFB kills all viruses, bacteria, fungi and spores within 45 s. However, the effect of DFB on spores on wood and Styrofoam was lower than in suspension (**Figure 1**). Virkon S was slightly less effective than DFB on spores in suspension, but the differences were not significant. Thirty minutes treatment (recommended by the manufacturer) of Virkon S on contaminated Styrofoam was significantly more effective than the treatment with DFB (**Figure 2C**). Virkon S has in a previous study been shown to kill 80% of *P. larvae* spores (9). In this study however, the biocidal effect ranged from 88.6 to 96.8% after 30 min treatment (**Figure 1**). The effect of both disinfectants on wood varied more than the effect on Styrofoam and in suspension, most likely due to difficulties recovering *P. larvae* from wood. This is probably because wood is more porous and absorbs the liquid with the spores. *P. larvae* spores can "hide" in wood,

making it more difficult for the disinfectant to access the bacterium. The wood and Styrofoam pieces used in this study were clean, i.e., they were not covered in wax or propolis. Any disinfectants will probably be less effective on used, non-cleaned hive material where large amounts of bacterial spores may be inaccessible to the disinfectants. It is therefore important that infected materials are thoroughly cleaned before being treated with disinfectants.

DATA AVAILABILITY STATEMENT

The original contributions presented in the study are included in the article/supplementary material, further inquiries can be directed to the corresponding author.

AUTHOR CONTRIBUTIONS

EF and AN developed the research concept. JK, EF, and AN designed and performed the experiments. JK, JMut, JMug, and AN co-wrote the manuscript. EF provided the resources, supervision, and funding assistance. All authors contributed to the article and approved the submitted version.

ACKNOWLEDGMENTS

We thank Karin Ullman for technical assistance and Preben Kristiansen for valuable comments, and we are thankful for the support from the Linnaeus-Palme international exchange program.

REFERENCES

1. Forsgren E, Stevanovic J, Fries I. Variability in germination and in temperature and storage resistance among *Paenibacillus larvae* genotypes. *Vet rinary Microbiol.* (2008) 129:342–9. doi: 10.1016/j.vetmic.2007.12.001
2. Haseman L. How long can spores of american foulbrood live? *Am Bee J.* (1961) 101:298–9.
3. Dobbelaere W, et al. Disinfection of wooden structures contaminated with *Paenibacillus larvae* subsp. *Larvae spores. J Appl Microbiol.* (2001) 91:212–216. doi: 10.1046/j.1365-2672.2001.01376.x
4. Genersch E. American Foulbrood in honeybees and its causative agent, *Paenibacillus larvae. J Invertebrate Pathol.* (2010) 103:S10–9. doi: 10.1016/j.jip.2009.06.015
5. Okayama A, Sákogawa T, Nakajima C, Hayama T. Sporicidal activities of disinfectants on *Paenibacillus larvae. J Vet Med Sci.* (1997) 59:953–4. doi: 10.1292/jvms.59.953
6. Del Hoyo M, Basualdo M, Torres J, Bedascarrasbure E. Use of DHT-Equpment for Disinfection of AFB-Contaminated Beehive Materials in Argentina. *Am Bee J.* (1998) 138:738–40.
7. Hernández A, et al. Assessment of in-vitro efficacy of 1% Virkon® against bacteria, fungi, viruses and spores by means of AFNOR guidelines. *Journal of Hospital Infection.* (2000) 46:203–209. doi: 10.1053/jhin.2000.0818
8. Nordström S, Fries I. A comparison of media and cultural conditions for identification of Bacillus larvae in honey. *J Apic Res.* (1995) 34:97–103. doi: 10.1080/00218839.1995.11100894
9. Hansen H, Brødsgaard CJ. American foulbrood: a review of its biology, diagnosis and control. *Bee World.* (1999) 80:5–23. doi: 10.1080/0005772X.1999.11099415

Conflict of Interest: The authors declare that the research was conducted in the absence of any commercial or financial relationships that could be construed as a potential conflict of interest.

frontiers | Frontiers in Veterinary Science

ORIGINAL RESEARCH
published: 27 May 2022
doi: 10.3389/fvets.2022.879805

Protective Effect of *Bifidobacterium lactis* JYBR-190 on Intestinal Mucosal Damage in Chicks Infected With *Salmonella pullorum*

Liangyu Yang[1,2], *Yuanhong Chen*[2], *Qian Bai*[2], *Xi Chen*[2], *Yunteng Shao*[2], *Ronghai Wang*[2], *Fengping He*[2]* *and Ganzhen Deng*[1]*

[1] Department of Clinical Veterinary Medicine, College of Veterinary Medicine, Huazhong Agricultural University, Wuhan, China,
[2] Department of Clinical Veterinary Medicine, College of Veterinary Medicine, Yunnan Agricultural University, Kunming, China

Pullorum is one of the most serious diseases that endanger the chicken industry. With the advent of the era of anti-antibiotics in feed, the replacement of antibiotics by probiotics has become the focus and hotspot of related research. In this study, hematoxylin-eosin (H&E) staining, immunohistochemistry (IHC) and enzyme-linked immunosorbent assay (ELISA) were used to observe the structural changes of intestinal mucosa in chicks infected with *Salmonella pullorum*, and to analyze TNF-α, IL-10, IFN-γ, proliferating cell nuclear antigen (PCNA), and secreted immunoglobulin A (sIgA) levels. The results showed that the intestinal villus height, villus height to crypt depth ratio (V/C), and muscle layer thickness of duodenum, jejunum and cecum in the JYBR-190 group were significantly higher than those of the infection group and antibiotic group. Furthermore, the levels of PCNA, sIgA and IL-10 in JYBR-190 group were significantly increased, whereas the expression of TNF-α and IFN-γ was significantly decreased. Taken together, *Bifidobacterium lactis* JYBR-190 has a protective effect on intestinal mucosal damage in chicks infected with *Salmonella pullorum*.

Keywords: ***Salmonella pullorum***, ***Bifidobacterium lactis***, **intestinal mucosa, inflammation, damage**

OPEN ACCESS

Edited by:
Kun Li,
Nanjing Agricultural University, China

Reviewed by:
Jin-Long Li,
Northeast Agricultural University, China
Pang Quanhai,
Shanxi Agricultural University, China

***Correspondence:**
Fengping He
hefengping@outlook.com
Ganzhen Deng
ganzhendeng@sohu.com

Specialty section:
This article was submitted to Veterinary Infectious Diseases, a section of the journal Frontiers in Veterinary Science

Received: *20 February 2022*
Accepted: *01 April 2022*
Published: *27 May 2022*

Citation:
Yang L, Chen Y, Bai Q, Chen X, Shao Y, Wang R, He F and Deng G (2022) Protective Effect of Bifidobacterium lactis JYBR-190 on Intestinal Mucosal Damage in Chicks Infected With Salmonella pullorum. Front. Vet. Sci. 9:879805. doi: 10.3389/fvets.2022.879805

INTRODUCTION

Pullorum is a widespread acute intestinal infectious disease caused by Salmonella Pullorum in the world. Salmonella pullorum was discovered by Rettger (1), and it can be transmitted vertically to the next generation of chicks. The morbidity and mortality of 2–3 week old chicks are extremely high (2), causing serious impact on the world chicken industry (3–5). In recent years, many countries have restricted the use of antibiotics to varying degrees due to the overuse of antibiotics resulting in drug resistance of animal-derived bacteria and drug residues, and the "banning of antibiotics" in feed has become an inevitable trend in the development of international animal husbandry (6, 7). Therefore, probiotics have gradually entered people's field of vision as an alternative to antibiotics.

Probiotics improve food safety and animal gut health by producing organic acids, activating the host immune system, and producing antimicrobial agents (8). Studies have shown that probiotics play an important role in stabilizing intestinal flora and controlling pathogen proliferation, and the addition of probiotics to feed increases host

and colonization resistance to enteric pathogens such as Salmonella and Campylobacter (9). Currently, Bifidobacterium strains such as Bifidobacterium longum, Bifidobacterium longum, Bifidobacterium longum, and Bifidobacterium suis have been used to modulate human and animal microflora (10, 11). Roselli et al. found that the mixture of Lactobacillus acidophilus and Bifidobacterium longum had a good preventive effect on trinitrobenzenesulfonic acid-induced colitis in mice. Zuo et al. found that Bifidobacterium infantis effectively attenuates colitis in mice by regulating Th1/Th17 cell-mediated immune responses (12–14). Other studies have shown that Bifidobacterium breve JCM1192 reduces the colonization of Salmonella typhimurium in the cecum by a competitive exclusion mechanism, and Bifidobacterium infantis BL2416 protects the gut by promoting the production of IFN-γ and TNF-α (15–17). Therefore, this study selected Bifidobacterium as the bacteria of interest to explore the protective effect of Bifidobacterium lactis JYBR-190 on the intestinal mucosa of chicks infected with S. pullorum.

MATERIALS AND METHODS

Bacterial Strains

Salmonella pullorum was isolated and preserved in this experiment and fed with 2.32×10^9 CFU at the median lethal dose (LD_{50}) to induce pullorum infection. Bifidobacterium lactis JYBR-190 dry powder was donated by Shandong Zhongke Jia Yiwan Bioengineering Co., Ltd. It was fed via drinking water at the ratio of 10 g JYBR-190 dissolved in 100 L water to obtain a concentration of $\sim 1 \times 10^{11}$ CFU/mL.

Animal Experiments

SPF fertilized eggs were purchased from Jinan Seth Poultry Technology Co., Ltd.. The hatching and animal experiments were performed in the laboratory of Yunnan Agricultural University. A total of 100 SPF chicks were randomly divided into five groups ($n = 20$): Group A, Group B, Group C, Group D, and Group E. Group A was fed a sterilized diet as the control group. Groups B, C, D, and E were orally administered 0.5 mL *S. pullorum* containing 2.32×10^9 CFU from the age of 7 days. Meanwhile, Group C received JYBR-190 with a concentration of 1.0×10^9 CFU/mL in the drinking water every day from the age of 1 day. JYBR-190 was first added to the drinking water of Group D every day after 24 h infection, and 0.15 g/kg of neomycin sulfate was added to the drinking water of group E every day after 24 h of infection. Each experimental group was reared in isolation, and the chicks were allowed to eat sterile diet and drinking water freely during the experiment. The mortality of chickens in each group from 7 days to 14 days was recorded, and the body weight of chickens in each group was weighed at 14 days of age. This study was approved by the Ethics Committee of Yunnan Agricultural University. All experimental procedures adhered to the institutional criteria for the care and use of laboratory animals.

Sample Collection

At the age of 14 days, 5 chicks were randomly selected from each group, and their duodenum, jejunum and cecum of about 2 cm were collected, and the intestinal contents were washed with PBS, fixed in 4% paraformaldehyde, and used for hematoxylin- Eosin (H&E) staining and immunohistochemistry (IHC). Another about 5 cm of duodenum, jejunum and cecum were taken, and the intestinal segment was washed with PBS and ground into tissue homogenate for the determination of secreted immunoglobulin A (sIgA) and intestinal cytokines.

Histological Analysis

Routine dehydration, clearing, paraffin immersion, and paraffin embedding were performed on fixed tissues. Two sets of 4 μm thick serial sections were prepared, one for H&E staining and the other for IHC staining. First soak the paraffin section in xylene twice for 8 min each time, then immerse in gradient alcohol for dewaxing, stain with hematoxylin for 3–5 min, differentiate with 1% hydrochloric acid-ethanol solution, turn blue with 1% ammonia solution, rinse with distilled water Sections were dehydrated with gradient alcohol, stained with eosin for 5 min, routinely dehydrated with paraffin sections, cleared with xylene for 5 min, and sealed with neutral gum. Two sections of the duodenum, jejunum and cecum of each chick were selected for sectioning, and three longest intestinal villi and crypts were selected for each section for measurement, and three visual fields were randomly selected to measure the thickness of the muscle layer. About 30 crypt depth/villus height and muscle thickness values were obtained for each group, and the whole intestinal section was imaged under a 20 × photographic microscope, each villus height and its corresponding crypt depth were measured, and this Ratio and mean of 3 sets of data values. The height of the intestinal villi was measured vertically from the tip of the intestinal villi to the opening of the intestinal gland; the depth of the crypt, the thickness of the muscle layer and the villus height were measured vertically from the opening of the intestinal gland to the mucosal muscle layer.

Immunohistochemical Analysis

Sections were routinely deparaffinized with distilled water, incubated with 3% H_2O_2 for 10 min at room temperature (RT) to inhibit endogenous peroxidase activity. Antigen activity in the sections was repaired with sodium citrate buffer for 10 min, and incubated with 3% BSA at RT in a humidified chamber closed for 30min. After removing the serum, the rabbit anti-proliferating cell nuclear antigen (PCNA) antibody (BS-2007R, 1:20; Beijing Biotechnology, China) was added, and incubated overnight at 4°C, before adding biotinylated goat anti-rabbit antibody (K009; KemeiBorui Technology, Beijing, China) and incubating at 25°C for 1 h. Horseradish peroxidase (HRP)-labeled streptavidin complex (SP9002; Beijing Zhongshan Jinqiao Biotechnology Co., Ltd., Beijing) was added and incubated at RT for 30 min. 3, 3'-Diaminobenzidine (DAB; Beijing Zhongshan Jinqiao Biotechnology Co., Ltd., Beijing) was added for 5–10 min, and the degree of staining was controlled by a microscope. Counterstained with hematoxylin for 3 min, dehydrated and transparentized for 5 min, dried and sealed with neutral glue.

5 slices were selected for each group, and 40× fields of view were selected for each slice. The mean optical density (OD) of intestinal PCNA immunopositive substances was determined using proplus (IPP) software 6.0.

Measurement of Intestinal SIgA and Cytokine Levels

Five groups of intestinal samples were ground into a homogenate in liquid nitrogen, and sIgA levels were measured by chicken sIgA ELISA kit (Shanghai Enzyme Link Biotechnology Co., Ltd., Shanghai, China). IL-10, TNF-α, and IFN-γ levels were measured according to IL-10, TNF-α and IFN-γ ELISA kits (Shanghai Enzyme Link Biotechnology Co., Ltd., Shanghai, China).

Statistical Analysis

Statistical analysis was performed using SPSS 13.0 (SPSS Inc., Chicago, IL). If the data obey normal distribution, one-way ANOVA is used; Otherwise, the multiple rank sum test is used.Data organization and analysis were performed with Graphpad Prism 8.0.1, and data measurements were performed using Image Proplus (IPP) software version 6.0. All data were expressed as mean ± standard deviation (SD) or percentage. $P < 0.05$ was considered statistically significant.

RESULTS

Mortality Rate and Average Body Weight of Different Treatment Groups

At 14 days of age, the mortality rate of blank control group A was 10%, and the mortality rate increased to 70% after infection with Salmonella pullorum. Compared with the infection group, feeding JYBR-190 before infection reduced the mortality rate to 33.3%, and feeding JYBR-190 and antibiotic treatment after infection reduced the mortality rate to 45% and 40%. The average weight of the blank control group was 71.25 g, while the average weight was reduced to 44.62 g by infection with Salmonella pullorum. Compared with the infection group, feeding JYBR-190 before infection increased the average body weight to 76.79 g, and feeding JYBR-190 and antibiotic treatment after infection increased the average body weight to 60.02 g and 58.35 g, respectively. The results show that feeding Bifidobacterium lactis JYBR-190 can reduce the mortality and weight loss caused by *Salmonella pullorum* infection, and feeding JYBR-190 before infection is more effective.

Pathological Changes of Duodenum, Jejunum and Cecum in Different Treatment Groups

Morphological observation of the duodenum showed that the duodenal villi in the blank control group had a complete structure, neatly arranged epithelial cells, and no obvious pathological changes (**Figure 1**). In the infection group, the villi structure was incomplete, the villus epithelial cells were dissolved and disappeared, the arrangement was disordered, and the intestinal glands had mild hyperplasia. In the JYBR-190 pre-fed group, the villi structure was relatively complete, the epithelial cells in the upper segment of villus were slightly shed, and the intestinal glands had mild hyperplasia, but the degree of lesions was milder than that in the infection group. The JYBR-190-fed group had a complete villi structure, neatly arranged epithelial cells, no epithelial shedding, and infiltration of lamina propria inflammatory cells. In the antibiotic group, the villous structure was incomplete, the villous epithelium was shed, and the intestinal glands had mild hyperplasia.

The jejunum morphological structure showed that the jejunal villi in the blank control group had a complete structure, neatly arranged epithelial cells, and no obvious pathological changes such as epithelial shedding or inflammatory cell infiltration (**Figure 1**). In the infection group, the jejunal

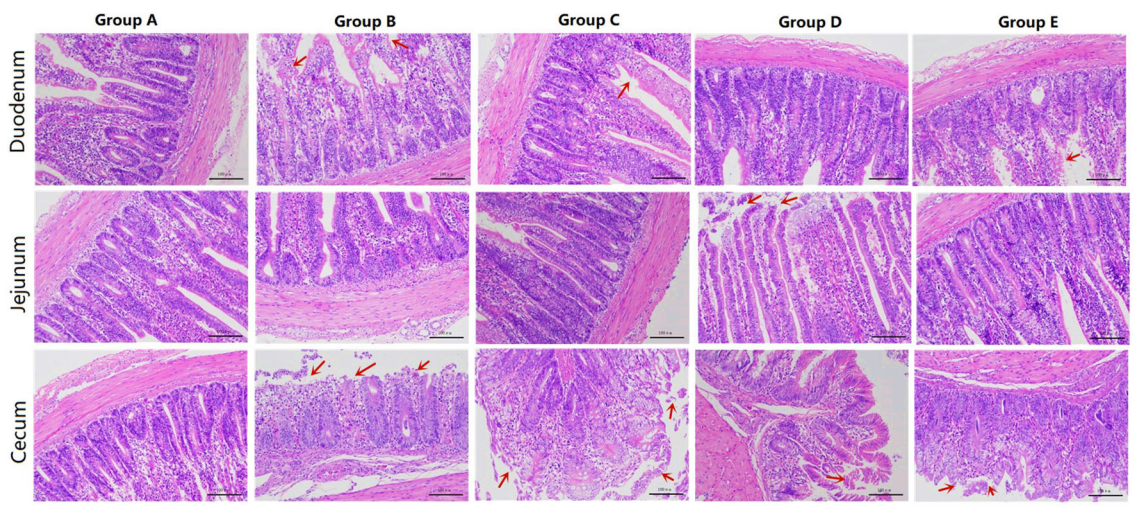

FIGURE 1 | HE sections of different treatment groups. Group A, control group; Group B, infection group; Group C, JYBR-190 pre-fed group; Group D, JYBR-190 fed group; Group E, antibiotic group.

villus epithelial cells were sloughed off and the upper villus epithelial cells were sloughed off more obviously, the cells were not arranged neatly, some inflammatory cells infiltrated the lamina propria and the basal part, and the intestinal gland cells proliferated. In the JYBR-190 pre-fed group, the villi structure was complete, and the epithelial cells were slightly disordered. In the antibiotic group and the JYBR-190 fed group, the epithelium of the villi fell off, and there were no other obvious lesions.

The cecum morphological structure found that some epithelial cells of the cecum villi were shed in the blank control group (**Figure 1**), and the others had no obvious lesions. In the infection group, the structure of the cecal villi was incomplete, epithelial cells were severely shed, a large number of inflammatory cells infiltrated the lamina propria and basal layer, and intestinal gland cells proliferated. The villous structure of the JYBR-190 pre-fed group was relatively complete, and the epithelial cells in the upper segment of the villi were partially shed. The intestinal villi in the JYBR-190 fed group were damaged, and the villus epithelial cells were necrotic and shed. Villous epithelial cell shedding and intestinal glandular hyperplasia were observed in the antibiotic group.

Changes in Villus Height, Crypt Depth, Villus Height and Crypt Depth, (V/C) Ratio and Muscle Thickness of Each Intestinal Segment in Different Treatment Groups

The histomorphology of duodenum in different treatment groups was observed, and the changes of duodenal villus height, crypt depth, V/C ratio and muscle layer thickness were analyzed. Changes in the depth of intestinal crypts showed that the depth of intestinal crypts in the Salmonella pullorum infection group was significantly higher than that in the blank control group. Compared with the Salmonella pullorum infection group, the depth of intestinal crypts in the JYBR-190 pre-fed, JYBR-190 fed, and antibiotic groups were reduced to varying degrees, and the difference was significant. The depth of the fossa decreased significantly (**Figure 2A**). Changes in intestinal villus height, V/C value and muscle layer thickness showed that the Salmonella pullorum infection decreased significantly the intestinal villus height, V/C value and muscle layer thickness compared with the blank control group. Compared with the Salmonella pullorum infection group, the intestinal villus height, V/C value and muscle layer thickness in the JYBR-190 pre-fed, JYBR-190

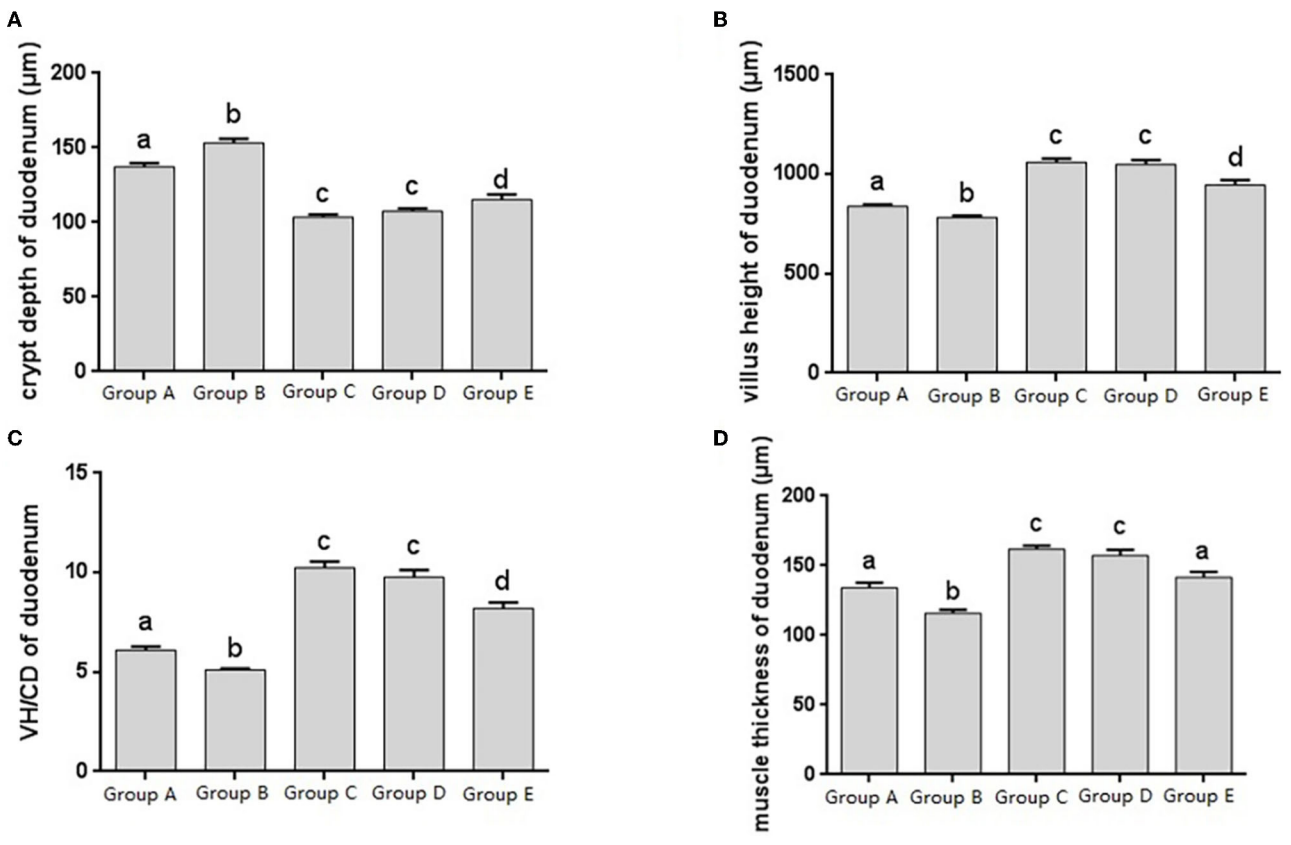

FIGURE 2 | Morphological changes in the duodenum of chicks after different treatments. **(A)** Crypt depth (CD) of the duodenum. **(B)** Villus height (VH) of the duodenum. **(C)** VH/CD of the duodenum. **(D)** Muscle thickness of duodenum. Group A, control group; Group B, infection group; Group C, JYBR-190 pre-fed group; Group D, JYBR-190 fed group; Group E, antibiotic group. Data are expressed as mean ± standard deviation (SD). Different lowercase letters on the columns indicate significant differences ($P < 0.05$); the same lowercase letters indicate no significant difference ($P > 0.05$).

fed, and antibiotic groups were increased to different degrees, and the difference was significant. The intestinal villi, V/C value and muscle layer thickness were significantly higher in the JYBR-190 pre-fed and fed groups than in the antibiotic group (**Figures 2B–D**). It indicated that feeding Bifidobacterium lactis JYBR-190 could increase the duodenal villus height, V/C value and muscle layer thickness, and decrease the depth of intestinal crypts.

The jejunal tissue morphology was observed in different treatment groups, and the changes in jejunal villus height, crypt depth, V/C ratio and muscle thickness were measured, and it was found that the change trend was roughly consistent with that of the duodenum (**Figures 3A–D**). The V/C value of the JYBR-190 pre-fed group was the highest among several (**Figure 3C**). It indicated that feeding Bifidobacterium lactis JYBR-190 could increase jejunal villus height, V/C value and muscle layer thickness, and reduce intestinal crypt depth. Feeding JYBR-190 before infection could even increase jejunal V/C value.

The histomorphology of cecum in different treatment groups was observed, and the changes of cecal villus height, crypt depth, V/C ratio and muscle layer thickness were analyzed. Changes in the depth of cecal crypts showed that the depth of intestinal crypts in the Salmonella pullorum infection group was significantly higher than that in the blank control group. Compared with the Salmonella pullorum infection group, the depth of intestinal crypts in the JYBR-190 pre-fed, JYBR-190 fed, and antibiotic groups were reduced to varying degrees, and the difference was significant (**Figure 4A**). The changes of cecal villus height, V/C value and muscle layer thickness showed that the Salmonella pullorum infection group decreased significantly the intestinal villus height, V/C value and muscle layer thickness compared with the blank control group. Compared with the Salmonella pullorum infection group, the intestinal villus height, V/C value and muscle layer thickness in the JYBR-190 pre-fed, JYBR-190 fed, and antibiotic groups were increased to different degrees, and the difference was significant. Compared with the antibiotic group, the intestinal villi and V/C values of the JYBR-190 pre-fed and fed groups were significantly higher (**Figures 4B,C**), and the difference in muscle layer thickness was not significant (**Figure 4D**). Before infection, the intestinal villi and V/C values of the JYBR-190 pre-fed group were the highest among several groups (**Figures 4B,C**). It indicated that feeding Bifidobacterium lactis JYBR-190 could increase cecal villus height and V/C value and reduce crypt depth, and feeding JYBR-190 before infection could increase cecal villus height and V/C value.

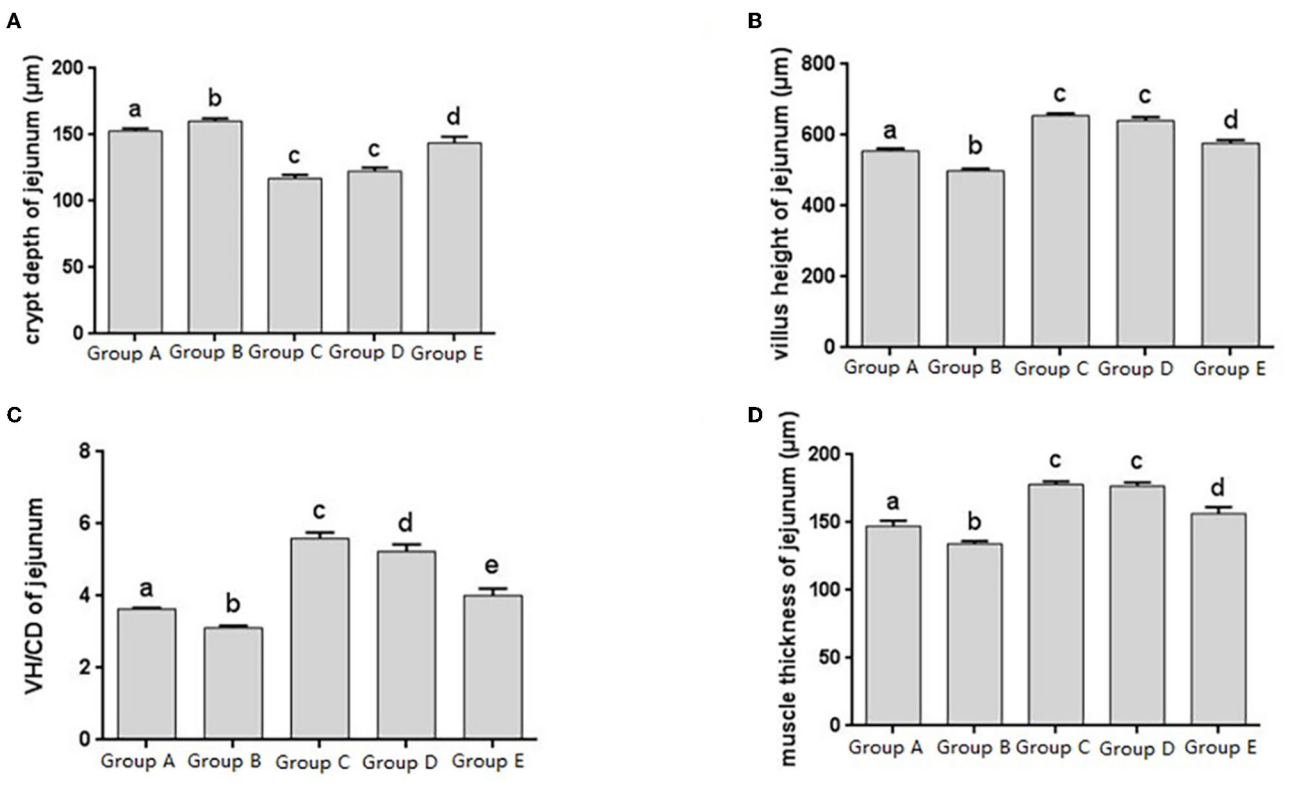

FIGURE 3 | Morphological changes in the jejunm of chicks after different treatments. **(A)** Crypt Depth (CD) of jejunum. **(B)** Villus height (VH) of jejunum. **(C)** VH/CD of jejunum. **(D)** Muscle thickness of jejunum. Group A, control group; Group B, infection group; Group C, JYBR-190 pre-fed group; Group D, JYBR-190 fed group; Group E, antibiotic group. Data are expressed as mean ± standard deviation (SD). Different lowercase letters on the columns indicate significant differences ($P < 0.05$); the same lowercase letters indicate no significant difference ($P > 0.05$).

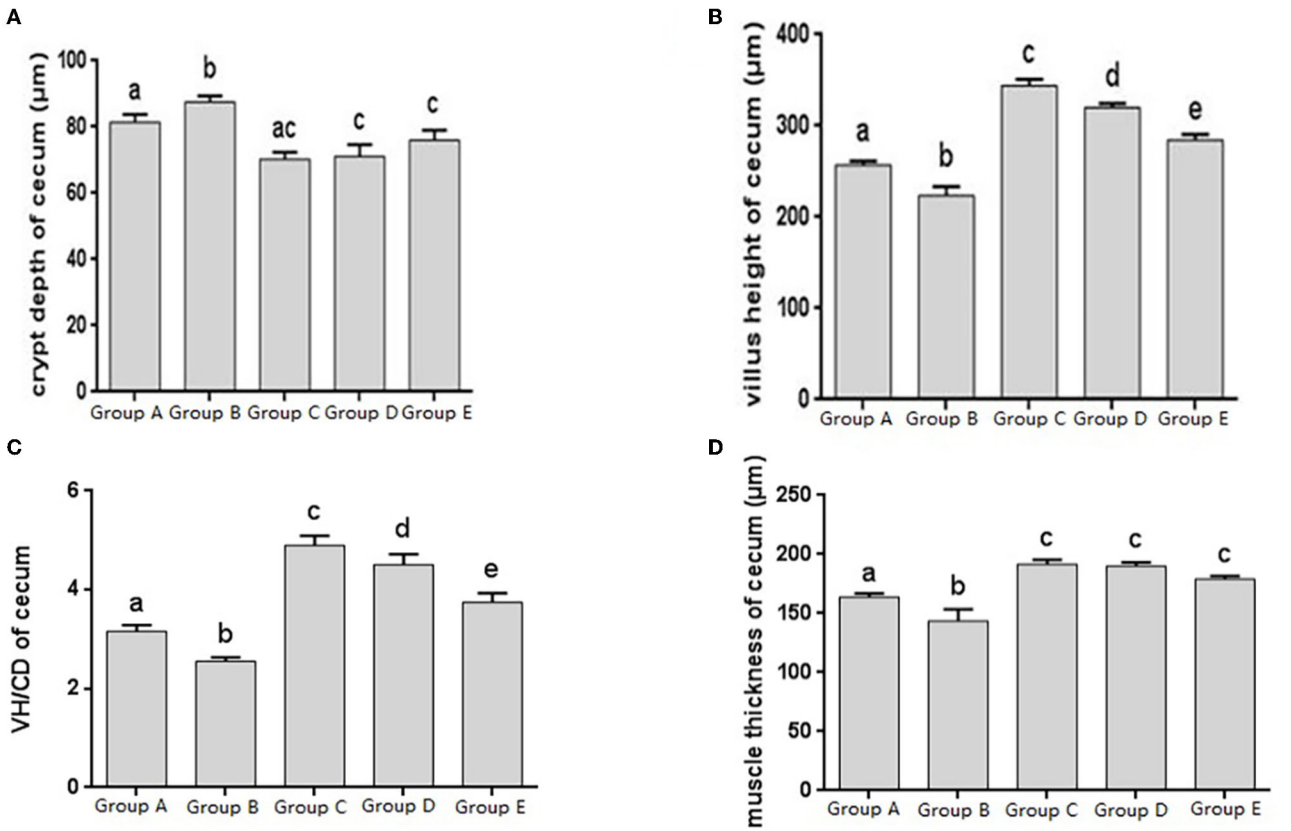

FIGURE 4 | Morphological changes in the cecum of chicks after different treatments. **(A)** Crypt Depth (CD) of the cecum. **(B)** Villus height (VH) of the cecum. **(C)** VH/CD of the cecum. **(D)** Muscle thickness of cecum. Group A, control group; Group B, infection group; Group C, JYBR-190 pre-fed group; Group D, JYBR-190 fed group; Group E, antibiotic group. Data are expressed as mean ± standard deviation (SD). Different lowercase letters on the columns indicate significant differences ($P < 0.05$); the same lowercase letters indicate no significant difference ($P > 0.05$).

Changes of PCNA Distribution and Level in Each Intestinal Segment in Different Treatment Groups

Proliferating cell nuclear antigen (PCNA), as an indicator of cell proliferation status, exists only in normal proliferating cells and tumor cells, and is closely related to cellular deoxyribonucleic acid (DNA) synthesis. The IHC results showed that PCNA was distributed in the nuclei and crypts of the basal epithelial cells of the duodenum, jejunum, and cecum villi (**Figure 5A**).

The expression levels of PCNA in the duodenum, jejunum and cecum showed that compared with the blank control group, the expression level of PCNA in the infection group was significantly lower. Compared with the infection group, the levels of PCNA in the JYBR-190 pre-fed, JYBR-190 fed, and antibiotic groups were significantly increased. The JYBR-190 pre-fed group was significantly higher than the antibiotic group (**Figures 5B–D**). It indicated that feeding Bifidobacterium lactis JYBR-190 could increase the expression of PCNA and promote the proliferation and repair of intestinal cells.

Detection Results of Protein Expression in Intestinal Tissue of Chicks in Different Treatment Groups (ELISA)

Changes of Intestinal Cytokine Levels in Different Treatment Groups

At 14 days of age, the expression levels of IL-10 in the intestinal tissue of chickens with different treatments are shown in **Figure 6**. The expression levels of IL-10 in the duodenum, jejunum and cecum showed that compared with the blank control group, IL-10 in the infection group was significantly decreased. Compared with the infection group, the level of IL-10 in the JYBR-190 pre-fed, JYBR-190 fed, and antibiotic groups were significantly increased, with the highest level of IL-10 found in the JYBR-190 pre-fed group.

Changes of TNF-α Protein Expression Levels in Chicks in Different Treatment Groups

At 14 days of age, the expression levels of TNF-α protein expression in the intestinal tissue of chickens with different treatments are shown in **Figure 7**. The expression levels of TNF-α protein expression in the duodenum, jejunum

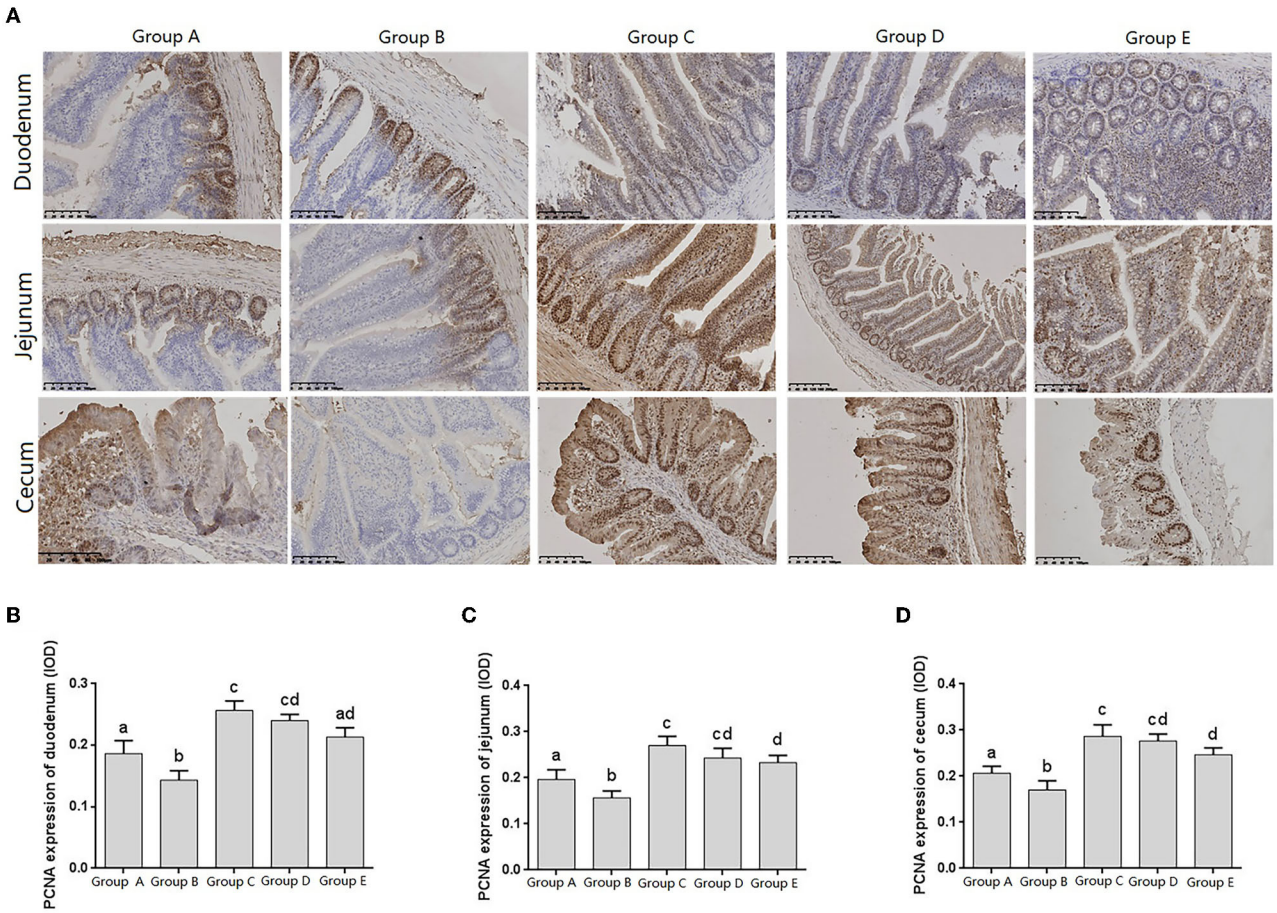

FIGURE 5 | Changes of PCNA distribution in intestine of chicks after different treatments. **(A)** Immunohistochemistry (IHC) staining of the distribution of PCNA in different treatment groups. **(B–D)** Levels of PCNA in different treatment groups. Group A, control group; Group B, infection group; Group C, JYBR-190 pre-fed group; Group D, JYBR-190 fed group; Group E, antibiotic group. Data are expressed as mean ± standard deviation (SD). Different lowercase letters on the columns indicate significant differences ($P < 0.05$); the same lowercase letters indicate no significant difference ($P > 0.05$).

and cecum showed that compared with the blank control group, TNF-α protein expression in the infection group was significantly increased. Compared with the infection group, the level of IL-10 in the JYBR-190 pre-fed, JYBR-190 fed, and antibiotic groups were significantly increased, with the highest level of IL-10 found in the JYBR-190 pre-fed group.

Changes of IFN-γ Protein Expression Levels in Chicks in Different Treatment Groups

At 14 days of age, the expression levels of IFN-γ protein expression in the intestinal tissue of chickens with different treatments are shown in **Figure 8**. The expression levels of IFN-γ protein expression in the duodenum, jejunum and cecum showed that compared with the blank control group, IFN-γ protein expression in the infection group was significantly increased. Compared with the infection group, the level of IFN-γ in the JYBR-190 pre-fed, JYBR-190 fed, and antibiotic groups significantly decreased, with the lowest level of IFN-γ found in the JYBR-190 pre-fed group.

Changes of SIgA Levels in Chicks in Different Treatment Groups

At 14 days of age, the expression levels of sIgA in the intestinal tissue of chickens in different treatment groups are shown in **Figure 9**. The expression of sIgA in duodenum and jejunum showed that compared with the blank control group, the sIgA in the infection group was significantly decreased. Compared with the infection group, the sIgA level in the JYBR-190 pre-fed, JYBR-190 fed, and antibiotic groups were significantly increased, with the highest sIgA level found in the JYBR-190 pre-fed group. The expression of sIgA in the cecum showed that compared with the blank control group, the sIgA in the infected group was significantly decreased. Compared with the infection group, in the JYBR-190 pre-fed, JYBR-190 fed, and antibiotic groups were significantly increased. Among the three groups, the sIgA level in the JYBR-190 pre-fed and fed groups were significantly

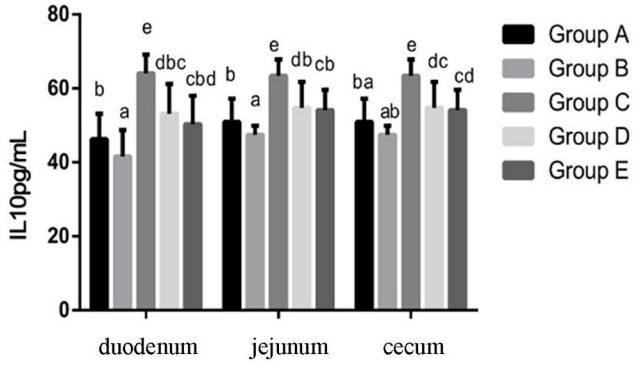

FIGURE 6 | Expression of IL-10 protein in duodenum, jejunum and cecum of different treatment groups. Group A, control group; Group B, infection group; Group C, JYBR-190 pre-fed group; Group D, JYBR-190 fed group; Group E, antibiotic group. Data are expressed as mean ± standard deviation (SD). Different lowercase letters on the columns indicate significant differences ($P < 0.05$); the same lowercase letters indicate no significant difference ($P > 0.05$).

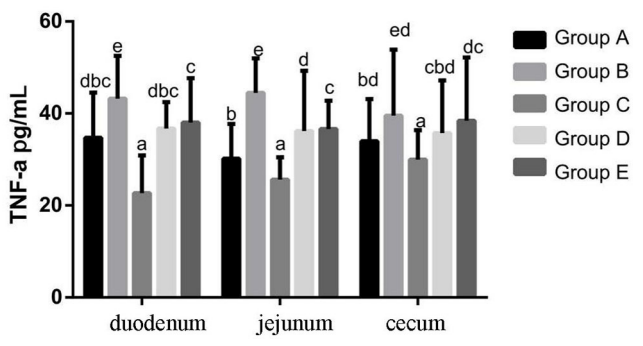

FIGURE 7 | TNF-α protein expression in duodenum, jejunum and cecum of different treatment groups. Group A, control group; Group B, infection group; Group C, JYBR-190 pre-fed group; Group D, JYBR-190 fed group; Group E, antibiotic group. Data are expressed as mean ± standard deviation (SD). Different lowercase letters on the columns indicate significant differences ($P < 0.05$); the same lowercase letters indicate no significant difference ($P > 0.05$).

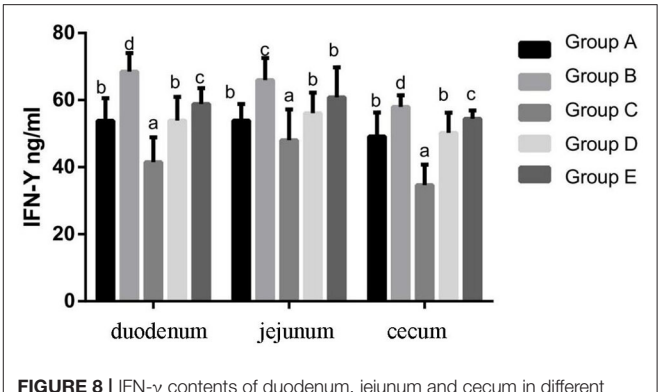

FIGURE 8 | IFN-γ contents of duodenum, jejunum and cecum in different treatment groups. Group A, control group; Group B, infection group; Group C, JYBR-190 pre-fed group; Group D, JYBR-190 fed group; Group E, antibiotic group. Data are expressed as mean ± standard deviation (SD). Different lowercase letters on the columns indicate significant differences ($P < 0.05$); the same lowercase letters indicate no significant difference ($P > 0.05$).

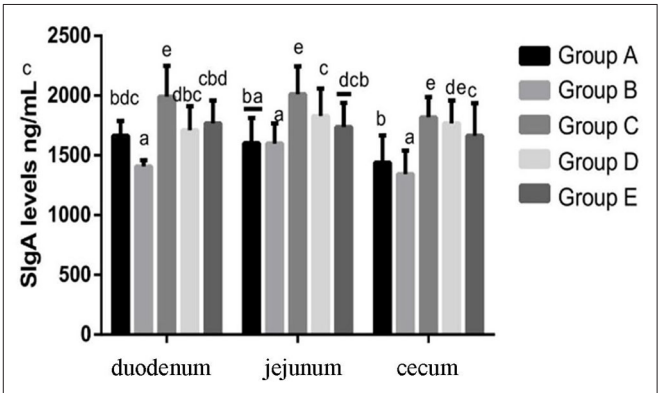

FIGURE 9 | Expression of sIgA Protein in Duodenum, Jejunum and Caecum in different treatment groups. Group A, control group; Group B, infection group; Group C, JYBR-190 pre-fed group; Group D, JYBR-190 fed group; Group E, antibiotic group. Data are expressed as mean ± standard deviation (SD). Different lowercase letters on the columns indicate significant differences ($P < 0.05$); the same lowercase letters indicate no significant difference ($P > 0.05$).

higher than that of the antibiotic group. It indicated that feeding Bifidobacterium lactis JYBR-190 increased the expression of sIgA in the duodenum, jejunum and cecum infected with pullorum, and feeding JYBR-190 before infection could promote the expression of sIgA in the duodenum and jejunum.

DISCUSSION

The duodenum, jejunum and cecum are important components of the intestinal barrier, and the height of the intestinal villi can directly affect the absorption area of the small intestine. The higher the height of the villi, the more mature epithelial absorbing cells, and the better the intestinal digestion and absorption. The depth of crypts reflects the rate of cell formation, and the ratio of villus height to crypt depth (V/C) reflects the strength of intestinal absorption to a certain extent. The higher the ratio, the stronger the intestinal digestion and absorption capacity. Samanya et al. found that Bacillus subtilis can increase the height of ileal villi in adult males and improve feed conversion efficiency (18). In this study, after chicks were infected with Salmonella pullorum, intestinal villus height, villus height ratio (V/C) and muscle thickness in duodenum, jejunum and cecum were significantly decreased, and the depth of intestinal crypts was significantly increased. This indicated that Salmonella pullorum infection caused damage to the intestinal mucosal structure of chicks. However, after treatment with Bifidobacterium lactis JYBR-190 or antibiotics, the villi height, ratio (V/C), and muscle thickness of each intestinal segment were significantly increased, feeding JYBR-190 before infection showed a better repair effect than feeding JYBR-190 and antibiotics after infection. These results indicate that Bifidobacterium lactis JYBR-190 has a protective effect on intestinal mucosal damage and alleviates intestinal inflammation

caused by Salmonella pullorum, which is consistent with the function of probiotics such as Bifidobacterium to improve intestinal inflammation.

Intestinal epithelial stem cells are the main repair cells after the intestinal mucosa is damaged, which can maintain the mechanical barrier function of the intestinal mucosa and prevent or reduce the invasion of intestinal bacteria. The expression of PCNA reflects the proliferation status of intestinal epithelial cells and repairability of intestinal mucosal epithelial injury (19). Wu et al. found that in abdominal infection, the role of intestinal mucosal epithelium was obvious, and the expression level of PCNA in the intestine increased, indicating that the proliferation and differentiation activities of intestinal epithelial stem cells were enhanced, thereby promoting the repair of intestinal mucosal damage. However, with infection the further aggravation of the PCNA index indicates that the intestinal epithelial cells are damaged, accompanied by a gradual decline in the proliferative capacity (20). This study found that the expression of PCNA in the duodenum, jejunum and cecum was significantly reduced after Salmonella pullorum infection, indicating that the proliferation and differentiation activities of epithelial stem cells were reduced, causing damage to the intestinal mucosa. The expression of PCNA in the duodenum, jejunum and cecum tissues of chicks fed JYBR-190 increased significantly, indicating that the proliferation and differentiation activities of epithelial stem cells were enhanced, and the repair of intestinal mucosal damage was promoted, indicating that feeding Bifidobacterium lactis JYBR- 190 can increase the expression of PCNA to promote the proliferation and repair of intestinal epithelial cells to maintain the stability of intestinal tissue structure.

Cytokines such as TNF-α, IL-10, and IFN-γ play an important role in the intestinal immune system. The increased secretion of pro-inflammatory factors such as IFN-γ and TNF-α can aggravate intestinal mucosal inflammation and apoptosis of intestinal mucosal epithelial cells. IL-10 is an anti-inflammatory cytokine in the body, which has a blocking effect on the development of immune inflammatory response, and plays a role in maintaining and regulating the intestinal and systemic immune homeostasis. A large number of studies have shown that after chicks are infected with Salmonella, the intestinal mucosa is damaged, resulting in the infiltration of inflammatory cells and the secretion of more inflammatory cytokines, thereby damaging the intestinal mucosa and expanding the chain reaction of intestinal inflammation. In this study, it was found that the expression of TNF-α and IFN-γ was significantly increased, and the expression of IL-10 was significantly decreased after the chicks were infected with Salmonella pullorum, indicating that the infection of Salmonella pullorum resulted in the imbalance of intestinal cell homeostasis and a serious immune disorder. However, after the infected chickens were fed with bifidobacteria, the protein expressions of IFN-γ, TNF-α and other cytokines secreted in the duodenum, jejunum and cecum tissues of chicks were significantly decreased, and the protein expression of IL-10 was significantly increased. In particular, the group fed JYBR-190 before infection was the most significant, indicating that bifidobacteria can inhibit the secretion of pro-inflammatory cytokines and promote the secretion of anti-inflammatory cytokines, thereby maintaining the balance of the intestinal immune system and relieving the intestinal inflammation caused by Salmonella pullorum infection.

sIgA is an important active substance for maintaining gut health, and secretory IgA also regulates the composition and function of gut microbiota, maintaining a mutually beneficial symbiosis between microorganisms and the host (21, 22). According to literature reports, probiotics such as Bifidobacterium lactis, Bifidobacterium bifidum, Lactobacillus and Bifidobacterium lactis can induce the host to secrete sIgA (23–25). After a long period of evolution, pathogenic microorganisms can synthesize an enzyme that hydrolyzes sIgA, which can hydrolyze the sIgA secreted by the intestinal mucosa, which is conducive to the colonization of pathogenic bacteria. In this study, it was found that the expression of sIgA protein in the duodenum, jejunum and cecum of the infected group decreased significantly after the chicks were infected with Salmonella, indicating that the intestinal mucosal immunity of the chicks decreased. However, feeding the chicks with Bifidobacterium lactis JYBR-190 after the expression of sIgA in the duodenum, jejunum and cecum increased significantly. Feeding Bifidobacterium lactis JYBR-190 can increase the expression of sIgA in the intestinal tissue of chicks, and can enhance the intestinal mucosal immunity of chicks to a certain extent.

CONCLUSION

Salmonella pullorum infection in chicks damage the intestinal barrier, manifesting as intestinal tissue damage and inflammation, while feeding Bifidobacterium pullorum can significantly reduce the intestinal damage and inflammation in chicks caused by Salmonella pullorum, indicating that Bifidobacterium lactis JYBR−190 has a protective effect on intestinal mucosal damage in chicks infected with Salmonella pullorum.

DATA AVAILABILITY STATEMENT

The original contributions presented in the study are included in the article/supplementary material, further inquiries can be directed to the corresponding authors.

ETHICS STATEMENT

The animal study was reviewed and approved by Institutional Animal Care and Use Committee of Yunnan Agricultural University.

AUTHOR CONTRIBUTIONS

GD, FH, and LY designed the study. LY, YC, QB, XC, and YS performed the study. LY, YC, QB, and RW analyzed the data. LY, GD, and FH wrote the manuscript. All authors read and approved the final manuscript.

REFERENCES

1. Rettger LF. Harvey SC. *Fatal septicemia in young chickens, or "white diarrhea". J Med Res.* (1908) 18:277–90.
2. Spalding M. Diseases of poultry. *J Wildl Dis.* 45 (2009) 251–6. doi: 10.7589/0090-3558-45.1.251
3. Barrow PA, Freitas Neto OC. Pullorum disease and fowl typhoid–new thoughts on old diseases: a review. *Avian Pathol.* (2011) 40:1–13. doi: 10.1080/03079457.2010.542575
4. Allen HK, Levine UY, Looft T, Bandrick M, Casey TA. Treatment, promotion, commotion: antibiotic alternatives in food-producing animals. *Trends Microbiol.* (2013) 21:114–9. doi: 10.1016/j.tim.2012.11.001
5. Wang Y, Li J, Xie Y, Zhang H, Jin J, Xiong L, et al. Effects of a probiotic-fermented herbal blend on the growth performance, intestinal flora and immune function of chicks infected with Salmonella pullorum. *Poult Sci.* (2021) 100:101196. doi: 10.1016/j.psj.2021.101196
6. Pan Z, Wang X, Zhang X, Geng S, Chen X, Pan W, et al. Changes in antimicrobial resistance among Salmonella enterica subspecies enterica serovar Pullorum isolates in China from 1962 to 2007. *Vet Microbiol.* (2009) 136:387–92. doi: 10.1016/j.vetmic.2008.11.015
7. Gao P, Ma C, Sun Z, Wang L, Huang S, Su X, et al. Feed-additive probiotics accelerate yet antibiotics delay intestinal microbiota maturation in broiler chicken. *Microbiome.* (2017) 5:91. doi: 10.1186/s40168-017-0315-1
8. Khan S, Moore RJ, Stanley D, Chousalkar KK. The gut microbiota of laying hens and its manipulation with prebiotics and probiotics to enhance gut health and food safety. *Appl Environ Microbiol.* (2020) 86:e00600–20. doi: 10.1128/AEM.00600-20
9. Gibson GR, Wang X. Regulatory effects of bifidobacteria on the growth of other colonic bacteria. *J Appl Bacteriol.* (1994) 77:412–20. doi: 10.1111/j.1365-2672.1994.tb03443.x
10. Abe F, Ishibashi N, Shimamura S. Effect of administration of bifidobacteria and lactic acid bacteria to newborn calves and piglets. *J Dairy Sci.* (1995) 78:2838–46. doi: 10.3168/jds.S0022-0302(95)76914-4
11. A.K. Misra, R.K. Kuila, Use of Bifidobacterium bifidum in the manufacture of bifidus milk and its antibacterial activity. *Dairy Sci Technol.* 72 (1992) 213–20. doi: 10.1051/lait:1992215
12. Roselli M, Finamore A, Nuccitelli S, Carnevali P, Brigidi P, Vitali B, et al. Prevention of TNBS-induced colitis by different Lactobacillus and Bifidobacterium strains is associated with an expansion of gammadeltaT and regulatory T cells of intestinal intraepithelial lymphocytes. *Inflamm Bowel Dis.* (2009) 15:1526–36. doi: 10.1002/ibd.20961
13. Zuo L, Yuan KT Yu L, Meng QH, Chung PC, Yang DH. Bifidobacterium infantis attenuates colitis by regulating T cell subset responses. *World J Gastroenterol.* (2014) 20:18316–29. doi: 10.3748/wjg.v20.i48.18316
14. Mi H, Dong Y, Zhang B, Wang H, Peter CCK, Gao P, et al. bifidobacterium infantis ameliorates chemotherapy-induced intestinal mucositis via regulating T cell immunity in colorectal cancer rats. *Cell Physiol Biochem.* (2017) 42:2330–41. doi: 10.1159/000480005
15. Ruiz L, Margolles A, Sánchez B. Bile resistance mechanisms in Lactobacillus and Bifidobacterium. *Front Microbiol.* (2013) 4:396. doi: 10.3389/fmicb.2013.00396
16. Gueimonde M, Garrigues C, van Sinderen D, de los Reyes-Gavilán CG, Margolles A. Bile-inducible efflux transporter from Bifidobacterium longum NCC2705, conferring bile resistance. *Appl Environ Microbiol.* (2009). 75:3153–60. doi: 10.1128/AEM.00172-09
17. Anand SK, Srinivasan RA, Rao LK. antimicrobial activity associated with Bifidobacterium bifidum-I, *Cult Dairy Prod J.* (1984). 19: 6–8.
18. Samanya M, Yamauchi KE. Histological alterations of intestinal villi in chickens fed dried Bacillus subtilis var. *natto Comp Biochem Physiol A Mol Integr Physiol.* (2002) 133:95–104. doi: 10.1016/S1095-6433(02)00121-6
19. Jain R, Aggarwal AK, Rechkoblit O. Eukaryotic DNA polymerases. *Curr Opin Struct Biol.* (2018) 53:77–87. doi: 10.1016/j.sbi.2018.06.003
20. Wu CT, Zheng YB. Expression of proliferating cell nuclear antigen of the intestinal mucosa during critical intraperitoneal infection. *Zhongguo Wei Zhong Bing Ji Jiu Yi Xue*. (2004). 16:738–9.
21. Gill HS. Probiotics to enhance anti-infective defences in the gastrointestinal tract. *Best Pract Res Clin Gastroenterol.* (2003) 17:755–73. doi: 10.1016/S1521-6918(03)00074-X
22. Fagarasan S, Kawamoto S, Kanagawa O, Suzuki K. Adaptive immune regulation in the gut: T cell-dependent and T cell-independent IgA synthesis. *Annu Rev Immunol.* (2010) 28:243–73. doi: 10.1146/annurev-immunol-030409-101314
23. Tezuka H, Abe Y, Iwata M, Takeuchi H, Ishikawa H, Matsushita M, et al. Regulation of IgA production by naturally occurring TNF/iNOS-producing dendritic cells. *Nature.* (2007) 448:929–33. doi: 10.1038/nature06033
24. Kim M, Ashida H, Ogawa M, Yoshikawa Y, Mimuro H, Sasakawa C. Bacterial interactions with the host epithelium. *Cell Host Microbe.* (2010) 8:20–35. doi: 10.1016/j.chom.2010.06.006
25. Martins FS, Silva AA, Vieira AT, Barbosa FH, Arantes RM, Teixeira MM, et al. Comparative study of Bifidobacterium animalis, *Escherichia coli, Lactobacillus casei*, and Saccharomyces boulardii probiotic properties. *Arch Microbiol.* (2009) 191:623–30. doi: 10.1007/s00203-009-0491-x

Conflict of Interest: The authors declare that the research was conducted in the absence of any commercial or financial relationships that could be construed as a potential conflict of interest.

frontiers | Frontiers in Veterinary Science

ORIGINAL RESEARCH
published: 20 June 2022
doi: 10.3389/fvets.2022.902052

The Probiotic Attributes and Anti-pseudorabies Virus Evaluation of *Lactobacillus* Isolates

Ming-Fan Yang[1†], *Wei Yan*[1†], *Yan Li*[1], *Shuai-Qi Li*[1], *Hong-Ying Chen*[1], *Qing-Qiang Yin*[1], *Xiao-Wei Dang*[2] *and Hong-Ying Zhang*[1*]

[1] *Zhengzhou Key Laboratory for Pig Disease Prevention and Control, College of Veterinary Medicine, Henan Agricultural University, Zhengzhou, China,* [2] *Henan Delin Biological Products Co., Ltd., Zhengzhou, China*

The emergence of pseudorabies virus (PRV) variants brings serious harm to the swine industry, and its effective treatments are limited at present. As one of the probiotics, the *Lactobacillus* species have beneficial characteristics of regulating the balance of intestinal flora, inhibiting the growth of pathogenic bacteria and viruses' proliferation, and improving self-immunity. In this study, *Lactobacillus plantarum* HN-11 and *Lactobacillus casei* HN-12 were selected and identified through morphology observation, Gram stain microscopy, 16S rRNA sequencing analysis, and specific amplification of the recA gene and pheS gene. All tested isolates exhibited rapid adaptation to the different conditions, excellent acid, and bile tolerance, and sensitivity to *Salmonella*, *Staphylococcus aureus,* and *Escherichia coli*. The antibiotic susceptibility assay displayed the isolates sensitive to most antibiotics and resistant to Lincomycin and Norfloxacin. Moreover, the supernatants of HN-11 and HN-12 inhibited PRV proliferation in ST cells. The results of animal experiments showed that supplementing the challenged mice with the supernatants of *Lactobacillus* isolates in advance delayed the course of the disease. PRV was detected in the heart, liver, spleen, lung, kidney, and brain tissues of dead mice in the test groups, and its copies in the lungs were significantly decreased compared with the control mice ($P < 0.05$). These findings proved the advantages of *L. plantarum* and *L. casei* as potential probiotic cultures, which could provide a basis for its application in microecological preparations and functional formulations.

Keywords: ***Lactobacillus plantarum*, *Lactobacillus casei*, probiotic potential, pseudorabies virus, antiviral**

OPEN ACCESS

Edited by:
Ambreen Ashar,
University of Agriculture, Pakistan

Reviewed by:
Neeta Agarwal,
Indian Veterinary Research Institute (IVRI), India
Aoyun Li,
Huazhong Agricultural University, China

***Correspondence:**
Hong-Ying Zhang
hongyingnd@163.com

†These authors have contributed equally to this work

Specialty section:
This article was submitted to Veterinary Infectious Diseases, a section of the journal Frontiers in Veterinary Science

Received: *22 March 2022*
Accepted: *16 May 2022*
Published: *20 June 2022*

Citation:
Yang M-F, Yan W, Li Y, Li S-Q, Chen H-Y, Yin Q-Q, Dang X-W and Zhang H-Y (2022) The Probiotic Attributes and Anti-pseudorabies Virus Evaluation of Lactobacillus Isolates. Front. Vet. Sci. 9:902052. doi: 10.3389/fvets.2022.902052

INTRODUCTION

Probiotics are defined as live microorganisms by WHO and exert a beneficial effect on the body if given in sufficient amounts (1). A fact that probiotics play an important role in regulating intestinal microecology had been determined (2). And the disturbance of intestinal microecology is related to the decline of the body's production performance, which in turn causes a variety of diseases. As the most widely used and extensively studied probiotic, *Lactobacillus* spp, such as *Lactobacillus plantarum*, *Lactobacillus casei*, and *Lactobacillus bifidum*, is known to prevent or treat gastrointestinal disorders in both humans and animals (3). A previous study confirmed that weaned piglets fed with diet supplements of *Lactobacillus* had a lower rate of diarrhea and mortality than those with the control diets by regulating intestinal flora disorders (4). In addition,

Lactobacillus species produce lactic acids, bacteriocins, and other metabolites to achieve the purpose of antibacterial, and many *Lactobacillus* preparations play an essential role in enhancing immunity (5). Remarkably, the antiviral effect of *Lactobacillus* and its metabolites has attracted attention globally in recent years (6).

As an epidemic swine pathogen, pseudorabies virus (PRV) causes significant economic losses to the global swine industry and is characterized by acute and high fever and neurological symptoms in piglets, abortions and stillbirths in sows, and digestive system diseases, such as vomiting, diarrhea, necrotizing enteritis, in adult pigs (7). Pseudorabies (PR) caused by PRV is a serious infectious disease, with mortality of nearly 100% in piglets (8). The swine is the natural host for PRV, and the virus can also infect most mammals, including cattle, rodents, and dogs (9). *Lactobacillus* isolates and their metabolites have been confirmed to exhibit antiviral activity against several human and animal viruses (10). However, there is no relevant research and report on *Lactobacillus* inhibiting PRV. Therefore, this study aimed to evaluate the probiotic properties of the *L. plantarum* and *L. casei* isolated from fermented silage and also to determine their antiviral activity against PRV, which provided the basis for its application in animal husbandry production.

MATERIALS AND METHODS

Samples, Cells, Viruses, and Animals

The corn silage samples used for the isolation of *Lactobacillus* in this study were collected from the silage cellars of a large-scale sheep farm in Henan Province, China.

Swine testicle (ST) cells were previously preserved in our laboratory and were cultured in Dulbecco's modified Eagle's medium (DMEM, Solarbio, Beijing, China) containing 10% (v/v) fetal bovine serum and 100 U mL^{-1} penicillin/streptomycin at 37°C and 5% CO_2 for 48 h. PRV was previously stored in our laboratory. The preparation of viral inoculum was as follows: The virus suspension was adsorbed on the ST monolayer cells for 1.5 h and washed three times with PBS and then added DMEM containing 2% fetal bovine serum to culture under 37°C and 5% CO_2 until the appearance of 80% CPE. Finally, the cells along with the culture medium were frozen and thawed thrice, and centrifuged for the supernatant. Female mice (3–4 weeks old, Kunming, SPF) were purchased from Henan Experimental Animal Center and allowed to eat and drink freely throughout the experiment.

Isolation and Genotypic Characterization

An amount of 10 g of each sample was cut into small pieces, suspended in PBS and the supernatant was plated on Man Rogosa Sharp (MRS) agar. The suspected bacteria colonies were randomly selected to striate on plates containing MRS agar and incubated at 37°C for 48 h, and then the colonies were purified and further evaluated for Gram reaction and morphology. To identify the isolates, the total genomic DNA of each isolate was extracted by the Rapid Bacterial Genomic DNA Isolation kit (Sangon Biotech, Shanghai, China) and amplified *via* PCR using a pair of primers (27F: 5′ - AGAGTTTGATCCTGGCTCAG-3′ and 1492R: 5′-TACGGCTACCTTGTTACGACT-3′). The PCR has carried out with the following program: denaturation at 95°C for 5 min, 35 cycles of 95, 52, and 72°C/45 s, and extension at 72°C for 10 min. After the amplification, 6 μL PCR products were separated by electrophoresis in a 1.2% (w/v) agarose gel, visualized by Gel Imaging System (Sigma, USA), and sequenced by TSINGKE company (Beijing, China). Finally, the sequencing results were compared with the known sequences in the database of NCBI using the BLAST program, and the phylogenetic tree was constructed using the neighbor-joining method with MEGA 7 software.

To identify the PCR products of the recA and pheS gene, the genomic DNA of the isolates HN-11 and HN-12 was amplified by specific primer pairs (pF: 5′ - CTATTTTTCGGTTGGTTGGTCG-3′, pR: 5′-TTG GCTGATGCACGGAAAG-3′, cF: 5′ -ATGGATCTTCAAACCA AACTTGAAC-3′ and cR: 5′ -TTAACCCTCCTGGCTGAAT TGC-3′), respectively. The PCR program was carried out above, and products were detected by 1.2% agarose gel electrophoresis.

Growth Curves

For growth curves, bacteria were grown on agar plates and a single colony was transferred to a 10 ml MRS broth and incubated overnight, then 6 mL fresh cultures were inoculated into 300 ml of MRS broth and incubated at 37°C for 18–36 h. The growth was monitored by measuring optical density (OD) at 600 nm for every 2 h interval, and pH was measured at the same time points.

Acid and Bile Tolerance

The acid and bile tolerance of isolates were checked according to the methods described previously with minor modifications (11). Acid tolerance was examined in MRS broth and adjusted to a final pH of 2.5 using 1N HCl. Specifically, 1 mL overnight cultured *Lactobacillus* isolates were inoculated into 9 ml MRS broth previously adjusted to pH 2.5 and cultured anaerobically at 37°C for 3 h. Bile tolerance was analyzed as above that 1 ml of overnight cultured isolates were inoculated into 9 ml MRS broth with 0.3% (w/v) oxgall bile salt (Sigma) and incubated at 37°C for 8 h. Then the plate counting method was used to measure the viable bacteria after incubation and the initial. Finally, the survival rate (%) of acid and bile tolerance was calculated as the percentage of the number of viable bacteria grown on MRS agar after incubation (N_1, lg CFU/mL) and the initial number of viable bacteria (N_0, lg CFU/mL) according to the formula: survival rate (%) $= N_1/ N_0 \times 100\%$.

Antibacterial Activity

The antibacterial activity of *Lactobacillus* isolates on indicator bacteria was evaluated by agar well diffusion assay as described previously (12). Indicator bacteria, such as *E. coli*, *S. aureus*, and *Salmonella*, were prepared in a bacterial suspension with a final concentration of 10^7 CFU ml^{-1} and inoculated into Luria-Bertani (LB) agar. The *Lactobacillus* suspension was injected into a well with a diameter of 5 mm which was punched in the LB agar plates as the experimental groups, and the wells were filled with MRS liquid medium as control groups. The antibacterial activity

was measured as the halos of the inhibition zone after incubation at 37°C for 48 h. The inhibitory effect was assessed by the width of the inhibition halos and ranked as highly sensitive (>15 mm), Moderately sensitive (10–15 mm), low sensitive (5–10 mm), and not sensitive (5 mm).

Antibiotic Susceptibility Assay

The isolates were evaluated for susceptibility to Penicillin, Cefamezin, Gentamicin, Clarithromycin, Lincomycin, Norfloxacin, and Rifampicin by the disc diffusion method using commercially available antibiotic disks. Bacteria cultures were diluted to suitable turbidity (0.6 OD at 600 nm) and spread on MRS agar. The antibiotic disks were placed at a suitable distance with sterile forceps. Then the plates were incubated at 37°C for 24–48 h. Zone of inhibition (mm) was measured, and the results were described as sensitive (S) or resistant (R) according to National Committee for Clinical Laboratory Standards (NCCLS).

Antiviral Assay *in vitro*

Isolate supernatants were tested for PRV inhibition *in vitro* in ST cells. Ten-fold serial dilutions of the viral inoculum were prepared, and each dilution was inoculated into 8 wells. After incubation for 72 h, CPE was observed and the viral titers in the wells were calculated as the 50% tissue culture infective dose ($TCID_{50}$/100 μL) using the Karber method. The *Lactobacillus* isolates were cultured anaerobically in MRS broth at 37°C for 16 h, and supernatants collected by centrifugation at 12,000 rpm for 5 min were adjusted with PBS to 10^8 CFU ml^{-1} and filter-sterilized 0.22-μm syringe filter. The cytotoxicity of isolates supernatants on ST cells were tested *in vitro* using a Cell Counting Kit-8 (CCK-8) assay. Different concentrations of supernatants were inoculated into a 96-well monolayer of ST cells, and the wells of blank control and virus control were also maintained. After the plate was incubated at 37°C with 5% CO_2 for 48–72 h, 10 μL of a CCK-8 solution was added, and OD at 450 nm was measured. The relative cell viability was counted as a percentage of that of the control based on the mean OD. ST Monolayers in 6-well plates were inoculated with three different safe and effective concentrations of the supernatants of *Lactobacillus* isolates after which it was infected with 100$TCID_{50}$ of PRV inoculum and allowed to absorb for 2 h as test groups, and quadruplicate wells of the virus control and blank control were also established. After the virus wells had developed 80% CPE, the plates were freeze-thawed thrice at −80°C. The mixtures were harvested and centrifuged to prepare the supernatants for the extraction of viral DNA. The PRV copies were determined using the fluorescence quantitative PCR (qPCR), and the primers and methods were the same as described previously (13).

Animal Treatments

After the adaptation period, a total of 48 Kunming mice in this part were randomly divided into the HN-11 group, HN-12 group, blank control group, and positive control group (n = 4), each group was set for three repetitions. And from day 8 to day 17, mice in the experiment groups and control groups were forced to accept the 1 mL supernatants of HN-11 and HN-12 at 10^8 CFU mL^{-1} and an equal volume of PBS, respectively. Afterward, mice in the HN-11, HN-12, and positive control groups were subcutaneously injected with 250 μL of

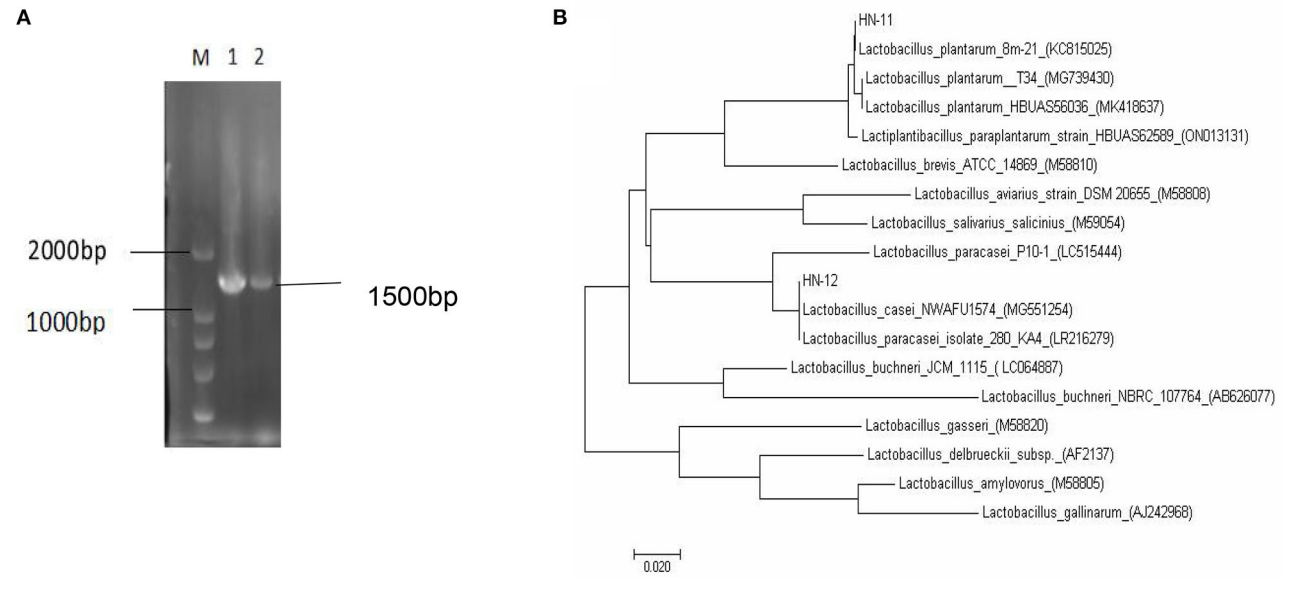

FIGURE 1 | The 16S rRNA gene sequence homology analysis of *Lactobacillus* isolates. **(A)** Amplified PCR products of about 1,500 bp; M. DNA marker DL2000; 1. isolate HN-11; 2. isolate HN-12. **(B)** Phylogenetic tree based on the 16S rRNA gene sequence of *Lactobacillus* isolates showing the relationship of isolates to other strains already present in GenBank. And the tree was rebuilt by the neighbor-joining method.

PRV inoculum with a proliferation titer of $10^{5.17}$TCID$_{50}$/100 μL according to previous experiments.

Sample Collection

The health status of the mice was closely observed and recorded, including diet, mental state, and morbidity. All dead mice were immediately dissected and their tissues, including heart, liver, spleen, lung, kidney, and brain, were collected. The viral DNA was extracted, and antigens were determined by qPCR as above.

Statistical Analysis

Experimental results were analyzed for statistical significance using GraphPad Prism (GraphPad, San Diego, USA). Independent Student *t*-test analysis was performed. $P < 0.05$ was defined as the statistical significance level. The values were expressed as the mean ± SD.

RESULTS

Isolation and Genotypic Characterization of Isolates

A total of 18 gram-positive colonies with typical *Lactobacillus* morphology, white in color and round in shape were selected and inoculated into MRS broth. The 16S rRNA gene sequence was matched with the reference sequence in the NCBI database to identify the organism. Blast analysis showed a similarity percentage ≥97% of homology to *Lactobacillus* species. The phylogenetic tree reconstructed by the neighbor-joining method

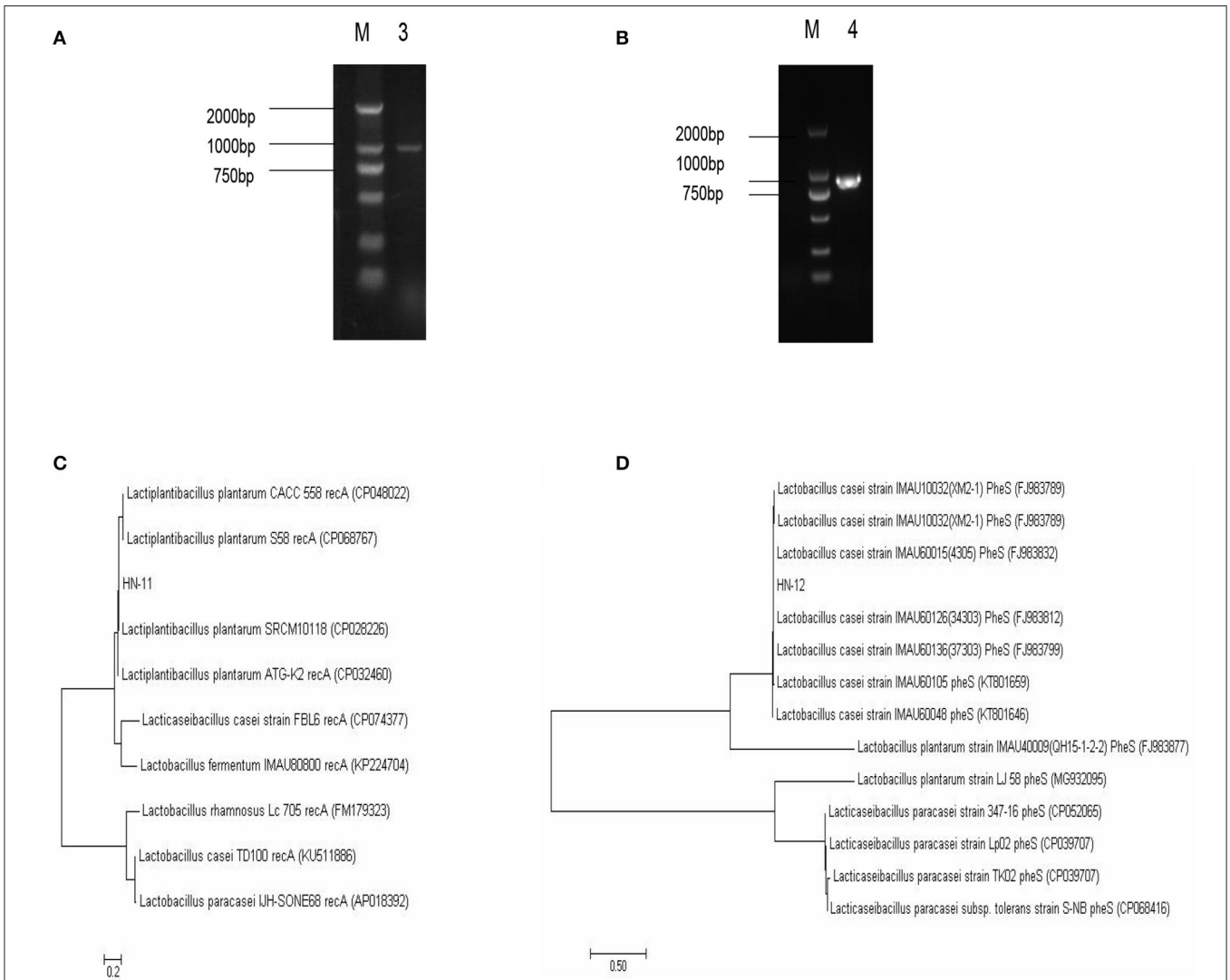

FIGURE 2 | The identification of *Lactobacillus* isolates by specific gene sequences. **(A,B)** Amplified PCR product of about 1,000 bp; M. DNA marker DL2000; 3. the specific amplification products of recA gene of *Lactobacillus plantarum* HN-11; 4. the specific amplification products of pheS gene of *Lactobacillus casei* HN-12. The phylogenetic tree based on the recA gene **(C)** and pheS gene **(D)** of *Lactobacillus* isolates shows the relationship of isolates to other strains already present in GenBank. And the tree was rebuilt by the neighbor-joining method.

reveals a phylogenetic relationship between the sequences of the 16S rRNA gene of the obtained strains (**Figure 1**).

The homology of the l6S rRNA of *Lactobacillus* species is too high to distinguish. Therefore, a specific pair of primers (pF and pR) was designed based on the conserved genes recA of *L. plantarum*, and the predicted amplified fragment length was 1,143 bp. Moreover, we also obtained specific primer pairs (cF and cR) based on the pheS gene sequences of the *L. casei* group, and the predicted amplified fragment length was 1,047 bp. The amplification products of the recA gene of the isolate HN-11 and the amplification product of the pheS gene of HN-12 were similar to the predicted results (**Figures 2A,B**). The target amplified sequence was analyzed by BLAST and the phylogenetic trees were reconstructed by the neighbor-joining method (**Figures 2C,D**). The result shows that the isolate HN-11 had high homology with *Lactiplantibacillus plantarum*

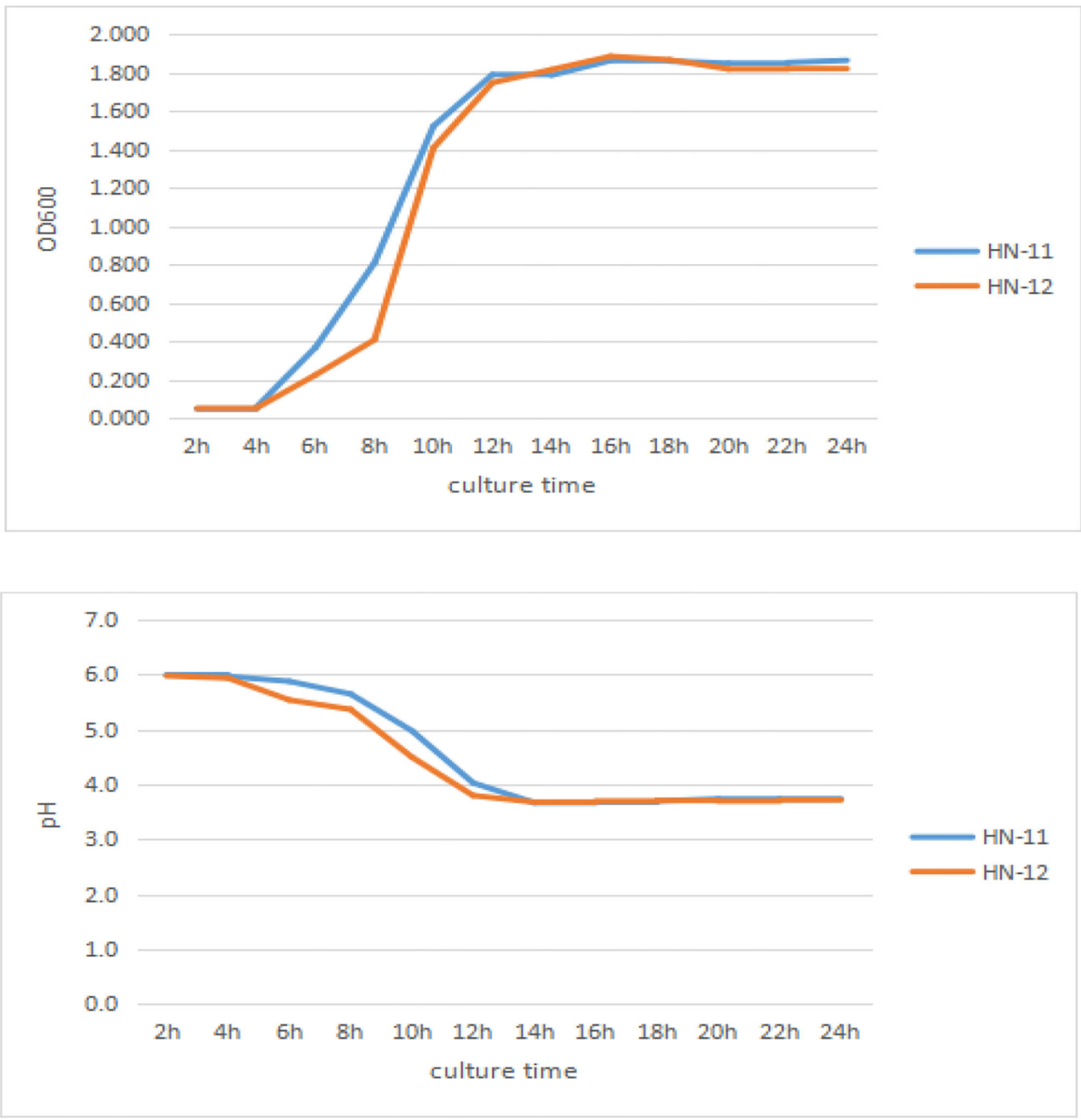

FIGURE 3 | Growth curves and acid production of the three isolates. The culture time was taken as abscissa, and OD_{600nm} value and pH value were taken as ordinate. HN-11 is labeled in blue, and HN-12 is labeled in orange.

TABLE 1 | Acid and bile tolerance of *Lactobacillus*[a].

Strains	Acid tolerance (pH: 2.5, 3 h)			Bile tolerance (0.3%, 8 h)		
	0 h (lg CFU/mL)	3 h (lg CFU/mL)	Survival rate (%)	0 h (lg CFU/mL)	8 h (lg CFU/mL)	Survival rate (%)
HN-11	7.78 ± 0.02	7.64 ± 0.05	98.20	8.08 ± 0.03	7.49 ± 0.03	92.70
HN-12	7.63 ± 0.05	7.36 ± 0.05	96.46	7.93 ± 0.04	7.28 ± 0.04	91.80

[a] *Each value is the mean ± SD of data.*

TABLE 2 | Antibacterial activity of *Lactobacillus* isolates determined by agar well diffusion assay[1].

Strains	Inhibition hale (mm)		
	Salmonella	***Staphylococcus aureus***	***Escherichia coli***
HN-11	18.73 ± 0.73	17.00 ± 0.16	7.47 ± 0.25
HN-12	17.00 ± 0.16	16.03 ± 0.21	7.80 ± 0.33

[1] *Results are shown as mean ± SD. Experiments were carried out thrice independently.*

TABLE 3 | Antibiotic susceptibility test of *Lactobacillus* isolates.

Antimicrobials	Strains	
	HN-11	HN-12
Cefamezin (30 ug)	S	S
Penicillin (10 U)	S	S
Gentamicin (10 ug)	S	S
Clarithromycin (15 ug)	S	S
Lincomycin (2 ug)	R	R
Norfloxacin (10 ug)	R	R
Rifampicin (5 ug)	S	S

S, sensitive; R, resistant.

strain SRCM101187 (CP028226), and isolate HN-12 had high homology with *L. casei* strain IMAU60126 (34303) (FJ983812). Above all, the isolates HN-11 and HN-12 were identified as *L. plantarum* and *L. casei*, respectively.

Growth Curves

As can be seen in **Figure 3**, the lag phase of three isolates lasted 4 h and three isolates reached the stationary phase after 16 h incubation, with a final OD_{600nm} of 1.7 or so. Good adaptation capability could help bacteria adapt to different environments, which might improve probiotic function in the gut. And the pH value of the isolates rapidly dropped to 3.72 at 14 h and last for a long time.

Acid and Bile Tolerance

Table 1 shows that the isolates showed a survival rate of more than 95% after incubation for 3 h at a pH of 2.5. They also survived in 0.3% bile and showed more than 90% of the survival rate after 8 h incubation. Despite a reduction of the viable count (lg CFU/ml) after incubation, the number of viable bacteria was still 10^7 CFU/ml above. A study has shown that the minimum number of viable bacteria for LAB to play a probiotic effect is 10^6 CFU/ml (14).

Antibacterial Activity

The isolates were evaluated for antibacterial activity against pathogenic bacteria by agar well diffusion assay (**Table 2**). In the assay, the strains HN-11 and HN-12 showed highly (>15 mm) sensitivity to *Salmonella* and *S. aureus*. On the other hand, they showed low sensitivity (6–10 mm) to *E. coli*.

Antibiotic Susceptibility Assay

The susceptibility patterns of three *Lactobacillus* isolates against seven antibiotics are shown in **Table 3**. Both the isolates were sensitive to Cefamezin, Penicillin, Gentamicin, Clarithromycin, and Rifampicin but resistant to Lincomycin and Norfloxacin.

Antiviral Assay *in vitro*

The virulence of the PRV inoculum was measured on ST cells as $10^{5.17}$ $TCID_{50}$/100 μL. And the maximum non-toxic dose of the supernatant of isolates was the dilution factor of 1:2. Therefore, the dilution gradient of *Lactobacillus* supernatant is 1:2, 1:4, and 1:8 in the next antiviral effect test. The DNA of the test groups and control groups was amplified, and the amplification results were analyzed as **Figure 4** that the copies of the virus in the test groups were lower than that in the virus control groups, and the copies decreased with the decrease of dilution factor of the supernatant, respectively.

Antiviral Assay *in vivo*

In this experiment, the mortality of mice after 7 days of challenge with PRV was shown in **Table 4** that the mice in the control group died on the 3 and 4 days after PRV challenge and no mice died in the blank control group. Some mice in the experimental group showed depression, decreased diet, severe pruritus, and accelerated breathing before death. The results showed that the protective effect of *Lactobacillus* isolates on the mice artificially infected with PRV inoculum was not significant, but it delayed the course of the disease. PRV was detected in the heart, liver, spleen, lung, kidney, and brain tissues of dead mice in the experimental group, and the viral load in tissues in the *Lactobacillus*-supplemented groups was lower than in the blank control group, but the difference was not significant ($p > 0.05$) (**Figure 5**). However, the viral load in lung tissues of the mice supplemented with isolate HN-11 was significantly reduced compared with the control mice ($P < 0.05$).

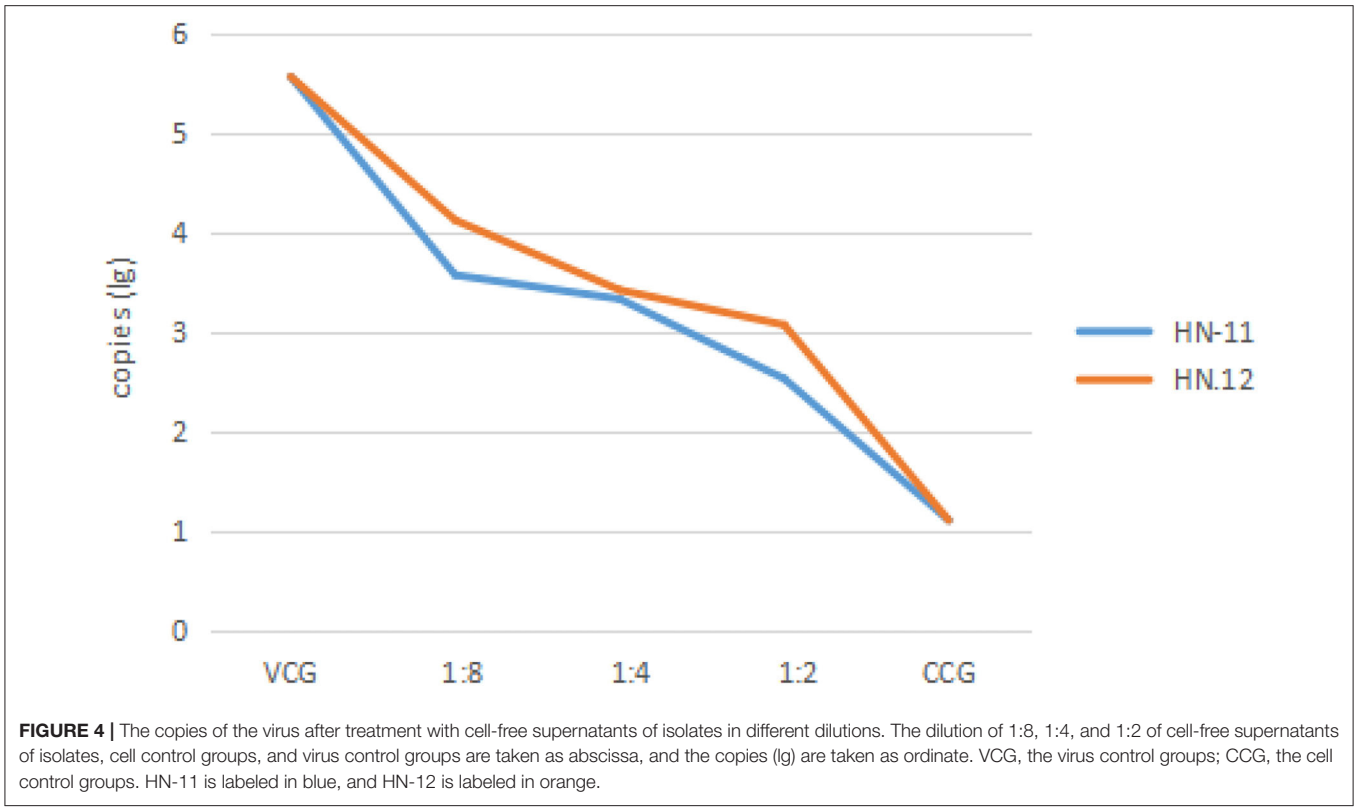

FIGURE 4 | The copies of the virus after treatment with cell-free supernatants of isolates in different dilutions. The dilution of 1:8, 1:4, and 1:2 of cell-free supernatants of isolates, cell control groups, and virus control groups are taken as abscissa, and the copies (lg) are taken as ordinate. VCG, the virus control groups; CCG, the cell control groups. HN-11 is labeled in blue, and HN-12 is labeled in orange.

TABLE 4 | Mortality results of experiments mice.

Date	The mortality of mice			
	Positive control group	Blank control group	HN-11 group	HN-12 group
1 dpi	0	0	0	0
2 dpi	0	0	0	0
3 dpi	6	0	4	6
4 dpi	6	0	4	3
5 dpi	0	0	2	2
6 dpi	0	0	2	0
7 dpi	0	0	0	1
Remaining mice	0	12	0	0

DISCUSSION

The health-promoting property of probiotics motivated the present study to isolate novel *Lactobacillus* with potential probiotic attributes. Any bacteria to be considered as potential probiotics should show high resistance to acidic conditions and bile salts (15). According to our study, both isolates had viability percentages of more than 90% against bile and higher tolerance to an acid environment, which is an important guarantee to ensure that *Lactobacillus* pass through the gastrointestinal barrier in the form of live bacteria. A total of 30 strains of *Lactobacillus* isolated from infants' feces were 58–97% survival in acid at pH 2.5 and 50–94% survival in 0.3% bile salts (3), which is similar to the results of this study. The efficacy of antimicrobial activity against pathogens exhibited by both isolates is beneficial for maintaining the intestinal flora balance, which is an important property of ideal probiotics. Śliżewska et al. (16) suggested several *Lactobacillus* strains as probiotic candidates for the development of functional feed due to the probiotic properties they exhibit, such as high survival rate and antagonistic activity, against pathogens. *L. plantarum* with excellent probiotic properties had been proved to relieve diarrhea caused by enterotoxigenic *E. coli* (ETEC) (17). Xu et al. (18) reported the antibacterial activity of *L. casei* NA-2 against *Bacillus cereus*, *S. aureus*, *S. typhimurium,* and *E. coli* O157:H7, together with its potential antibacterial properties of exopolysaccharide (EPS). An increasing data has shown the EPS from *Lactobacillus* exerts antibacterial activities by inhibiting biofilm formation and dispersing of various bacteria, such as *S. aureus* (19), *E. coli* (16), *Listeria monocytogenes*, *S. typhimurium,* and *P. aeruginosa* (20). Further studies are required to determine the EPS product secreted by the present strains to differentiate them from previous strains.

Through TANJA, it was confirmed the antiviral activity of probiotics and their metabolites in *in vitro* cell model for the first time in 2007 (21). Since then, the cell infection model has been widely used in probiotic antiviral tests. Previous reports found that *L. plantarum* metabolites can inhibit the adsorption of transmissible gastroenteritis virus (TGEV) on ST cells (22).

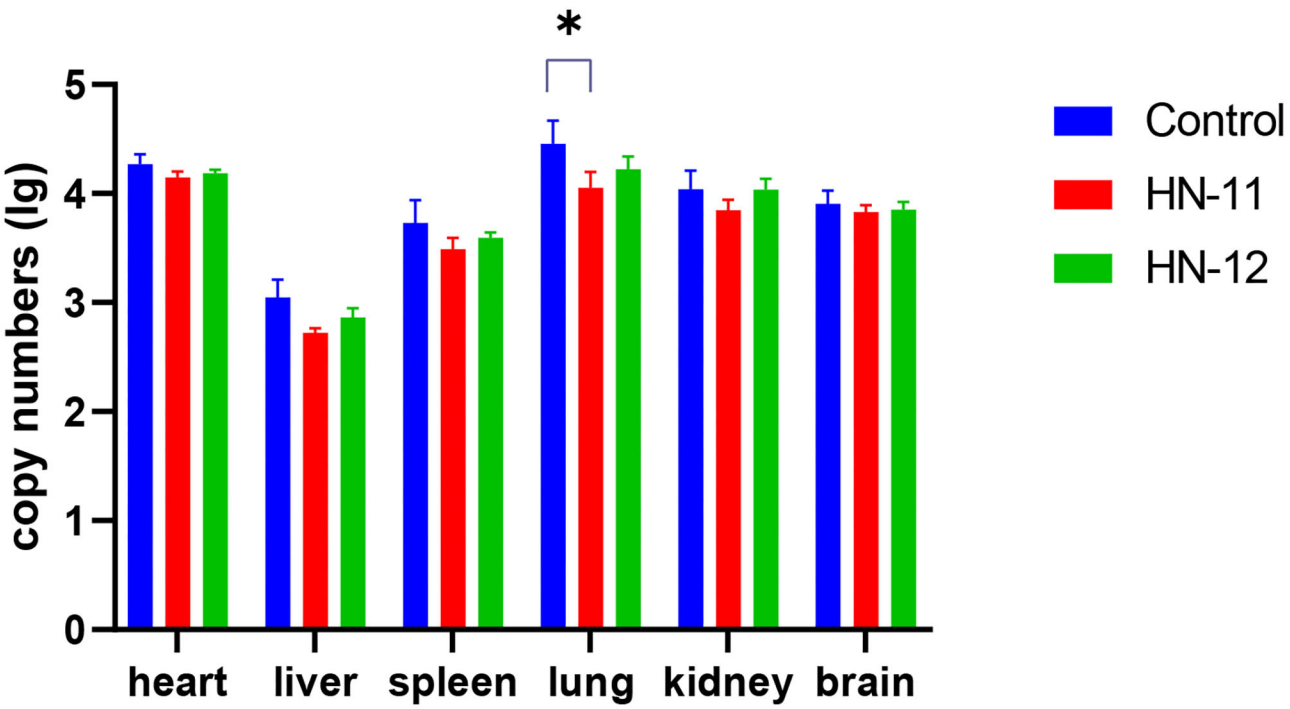

FIGURE 5 | The copies of PRV in mice tissues. The heart, liver, spleen, lung, kidney, and brain tissues of the positive control group, HN-11 group, and HN-12 group are taken as abscissa, and the copies (lg) are taken as ordinate (*$P < 0.05$).

Moreover, both *L. plantarum* metabolites and *L. plantarum* exopolysaccharides showed a good inhibitory effect on porcine epidemic diarrhea virus (PEDV) (23) and rotaviruses (RV) (24), and the treatments that exerted the excellent effects have been repeatedly proved. This could be due to the complex composition of metabolites, which blocks virus adsorption, alleviates inflammatory responses, and induces immunity (14). We herein observed that PRV inhibition on the ST model by isolated supernatant was concentration-dependent. Currently, there is a lack of animal test models, but the results of this test showed that *Lactobacillus* isolates were indeed impossible to independently complete the task of antiviral on mice model, but probiotics can still be supplemented clinically to assist vaccines or antiviral drugs to achieve a better effect. As previously reported, *L. acidophilus* had significant immuno-potentiating effects and was suggested as a safe oral adjuvant for RV vaccines in neonates gnotobiotic pigs (25). And further studies are required to explore the antiviral effect of specific substances of probiotic metabolites.

Lactobacillus isolates (HN-11 and HN-12) had been confirmed to have excellent probiotic properties and the obtained data showed the supernatants all make a certain contribution in inhibiting the proliferation of PRV *in vitro* and *in vivo*. In an era defined by severe antibiotic resistance in bacterial pathogens, probiotic feeding may represent a potential effect on reducing antimicrobial use and restoring animal health.

DATA AVAILABILITY STATEMENT

The original contributions presented in the study are included in the article/supplementary material, further inquiries can be directed to the corresponding author/s.

ETHICS STATEMENT

The animal study was reviewed and approved by the Henan Agriculture University Animal Care and Use Committee [license number SCXK (Henan) 2013-0001].

AUTHOR CONTRIBUTIONS

M-FY and WY have made substantial contributions to the conception, design of the work, acquisition, and analysis. YL and S-QL carried out interpretation of data. H-YC discussed and prepared the final report. Q-QY and X-WD contributed to the drafting of the work. H-YZ has completed the revision of the entire paper and provided financial support. All authors have read and approved the final manuscript.

FUNDING

This study was supported by the Project for National Natural Science Foundation of China-Research on Bidirectional Immunomodulatory Effects of Radix Isatidis polysaccharide on PRRSV-infected 3D4/21 cells (31972731).

REFERENCES

1. Heilig H, Zoetendal E, Vaughan E, Marteau P, Akkermans A, de Vos W. Molecular diversity of *Lactobacillus* spp. and other lactic acid bacteria in the human intestine as determined by specific amplification of 16S ribosomal DNA. *Vet Microbiol.* (2002) 68:114–23. doi: 10.1128/AEM.68.1.114-123.2002
2. Ma Z, Cheng Y, Wang S, Ge J, Shi H, Kou J. Positive effects of dietary supplementation of three probiotics on milk yield, milk composition and intestinal flora in Sannan dairy goats varied in kind of probiotics. *J Anim Physiol Anim Nutr.* (2020) 104:44–55. doi: 10.1111/jpn.13226
3. Jomehzadeh N, Javaherizadeh H, Amin M, Saki M, Al-Ouqaili M, Hamidi H, et al. Isolation and identification of potential probiotic *Lactobacillus* species from feces of infants in southwest Iran. *Int J Infect Dis.* (2020) 96:524–30. doi: 10.1016/j.ijid.2020.05.034
4. Zhang L, Xu Y, Liu H, Lai T, Ma J, Wang J, et al. Evaluation of *Lactobacillus rhamnosus* GG using an *Escherichia coli* K88 model of piglet diarrhoea: effects on diarrhoea incidence, faecal microflora and immune responses. *Vet Microbiol.* (2010) 141:142–8. doi: 10.1016/j.vetmic.2009.09.003
5. Qian Z, Zhao D, Yin Y, Zhu H, Chen D. *Lactobacillus* antibacterial activity of strains isolated from mongolian yogurt against. *Biomed Res Int.* (2020) 2020:3548618. doi: 10.1155/2020/3548618
6. Jiang X, Hou X, Tang L, Jiang Y, Ma G, Li Y. A phase trial of the oral Lactobacillus casei vaccine polarizes Th2 cell immunity against transmissible gastroenteritis coronavirus infection. *Appl Microbiol Biotechnol.* (2016) 100:7457–69. doi: 10.1007/s00253-016-7424-9
7. Lin J, Li Z, Feng Z, Fang Z, Chen J, Chen W, et al. Pseudorabies virus (PRV) strain with defects in gE, gC, and TK genes protects piglets against an emerging PRV variant. *J Vet Med Sci.* (2020) 82:846–55. doi: 10.1292/jvms.20-0176
8. Gou H, Bian Z, Cai R, Chu P, Song S, Li Y, et al. RIPK3-dependent necroptosis limits PRV replication in PK-15 cells. *Front Microbiol.* (2021) 12:664353. doi: 10.3389/fmicb.2021.664353
9. Ren C, Hu W, Zhang J, Wei Y, Yu M, Hu T. Pseudorabies establishment of inflammatory model induced by virus infection in mice. *J Vet Sci.* (2021) 22:e20. doi: 10.4142/jvs.2021.22.e20
10. Carucci L, Coppola S, Luzzetti A, Giglio V, Vanderhoof J, Berni Canani R. The role of probiotics and postbiotics in modulating the gut microbiome-immune system axis in the pediatric age. *Minerva Pediatr.* (2021) 73:115–27. doi: 10.23736/S2724-5276.21.06188-0
11. Kang W, Pan L, Peng C, Dong L, Cao S, Cheng H, et al. Isolation and characterization of lactic acid bacteria from human milk. *J Dairy Sci.* (2020) 103:9980–91. doi: 10.3168/jds.2020-18704
12. Davoodabadi A, Soltan Dallal M, Rahimi Foroushani A, Douraghi M, Sharifi Yazdi M, Amin Harati F. Antibacterial activity of *Lactobacillus* spp. isolated from the feces of healthy infants against enteropathogenic bacteria. *Anaerobe.* (2015) 34:53–8. doi: 10.1016/j.anaerobe.2015.04.014
13. Tian R, Jin Y, Xu T, Zhao Y, Wang Z, Chen H. Development of a SYBR green I-based duplex real-time PCR assay for detection of pseudorabies virus and porcine circovirus 3. *Mol Cell Probes.* (2020) 53:101593. doi: 10.1016/j.mcp.2020.101593
14. Maragkoudakis P, Chingwaru W, Gradisnik L, Tsakalidou E, Cencic A. Lactic acid bacteria efficiently protect human and animal intestinal epithelial and immune cells from enteric virus infection. *Int J Food Microbiol.* (2010) 141:S91–7. doi: 10.1016/j.ijfoodmicro.2009.12.024
15. Celiberto L, Pinto R, Rossi E, Vallance B, Cavallini D. Isolation and characterization of potentially probiotic bacterial strains from mice: proof of concept for personalized probiotics. *Nutrients.* (2018) 10:1684. doi: 10.3390/nu10111684
16. Śliżewska K, Chlebicz-Wójcik A, Nowak A. Probiotic properties of new *Lactobacillus* strains intended to be used as feed additives for monogastric animals. *Probiotics Antimicrob Proteins.* (2021) 13:146–62. doi: 10.1007/s12602-020-09674-3
17. Yue Y, He Z, Zhou Y, Ross R, Stanton C, Zhao J, et al. *Lactobacillus plantarum* relieves diarrhea caused by enterotoxin-producing *Escherichia coli* through inflammation modulation and gut microbiota regulation. *Food Funct.* (2020) 11:10362–74. doi: 10.1039/D0FO02670K
18. Xu X, Peng Q, Zhang Y, Tian D, Zhang P, Huang Y, et al. Antibacterial potential of a novel *Lactobacillus casei* strain isolated from Chinese northeast sauerkraut and the antibiofilm activity of its exopolysaccharides. *Food Funct.* (2020) 11:4697–706. doi: 10.1039/D0FO00905A
19. Wong C, Khoo B, Sasidharan S, Piyawattanametha W, Kim S, Khemthongcharoen N, et al. Inhibition of *Staphylococcus aureus* by crude and fractionated extract from lactic acid bacteria. *Benef Microbes.* (2015) 6:129–39. doi: 10.3920/BM2014.0021
20. Kim J, Jang H, Lee N, Paik H. *Lactobacillus brevis* antibacterial and antibiofilm effect of cell-free supernatant of KCCM 202399 isolated from Korean fermented food against KCTC 5458. *Microbiol Biotechnol.* (2022) 32:56–63. doi: 10.4014/jmb.2109.09045
21. Botić T, Klingberg T, Weingartl H, Cencic A. A novel eukaryotic cell culture model to study antiviral activity of potential probiotic bacteria. *Int J Food Microbiol.* (2007) 115:227–34. doi: 10.1016/j.ijfoodmicro.2006.10.044
22. Kumar R, Seo B, Mun M, Kim C, Lee I, Kim H, et al. Putative probiotic *Lactobacillus* spp. from porcine gastrointestinal tract inhibit transmissible gastroenteritis coronavirus and enteric bacterial pathogens. *Trop Anim Health Prod.* (2010) 42:1855–60. doi: 10.1007/s11250-010-9648-5
23. Huang S, Yu Q, Xie L, Ran L, Wang K, Yang Y, et al. Inhibitory effects of *Lactobacillus plantarum* metabolites on porcine epidemic diarrhea virus replication. *Res Vet Sci.* (2021) 139:32–42. doi: 10.1016/j.rvsc.2021.07.002
24. Kim K, Lee G, Thanh H, Kim J, Konkit M, Yoon S, et al. Exopolysaccharide from *Lactobacillus plantarum* LRCC5310 offers protection against rotavirus-induced diarrhea and regulates inflammatory response. *J Dairy Sci.* (2018) 101:5702–12. doi: 10.3168/jds.2017-14151
25. Zhang W, Azevedo M, Wen K, Gonzalez A, Saif L, Li G, et al. Probiotic *Lactobacillus acidophilus* enhances the immunogenicity of an oral rotavirus vaccine in gnotobiotic pigs. *Vaccine.* (2008) 26:3655–61. doi: 10.1016/j.vaccine.2008.04.070

Conflict of Interest: X-WD is employed by Henan Delin Biological Products Co., Ltd.

The remaining authors declare that the research was conducted in the absence of any commercial or financial relationships that could be construed as a potential conflict of interest.

Publisher's Note: All claims expressed in this article are solely those of the authors and do not necessarily represent those of their affiliated organizations, or those of the publisher, the editors and the reviewers. Any product that may be evaluated in this article, or claim that may be made by its manufacturer, is not guaranteed or endorsed by the publisher.

frontiers | Frontiers in Veterinary Science

ORIGINAL RESEARCH
published: 20 July 2022
doi: 10.3389/fvets.2022.946814

Characterization and Preliminary Application of Phage Isolated From *Listeria monocytogenes*

Tianhao Li[1†], Xuehui Zhao[1†], Xuejian Wang[2], Zijian Wang[3], Changqing Tian[1], Wenjing Shi[1], Yumei Qi[1], Huilin Wei[1], Chen Song[1], Huiwen Xue[1] and Huitian Gou[1*]*

[1] College of Veterinary Medical, Gansu Agricultural University, Lanzhou, China, [2] Infectious Diseases Section, Xigu District Animal Disease Prevention and Control Center, Lanzhou, China, [3] Infectious Diseases Section, Gansu Province Animal Disease Prevention and Control Center, Lanzhou, China

OPEN ACCESS

Edited by:
Kun Li,
Nanjing Agricultural University, China

Reviewed by:
Houqiang Luo,
Wenzhou Vocational College of Science and Technology, China
Xu-Jie Zhang,
Huazhong Agricultural University, China
Yujuan Suo,
Shanghai Academy of Agricultural Sciences, China

***Correspondence:**
Huiwen Xue
xuehw@gsau.edu.cn
Huitian Gou
gouht@gsau.edu.cn

†These authors have contributed equally to this work and share first authorship

Specialty section:
This article was submitted to Veterinary Infectious Diseases, a section of the journal Frontiers in Veterinary Science

Received: 18 May 2022
Accepted: 20 June 2022
Published: 20 July 2022

Citation:
Li T, Zhao X, Wang X, Wang Z, Tian C, Shi W, Qi Y, Wei H, Song C, Xue H and Gou H (2022) Characterization and Preliminary Application of Phage Isolated From Listeria monocytogenes. Front. Vet. Sci. 9:946814. doi: 10.3389/fvets.2022.946814

Listeria monocytogenes (LM) is one of the four major foodborne bacteria that cause bacteremia and meningitis. To explore the control of listeriosis with natural phages, we used the double-layer agar plate method to isolate LM from slaughterhouse sewage and designated LP8. The result of electron microscopy indicated that the phage belonged to the family of *Myoviridae*. Whole-genome sequencing indicated that the genome size of LP8 is 87,038 bp and contains 120 genes. Mice were infected with LM and treated with penicillin G sodium, LP8, and the combination of these two. From the levels of lymphocyte subsets (CD^{4+}, CD^{8+}), the expression of cytokines (TNF-α, IL1β, IL-10, and IFN-γ), observation of pathological changes in organs (heart, liver, spleen, kidney, and brain), and the bacterial load of the spleen, we concluded the therapeutic effect of LP8 against listeriosis and demonstrate the feasibility of a combined therapy to reduce the use of antibiotics. This provides a new avenue for the treatment of listeriosis.

Keywords: ***Listeria monocytogenes*, Phage, Isolation, characterization, combination therapy**

HIGHLIGHTS

- A Listeria monocytogenes phage LP8 was isolated from slaughterhouse sewage. It was DNA virus, genome size was 87,038 bp, coded 120 genes and belong to Myoviridae.
- The combination of LP8 and antibiotics can make up for the influence of the biological activity of the phage itself on the treatment. Meanwhile, the addition of phage can reduce the use of antibiotics and achieve the effect of reducing and limiting resistance.

INTRODUCTION

Listeria monocytogenes (LM) is one of the four major foodborne pathogens that cause bacteremia and meningitis. LM can survive under various stress conditions, including extreme temperature, drought, low pH, and high salinity (1–4). In recent years, Listeria has been shown to include 27 species. However, only two strains, *L. monocytogenes* and *L. ivanovii,* can cause human and animal diseases (5). Hence, the risk of infection from contaminated food increases after refrigeration (6). About 20 to 65% of the deaths from foodborne infections are caused by LM in food hygiene events in the United States (7–9). In 2018, the fatality rate of listeriosis among detected cases in EU countries was 15.6% (10). It is generally accepted that 99% of infections caused by LM are non-invasive infections through the fecal-oral route, secondary to invasive infections (11). The diseases caused by LM are predominantly treated with drugs, such as penicillin, fluoroquinolones,

cephalosporins, and vancomycin (12). LM carried the *plcb* and *iap* genes, which make the bacterium highly resistant to drugs, such as penicillin and erythromycin (13). *L. monocytogenes* can cross the intestinal barrier by the active invasion of host cells, which is mainly triggered by internalins InlA and InlB. Other virulence factors, such as listeriolysin O (LLO) and phospholipases are activated by the low pH inside the phagolysosome and allow the bacteria to escape into the cytoplasm (14). After the release into the host cell cytoplasm, *L. monocytogenes* can multiply and spread to neighboring cells, driven by ActA-mediated polymerization of host-cell actin (15). This strategy enables the pathogen to cross host tissue barriers, such as the placental and the blood-brain barrier.

Bacteriophages (phage) are viruses that infect bacterial hosts but are not harmful to eukaryotic organisms. Phages cannot replicate independently of their bacterial hosts. Their host ranges are determined by various factors, including the specificity of the phages' host-binding protein and the host's resistance (16). In recent years, phages have been used as alternatives to antibiotics indicating large potential. However, the high specificity for host bacteria and sensitivity to environmental factors (temperature, pH, etc.) might be limited to the use of phages on a large scale. Therefore, cocktail, phage transformation, and other methods have been proven to be effective measures to overcome the above shortcomings (17). In recent years, to face the emerging drug resistance problem of *Listeria monocytogenes* the use of phages to treat listeriosis will become a feasible approach.

In this study, an LM phage was isolated from slaughterhouse sewage. The morphology, biological characteristics, and whole-genome sequence of the phage were analyzed. To assess the effects of the phage intervention, a mouse model of LM infection was established and treated with the phage, antibiotic, or a phage–antibiotic mixture, as well as comprehensive analysis of lymphocyte subsets, cytokines, pathological changes, and bacterial load.

MATERIALS AND METHODS

Mouse Experiments and Ethics

Female 6∼8-week-old Kunming mice (SPF Standard Animal Laboratory, Lanzhou University Medical Laboratory Center, Lanzhou, China) were housed in a vector-free animal facility, under controlled environmental conditions with a 12-h day-night cycle, and free access to food and water. All animals followed the relevant protocols of animal welfare of the Gansu agricultural university college of veterinary medicine (Lanzhou, China).

Kunming mice are the outbred mice with the largest production and usage in China. The gene pool is large, the gene heterozygosity rate is high, and it is characterized by strong disease resistance and adaptability, as well as high reproduction and survival rates.

Strains

Among the tested 50 *Listeria* strains, four standard strains (NCTC 19890, ATCC 19112, ATCC 19111, and ATCC 19115) and 46 wild strains (18 strains of *L. monocytogenes*, 10 strains of *L. welshimeri,* and 22 strains of *L. innocua*) were all wild strains isolated from beef and mutton samples in parts of Gansu province in previous work in this laboratory. After programmed thawing, they were used to inoculate into tryptic soy broth supplemented with yeast extract (TSB-YE; Solarbio, Beijing, China) and cultured overnight at 37°C with shaking at 220 pm.

Phage Isolation and Characterization

The sewage was centrifuged at 3,000×g for 30 min at 4°C, and filtered through a.22 μm filter. The double-layer agar plate method was used for phage separation (18). A plaque was aspirated into a 1.5 mL sterile centrifuge tube containing 500 μL of magnesium sulfate buffer (Solarbio, Beijing, China), and lysed statically for 4 h at 4°C. The lysate was incubated on double-layer agar plates. The above steps were repeated 5 6 times to purify the phage.

The bacterial culture fluid (100 μL) and lysate (100 μL) were added to 100 mL of TSB-YE, and the mixture was cultured overnight at 37°C with shaking. Polyethylene glycol 8,000 (Solarbio, Beijing, China) was used to prepare a high-titer phage solution. To determine the phage host spectrum, the phage was separately cultured with 50 strains of *Listeria* spp, the plaque-forming units (pfu) were counted, and the electroplating efficiency (EOP) was calculated as follows: EOP = phage titer in the test bacteria/phage titer in the host bacteria(Host bacteria is the bacteria in which the phage was originally isolated. Test bacteria is the bacteria used to test excepted host bacteria) (19). The phage solution was stained with phosphotungstic acid and observed with transmission electron microscopy (Hitachi HT 7,700, Hitachi Ltd, Tokyo, Japan).

Different phage/bacterium ratios were tested to determine the optimal multiplicity of infection of phage (MOI = 0.001, 0.01, 0.1, 1, 10, or 100). Under the optimal conditions for infection, bacterial and phage cultures were subjected to gradients of temperature (25°C, 35°C, 45°C, 55°C, 65°C, and 75°C) and pH (2, 4, 6, 8, 10, and 12), and different solvents (methanol, ethanol, glycerol, isoamyl alcohol, magnesium sulfate buffer, and chloroform) to determine optimal growth conditions, and their growth was measured per 10 min to 2 h. The data were used to construct one-step growth curves.

Phage Genome-Wide Analysis

The genome was extracted from the phage with the Tris-HCL method (20). The genome was digested with DNase I, RNase I, and mung bean nuclease (Solarbio) to determine the genome type. The phage genome was scanned and sequenced with Illumina sequencing technology. The databases RefSeq nonredundant (Nr) protein (RefSeq: NCBI Reference Sequence Database, nih.gov), Clusters of Orthologous Groups of proteins (COG, https://www.ncbi.nlm.nih.gov/research/cog), Kyoto Encyclopedia of Genes and Genomes (KEGG, https://www.kegg.jp/kegg/), Swiss-Prot (www.sib.swiss/swiss-prot), and Gene Ontology (http://www.geneontology.org/GO.indices.html) were used to annotate the genes. Finally, the SnapGene software (Insightful Science; available at snapgene.com) was used to analyze the distributions and functions of the genes.

Listeriosis Infection Model and Phage Intervention

Sixty female Kunming mice were randomly divided into a blank control group, toxic reaction group, antibiotic treatment group, phage treatment group, and combined treatment group (**Appendix 1**). About 100 μL bacterial culture with $OD_{600} = 0.6$ (which is equivalent to a bacterial concentration of 2.09×10^{10}CFU/mL, **Appendix 2**) was injected into each mouse. The phage injection was converted according to the detected optimal MOI (bacterial concentration × MOI), and the injection volume was 100 μL. Among the six antimicrobial drugs, ATCC19111 had the highest resistance to penicillin G sodium and was sensitive to other antibiotics. In addition, among many antibiotics, β-lactam antibiotics are the most widely used. Finally, penicillin G sodium was selected as the tested antibiotic (**Appendix 3**). According to the *in vitro* plate bacteriostatic test, the minimum inhibitory concentration of single penicillin G sodium is 11 mg/L (**Appendix 4**), and the minimum inhibitory concentration of the combination with phage LP8 is 7 mg/L (**Appendix 5**).

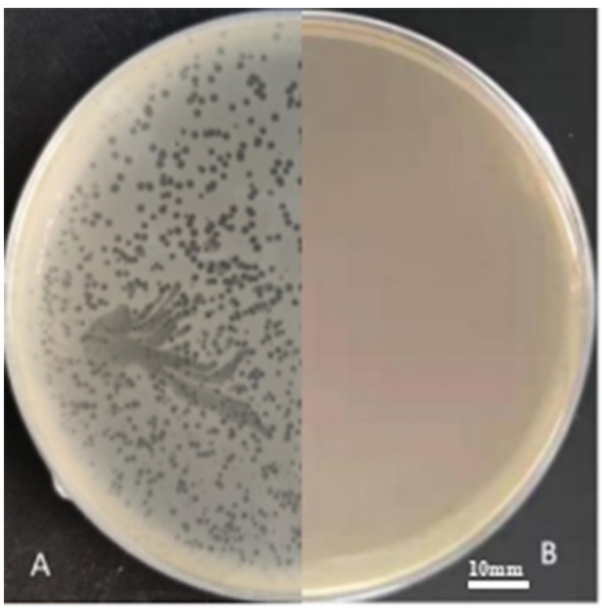

FIGURE 1 | LP8 plaques observed on plate. The host strain was ATCC19111 (1/2a). The plaques, approximately 2 mm in diameter, were seen on the plate. **(A)** is separation plate. **(B)** is blank plate.

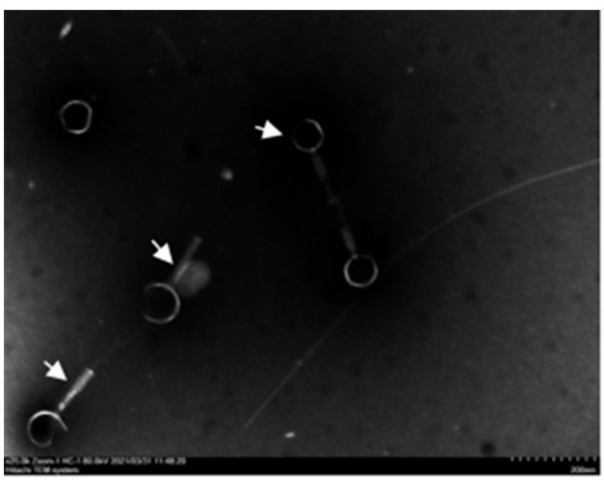

FIGURE 2 | Transmission electron microscopy (TEM) image of LP8. White arrows in the figure indicate phage. The phage has a hollow needle-like structure; the tail consists of an envelope and the base consists of a tail needle. The average diameter of the phage head is 80 nm and the average length of the tail is 120 nm. Scale bar: 200 nm.

Sample Detection

Peripheral blood (100 μL) was collected from each mouse and 5 μL of allophycocyanin (APC)-conjugated anti-mouse CD^{3+} antibody (**0.2** mg/mL), 2 μL of phycoerythrin (PE)-conjugated anti-mouse CD^{4+} antibody (**0.5** mg/mL), or 5 μL of fluorescein isothiocyanate (FITC)-conjugated anti-mouse CD^{8+} antibody (**0.2** mg/mL) (BioLegend, San Diego, CA, USA) were added to the sample to stain. All samples from each group were analyzed with flow cytometry. Treestar FlowJo v10.0 was used to analyze the data.

Mouse serum was collected to test the expression of cytokines, tumor necrosis factor α (TNF-α), interleukin 1β (IL-1β), interleukin 10(IL-10), and interferon γ (IFN-γ). ELISAs kit (Jiangsu ELISA Co., Ltd, Jiangsu, China) was used to test the above value and detailed operation according to kit instructions.

Heart, liver, spleen, kidney, and brain tissues were sampled from each mouse and steeped in 4% formaldehyde. Sections

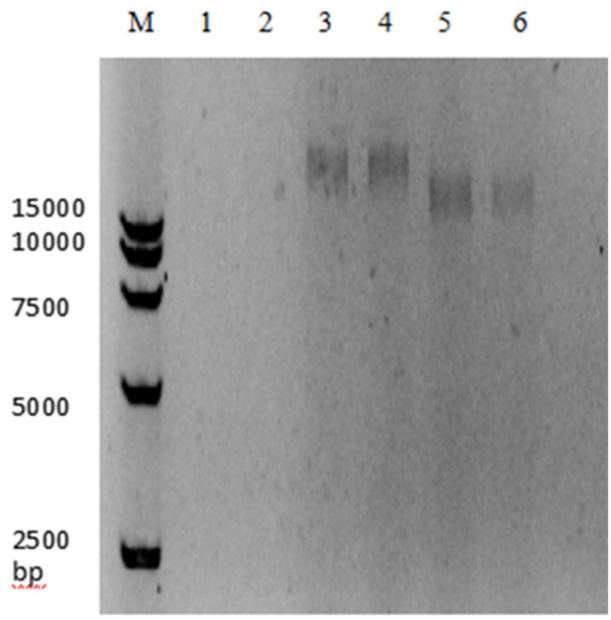

FIGURE 3 | Digestion electrophoresis of LP8 phage genome. M, DNA Marker 15,000;1, 2, DNase;3, 4, RNase;5, 6, Mung bean nuclease.

(3 μm) were cut, stained with HE, and observed microscopically at 400× magnification (Olympus Corporation, Japan). Sections were also stained with Giemsa and observed at 1,000× magnification.

The spleens were collected aseptically from each group of mice and pooled according to the group in sterile 1.5-mL centrifuge tubes. Sterilized stainless-steel balls and 1 mL of phosphate-buffered saline (PBS) were added, and the tissues were ground for 300 s with a high-throughput tissue grinder (Ningbo Biotechnology Co., Ltd, Zhejiang, China). Each spleen suspension was diluted with PBS (10^{-1}, 10^{-3}, 10^{-5}, 10^{-7}, and 10^{-9}), and an aliquot (100 μL) of each dilution was added to a solid TSB-YE medium, incubated at 37°C for 12 h, and colonies were counted. Five biological replicates were analyzed per sample.

Data Analysis

All comparisons among groups were analyzed with an independent- samples *t-test* and analysis of variance (ANOVA), with the SPSS software. The data were analyzed and visualized with the Origin software (Origin Lab Corporation Northampton, MA, USA).

RESULTS

Isolation and Identification of Phage

In three slaughterhouse sewage samples, a total of four phages were isolated and named LP1, LP2, LP3, and LP4. After purification, it was found that LP1 and LP2 were not *Listeria monocytogenes* phages, while LP3 and LP4 were found to be the same phage by whole genome sequencing. To distinguish, LP3 and LP4 are uniformly named LP8 for subsequent experiments (**Figure 1**). Host spectrum showed that LP8 lysed 18 strains of *L. monocytogenes* and 5 strains of *L. welshimeri* (**Appendix 6**). Transmission electron microscopy showed that LP8 belongs to *Myoviridae* (**Figure 2**). The optimal MOI for LP8 was 1, the optimal growth temperature was 45°C, the optimal pH was 7, and isopentyl alcohol could lead to the LP8 inactivity (**Appendix 7**).

Phage Genome Analysis

The genome of the LP8 phage was double-stranded DNA (**Figure 3**). Whole-genome sequencing indicated that the genome size of LP8 was 87,038 bp and encoded 120 genes. These genes encoded proteins involved in phage synthesis, invasion, assembly, signal transduction, and related functions (**Figure 4**). The non-structural proteins were predominantly involved in regulatory roles and signal transduction.

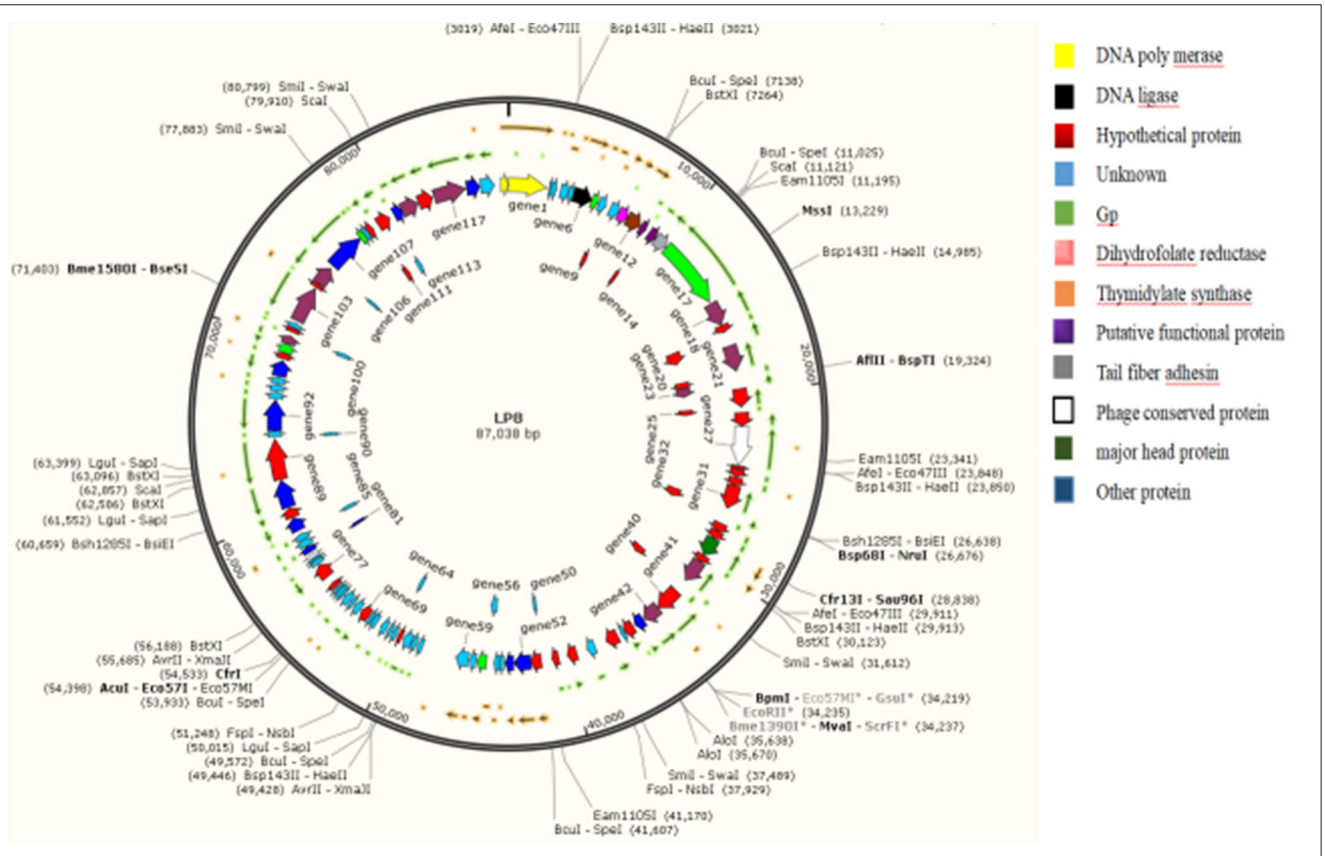

FIGURE 4 | Whole-genome map of LP8. Length of the phage LP8 genome is 87,038 bp, with a total of 120 coding genes. Length of the coding region accounts for 87.69% of the genome length. Six genes encode proteins involved in phage synthesis, 20 genes encode proteins involved in phage-related biological processes, and 11 genes encode proteins involved in molecular functions such as binding or catalysis.

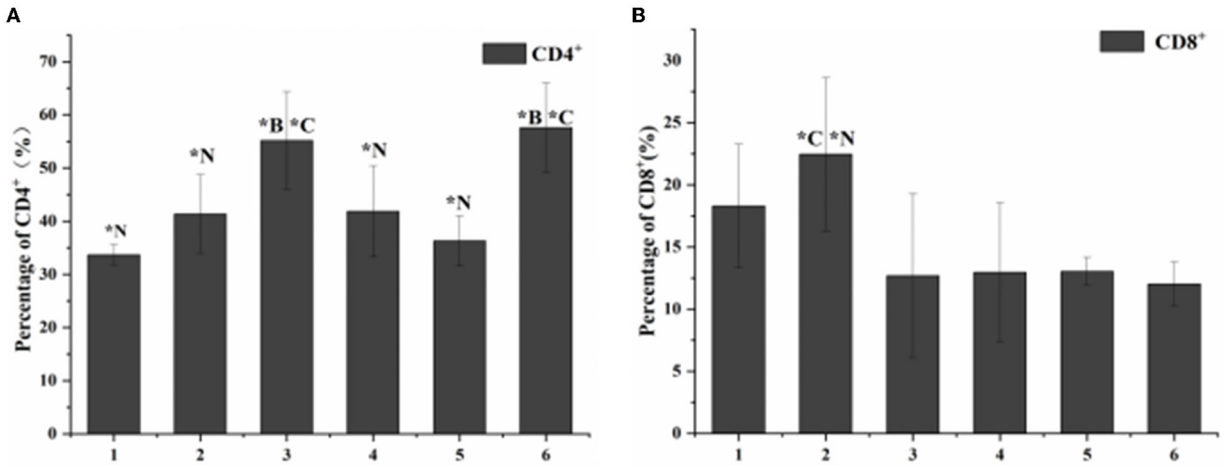

FIGURE 5 | Statistical chart of the proportion of lymphocyte subsets. 1. Blank control group. 2. Toxic group. 3. Penicillin G sodium treatment group. 4. Phage therapy group. 5. Combination therapy group. 6. Non-intervention group. The values are means and standard deviations (SD) ($n = 5$). ***C** < 0.05. Each group vs. combination therapy group. ***B** < 0.05. Each group vs. blank control group. ***N** < 0.05. Each group vs. non-intervention group.

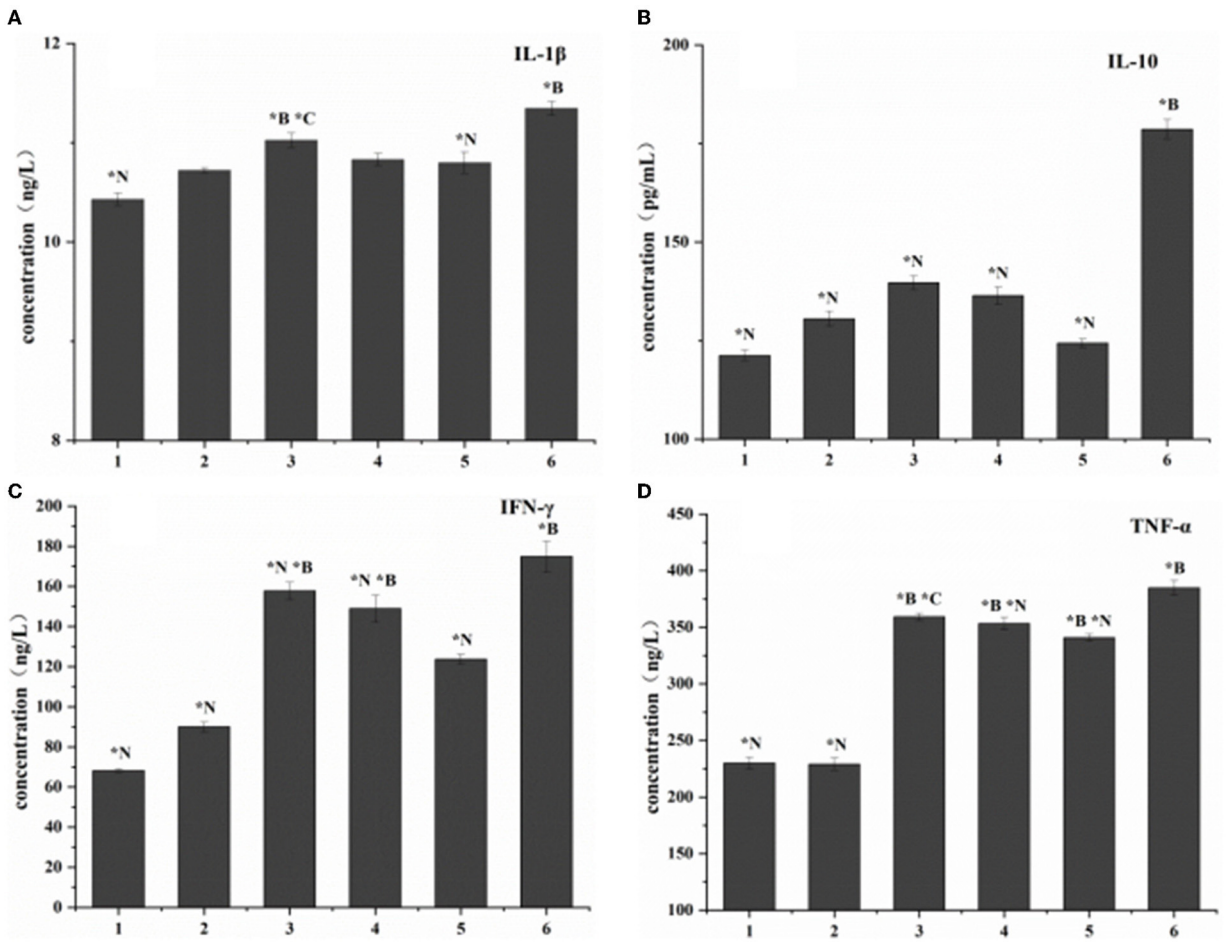

FIGURE 6 | Cytokine expression in listeriosis model. 1. Blank control group. 2. Toxic group. 3. Penicillin G sodium treatment group. 4. Phage therapy group. 5. Combination therapy group. 6. Non-intervention group. The values are means and standard deviations (SD) ($n = 5$). ***C**<0.05. Each group vs. combination therapy group. ***B** < 0.05. Each group vs. blank control group. ***N**<0.05. Each group vs. non-intervention group.

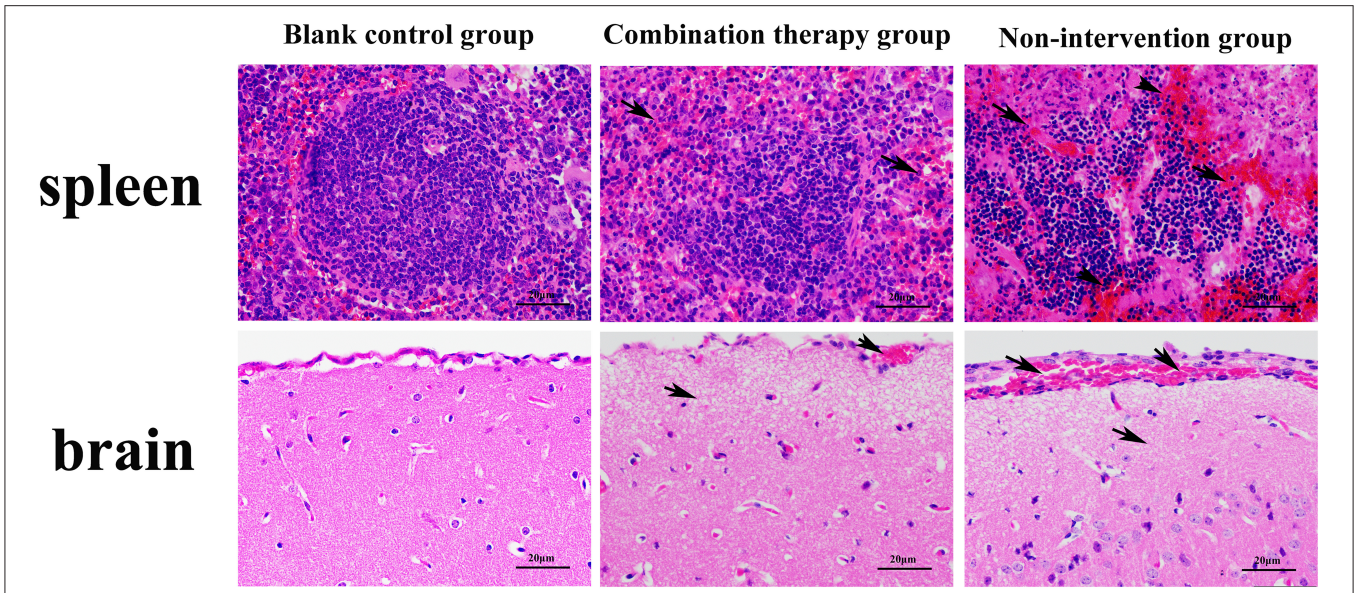

FIGURE 7 | Giemsa staining of mouse parenchyma (×1,000). Red arrow indicates bacteria with the typical form of LM. LM was not detected in the blank control group and non-intervention group.

The phage sequence was uploaded to the NCBI database (GenBank: OK283618.1).

Evaluation of Therapeutic Effects of LP8

According to the results of flow cytometry, the proportion of CD^{4+} cells in the blank control group was 34%, while the proportion of CD^{8+} cells was 16%. The proportion of CD^{4+} and CD^{8+}cells in the toxicity group was 41 and 25%. The proportion of CD^{4+} and CD^{8+}cells in the antibiotic treatment group was 56 and 12%. The proportion of CD^{4+} and CD^{8+}cells in the phage-treated group was 42 and 13%, respectively. The proportion of CD^{4+} and CD^{8+} cells in the combined treatment group were 37 and 16%. The proportion of CD^{4+} and CD^{8+}cells in the non-intervention group was 58 and 11% (**Figure 5**).

Compared with the blank control group, the expression levels of the four cytokines (TNF-α, IL-1β, IL-10, and IFN-γ) increased *in vivo* in all treatment groups. The no-intervention group had the highest expression levels. Among the three treatment groups, the cytokine expression in the combined treatment group had the smallest change (**Figure 6**).

For pathological changes, the results for the no-intervention group showed that LM caused severe hemorrhagic necrosis in the spleen, meningeal local hemorrhage, hemorrhagic necrosis and atrophy of glomeruli, diffuse hemorrhage of the liver accompanied by severe edema, and atrophy and rupture of the cardiac myocardial fibers (**Figure 7**). In the late stage, symptoms such as secondary bacteremia and meningitis appeared, and the kidneys, heart, and liver displayed various degrees of atrophy (**Appendix 8**). Bacteria with the typical morphology of LM were found in the parenchymal organs, especially in the spleen and brain (**Figure 8**).

There was no bacterial growth on the plates in the blank control group or the toxic reaction group. The bacterial load was highest in the no-intervention group with 1.23×10^{12} CFU/mL. The load in the phage treatment group was 6.27×10^{9} CFU/mL, and the antibiotic treatment group was 1.97×10^{10} CFU/mL. However, the combination therapy group was 1.05×10^{8} CFU/mL (**Figure 9**).

DISCUSSION

First, LP8 was isolated from slaughterhouse sewage contaminated with LM. Whole-genome sequencing showed that the genome is 87,038 bp. LP8 belongs to the family of *Myoviridae*. By comparing the whole genome sequence of LP8, the coding region of the phage genome was more than 80% of the genome size. Among the genes encoded, 76 genes were highly similar to some genes from *Salmonella*, *Escherichia,* and *Citrobacter* phages, with maximum single coverage of 7% and cumulative coverage of 38.4%. For the 120 genes, the similarity of BLAST from the NCBI is low, and the function of 44 genes is unknown. The above phenomenon indicates that LP8 may have undergone a complex process of horizontal gene transfer, mutation, and recombination during the evolution process (21, 22).

At present, the LISTEX^{TM} P100 is used to prevent and control food safety incidents caused by LM (23). The reagents are largely based on six species of LM phage, and this cocktail therapy is used to deal with the problem of the high specificity of a single phage. Compared with LISTEX^{TM} P100, LP8 has a shorter action time and wider temperature range for activity. It is also effective in combination with antibiotics. LP8 has a greater capacity for cross-species lysis and a shorter incubation period than other reported LM phages (24, 25).

Song et al. measured the one-step growth curve of LM phages LP020, LP027, and LP094, and the results showed that the incubation period of these three LM phages was 45∼60 min (25). However, the incubation period of LP8 was 23 min, reaching the

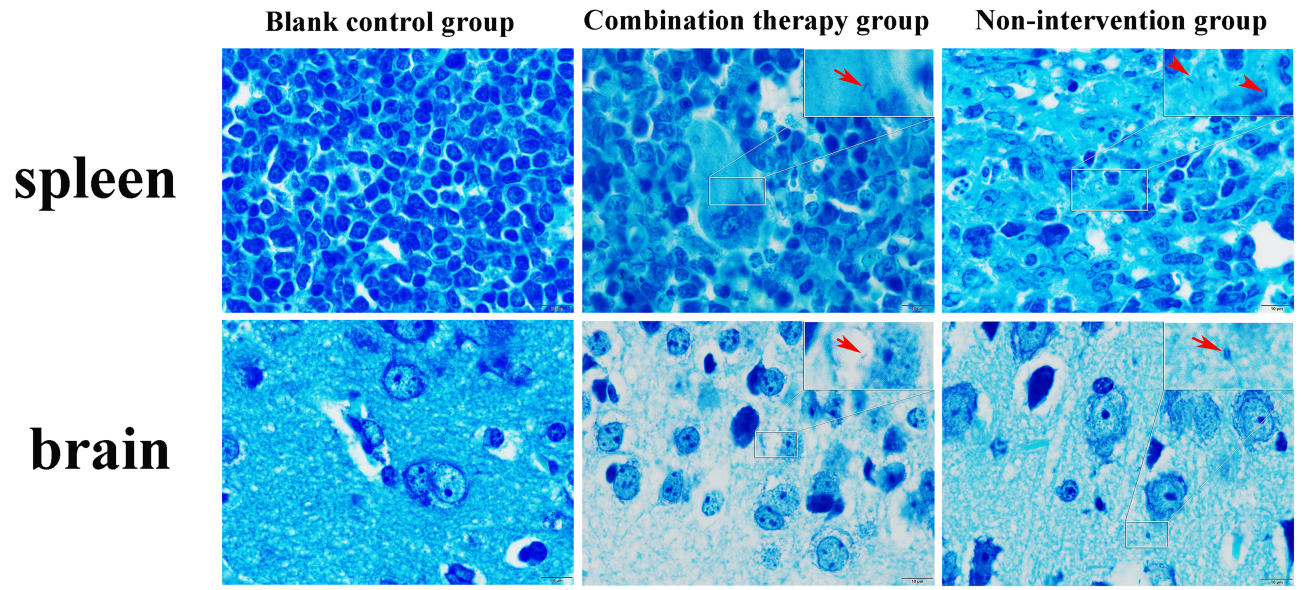

FIGURE 8 | Spleen bacterial load in the listeriosis model. **(A)** Blank control group. **(B)**. Toxic reaction group. **(C)** Penicillin G sodium treatment group. **(D)** Phage Therapy Group. **(E)** Combination Therapy Group. **(F)** Non-intervention group. The values are means and standard deviations (SD) ($n = 5$). *C < 0.05. Each group vs. combination therapy group. *N < 0.05. Each group vs. non-intervention group.

plateau after 80 min. The four phages with the highest efficiency were all above 1×10^{10} PFU·mL^{-1} and had the same effect, but LP8 acted faster. Lee et al. isolated two LM phages LMP1 and LMP7 from chicken manure samples, which showed lytic activity in ATCC7644, ATCC15313, ATCC19114, and ATCC19115 (26). In addition to 18 strains of LM, LP8 also showed lytic activity against five strains of *L. welshimer* (9-2, 4-40, C10, C59, 4-43), indicating that LP8 had cross-species lytic activity.

L. monocytogenes is classified into four evolutionary lines (I, II, III, and IV) and four molecular serogroups (IIa, IIc, IIb, and IVb), which cover different serotypes (1/2a, 3a, 1/2c, 3c, 1/2b, 3b, 4b, 4d, and 4e) (27–29). Several studies have indicated strains divergence regarding their ability to persist in the environment, as well as their virulence potential (29), because the serotyping of *L. monocytogenes* is based on the difference between the A antigenic site and the O antigenic site on the surface of the bacteria. LP8 can lyse 18 strains of *L. monocytogenes*, among which the lysis ability is generally higher for the strains with serotype 1/2a; therefore, we suspect that the recognition of *L. monocytogenes* by LP8 is related to the A and O antigens on the bacterial surface. In addition, LP8 has a lytic activity to five strains of *L. welshimeri*. According to our evolutionary analysis of the 16s RNA of 10 strains of *L. welshimeri*, the five strains that LP8 can lyse with are located on the same evolutionary branch. LP8 had no lytic activity against 22 strains of *L. innocua*, which may be related to the different surface sites of the bacteria.

The results of the three treatment groups in this study showed that the lymphocyte subsets decreased, and the expression of cytokines increased, proving that the three methods had an intervention effect on LM infection. Because of their

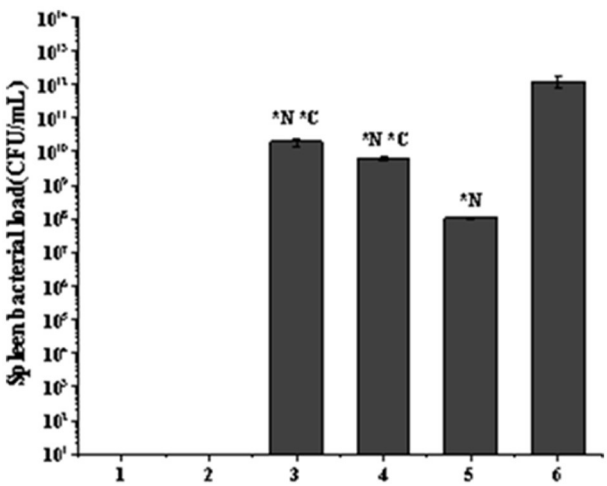

FIGURE 9 | Hematoxylin–eosin staining microscopy of spleen and brain (×400). Black arrow in the figure indicates the location of the lesion. Compared with the blank control group, the non-intervention group showed partial splenic corpuscle disappearance from spleen; apoptosis of a large number of lymphocytes, accompanied by a certain degree of hemorrhage, and the boundary of the germinal center was blurred. Partial meningeal hyperemia, cerebral cortex tissue shows watery degeneration, and the nerve cells are necrotic and atrophied, which is typical of sepsis and meningitis.

biological activity and composition, phages are susceptible to complex environments, so combining them with antibiotics can compensate for some shortcomings of the phages themselves (30, 31). In addition, the effect of the combination group

was better than that of the single administration group, indicating that the addition of phage can reduce the use of antibiotics. In the future, genetically modified phages could specifically replace resistant genes in bacterial genomes, making bacteria susceptible to antibiotics again (32). This also demonstrates the potential of phage-antibiotic combinations as novel biologics.

CONCLUSION

This study confirms that LP8, an LM phage isolated from slaughterhouse sewage, was effective for LM and *L. welshimeri*. The combination of LP8 and antibiotics can compensate for the impact of the biological activity of the phage in the treatment. Furthermore, the addition of phage can reduce the use of antibiotics and achieve the effect of reducing and limiting antibiotics finally.

DATA AVAILABILITY STATEMENT

The datasets presented in this study can be found in online repositories. The names of the repository/repositories and accession number(s) can be found below: https://www.ncbi.nlm.nih.gov/genbank/, OK283618.1.

ETHICS STATEMENT

The animal study was reviewed and approved by Animal Welfare and Ethics Committee of Gansu Agricultural University.

AUTHOR CONTRIBUTIONS

This article is provided by HG and HX to provide design ideas, guide the experimental process, follow-up data analysis and paper writing. TL is engaged in related experimental work, data analysis and paper writing. XW and ZW provide relevant experimental sample collection work. XZ and CT assisted in phage isolation. WS and YQ assisted in phage identification. HW and CS assisted in mouse experiments. All authors contributed to the article and approved the submitted version.

FUNDING

This work was supported by the National Nature Science Foundation of China (nos. 32060822, 31960726, and 31560700), Key Research and Development Program of Gansu Province (no. 20YF8-FA136), National Key Research and Development Program of China (no. 2019YFC1605705), Gansu Agricultural University Youth Tutor Support Fund (no. GAU-QDFC-2020-10), and Gansu Excellent Postgraduate Innovation Star Project (no. 2021CXZX-390). We are indebted to international science editing for the critical correction of this manuscript.

SUPPLEMENTARY MATERIAL

The Supplementary Material for this article can be found online at: https://www.frontiersin.org/articles/10.3389/fvets.2022.946814/full#supplementary-material

REFERENCES

1. Ming X, Daeschel MA. Nisin resistance of foodborne bacteria and the specific resistance responses of *Listeria monocytogenes* Scott A. *J Food Prot.* (1993) 56:944–8. doi: 10.4315/0362-028X-56.11.944
2. Keto-Timonen R, Tolvanen R, Lunden J, Korkeala H. An 8-year surveillance of the diversity and persistence of *Listeria monocytogenes* in a chilled food processing plant analyzed by amplified fragment length polymorphism. *J Food Prot.* (2007) 70:1866–73. doi: 10.4315/0362-028X-70.8.1866
3. Camargo AC, Woodward JJ, Call DR, Nero LA. *Listeria monocytogenes* in food-processing facilities, food contamination, and human Listeriosis: the Brazilian scenario. *Foodborne Pathog Dis.* (2017) 14:623–36. doi: 10.1089/fpd.2016.2274
4. Cheng C, Liu F, Jin H, Xu X, Xu J, Deng S, et al. The DegU orphan response regulator contributes to heat stress resistance in *Listeria monocytogenes*. *Front Cell Infect Microbiol.* (2021) 11:761335. doi: 10.3389/fcimb.2021.761335
5. Allerberger F, Wagner M. Listeriosis: a resurgent foodborne infection. *Clin Microbiol Infect.* (2010) 16:16–23. doi: 10.1111/j.1469-0691.2009.03109.x
6. Hof H, Nichterlein T, Kretschmar M. When are *Listeria* in foods a health risk? *Trends Food Sci Technol.* (1994) 5:185–90. doi: 10.1016/0924-2244(94)90103-1
7. Gould LH, Walsh KA, Vieira AR, Herman K, Williams IT, Hall AJ, et al. Surveillance for foodborne disease outbreaks—United States, 1998–2008. *MMWR Surveill Summ Morb Mortal Wkly Rep.* (2013) 62:1–34.
8. Dewey-Mattia D, Manikonda K, Hall AJ, Wise ME, Crowe SJ. Surveillance for foodborne disease outbreaks — United States, 2009–2015. *MMWR Surveill Summ Morb Mortal Wkly Rep.* (2018) 67:1–11. doi: 10.15585/mmwr.ss6710a1
9. Lee BH, Cole S, Badel-Berchou XS, Guillier L, Felix B, Krezdorn N, et al. Biofilm formation of *Listeria monocytogenes* strains under food processing environments and pan-genome-wide association study. *Front Microbiol.* (2019) 10:2698. doi: 10.3389/fmicb.2019.02698
10. Lüth S, Halbedel S, Rosner B, et al. Backtracking and forward checking of human listeriosis clusters identified a multiclonal outbreak linked to *Listeria monocytogenes* in meat products of a single producer. *Emerg Microbes Infect.* (2020) 9:1600–8. doi: 10.1080/22221751.2020.1784044
11. Halimi B, Dortu C, Arguelles-Arias A, Thonart P, Joris B, Fickers P, et al. Antilisterial activity on poultry meat of amylolysin, a bacteriocin from *Bacillus amyloliquefaciens* GA1. *Probiotics Antimicrob Proteins.* (2010) 2:120–5. doi: 10.1007/s12602-010-9040-9
12. Temple ME, Nahata MC. Treatment of listeriosis. *Ann Pharmacother.* (2000) 34:656–61. doi: 10.1345/aph.19315
13. Skowron K, Wałecka-Zacharksa E, Grudlewska K, Wiktorczyk N, Kaczmarek A, Gryń G, et al. Characteristics of *Listeria monocytogenes* strains isolated from milk and humans and the possibility of milk-borne strains transmission. *Pol J Microbiol.* (2019) 68:353–69. doi: 10.33073/pjm-2019-038
14. Grosboillot V, Keller I, Ernst C, Loessner MJ, Schuppler M. Ampicillin treatment of intracellular *Listeria monocytogenes* triggers formation of persistent, drug-resistant L-form cells. *Front Cell Infect Microbiol.* (2022) 12:869339. doi: 10.3389/fcimb.2022.869339
15. Radoshevich L, Cossart P. *Listeria Monocytogenes*: toward a complete picture of its physiology and pathogenesis. *Nat Rev Microbiol.* (2018) 11:32–46. doi: 10.1038/nrmicro.2017.126
16. Clokie MR, Millard AD, Letarov AV, Heaphy S. Phages in nature. *Bacteriophage.* (2011) 1:31–45. doi: 10.4161/bact.1.1.14942
17. Monteiro R, Pires DP, Costa AR, Azeredo J. Phage Therapy: Going Temperate? *Trends Microbiol.* (2019) 27:368–78. doi: 10.1016/j.tim.2018.10.008
18. Jofre J, Muniesa M. Bacteriophage isolation and characterization: phages of Escherichia coli. *Methods Mol Biol.* (2020) 2075:61–79. doi: 10.1007/978-1-4939-9877-7_4

19. Guo Y, Li J, Islam MS, Yan T, Zhou Y, Liang L, et al. Application of a novel phage vB_SalS-LPSTLL for the biological control of Salmonella in foods. *Food Res Int.* (2021) 147:110492. doi: 10.1016/j.foodres.2021.110492
20. Tovkach FI, Zhuminska GI, Kushkina AI. Long-term preservation of unstable bacteriophages of enterobacteria. *Mikrobiol Z.* (2012) 74:60–6.
21. Dion MB, Oechslin F, Moineau S. Phage diversity, genomics and phylogeny. *Nat Rev Microbiol.* (2020) 18:125–38. doi: 10.1038/s41579-019-0311-5
22. Olszak T, Latka A, Roszniowski B, Valvano MA, Drulis-Kawa Z. Phage life cycles behind bacterial biodiversity. *Curr Med Chem.* (2017) 24:3987–4001. doi: 10.2174/0929867324666170413100136
23. Poaska M, Sokoowska B. Bacteriophages—a new hope or a huge problem in the food industry. *AIMS Microbiol.* (2019) 5:324–46. doi: 10.3934/microbiol.2019.4.324
24. Trudelle DM, Bryan DW, Hudson LK, Denes TG. Cross-resistance to phage infection in *Listeria monocytogenes* serotype 1/2a mutants. *Food Microbiol.* (2019) 84:103239. doi: 10.1016/j.fm.2019.06.003
25. Song Y, Peters TL, Bryan DW, Hudson LK, Denes TG. Characterization of a novel group of *Listeria* phages that target serotype 4b *Listeria monocytogenes*. *Viruses.* (2021) 13:671. doi: 10.3390/v13040671
26. Lee S, Min GK, Lee HS, Heo S, Kwon M, Kim GB, et al. Isolation and characterization of listeria phages for control of growth of *Listeria monocytogenes* in milk. Hangug Chugsan Sigpum Haghoeji = Korean. *J Food Sci Anim Resour.* (2017) 37:320–8. doi: 10.5851/kosfa.2017.37.2.320
27. Doumith M, Buchrieser C, Glaser P, Jacquet C, Martin P, et al. Differentiation of the major *Listeria monocytogenes* serovars by multiplex PCR. *J Clin Microbiol.* (2004) 42:3819–22. doi: 10.1128/JCM.42.8.3819-3822.2004
28. Matle I, Mbatha KR, Madoroba EA. Review of *Listeria monocytogenes* from meat and meat products: epidemiology, virulence factors, antimicrobial resistance and diagnosis. *Onderstepoort J Vet Res.* (2020) 87:a1869. doi: 10.4102/ojvr.v87i1.1869
29. Orsi RH, den Bakker HC, Wiedmann M. *Listeria monocytogenes* lineages: Genomics, evolution, ecology, and phenotypic characteristics. *Int J Med Microbiol.* (2011) 301:79–96. doi: 10.1016/j.ijmm.2010.05.002
30. Gordillo Altamirano FL, Barr JJ. Phage therapy in the postantibiotic era. *Clin Microbiol Rev.* (2019) 16:e00066–18. doi: 10.1128/CMR.00066-18
31. Abedon ST. Phage-Antibiotic Combination Treatments: Antagonistic Impacts of Antibiotics on the Pharmacodynamics of Phage Therapy? *Antibiotics.* (2019) 11:182. doi: 10.3390/antibiotics8040182
32. Sagona AP, Grigonyte AM. MacDonald PR, Jaramillo A. Genetically modified bacteriophages. *Integr Biol.* (2016) 18:465–74. doi: 10.1039/C5IB00267B

Conflict of Interest: The authors declare that the research was conducted in the absence of any commercial or financial relationships that could be construed as a potential conflict of interest.

Publisher's Note: All claims expressed in this article are solely those of the authors and do not necessarily represent those of their affiliated organizations, or those of the publisher, the editors and the reviewers. Any product that may be evaluated in this article, or claim that may be made by its manufacturer, is not guaranteed or endorsed by the publisher.

frontiers | Frontiers in Veterinary Science

TYPE Original Research
PUBLISHED 26 July 2022
DOI 10.3389/fvets.2022.947522

OPEN ACCESS

EDITED BY
Kun Li,
Nanjing Agricultural University, China

REVIEWED BY
Awais Ghaffar,
University of Calgary, Canada
Abdul Rahman Omar,
Putra Malaysia University, Malaysia

*CORRESPONDENCE
Iqra Zaheer
dr.iqzaheer@gmail.com
Wei Chen
cwei010230@163.com

SPECIALTY SECTION
This article was submitted to Veterinary Infectious Diseases, a section of the journal Frontiers in Veterinary Science

RECEIVED 18 May 2022
ACCEPTED 30 June 2022
PUBLISHED 26 July 2022

CITATION
Zaheer I, Chen W, Khan A, Elokil A, Saleemi MK, Zaheer T and Khan MZ (2022) Immunopathological comparison of *in ovo* and post-hatch vaccination techniques for infectious bursal disease vaccine in layer chicks. *Front. Vet. Sci.* 9:947522. doi: 10.3389/fvets.2022.947522

Immunopathological comparison of *in ovo* and post-hatch vaccination techniques for infectious bursal disease vaccine in layer chicks

Iqra Zaheer[1]*, Wei Chen[2]*, Ahrar Khan[3], Abdelmotaleb Elokil[4], Muhammad Kashif Saleemi[1], Tean Zaheer[5] and Muhammad Zargham Khan[1]

[1]Department of Pathology, University of Agriculture, Faisalabad, Pakistan, [2]Institute of Animal Science, Guangdong Academy of Agricultural Sciences, Animal Nutrition and Feed Science in South China, Ministry of Agriculture and Rural Affairs, State Key Laboratory of Livestock and Poultry Breeding, Key Laboratory of Guangdong Public Laboratory of Animal Breeding and Nutrition, Guangdong Key Laboratory of Animal Breeding and Nutrition, Guangzhou, China, [3]Department of Animal Science & Technology, Shandong Vocational Animal Sciences and Veterinary College, Weifang, China, [4]Department of Animal Production, Faculty of Agriculture, Benha University, Benha, Egypt, [5]Department of Parasitology, University of Agriculture, Faisalabad, Pakistan

This study was designed to compare immunopathological effects of *in ovo* vaccination with post-hatch vaccination against IBD in White Leghorn chicks. A total of 189 embryonated eggs were divided into six groups. At day 18 of incubation, groups A–C were administered *in ovo* with 228E, Winterfield 2512:10/3 and 2512/90:10/2.7, respectively, group D (post-hatch vaccination) and group E as shamed control (for quality evaluation of *in ovo* vaccination technique), and group F as control. The results showed that antibody titers against IBD detected by ELISA on days 2, 17, and 28 were significantly higher in all *in ovo* groups as compared to control groups E and F. On day 17, all vaccinated groups (*in ovo* and post-hatch vaccinated) showed no significant differences in antibody titers among themselves; however, at day 28, only the post-hatch group showed significantly higher antibody titers followed by *in ovo* vaccinated groups. The cell-mediated immunity determined by PHA-P assay was significantly higher in all vaccinated groups than the non-vaccinated groups. No clinical signs of IBD infection were observed in any of the vaccinated groups. There was only increase in bursa size of groups vaccinated with intermediate plus strains (groups A, C, and D) at day 28. The histopathology showed that all the treatment groups had mild lesions induced by IBD virus in bursa. This study concluded that *in ovo* vaccination with live IBD vaccines provides protective immunity to the chickens even in the presence of IBD-specific MDA; therefore, the onset of immunity was much earlier than the post-hatch vaccination and *in ovo* groups also maintained protective immunity against IBD for longer time.

KEYWORDS

IBD, *in-ovo*, vaccine, immunopathology, layers

Introduction

Infectious bursal disease virus (IBDV) is a dsRNA virus of birnaviridae family having two serotypes (serotypes I and II), of both only serotype I is responsible for infectious bursal disease (IBD) in chicken also known as "Gumboro diseases." The virus is difficult to be inactivated by ordinary physical and chemical methods. Therefore, it persists for longer durations in poultry houses. Longer persistence of the diseases in commercial poultry flocks is of prime economic concern that may adversely affect the health and welfare of the flocks (1, 2). Infectious bursal disease is highly contagious in young chicken with acute onset and primarily targets the lymphoid tissue with special affinity to bursa of Fabricius (3, 4). At days 3–4 of post-infection (PI), bursa shows hypertrophy, hyperemia, and edema. At days 5–6 of PI, the bursa regains its normal size and by day 8 gets atrophied to one-third of its normal size. The birds suffer from severe dehydration and exhibit hypertrophy, whitish urate crystal deposits with cell debris in kidneys (5). IBD virus-induced immunosuppression (6) predisposes the young chicks to opportunistic pathogens and prevents the development of adequate immune response to the commonly used vaccines (7). The degree of immunosuppression, mortality rate, clinical signs, and severity of bursal lesions depend upon the age and immune status of the bird and pathogenicity of viral strains (5).

Despite intensive vaccination regimens, IBD still stands as an economically important disease of poultry (8). In field environment, mostly IBD vaccine is administered in drinking water to the chicks. However, *in ovo* vaccine delivery has shown to induce protective immunity as well (9, 10). The concept of *in ovo* vaccination evolved by successful experimental administration of Marek's disease virus (MDV) vaccine to chicken embryos which protected the chicks from MDV challenge later in life (11). Following this successful study, this concept of vaccinating the chicken embryos further developed and the chicken embryos were vaccinated with IBD vaccine alone and in combination with MD vaccine, both of which presented the same conclusion as the previous study (12).

In ovo vaccine administration against IBD virus at 18th day of incubation minimizes the susceptibility window, i.e., the duration between the vaccine administration and an early exposure to the IBD virus as compared to routine post-hatch vaccine administration (13). The recent studies have revealed that in comparison with the vaccine administered after hatching, the *in ovo* vaccination approach stimulated both the innate and adaptive immunity in young chicks (13). The IBD virus exposure induced systemic humoral immunity as well as the cell-mediated immune (CMI) response (14). The local immune response may also play a remarkable role in building protection against IBD virus challenge as the IBD virus *via* gut-associated tissue enters the circulation and then gets distributed to other organs (15).

Although conventional vaccination strategies are still in use but *in ovo* vaccination is also being adopted in many parts of the world (16), however, there is less information about the immunopathological sequelae of administering live vaccines by *in ovo* route as the embryos lack fully developed immune system. Therefore, present experimental study was designed to investigate the pathological changes associated with *in ovo* administration of IBD live vaccines and comparison of immune response elicited by *in ovo* vaccination with that of post-hatch vaccination against IBD followed in field conditions.

Materials and methods

Experimental design

A total of 189 fertile hatching eggs from White Leghorn (WLH) layer breeder flock were procured from a commercial hatchery. The eggs were clean and shifted to the setter of disinfected incubator in the hatchery at Department of Poultry Science, University of Agriculture Faisalabad. At day 18 of incubation, eggs were candled and only the viable embryos were selected. The egg shell surfaces of all groups except group F (Control) were disinfected with alcohol and groups A, B, C, and E inoculated *in ovo via* air cell route, using a 2.5-cm 23-gauge needle with individual dose (0.1 ml) of vaccine (17) per egg. Gentamicin sulfate was added at dose rate of 1 mg /ml inoculums (18) to avoid bacterial contamination. The virus particles per dose for group A were (2-3 log10 EID_{50}), B (10^{3} EID_{50}), and C ($10^{2.7}$ EID_{50}). The eggs of group E served as shamed control and were inoculated with sterilized physiological saline (19). A number of eggs in groups A, B, C, D, E, and F were 33, 32, 32, 32, 30, and 30 eggs, respectively. After that, the eggs were placed in labeled porous bags. These egg-containing bags were then carefully shifted to the hatcher of disinfected incubator till day 21 of incubation. The embryonated eggs of commercial layer were from same batch used for *in ovo* vaccination and post-hatch study.

After hatching, the chicks were shifted to the experimental poultry house at Department of Clinical Medicine and Surgery, University of Agriculture Faisalabad. Birds of each group were kept in separate cages and were provided drinking water and feed *ad libitum*. The hatchlings of the *in ovo* vaccinated groups (A, B, C), group D (used for post-hatch vaccination), shamed control (E), and negative control (F) were used in post-hatch experiment of 28 days. The experimental design of chicks is given in Table 1.

The only group D was administered post-hatch IBD vaccine by intraocular route (20) at days 08 and 16 as per field practice. However, all the groups were vaccinated with live vaccines *via* eye drop route against Newcastle disease (ND) and infectious bronchitis (IB) at day 5 of age. The duration of experiment was 28 days (because the susceptibility window for IBD infection in

TABLE 1 Experimental design for chicks.

Groups	IBDV strains	Route of vaccine	Description
A	Nobilis Gumboro 228-E Intermediate plus strains	*In ovo*	No post-hatch vaccination of IBD.
B	Winterfield 2512: 10/3 Intermediate strain	*In ovo*	
C	Winterfield 2512/90: 10/2.7 Intermediate plus strains	*In ovo*	
D	Winterfield 2512/90: 10/2.7 Intermediate plus strains	Eye drop	IBD post-hatch vaccination on days 08 and 16.
E	Shamed control	*In ovo*	Physiological saline solution (no vaccination of IBD)
F	Control	–	No intervention

layer chicks is at 3–4 weeks of age (21). A total of six birds from each group were bled at days 2 and 28 for collection of blood and visceral organs for evaluation of different parameters. The blood was collected for serum. The bursal tissues were collected at days 2 and 28 and fixed in 10% neutral buffered formalin for histopathology.

Parameters studied

The percent hatchability was determined. Clinical signs were recorded two times daily and body weights weekly. On days 2 and 28, necropsy examination was done to explore any gross changes in the organs. The preserved tissues were processed for histopathological studies (22).

To determine **cell-mediated immunity,** the cutaneous lymphoproliferative response to phytohemagglutinin (PHA-P) was assessed *in vivo* at 24, 48, and 72 h as cutaneous basophilic hypersensitivity response = skin thickness in the right foot (PHA-P Ag)—skin thickness in the left foot (control) (23). Humoral immunity was determined using ELISA (Iddex Labs USA). The bursa: body weight index was determined by formula of (24):

$$\text{BW ratio} = \frac{\text{Bursal weight}}{\text{Body weight}} \times 100$$

$$\text{Bursa: BW index} = \frac{\text{Bursa: Body weight of vaccinated group}}{\text{Mean bursa: Body weight of control}}$$

Organ weights of immune organs (bursa, thymus, and spleen) were studied by taking average of six replicates, as absolute organ weights and relative organ weights. The formula for relative organ weight was:

$$\text{Relative organ weight} = \frac{\text{Absolute organ weight}}{\text{Body weight}}$$

The data obtained were subjected to one-way analysis of variance and group means were compared by Duncan's multiple range test (DMR) ($p \leq 0.05$) using M Stat-C software package. All the experimental protocols and use of animal were approved by Graduate Studies Research Board (GSRB) of University of Agriculture Faisalabad.

TABLE 2 Hatchability in different groups of the White Leghorn chicks administered live IBD vaccines *in ovo* and post-hatch period.

Groups	Total no. of fertile hatching eggs	Hatchability #	Hatchability (%)
A	33	31	93.93
B	32	30	93.75
C	32	30	93.75
D	32	31	96.86
E	30	30	100
F	30	29	96.67

Results

Hatchability

The percent hatchability varied among different groups. The highest percent hatchability was seen in group E followed by groups D, F, A, B, and C. It has been presented in Table 2.

Clinical signs

During the whole period of study, none of the birds from any group presented any clinical sign of disease based upon the parameters of their alertness, hydration status, and fecal consistency.

Body weights

Body weights determined at weekly intervals of different groups have been presented in Table 3. No significant difference was found in the weekly body weights among all groups.

TABLE 3 Body weights (mean ± SD) of the White Leghorn chicks administered live IBD vaccines *in ovo* and post-hatch period.

Groups	Vaccine	Route	Body weight (mean ± SD)			
			Week 1	Week 2	Week 3	Week 4
A	Nobilis Gumboro 228-E Intermediate plus strains	*In ovo*	38.89 ± 1.90	59.13 ± 2.55	107.28 ± 6.34	160.55 ± 3.43
B	Winterfield 2512: 10/3 Intermediate strain	In ovo	39.45 ± 2.66	60.96 ± 3.32	99.67 ± 7.23	162.87 ± 5.54
C	Winterfield 2512/90: 10/2.7 Intermediate plus strains	*In ovo*	41.62 ± 3.09	60.65 ± 3.64	102.27 ± 10.67	158.14 ± 12.17
D	Winterfield 2512/90: 10/2.7 Intermediate plus strains	Eye drop	40.48 ± 4.10	58.0 ± 5.60	106.19 ± 10.09	159.27 ± 12.15
E	Shamed control	*In ovo*	39.39 ± 3.28	59.82 ± 3.55	104.85 ± 13.12	160.15 ± 9.46
F	Control		39.87 ± 4.74	57.83 ± 6.17	106.45 ± 10.19	159.86 ± 11.88

Values denoted by different alphabets in each column are significantly different ($p \leq 0.05$).

Gross lesions

At day 2 after hatching, all organs including bursa of Fabricius, spleen, kidney, and thymus grossly appeared normal in all groups. At day 28 after hatching, groups E and F showed the normal size of the bursa. However, the bursa of groups A, C, and D was swollen two times their original size followed by those of group B which presented moderate swelling (Figure 1). Other organs such as spleen, kidney, and thymus presented the normal gross appearance.

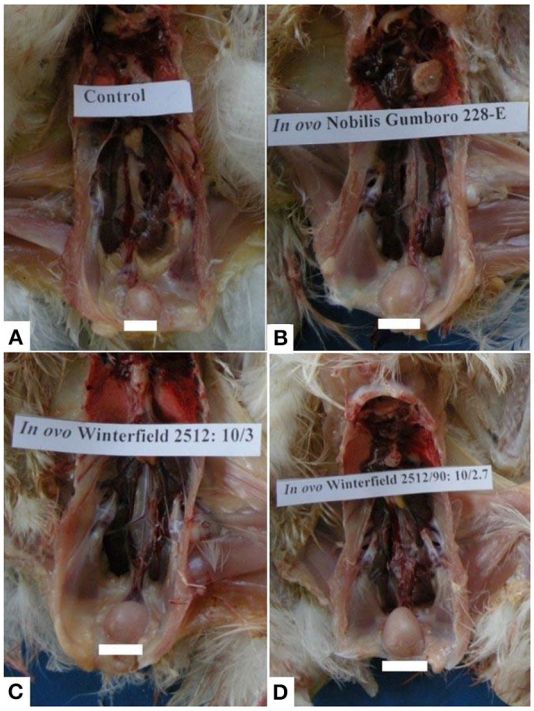

FIGURE 1
Bursa of Fabricius of layer chicks at day 28. **(A)** Control group (normal size of bursa) whereas bursal hypertrophy **(B–D)** in group A (*in ovo* 228 E), group B (*in ovo* Winterfield 2512: 10/3) and group C (*in ovo* Winter field 2512: 10/2.7) in comparison with control group F.

Histopathological lesions

Bursa of Fabricius

Group A (in ovo Nobilis Gumboro 228 E)

At day 2, the medulla of follicles exhibited mild degree of lymphocytic depletion. However, the surface epithelium was intact. There were prominent dark condensed nuclei (pyknotic) depicting the necrosis in few follicles. A thin layer of cells was present between cortex and medulla. Follicles appeared larger in size compared with follicles of other groups. At day 28, the interfollicular connective tissue was minimal. Medulla was not as densely packed as cortex, and it mainly contained small cells with scarce cytoplasm, some larger cells (macrophages), and fibroblasts. Cortex was densely packed with small and large cells with little cytoplasm. Medullae of bursal follicles also showed some scattered cells with pyknotic nuclei. The cortex contained some empty spaces (Figure 2B).

Group B (in ovo Winterfield 2512: 10/3)

At day 2, the empty spaces and pyknotic nuclei in the medulla of follicles appeared lesser in number as compared to groups A and E while at day 28, surface epithelium was intact and interfollicular connective tissue was thinner than group A. There was clearly demarcated cortex and medulla and the cortical cells were larger than medullary cells. Both cortex and medulla were not as densely packed as that of group A. Some cells with pyknotic nuclei and large cells (macrophages) were

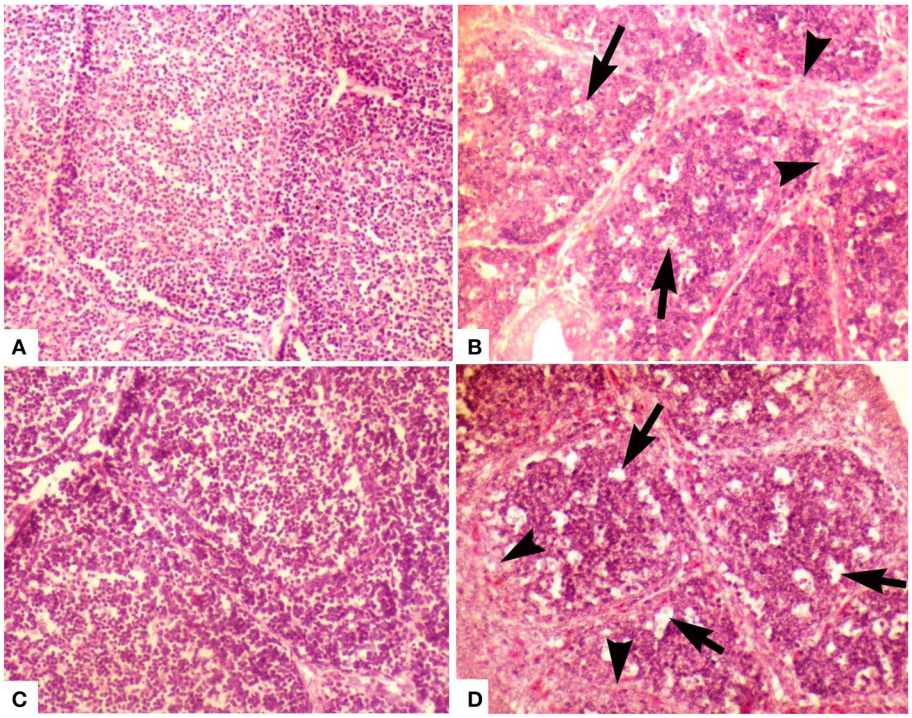

FIGURE 2
Photomicrograph of bursa of Fabricius of layer chicken on day 28. **(A)** Developed cortex and medulla (post-hatch vaccination group D), **(B)** (group A *in ovo* 228 E) and **(C)** showing demarcated cortex and medulla (group B) (*in ovo* Winterfield 2512: 10/3) (H&E staining at 200×) **(D)** (group C *in ovo* Winterfield 2512: 10/2.7) showing vacuolar degeneration (arrows), polymorphic cells in the medullary region and interfollicular connective tissue fibrosis (arrow heads).

present in medulla. Most of the cells present in medulla were small with thin rim of cytoplasm. In medulla, lesser fibroblasts and at some places, segmented cells and macrophages were seen more frequently than in group A (Figure 2C).

Group C (in ovo Winterfield 2512: 10/2.7)

At day 2, follicular size was variable being smaller in some parts of the bursal tissue while normal in other parts. Lesser pyknotic cells were observed as compared to group A suggesting necrosis in a few follicles. Empty spaces were seen in the follicles; however, the surface epithelium of the organ was found intact. Similar pattern was present day 28 (Figure 2D).

Group D (post-hatch Winterfield 2512/90: 10/2.7 eye drop vaccination)

At day 2, empty spaces in the medulla of the follicles were minimum compared with other groups. Medulla and cortex almost indistinguishably separated from each other by a very fine layer of cortical rim around the medulla. The connective tissue was lesser than that observed in group E. The surface epithelium of the bursa of Fabricius was found intact. The interfollicular connective tissue was thin even at day 28. There has been a clear demarcation of cortex and medulla. Medulla was denser than those of groups A, B, and C. Large cells (macrophages) were also present in the medullae; however, there was less fibroblast activity in medulla as compared to groups A and C (Figure 2A).

Group E (in ovo shamed control)

Some empty spaces were observed in the medullae of follicles. Medulla and cortex were almost indistinguishable, and a very fine layer of cortical rim formed around the medulla. The connective tissue was thinner than that observed in group F. The surface epithelium of the organ was intact. There was clearly demarcated cortex and medulla. Cortex and medulla were denser than the groups A, B, C, and D. In medulla, most of the cells were small with thin rim of visible cytoplasm, and some macrophages and fibroblasts were also observed.

Group F (control)

At day 2, medullary portion of bursal follicles exhibited least empty spaces. Interfollicular connective tissue was prominent. The epithelial folds on the surface of the organ were intact. All follicles showed larger medulla and a thin rim of cortical cells was surrounding it. At day 28, surface epithelium was intact. There was clearly demarcated cortex and medulla. Cortex and medulla were denser than those of groups A, B, C, and D. In medulla, most of the cells were small with thin rim of

TABLE 4 Lymphoproliferative response against PHA-P in White Leghorn chicks administered IBD live vaccines by *in ovo* and post-hatch (mean ± SD).

Group	PHA-P response (Skin thickness in mm)		
	24 h	48 h	72 h
Day 8			
A Nobilis Gumboro 228-E Intermediate plus strains (*In ovo* vaccination)	0.88 ± 0.07 a	0.83 ± 0.06 ab	0.75 ± 0.02 b
B Winterfield 2512: 10/3 Intermediate strain (*In ovo* vaccination)	0.82 ± 0.03 b	0.79 ± 0.03 b	0.76 ± 0.02 b
C Winterfield 2512/90: 10/2.7 Intermediate plus strains (*In ovo* vaccination)	0.90 ± 0.06 a	0.87 ± 0.07 a	0.83 ± 0.09 a
D Winterfield 2512/90: 10/2.7 Intermediate plus strains (Post-hatch vaccination)	0.08 ± 0.04 c	0.06 ± 0.03 c	0.04 ± 0.02 c
E Shamed control	0.08 ± 0.04 c	0.07 ± 0.04 c	0.05 ± 0.03 c
F Control	0.09 ± 0.03 c	0.06 ± 0.02 c	0.04 ± 0.02 c
Day 21			
A (228E)	0.56 ± 0.02 b	0.51 ± 0.03 b	0.44 ± 0.03 c
B Winterfield 2512: 10/3	0.57 ± 0.04 b	0.53 ± 0.05 b	0.50 ± 0.05 b
C Winterfield 2512/90: 10/2.7	0.56 ± 0.02 b	0.52 ± 0.02 b	0.45 ± 0.03 c
D Post-hatch vaccination	0.77 ± 0.04 a	0.67 ± 0.03 a	0.59 ± 0.05 a
E Shamed control	0.07 ± 0.01 c	0.04 ± 0.01 c	0.03 ± 0.01 d
F Control	0.08 ± 0.02 c	0.05 ± 0.02 c	0.03 ± 0.01 d

Values denoted by different alphabets in each column are significantly different ($p \leq 0.05$).

visible cytoplasm, and some macrophages and fibroblasts were also observed.

Cell-mediated immunity

Lymphoproliferative response to PHA-P as elicited by the thickness of skin at the site of injection has been presented in Table 4. At day 8 of age, it was significantly higher in groups A and C compared with control 24 h post-injection. The response was significantly lower in group B compared with groups A and C. The significantly lowest response was observed in groups D, E, and F. At 48 h post-injection, group B showed significantly lower response and all other groups showed similar trend as it was at 24 h. At 72 h post-injection, significantly higher response was observed in group C followed by groups A and B. At day 21 of age, response to PHA-P at 24 and 48 h post-injection was significantly higher in group D whereas groups A, B, and C showed significantly lower response from group D. The groups E and F showed significantly lower values than all other groups. At 72 h post-injection, significantly higher response was observed in group D followed by group B. The groups A and C showed significantly lower response from group B, whereas the groups E and F showed significantly lower response from all other groups.

TABLE 5 ELISA log_2 titers of the White Leghorn chicks administered live IBD vaccines *in ovo* and post-hatch (means ± SD).

Groups	ELISA log_2 Titers		
	Day 2	Day 17	Day 28
A 228E	10.98 ± 0.33 a	9.39 ± 0.13 a	8.06 ± 0.80 b
B Winterfield 2512: 10/3	10.97 ± 0.31 a	8.66 ± 0.70 a	7.94 ± 1.08 b
C Winterfield 2512/90: 10/2.7	10.86 ± 0.09 a	9.33 ± 0.75 a	8.36 ± 0.66 b
D Post-hatch vaccination	9.76 ± 0.224 b	8.83 ± 0.83 a	9.54 ± 0.61 a
E Shamed	9.93 ± 0.31 b	6.65 ± 0.48 b	6.95 ± 1.63 cd
F Control	9.85 ± 0.32 b	6.54 ± 0.79 b	6.74 ± 0.58 d

Values denoted by different alphabets in each column are significantly different ($p \leq 0.05$).

Humoral immunity

At day 2 of age, the White Leghorn (WLH) chicks showed significantly highest ELISA log_2 titers in groups A, B, and C while significantly lower in groups D, E, and F. At day 17 of age, the ELISA titers were significantly highest in groups A, B, C, and D whereas significantly lower titers were observed in groups E and F. At day 28 of age, significantly higher titers were observed in group D followed by groups A, B, and C compared with control (Table 5).

Absolute organ weights

The results of absolute organ weights results have been presented in Table 6. At day 2 of age, the White Leghorn chicks of groups A and C showed significantly highest absolute weight of bursa, followed by group B. The significantly lowest bursal weight was observed in groups D, E, and F. The thymus weight was significantly higher in groups A, B, and C whereas

TABLE 6 Absolute organ weights (mean ± SD) of the White Leghorn chicks administered live IBD vaccines *in ovo* and post-hatch.

Groups	Bursa of Fabricius	Thymus	Spleen
Day 2			
A	0.09 ± 0.01 ab	0.08 ± 0.01 a	0.041 ± 0.00 ab
B	0.08 ± 0.01 b	0.07 ± 0.01 a	0.043 ± 0.00 a
C	0.10 ± 0.01 a	0.08 ± 0.00 a	0.048 ± 0.01 a
D	0.03 ± 0.001 c	0.039 ± 0.001 b	0.026 ± 0.001 c
E	0.02 ± 0.00 c	0.04 ± 0.01 b	0.031 ± 0.00 bc
F	0.02 ± 0.00 c	0.04 ± 0.01 b	0.023 ± 0.00 c
Day 10			
A	0.24 ± 0.01 a	0.17 ± 0.02 ab	0.11 ± 0.02 a
B	0.21 ± 0.02 b	0.13 ± 0.02 bc	0.09 ± 0.02 b
C	0.25 ± 0.02 a	0.18 ± 0.02 a	0.06 ± 0.01 c
D	0.167 ± 0.03 c	0.120 ± 0.05 c	0.062 ± 0.01 c
E	0.15 ± 0.02 d	0.10 ± 0.01 c	0.09 ± 0.02 b
F	0.14 ± 0.02 e	0.09 ± 0.01 c	0.06 ± 0.01 c
Day 17			
A	0.57 ± 0.04 a	0.27 ± 0.02 a	0.15 ± 0.01 a
B	0.38 ± 0.03 b	0.24 ± 0.03a	0.12 ± 0.04 bc
C	0.53 ± 0.05 a	0.26 ± 0.03 a	0.14 ± 0.03 ab
D	0.58 ± 0.06 a	0.27 ± 0.04 a	0.15 ± 0.03 a
E	0.38 ± 0.02 b	0.19 ± 0.01 b	0.10 ± 0.01 bc
F	0.35 ± 0.03 b	0.18 ± 0.02b	0.09 ± 0.02 c
Day 28			
A	0.83 ± 0.04 b	0.87 ± 0.07 c	0.33 ± 0.02 b
B	0.83 ± 0.03 b	1.02 ± 0.04 b	0.34 ± 0.02 b
C	0.84 ± 0.09 b	0.98 ± 0.06 b	0.33 ± 0.02 b
D	1.10 ± 0.11 a	1.73 ± 0.05a	0.40 ± 0.06 a
E	0.603 ± 0.02 c	0.613 ± 0.07 d	0.273 ± 0.03 c
F	0.557 ± 0.03 c	0.60 ± 0.08 d	0.24 ± 0.02 c

Values denoted by different alphabets in each column are significantly different ($p \leq 0.05$).

TABLE 7 Relative organ weights (mean ± SD) of the White Leghorn chicks administered live IBD vaccines *in ovo* and post-hatch.

Groups	Bursa of Fabricius	Thymus	Spleen
Day 2			
A	0.23 ± 0.01 a	0.20 ± 0.02 a	0.11 ± 0.01 a
B	0.20 ± 0.01 b	0.18 ± 0.02 b	0.11 ± 0.02 a
C	0.24 ± 0.01 a	0.20 ± 0.01 a	0.12 ± 0.02 a
D	0.065 ± 0.01 c	0.096 ± 0.01 c	0.066 ± 0.02 c
E	0.06 ± 0.01 c	0.09 ± 0.01 c	0.08 ± 0.01 b
F	0.06 ± 0.01 c	0.09 ± 0.01 c	0.06 ± 0.02 c
Day 10			
A	0.39 ± 0.02 a	0.29 ± 0.04 a	0.18 ± 0.04 a
B	0.34 ± 0.01 b	0.22 ± 0.03 b	0.14 ± 0.03 ab
C	0.40 ± 0.01 a	0.30 ± 0.05 a	0.10 ± 0.03 c
D	0.290 ± 0.06 c	0.205 ± 0.07 b	0.107 ± 0.02 bc
E	0.25 ± 0.02 d	0.17 ± 0.02 b	0.15 ± 0.03 a
F	0.24 ± 0.02 d	0.17 ± 0.01 b	0.10 ± 0.01 c
Day 17			
A	0.53 ± 0.04 a	0.25 ± 0.03 a	0.14 ± 0.02 a
B	0.38 ± 0.01 b	0.24 ± 0.03 a	0.12 ± 0.04 ab
C	0.52 ± 0.01 a	0.25 ± 0.03 a	0.14 ± 0.03 a
D	0.55 ± 0.05 a	0.26 ± 0.05 a	0.14 ± 0.03 a
E	0.363 ± 0.05 bc	0.186 ± 0.02 b	0.098 ± 0.01 bc
F	0.33 ± 0.02 c	0.17 ± 0.01 b	0.09 ± 0.02 c
Day 28			
A	0.52 ± 0.02 b	0.54 ± 0.05 c	0.21 ± 0.01 b
B	0.51 ± 0.02 b	0.63 ± 0.03 b	0.21 ± 0.01 b
C	0.53 ± 0.05 b	0.63 ± 0.08 b	0.21 ± 0.02 b
D	0.69 ± 0.03 a	1.08 ± 0.08 a	0.25 ± 0.03 a
E	0.38 ± 0.03 c	0.38 ± 0.06 d	0.17 ± 0.02 c
F	0.36 ± 0.02 c	0.38 ± 0.07 d	0.15 ± 0.01 d

Values denoted by different alphabets in each column are significantly different ($p \leq 0.05$).

significantly lowest thymus weight was observed in groups D, E, and F. The absolute weight of spleen was significantly highest in groups A, B, and C followed by group E and significantly lowest was in groups D and E. At day 28, significantly highest weight of bursa was observed in group D, followed by groups A, B, and C. The significantly lowest bursal weights were observed in groups E and F. The absolute thymic weights were the highest in group D followed by groups B and C which were succeeded by group A. The significantly lowest thymic weight was observed in groups E and F. The absolute weight of spleen was significantly highest in group D followed by groups A, B, and C. The significantly lowest weight of spleen was observed in groups E and F.

Relative organ weight

The results of relative organ weights results have been presented in Table 7. The relative organ weights of WL chicks calculated at days 2, 10, and 17 of age showed that the relative weight of bursa and thymus was significantly higher in groups A and C followed by group B which was succeeded by significantly lowest groups D, E, and F. The relative weight of spleen was significantly the highest in groups A, B, and C compared with F. At day 28, the relative weight of bursa and thymus was significantly highest in group D, followed by groups A, B, and C in comparison with E and F. The relative weight of thymus was significantly the higher in group D, followed by groups B and C compared with groups E and F. The relative weight of spleen was significantly highest in group A followed by groups A, B, and C, which were succeeded by group E. The significantly lower relative splenic weights were observed in group F.

Bursa: Body weight index (BB index)

The results are presented in Table 8. The BB index of WL chicks at day 2 of age was significantly highest in groups A and C followed by group B whereas significantly lowest BB index was

TABLE 8 Bursa: Body weight index of the White Leghorn chicks administered live IBD vaccines *in ovo* and post-hatch period at days 2, 10, 17, and 28.

Groups	Bursa: body weight index			
	Day 2	Day 10	Day 17	Day 28
A (228E)	4.003 ± 0.21 a	1.656 ± 0.07 a	1.612 ± 0.11 a	1.441 ± 0.04 b
B (Winterfield 2512: 10/3)	3.542 ± 0.22 b	1.411 ± 0.06 b	1.160 ± 0.04 b	1.416 ± 0.04 b
C (Winterfield 2512/90: 10/2.7)	4.201 ± 0.26 a	1.681 ± 0.06 a	1.582 ± 0.03 a	1.481 ± 0.14 b
D (Post-hatch vaccination)	1.14 ± 0.14 c	1.21 ± 0.224 d	1.676 ± 0.15 a	1.907 ± 0.09 a
E (Shamed)	1.000 ± 0.09 c	1.053 ± 0.08 c	1.10 ± 0.152 b	1.05 ± 0.08 c

Values denoted by different alphabets in each column are significantly different ($p \leq 0.05$).

recorded in group D. At day 10 of age, BB index was significantly highest in groups A and C succeeded by group B followed by group E while significantly lowest BB index was recorded in group D. At day 17 of age, groups B and E showed significantly lower BB index whereas other groups showed significantly higher BB index which was non-significantly different among themselves. At day 28, group D showed significantly highest BB index followed by groups A, B, and C whereas group E showed significantly lowest BB index.

Histomorphometry of bursa of Fabricius

The histomorphometry of bursa of Fabricius at 2 day of age of birds showed significantly highest follicular diameter in group B, followed by groups D, E, and F, whereas significantly lowest follicular diameter was observed in groups A and C. The cortex diameter was significantly higher in group B and C compared with control group F. However, there was a non-significant difference among groups B and D, E, and F. The diameter of medulla was significantly higher in groups B and D, succeeded by groups E and F. The interfollicular tissue was significantly highest in groups A, C, D, and E as compared to control whereas significantly lower interfollicular connective tissue was observed in group B compared with control (Table 9).

At day 28, the follicular diameter was significantly higher in groups A and D whereas it was compared with control group F. The diameter of the cortex was significantly higher in groups A, B, D, and E as compared to control group whereas it was significantly lower in group C. The diameter of medulla was significantly higher in groups A and D in comparison with group F. The interfollicular connective tissue showed no significant difference among all groups.

Discussion

Infectious bursal disease is a highly contagious and immunosuppressive disease of economic importance for commercial poultry (8). Chickens of all breeds are susceptible to IBD; however, White Leghorn shows higher morbidity and mortality rate. Vaccination is the principle control strategy for IBD (3) and contributes to minimize the IBD-related losses. However, there is no vaccine and vaccination technique which could provide 100% protection. Hence, a rational and economically viable control strategy is required to culminate the disease (6).

In ovo vaccination of chick embryos is among contemporary vaccination strategies. The concept of this vaccination protocol is to stimulate the developing immune system in late embryonic life against probable IBDV challenge in post-hatch life. The *in ovo* vaccination reduces the cost of labor and can initiate primary immune response even in the presence of maternal antibodies (7, 25). Some studies suggested that there are few live vaccines used in post-hatch vaccination regimes which can be considered for *in ovo* administration without any detrimental effects on the survival of chicken embryos (26).

The results of this study revealed that all groups administered physiological saline or live vaccines *via in ovo* route produced hatchability percentage of 90.91, 93.75, 90.63, and 100% in groups A (intermediate plus strain; Nobilis Gumboro 228 E), B (intermediate strain; Winterfield 2512: 10/3), C (intermediate plus strain; Winterfield 2512/90:10/2.7), and E (shamed; physiological saline), respectively. This finding indicates that neither *in ovo* administration technique nor the post-hatch delivery of live IBD vaccines negatively affected the hatchability percentage or the survival of newly hatched chicks. Our findings are in line with the suggestions of Romao et al. (19) and Saeed et al. (27). However, the hatchability percentage in this experiment was higher than that of commercial hatcheries because all non-viable eggs were discarded at day 18 of incubation after candling as suggested by Moura et al. (28).

None of the vaccine treatment groups irrespective of vaccination method (whether *in ovo* or post-hatch vaccination) showed clinical presentation of disease. The results suggested that the birds, of which their embryos subjected to *in ovo* vaccination, did not undergo much stress to yield post-hatch clinical IBD. Similarly, Hedayati et al. (29) and De Wit et al. (25) reported no clinical signs or ailment in chicks administered *in ovo* IBD vaccines.

The body weights of the layer type chick vaccinated (*in ovo* or post-hatch vaccinated) with intermediate vaccinal strain (Winterfield 2512: 10/3), and intermediate plus strains (Nobilis Gumboro 228 E and Winterfield 2512/90:10/2.7) showed no significant differences from the control negative groups. Otsyina et al. (30) demonstrated no deleterious effect of intermediate plus vaccination of White Leghorn chicks upon body weights.

TABLE 9 Histomorphometery of bursa of Fabricius of the White Leghorn chicks administered live IBD vaccines *in ovo* and post-hatch period at days 2 and 28 of age.

Groups	Follicle diameter μm (mean ± SD)	Cortex diameter μm (mean ± SD)	Medulla diameter μm (mean ± SD)	Interfollicular connective tissue μm (mean ± SD)
Day 2				
A (228E)	99.62 ± 11.02c	10.03 ± 2.22b	79.55 ± 9.32c	10.03 ± 2.22ab
B (Winterfield 2512: 10/3)	144.77 ± 18.38a	12.18 ± 3.24ab	120.40 ± 12.16a	7.17 ± 3.51b
C (Winterfield 2512/90: 10/2.7)	100.33 ± 12.06c	15.05 ± 3.60a	70.23 ± 12.36c	11.47 ± 2.22a
D (Post-hatch vaccination)	126.85 ± 23.35b	10.03 ± 2.22b	106.78 ± 24.69ab	9.32 ± 3.24ab
E (Shamed)	123.27 ± 7.02b	11.47 ± 2.22b	100.33 ± 7.02b	7.88 ± 3.24ab
F (Control)	118.97 ± 12.66b	10.03 ± 2.22b	98.90 ± 9.02b	11.47 ± 2.22a
Day 28				
A (228E)	342.57 ± 46.29a	50.88 ± 20.43a	240.80 ± 21.07a	17.20 ± 3.85a
B (Winterfield 2512: 10/3)	255.13 ± 11.75b	31.53 ± 7.02ab	192.07 ± 16.01b	15.77 ± 3.51a
C (Winterfield 2512/90: 10/2.7)	229.33 ± 16.91b	25.80 ± 6.08b	177.73 ± 7.02b	16.48 ± 3.24a
D (Post-hatch Vaccination)	326.80 ± 69.87a	48.02 ± 17.07a	230.77 ± 44.66a	16.48 ± 4.23a
E (Shamed)	258 ± 39.60b	41.57 ± 18.78ab	174.87 ± 19.36b	16.48 ± 5.03a
F (Control)	260.15 ± 54.51b	42.28 ± 22.33ab	175.58 ± 21.49b	15.05 ± 3.60a

Values denoted by different alphabets in each column are significantly different ($p \leq 0.05$).

Similarly, Ashash et al. (7) and De Wit et al. (25) have shown that *in ovo* vaccination against IBD with live vaccines does not interfere with the body weights of the chickens.

The absolute and relative bursal weight in this study was significantly higher in chicks administered *in ovo* intermediate plus strains (Nobilis Gumboro 228 E and Winterfield 2512/90:10/2.7) than all other groups at day 2 and 10. On day 17, the highest bursal weight was recorded in chicks administered *in ovo* and intermediate plus strains (Nobilis Gumboro 228 E and Winterfield 2512/90:10/2.7) and the post-hatch vaccinated group. On day 28, the significantly highest bursal weight was recorded in chicks of post-hatch vaccinated group. These findings were contrary to the findings of Rautenschlein et al. (31) who reported a decrease in bursal weight of broiler chicks administered intermediate plus vaccine. A similar trend was observed in the relative weight of the broiler chicks administered *in ovo* intermediate plus vaccines. Different authors have shown decreased bursal weights in White Leghorn chicks administered intermediate plus vaccines (30). An absence of decrease in bursal weight of chicks administered intermediate plus vaccine by *in ovo* technique indicated that the negative effect of intermediate plus vaccine upon bursal weight was prevented and it could be helpful in the prevention of possible immunosuppression caused by these stronger vaccines.

The bursa showed minor histopathological changes in *in ovo* vaccinated groups. Similarly, the bursa of post-hatch vaccinated group showed mild lesions as investigated by Rautenschlein et al. (31) and Giambrone et al. (32).

The humoral immunity determined by ELISA showed that the IBD-specific antibody titers were significantly higher for *in ovo* vaccinated groups than control and shamed group at day 2 post-hatching, and similar observations have been reported by Corley et al. (9) and Coletti et al. (33), whereas at day 17, the antibody titers of all vaccinated groups (*in ovo* and post-hatch vaccinated) were showed significantly higher titers than control negative and shammed control groups; however, all vaccinated groups showed non-significant difference in titers among themselves. At day 28, the post-hatch vaccination group showed significantly highest antibody titers. In some recent studies, it has been determined that live vaccines of IBD do not interfere with the maternal antibodies of the commercial chicken in embryonic life or at early post-hatch vaccination; rather, the multiplication of live vaccine virus slows down due to unknown mechanisms (7, 25). Moreover, the mean titers in breeder flock were 9.5 (ELISA $\log_2$ titers). Despite the higher levels of maternal antibodies transferred to the experimental/ commercial flock, none of the vaccination method of vaccine strain's antibody titers seemed to be affected by breeders' antibody level in this study.

The cell-mediated immune response to PHA-P antigen at day 8 was statistically non-significant between both *in ovo* administered intermediate plus strains but were significantly higher than intermediate strain. While at day 21, the post-hatch vaccinated group showed significantly higher response to PHA-P antigen followed by a non-significant difference among *in ovo* vaccinated groups (irrespective of different levels of virulence of vaccinal strains). However, all vaccinated groups showed

significantly higher responses than control group. Sharma et al. (34), however, reported opposite results using the field isolates of IBDV. A reason for the difference in the present result and those of Sharma et al. (34) could be that they used field isolates of IBDV, which might be high in virulence compared to vaccinal strains used in the present study. The purpose of monitoring CMI using PHA-P assay was to assess whether there had been any kind of immunosuppression (in peripheral t-cell activity) in response to live IBD vaccines (especially intermediate and intermediate plus vaccines), which was not observed in this study.

Conclusion

From the results of this study, it might be concluded that *in ovo* vaccinating approach reduces the susceptibility period of chickens to field IBDV challenge and the birds' immune organs start getting functional even before hatching. In comparison with the post-hatch vaccination strategy, the *in ovo* vaccinated chickens not only develop humoral and cell-mediated immunity much earlier, but also the antibody induction is higher in birds vaccinated *via in ovo* route.

Data availability statement

The datasets presented in this article are not readily available because not applicable. Requests to access the datasets should be directed to dr.iqzaheer@gmail.com.

Ethics statement

The animal study was reviewed and approved by Institutional Bioethics Committee, University of Agriculture, Faisalabad.

Author contributions

IZ, AK, MS, and MK contributed to conception and design of the study. IZ and TZ organized the database. IZ performed the statistical analysis. IZ and MK wrote the first draft of the manuscript. IZ, MS, TZ, AE, and WC wrote sections of the manuscript. WC and AE were partial funding collaborators in this project. All authors contributed to manuscript revision, read, and approved the submitted version.

Funding

This work was supported by the National Key Research and Development Program (Grant Nos. 2018YFE0128200 and 2021YFD1300405), Fund for China Agricultural Research System (CARS-42-13), Modern Agricultural Industry Technology System Innovation Team of Guangdong Province (2019KJ137), Key Project of the Science and Technology Program of Guangzhou City (Grant No. 2019A050505007), Foreign Expert Project (QNL20200130001), the Science and Technology Program of Guangdong Province (2021A0505050003), Special Fund for Scientific Innovation Strategy-Construction of High Level Academy of Agriculture Science (R2020PY-JX008), and the Science and Technology Program of Guangdong Academy of Agricultural Sciences (202106TD), opening project for State Key Laboratory of Livestock and Poultry Breeding (2021GZ06).

Conflict of interest

The authors declare that the research was conducted in the absence of any commercial or financial relationships that could be construed as a potential conflict of interest.

Publisher's note

References

1. Lin X, Mohsin M, Abbas RZ, Li L, Chen H, Huang C, et al. Evaluation of immunogenicity and protective efficacy of Eimeria maxima immune mapped protein 1 with EDA adjuvant in chicken. *Pak Vet J.* (2020) 40:209–13. doi: 10.29261/pakvetj/2020.043

2. Ali M, Khan MUR, Aslam A, Rehman HU, Masood S, Masood A, et al. Comparative molecular characterization and pathogenicity of H9N2 avian influenza virus in commercial poultry flocks in Pakistan. *Pak Vet J.* (2021) 41:451–5. doi: 10.29261/pakvetj/2021.047

3. Eterradossi YMS. Infectious bursal disease. In: Swayne DE, editor. *Diseases of poultry. 14th ed.* New York: Wiley Blackwell (2020). p. 257–83. doi: 10.1002/9781119371199.ch7

4. Ma J, Yu Y, Zhang H, Mo H, Ou C, Wang X, et al. Over-expression of Rab1 gene during infectious bursal disease virus infection in layer chicken. *Pak Vet J.* (2016) 36:73–6.

5. Van Den Berg TP, Eterradossi N, Toquin D, Meulemans G. Infectious bursal disease (Gumboro disease). *Rev Sci Tech OIE.* (2000) 19:527–43. doi: 10.20506/rst.19.2.1227

6. Van den Berg TP. Acute infectious bursal disease in poultry: a review. *Avian Pathol.* (2000) 29:175–94. doi: 10.1080/03079450050045431

7. Ashash U, Noach C, Perelman B, Costello C, Sansalone P, Brazil T, et al. In ovo and day of hatch application of a live infectious bursal

disease virus vaccine to commercial broilers. *Avian Dis.* (2019) 63:713–20. doi: 10.1637/aviandiseases-D-19-00087

8. Saeed NM. Sequence analysis and comparison of infectious bursal disease virus affecting indigenous kurdish breed and broiler chickens in Sulaymaniyah, Kurdistan Region of Iraq. *Pak Vet J.* (2021) 41:249–53. doi: 10.29261/pakvetj/2021.017

9. Corley MM, Giambrone JJ, Dormitorio TV. Detection of infectious bursal disease vaccine viruses in lymphoid tissues after in ovo vaccination of specific-pathogen-free embryos. *Avian Dis.* (2001) 45:897–905. doi: 10.2307/1592869

10. Shah MU, Aslam A, Mustafa G, Zahid B, Imran MS. Effect of mentofin and asimirus on humoral immune response and tissue changes in infectious bursal disease vaccinated broiler birds. *Pak Vet J.* (2018) 38:56–60. doi: 10.29261/pakvetj/2018.011

11. Sharma JM, Burmester BR. Resistance of Marek's disease at hatching in chickens vaccinated as embryos with the turkey herpesvirus. *Avian Dis.* (1982) 26:134–49. doi: 10.2307/1590032

12. Sharma JM. Embryo Vaccination with infectious bursal disease virus alone or in combination with marek's disease vaccine. *Avian Dis.* (1985) 29:1155–69. doi: 10.2307/1590469

13. Negash T, Al-Garib SO, Gruys E. Comparison of in ovo and post-hatch vaccination with particular reference to infectious bursal disease, a review. *Vet Q.* (2004) 26:76–87. doi: 10.1080/01652176.2004.9695170

14. Yeh HY, Rautenschlein S, Sharma JM. Protective immunity against infectious bursal disease virus in chickens in the absence of virus-specific antibodies. *Vet Immunol Immunopathol.* (2002) 89:149–58. doi: 10.1016/S0165-2427(02)00206-4

15. Muller R, Weiss IK, Reinacher M, Weiss E. Immunofluorescence studies of early virus propagation after oral infection with infectious bursal disease virus (IBDV). *Zentralbl Veterinarmed B.* (1979) 26:345–52. doi: 10.1111/j.1439-0450.1979.tb00823.x

16. Khatri M, Sharma JM. Response of embryonic chicken lymphoid cells to infectious bursal disease virus. *Vet Immunol Immunopathol.* (2009) 127:316–24. doi: 10.1016/j.vetimm.2008.10.327

17. McCarty JE, Brown TP, Giambrone JJ. Delay of infectious bursal disease virus infection by *in ovo* vaccination of antibody-positive chicken eggs. *J Appl Poult Res.* (2005) 14:136–40. doi: 10.1093/japr/14.1.136

18. Senne DA. Virus propagation inembryonating eggs. In: Swayne DE, Glisson JR, Jackwood MW, Pearson JE, Reed WM, editor. *Laboratory Manual for The Isolation and Identification of Avian Pathogens. 4th Ed.* American association of avian pathologists. Pennsylvannia: Kennett Square (1998). p. 235–40.

19. Romao JM, de Moraes TV, Salles RR, Cardoso WM, Buxade CC. Effect of in ovo vaccination procedures on japanese quail embryos (*Coturnix japonica*) and incubation performance. *Ci Anim Bras.* (2001) 12:584–92. doi: 10.5216/cab.v12i4.5234

20. Kim IJ, Gagic M, Sharma JM. Recovery of antibody producing ability and lymphocyte repopulation of bursal follicles in chickens exposed to infectious bursal disease virus. *Avian Dis.* (1999) 43:401–13. doi: 10.2307/1592637

21. Sultana R, Hussain SA, Ilyas S, Ch A, Anjum R, Zaidi FH. Epidemiology of infectious bursal disease in broiler and layer flocks in and around Lahore, Pakistan. *Punjab Univ J Zool.* (2008) 23:067–72.

22. Bancroft JD, Gamble M. *Theory and Practise of Histological Techniques. 5th ed.* London: Churchill Livingstone (2008).

23. Ul-Hassan Z, Zargham Khan M, Khan A, Javed I. Immunological status of the progeny of breeder hens kept on ochratoxin A (OTA)- contaminated diet. *J Immunotoxicol.* (2011) 8:122–30. doi: 10.3109/1547691X.2010.547886

24. Thangavelu A, Raj AGD, Elankumaran S, Manohar BM, Koteeswaran A, Venugopalan AT, et al. Pathogenicity and immunosuppressive properties of infectious bursal disease virus field isolates and commercial vaccines In India. *Trop Anim Health Prod.* (1998) 30:167–76. doi: 10.1023/A:1005059619825

25. de Wit JJ, Jorna I, Finger A, Loeb V, Dijkman R, Ashash U, et al. *In ovo* application of a live infectious bursal disease vaccine to commercial broilers confers proper immunity. *Avian Pathol.* (2021) 50:531–9. doi: 10.1080/03079457.2021.1986618

26. Mast J, Meulemans G. *Attenuated mutant Newcastle disease virus strains for in ovo vaccination, method for preparing and their use.* European Patent WO 03/030932 Al (2003).

27. Saeed M, Babazadeh D, Naveed M, Alagawany M, Abd El-Hack ME, Arain MA, et al. In ovo delivery of various biological supplements, vaccines and drugs in poultry: current knowledge. *J Sci Food Agric.* (2019) 99:3727–39. doi: 10.1002/jsfa.9593

28. Moura L, Vakharia V, Liu M, Song H. *In ovo* vaccine against infectious bursal disease. *Int J Poult Sci.* (2007) 6:770–5. doi: 10.3923/ijps.2007.770.775

29. Hedayati A, Nili H, Bahonar A. Comparison of pathogenicity and serologic response of four commercial infectious bursal disease live vaccines. *Arch Razi Inst.* (2005) 59:65–73. doi: 10.22092/ARI.2005.103814

30. Otsyina HR, Anim JA, Aning KG. Protective efficacy of commercial live vaccines against very virulent infectious Bursal disease virus (vvIBDV) in Ghana. *Vet Med Anim Health.* (2009) 1:023–7.

31. Rautenschlein S, Kraemer CH, Vanmarcke J, Montiel E. Protective efficacy of intermediate and intermediate plus infectious bursal disease virus (IBDV) vaccines against very virulent IBDV in commercial broilers. *Avian Dis.* (2005) 49:231–7. doi: 10.1637/7310-112204R

32. Giambrone JJ, Dormitorio T, Brown T. Safety and efficacy of in ovo administration of infectious bursal disease viral vaccines. *Avian Dis.* (2001) 45:144–8. doi: 10.2307/1593021

33. Coletti M, Del Rossi E, Franciosini MP, Passamonti F, Tacconi G, Marini C. Efficacy and safety of an infectious bursal disease virus intermediate vaccine in ovo. *Avian Dis.* (2001) 45:1036–43. doi: 10.2307/1592885

34. Sharma JM, Dohms JE, Metz AL. Comparative pathogenesis of serotype 1 and variant serotype 1 isolates of infectious bursal disease virus and their effect on humoral and cellular immune competence of specific-pathogen-free chickens. *Avian Dis.* (1989) 33:112–24. doi: 10.2307/1591076

frontiers | Frontiers in Veterinary Science

TYPE Original Research
PUBLISHED 08 August 2022
DOI 10.3389/fvets.2022.938822

OPEN ACCESS

EDITED BY
Kun Li,
Nanjing Agricultural University, China

REVIEWED BY
Xiaojian Gao,
Yangzhou University, China
Xinyu Zhu,
Duke University, United States

*CORRESPONDENCE
Huanying Pang
phying1218@163.com

SPECIALTY SECTION
This article was submitted to Veterinary Infectious Diseases, a section of the journal Frontiers in Veterinary Science

RECEIVED 08 May 2022
ACCEPTED 14 July 2022
PUBLISHED 08 August 2022

CITATION
Zhang W, Chen L, Feng H, Wang J, Zeng F, Xiao X, Jian J, Wang N and Pang H (2022) Functional characterization of *Vibrio alginolyticus* T3SS regulator ExsA and evaluation of its mutant as a live attenuated vaccine candidate in zebrafish (*Danio rerio*) model. *Front. Vet. Sci.* 9:938822. doi: 10.3389/fvets.2022.938822

Functional characterization of *Vibrio alginolyticus* T3SS regulator ExsA and evaluation of its mutant as a live attenuated vaccine candidate in zebrafish (*Danio rerio*) model

Weijie Zhang[1,2], Liangchuan Chen[1,2], Haiyun Feng[1,2], Junlin Wang[1,2], Fuyuan Zeng[1,2], Xing Xiao[1,2], Jichang Jian[1,2], Na Wang[3] and Huanying Pang[1,2]*

[1]Fisheries College, Guangdong Ocean University, Zhanjiang, China, [2]Guangdong Provincial Key Laboratory of Aquatic Animal Disease Control and Healthy Culture & Key Laboratory of Control for Diseases of Aquatic Economic Animals of Guangdong Higher Education Institutes, Zhanjiang, China, [3]Chinese Academy of Inspection and Quarantine, Beijing, China

Vibrio alginolyticus, a Gram-negative bacterium, is an opportunistic pathogen of both marine animals and humans, resulting in significant losses in the aquaculture industry. Type III secretion system (T3SS) is a crucial virulence mechanism of *V. alginolyticus*. In this study, the T3SS regulatory gene *exsA*, which was cloned from *V. alginolyticus* wild-type strain HY9901, is 861 bp encoding a protein of 286 amino acids. The Δ*exsA* was constructed by homologous recombination and Overlap-PCR. Although there was no difference in growth between HY9901 and Δ*exsA*, the Δ*exsA* exhibited significantly decreased extracellular protease activity and biofilm formation. Besides, the Δ*exsA* showed a weakened swarming phenotype and an ∼100-fold decrease in virulence to zebrafish. Antibiotic susceptibility testing showed the HY9901Δ*exsA* was more sensitive to kanamycin, minocycline, tetracycline, gentamicin, doxycycline and neomycin. Compared to HY9901 there were 541 up-regulated genes and 663 down-regulated genes in Δ*exsA*, screened by transcriptome sequencing. qRT-PCR and β-galactosidase reporter assays were used to analyze the transcription levels of *hop* gene revealing that *exsA* gene could facilitate the expression of *hop* gene. Finally, *Danio rerio*, vaccinated with Δ*exsA* through intramuscular injection, induced a relative percent survival (RPS) value of 66.7% after challenging with HY9901 wild type strain. qRT-PCR assays showed that vaccination with Δ*exsA* increased the expression of immune-related genes, including *GATA-1*, *IL6*, *IgM*, and *TNF-α* in zebrafish. In summary, these results demonstrate the importance of *exsA* in *V. alginolyticus* and provide a basis for further investigations into the virulence and infection mechanism.

KEYWORDS

type III secretory system, characteristics, live attenuated vaccine, *Vibrio alginolyticus*, *exsA* gene

Introduction

Vibrio alginolyticus, which is a gram-negative halophilic bacterium, is diffusely distributed in nature occurring in both fresh and saltwater (1, 2). Obviously, Vibriosis disease outbreaks cause significant setbacks to aquaculture. *V. alginolyticus* was considered a serious pathogenic bacterium for many marine vertebrates, including cultured fish species such as turbot, *Larimichthys crocea*, grouper, as well as invertebrates, such as shrimp and shellfish (3, 4). It is also a zoonotic bacterium that can cause food poisoning in humans, including diarrheal and septicemia (5). Antibiotic treatment is the traditional measure used to treat *V. alginolyticus* infections, and this is considered a serious concern for the escalation of antibiotic resistant Vibrios (6). Hence, it is imperative to achieve a better understanding of the pathogenic mechanisms of *V. alginolyticus* to facilitate the discovery of more effective therapies.

Type III secretion system (T3SS) plays an important role in pathogenic process, and its structural components are highly conserved among bacterial species (7–9). ExsA, as is a member of the AraC/XylS family of DNA-binding proteins, is the main transcriptional activator of T3SS gene expression (10). And A previous study showed that the expression of ∼40 gene products constituting the T3SS was regulated by 10 ExsA-dependent promoters (11). Qu et al. (12) showed that deletion of *exsA* suppressed the production of T3SS pilus (PopB/D) and effector protein (ExoT/U) in *Pseudomonas aeruginosa*. Moreover, T3SS1 expression in *V. parahaemolyticus* is genetically regulated by the ExsACDE cascade in which the master transcription factor ExsA positively regulates T3SS1 expression (13, 14). Zhou speculated that ExsA could act directly on the T3SS1 promoter sequence in view of the result that ExsA can bind the upstream region of VP1668 and VP1687 (15). To summarize, the ExsA protein exhibits significant functions during many Gram-negative bacteria pathogenesis.

When *V. alginolyticus* infects the host cell, it secretes effector proteins through T3SS, thus subverting host cellular functions and resulting in cell death (16). HopPmaJ, as a type III system effector (T3SE), is considered an important virulence factor in *V. alginolyticus*. Pang et al. (17) found HopPmaJ encoded by *hop* gene in *V. alginolyticus* is pathogenic to the orange-spotted grouper (*Epinephelus coioides*), which exhibits symptoms of ulceration, hemorrhage of liver and kidney, and swelling. Furthermore, a later study revealed that regulatory protein TyeA could up-regulated the expression of HopPmaj (18). While the T3SS is highly conserved, the regulators are unique proteins with very specialized functions critical to virulence. It was reported that T3SS of *V. alginolyticus* is similar to T3SS1 of *Vibrio* parahaemolyticus in genome analysis (19), but the regulator ExsA in *V. alginolyticus* T3SS remains poorly understood.

To better understand the function of ExsA in the *V. alginolyticus* T3SS, we constructed a HY9901Δ*exsA* mutant strain, and then studied the physiology and pathogenicity of HY9901Δ*exsA*. Besides, the differentially expressed genes between HY9901 and HY9901Δ*exsA* were investigated by transcriptome sequencing. Furthermore, we have evaluated the protective efficacy of Δ*exsA*, and found that the Δ*exsA* mutant could be used as a live attenuated vaccine to combat *V. alginolyticus* in zebrafish.

Materials and methods

Bacterial strains, experimental fish and plasmid

In this study, *V. alginolyticus* HY9901 was isolated from diseased red snapper (*Lutjanus sanguineus*) (20). *E. coli* S17-1 (λ Pir) and suicide plasmid pDM4 were kept in our laboratory (Table 1).

Experimental fish

Healthy zebrafish (*Danio rerio*) were purchased from a commercial fish farm in Guangzhou, China, 3–4 cm long and 0.3 g in weight. The zebrafish were tested by the bacterial recovery assay, kept in freshwater in the circulatory system at 28°C for 2 weeks before the experiment.

Reagents and primers

TIANamp Bacteria DNAKit (Beijing, Tiangen Biotech Co., Ltd.); Easy PureTMQuick GelExtraction Kit and Easy PureTMPlasmid MiniPrepKit (Beijing, TransGen Biotech Co., Ltd.); pDM4 vector, ExTaqDNA polymerase, Prime START MHS DNA polymerase, BglII, SalI, and T4DNA ligase were all purchased from TaKaRa (Japan). The primers were synthesized by Guangzhou Sangon Biotech Co., Ltd.

Cloning and sequencing of the *exsA* gene from *V. alginolyticus* HY9901

A pair of primers *exaA*-F/*exsA*-R were designed based on the *V. alginolyticus* gene sequence (GenBank Number: GU074526.1) (Table 2). PCR was performed according to the previous study of Zhou et al. (18). PCR products were run on 1.5% agarose gels, visualized with ethidium bromide. Then, the recovered PCR products were cloned into the pMD18-T vector, and transformed into *E. coli* DH5α (Table 1). The inserted fragment was sequenced by Sangon Biological Engineering Technology & Services Co., Ltd. (Guangzhou, China). The similarity analyses were based on the method of Pang et al. (22).

TABLE 1 Bacterial strains and plasmids used in this study.

Strains and primers	Relevant characteristics	Source
V.alginolyticus HY9901	Isolated from diseased red snapper (*Lutjanus sanguineus*)	(20)
Δ*exsA*	*exsA* deletion mutant; Apr	This study
E. coli DH5α	supE44 1lacU169 (ϕ80 lacZDM15) hsdR17 recA1 gyrA96 thi-1 relA1	TakaRa
S17-1λpir	T prSmrrecA thi pro hsdR-M+RP4:2-Tc: Mu: K m T n7λpir	(18)
pDM4	A suicide vector with ori R6K sacB; Cmr	(21)
pDM4_exsA_A1F +A2R	Flanking region sequences of exsA cloned into pDM4	This study
pME6522-*hop–lacZ*	Promoter sequences of hop cloned into pME6522	This study
S17-*hop*–lacZ	S17 carrying pME6522-hop–lacZ	This study
hop–lacZ: Δ*exsA*	Promoter sequences of hop was inserted in the upstream of lacZ gene in Δ*exsA* strain	This study
hop–lacZ: HY9901	Promoter sequences of hop was inserted in the upstream of lacZ gene in HY9901 strain	This study

Construction of in-frame deletion mutant of *exsA* gene

The in-frame deletion of *exsA* in the *V. alginolyticus* was generated according to the previous study (23). For the construction of Δ*exsA*, two pairs of primers were firstly designed to obtain the *exsA* upstream homologous arm fragment A (Primers: *exsA*-A1-F and *exsA*-A1-R) and downstream homologous arm fragment B (Primers: *exsA*-A2-F and *exsA*-A2-R). Both fragments contained a 10 bp overlapping sequence and were used as templates for the subsequent PCR procedure, which used primers *exsA*-A1-F and *exsA*-A1-R. The PCR product was ligated into suicide vector pMD4 to generate pMD4-Δ*exsA*. Then, the recombinant suicide plasmid was used to transform into *E. coli* S17-1. The single crossover mutants were acquired by transferring the resulting plasmid directly into *V. alginolyticus* HY9901. Ten percentage sucrose TSA plates were used to select the deletion mutants. HY9901Δ*exsA* was subsequently confirmed by PCR and sequencing using primers *exsA*-F and *exsA*-R.

Characterization of the Δ*exsA*

The Δ*exsA* phenotype characterized by growth, genetic stability, extracellular protease (ECPase) activity, swarming motility and biofilm Formation. The experimental method of genetic stability was based on previous studies our research group undertook (18). In brief, ΔexsA were seeded into a Tryptic Soya agar (TSA) plate, passed randomly for 30 generations. Its genetic stability was determined by PCR. Growth curves were determined using the method of Wu et al. (24). Extracellular protease activity assay was performed referring to Windle and Kelleher (25). HY9901 and Δ*exsA* were inoculated onto TSA plates coated with sterile cellophane, and then cultured at 28°C for 24 h, washed with PBS, centrifuged at low temperatrue for 30 min, and filtered the supernatant using a 0.22 μm porous membrane. The protease activity of the supernatant was measured at OD_{442} using an azocasein trichloroacetic acid colorimetric assay solution.

Biofilm formation was measured with the method of Zhou et al. (18). Swarming motility was assayed according to the previous method described by Mathew et al. (26). LD_{50} of HY9901 and Δ*exsA* were assessed by the previous study of Chen et al. (27). In brief, a total of 330 fish were blindly separated into three groups. The zebrafish in experimental group were injected with 5 μL HY9901 and Δ*exsA* suspended in PBS containing 10^4-10^8 CFU/mL, while negative control group was injected with 5 μL of PBS. Fish were monitored for 14 days or until no morbidities occurred, and LD_{50} of HY9901 and Δ*exsA* was calculated. All experiments were carried out triplicate.

Antibiotic susceptibility testing was performed. Briefly, HY9901 and Δ*exsA* were seeded into TSA plates, and then 30 different antibiotics disks were respectly added into the plates. The plates were incubated for 16 h at 28°C and the diameters of the inhibition zones were measured by Vernier calipers. All experiments were carried out triplicate.

Transcriptome sequencing

With reference to the method described previously (22), HY9901 and Δ*exsA* cells were cultured in DMEM media at 28°C. The bacterial cells were harvested after 12 h. The series of experiments, including mRNA extraction, RNA fragmentation, cDNA synthesis and RNA-Seq library construction, were conducted by Novogene Co., Ltd. The data generated from the Illumina platform were used for bioinformatics analysis using I-Sanger Cloud Platform (www.i-sanger.com). Besides, the GO terms of the different expression genes were analyzed with the Goatools tool (EMBL, European Molecular Biology Laboratory).

TABLE 2 Sequences of primers used in this study.

Primer name	Primer sequence (5′-3′)	Accession number
ExsA-A1-F	TGAAGATCTTATCTCGCTCCTTGAACAC	This study
ExsA-A1-R	TAGCCACTTGTTTCTACCCTTCATTATTTTGA	
ExsA-A2-F	AGGGTAGAAACAAGTGGCTATCGCGAAATGAA	This study
ExsA-A2-R	AGCGTCGACCAGACGAGAGTTGATGTAGT	
ExsA-F	ATGGATGTGTCAGGCCAACTA	This study
ExsA-R	TCATTTCGCGATAGCCACTTG	
TNF-α-F	TAGAACAACCCAGCAAAC	NC_007130.7
TNF-α-R	ACCAGCGGTAAAGGCAAC	
IL-6-F	GGTCAGACTGAATCGGAGCG	NM_001079833.1
IL-6-R	CAGCCATGTGGCGAACG	
IL-1β-F	TGGACTTCGCAGCACAAAATG	AY340959.1
IL-1β-R	GTTCACTTCACGCTCTTGGATG	
IgM-F	GTTCCTGACCAGTGCAGAGA	AF246193
IgM-R	CCTGATCACCTCCAGCATAA	
TLR5-F	GAAACATTCACCTGGCACA	NC_007131.7
TLR5-R	CTACAACCAGCACCACCAGAATG	
IL-8-F	GTCGCTGCATTGAAACAGAA	XM_001342570.2
IL-8-R	CTTAACCCATGGAGCAGAGG	
IL-6R-F	GCATGTGCTTAAAGTATCCTGGTC	NM_001114318.1
IL-6R-R	TGCAAATTGTGGTCGGTATCTC	
c/ebpβ-F	GCCGTACCAGACTGCTCCGA	NC_007119.7
c/ebpβ-R	AGCCGCTTCTTGCCTTTCCC	
Gata-1-F	GCCTGATAAACTGAATTTAGTA	NC_007122.7
Gata-1-R	GTCGTGCAAAAGAATTATGTGA	
β-actin-F	ATGGATGAGGAAATCGCTGCC	NM_131031.1
β-actin-R	CTCCCTGATGTCTGGGTCGTC	
hop-F	CTTCGCTTTCGGTTTGCT	KX245315
hop-R	AATACCATCCCACCCTGT	
16S-F	TTGCGAGAGTGAGCGAATCC	NR_044825.2
16S-R	ATGGTGTGACGGGCGGTGTG	
q-CheA-F	CCGCAGTTACCACATCAAGG	This study
q-CheA-R	GCCAGAATCTAAACCAGTCGC	
q-FlaE-F	GTTTGCTTGGTAGTTGCGTTGT	This study
q-FlaE-R	GGCTTAGCGAAAGTGAGTGGA	
q-FlaG-F	AATCGTCACCACATCTCGTCC	This study
q-FlaG-R	AAAGCCGTCAAGAACTGAACAA	
q-FliN-F	GCCGTGAGCAATCAAAGTACC	This study
q-FliN-R	GCGAAGATGAGCGTCGTAAA	
q-FliS-F	TGTCCAAAATTCATCCAACC	This study
q-FliS-R	GGAAAACCTACGCCAGCT	
q-CysN-F	TAATCGGTCGCTTACTCCAT	This study
q-CysN-R	GCAAGGTCGGGCTTTTCA	
q-KdsA-F	ATCGTTGAGAAGTTCGCAGAG	This study
q-KdsA-R	GATGGGTCACGCATTTGTAGT	
q-MinD-F	ACGGCTTGGCTTTCTGGA	This study
q-MinD-R	CGTGACTCTGACCGCATTCT	

Validation of transcriptome data

qRT-PCR was used to validate the different expression genes obtained from transcriptome analysis. The related-gene primers sequences were tabulated in Table 2. Besides, the 16 s rRNA gene was used as the internal reference. RNA was extracted, synthetic cDNA and real-time PCR was based on the method of previous study (28).

hop gene expression analysis

Detection of HopPmaJ mRNA expression by qRT-PCR after deletion of *exsA* gene

In order to facilitate T3SS secretion, HY9901 and HY9901Δ*exsA* were cultured in DMEM media for 16 h. The primers for *hop* are shown in Table 2. 16S rRNA is used as an internal reference. RNA was extracted, synthetic cDNA and real-time PCR was based on the method of previous study (28).

β-galactosidase reporter assay

The β-galactosidase reporter assay was carried out as previously described (29). In brief, the recombinant plasmid PME6522 containing the promoter region of *hop* was introduced to HY9901 and HY9901Δ*exsA*, and a LacZ reporter assay was employed to measure the activity and regulation of promoters. The recombinant plasmid PME6522 and related-gene primers are, respectively, shown in Tables 1, 2. The experiments were carried out triplicate.

Vaccination

The concentration of Δ*exsA* in LD_{50} experiment is 10^5 cfu/mL, which is not lethal to zebrafish (Table 3). Vaccination was undertaken according to Zhou et al. (18). Briefly, zebrafish were randomly separated into two groups with 80 fish per group. The water temperature was adjusted to 28°C.Fish in the Δ*exsA* group were injected with 5 μL Δ*exsA* bacterial solution (10^5 cfu/mL), while control fish were injected with 5 μL PBS. The experiment was repeated three times.

Vaccine safety evaluation

The number of HY9901Δ*exsA* in livers and spleens of selected from three fish in HY9901Δ*exsA* group were investigated to further assess safety of live attenuated HY9901Δ*exsA* vaccine. Briefly, fish were weighed and euthanized to sample liver and spleen once daily for seven consecutive days. All the samples were weighed, homogenized in 1 mL of sterile PBS. The homogenates were diluted serially and spread on TCBS plates, and the plates were incubated at 28°C for 16 h. Colony numbers were counted visually and colonies measuring at least 50 μm were counted. The bacteria counts were calculated by dividing the weights of the tissues and from the mean of three samples. Besides, the identities of the HY9901Δ*exsA* isolates were confirmed by colonial morphology and PCR.

Immune-related gene of zebrafish expression analysis

Briefly, liver and spleen samples were taken from three fish from each group, respectively, at 1 day before the challenge. The expression levels of immune-related genes were determined by qRT-PCR. Primers are shown in Table 2, and β-actin was used as internal reference. Detailed experimental steps refer to the previous study of Li et al. (28).

Routine H&E stained sections were analyzed for histopathology

To evaluate the safety of the Δ*exsA* vaccines, livers and spleens of selected from three fish from each group were fixed in neutral buffered 10% formalin, embedded in paraffin and processed for routine histopathological examination. Detailed experimental steps refer to our previous study (30).

Challenge experiment

Fish were challenged 28 days post vaccination. zebrafish ($n = 30$) were given intramuscular injection of 5 μL 1×10^8 cfu mL^{-1} of *V. alginolyticus* HY9901. The relative percent survival (RPS) of post-challgenged fishes were measured per day in a 14-day time frame. The experiment was repeated three times.

Statistical analyses

Statistical analyses were conducted using SPSS 17.0 (SPSS Inc., USA). The statistical significance of differences between the wild-type strain and Δ*exsA* mutant, were determined using the Student's *t*-test. Group differences were determined by Duncan's test. Data was considered statistically significant when $p < 0.05$.

Ethics statement

All animal experiments were conducted strictly based on the recommendations in the "Guide for the Care and

TABLE 3 Experiment of LD_{50}.

Concentration (CFU/mL)	HY9901	Mortality rate (%)	Δ*exsA*	Mortality rate (%)	Control (PBS)	Mortality rate (%)
10^8	10 × 3	90	10 × 3	50	–	
10^7	10 × 3	80	10 × 3	40	–	
10^6	10 × 3	60	10 × 3	10	–	
10^5	10 × 3	20	10 × 3	0	–	
10^4	10 × 3	20	10 × 3	0	–	
0 (PBS)	–		–		10 × 3	0

Use of Laboratory Animals" set by the National Institutes of Health. The animal protocols were approved by the Animal Ethics Committee of Guangdong Ocean University (Zhanjiang, China).

Biosecurity

The bacteria protocols were approved by the Biosecurity Committee of Guangdong Ocean University (Zhanjiang, China).

Results

Cloning of *exsA* gene and construction of mutant

The exsA gene is 861 bp long, and encodes 286 amino acids (aa) with a predicted molecular weight of 32.549 kDa and a theoretical isoelectric point of 6.0 (*exsA* accession no. MN385414) (Figures 1A,B). To understand the potential function of ExsA in *V. alginolyticus*, an untagged in-frame deletion mutant strain HY9901Δ*exsA* was constructed by Overlap PCR and a dual selection strategy. HY9901 was determined by PCR by generating a fragment of 1,811 bp, while Δ*exsA* was determined by PCR by generating a fragment of 1,019 bp (Figure 2).

Characterization of the *exsA*

HY9901Δ*exsA* was genetically stable

After 30 generations of continuous blind transmission of HY9901Δ*exsA*, the *PCR* genome of HY9901Δ*exsA* and wild-type strain HY9901 using primers ExsA-F/ExsA-R, a fragment of 861 bp was obtained for HY9901, while Δ *exsA* is negative. This result indicates that Δ*esxA* has deleted the gene *esxA*, which can stabilize the inheritance (Figure 3A).

HY9901 and HY9901Δ*exsA* did not differ for growing

There were no significant differences in growth rates between wild-type strain HY9901 and HY9901Δ*exsA* ($p > 0.05$). The exponential growth phase of the two bacterial strains was from 0 to 4 h, with growth stationary at 16 h, $OD_{600} \approx 1.8$ (Figure 3B).

The *exsA* is a positive contributor to extracellular protease activity

ECP is a crucial virulence factor, and have a variety of protease activities. After deletion of *exsA* gene, the extracellular protease activity of Δ*exsA* was decreased compared to the wild-type strain HY9901 ($p < 0.01$) (Figure 3C).

The biofilm formation ability of HY9901Δ*exsA* decreased impressively

Biofilms are organized groups of microorganisms, usually formed on abiotic or natural surfaces, where organisms are embedded into a matrix composed of extracellular polymers. In comparison to the development observed in HY9901 wild type strain by confocal microscopy, Δ*exsA* showed a decline in biofilm formation capability ($p < 0.01$) (Figure 3D; Table 4).

The HY9901Δ*exsA* showed an attenuated swarming phenotype

The result of swarming assay was showed in the Table 3. As for swarming activity, the swarming circle of the wild strain HY9901was 29.2 ± 1.2 mm, and Δ*exsA* was 26.6 ± 0.3 mm. The result indicated that the swarming ability of HY9901Δ*exsA* was significantly weakened (Figure 3E; Table 4).

LD_{50} determination

In this study, zebrafish were used as models to evaluate the virulence of the HY9901 and Δ*exsA*. The results showed that the 50% lethal dose of Δ*exsA* was 100 times higher than that of wild strain (Tables 3, 4). All of the dead fish exhibited the clinical

A

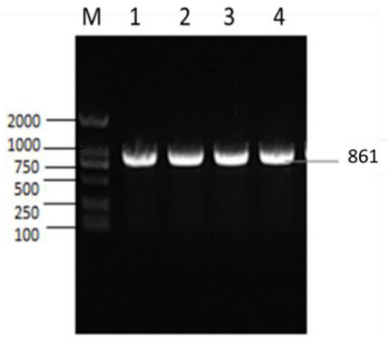

B

```
1          ATGGATGTGTCAGGCCAACTAAACTCAGAAAGGGTCGACTCGAGTTCACGAAAAATTCGT
1           M  D  V  S  G  Q  L  N  S  E  R  V  D  S  S  S  R  K  I  R

61         AGTTTTTCCTGCTATGAAAAATCTGACGAAGTATTTCACTCAGACCAGTCTCACATTGTT
21          S  F  S  C  Y  E  K  S  D  E  V  F  H  S  D  Q  S  H  I  V

121        GTCGTTCACAATGGTCAGCTTCGAGTGCAAACAGGTGATTGCACAATCGATGTTGCTGCA
41          V  V  H  N  G  Q  L  R  V  Q  T  G  D  C  T  I  D  V  A  A

181        GAAAATGGGGTATTTCTATCTCAAGGGGATTACTTGTTAGAGTACTCTCCGCTAGATGGG
61          E  N  G  V  F  L  S  Q  G  D  Y  L  L  E  Y  S  P  L  D  G

241        GCATACAAAGCGTCGATTATTGCTTACGACAATGAACTCGTTAGTCAGTTGCTGCAAAAA
81          A  Y  K  A  S  I  I  A  Y  D  N  E  L  V  S  Q  L  L  Q  K

301        CACAGTGATCTCTTGATGATGCTGCCTAAGGTAGACAAAGTTTGTTCTGGTTTGTTTACT
101         H  S  D  L  L  M  M  L  P  K  V  D  K  V  C  S  G  L  F  T

361        TTTGGTTTGAACATACTCGTTGAACAAGTGCTTTCTAGCATGCAGACGCTTGAGCAACAA
121         F  G  L  N  I  L  V  E  Q  V  L  S  S  M  Q  T  L  E  Q  Q

421        GCGTACCCTGATGCCATTATGTGCCTAAAATACGAAGAACTACTCATTCTCTTGCTACAC
141         A  Y  P  D  A  I  M  C  L  K  Y  E  E  L  L  I  L  L  L  H

481        AGCAAAGGAGGAGAATCACTGTATGCGTTGCTGTCACAACAAACAAACCGTACGTCGGAA
161         S  K  G  G  E  S  L  Y  A  L  L  S  Q  Q  T  N  R  T  S  E

541        CGGTTACGTCGATTTATGGAACAGCATTACTTAAAAGAATGGAAGTTGACAGACTACGCG
181         R  L  R  R  F  M  E  Q  H  Y  L  K  E  W  K  L  T  D  Y  A

601        CAGGAGTTTGGTGCCAGCTTAACCACTTTTAAAGAGCTTTTTAATGAGCACTATGGCATT
201         Q  E  F  G  A  S  L  T  T  F  K  E  L  F  N  E  H  Y  G  I

661        TCTCCAAGAGCCTGGATCAGTGAGCGTCGACTACTGCATGCTCATAAACTGCTGTTGACG
221         S  P  R  A  W  I  S  E  R  R  L  L  H  A  H  K  L  L  L  T

721        AGCAAGATGAGCATCGTAGATGTGGCGATGGAGGCAGGGTTTTCCAGCCAGTCTTACTTT
241         S  K  M  S  I  V  D  V  A  M  E  A  G  F  S  S  Q  S  Y  F

781        ACGCAGAGTTACCGTCGTCGTTTTGGAACGACCCCAAGCCGCGTACGTTCGGGAGACGAT
261         T  Q  S  Y  R  R  R  F  G  T  T  P  S  R  V  R  S  G  D  D

841        CAAGTGGCTATCGCGAAATGA
281         Q  V  A  I  A  K  *
```

FIGURE 1
(A) Cloning of *exsA* gene. M: DL2000 marker. Lane 1-4: The 861 bp fragment amplified from genomic DNAs of HY9901 using primer pairs of ExsA-F/ExsA-R. **(B)** *exsA* gene nucleotide and its encoded amino acid sequence.

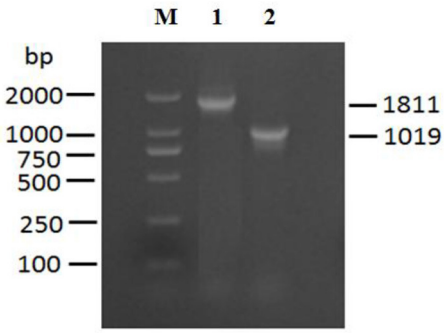

FIGURE 2
Construction and confirmation of the knockout mutant strain HY9901Δ*exsA*. M: DL2000 marker, Lane 1. A fragment of 1,811 bp is obtained for HY9901 using primer pairs of *exsA*-A1-F/*exsA*-A2-R. Lane 2. A fragment of 11,019 bp is obtained for HY9901Δ*esxA* using primer pairs of *exsA* -A1-F/*exsA*-A2-R.

symptoms of Vibriosis such as ulcers on the skin, hemorrhagic and swelling in the liver and kidney. The results showed that the virulence of HY9901Δ*exsA* was significantly decreased when compared with the HY9901 ($p < 0.01$).

Antibiotic susceptibility

The susceptibility of the wild strain HY9901 and Δ*exsA* to 30 antibiotics was determined by disc diffusion method. The result was as follows. The HY9901 was highly resistant to chloramphenicol, while the Δ*exsA* had a zone of inhibition against chloramphenicol. Besides, the Δ*exsA* was more sensitive to kanamycin, minocycline, tetracycline, gentamicin, doxycycline and neomycin (Table 5).

Transcriptome sequencing analysis of HY9901 and strain Δ*exsA*

The transcriptome sequencing analysis identified a total of 541 upregulated and 663 downregulated differentially expressed genes (DEGs) in Δ*exsA* compared to HY9901 (Figure 4A; Supplementary Table S1). These DEGs were enriched by GO function. Go analysis showed that DEGs of HY9901 and strain Δ*exsA* were related to locomotion, movement of cell or subcellular component and bacterial-type flagellum-dependent cell motility (Figure 4B). We also identified the virulence genes in HY9901 and Δ*exsA* in the transcriptome sequencing data. Compared with HY9901, genes in biofilm formation (*crp*, *fis*, *flrA*, *ompT*), bacterial secretion (*gspC*, *lip*), two-component system (*epsP*, *pfeR*, *phoA*,) and lipopolysaccharide biosynthesis (*lpxK*,) were at lower expression level in Δ*exsA*.

Validation of transcriptome data at the mRNA level

To verify our transcriptome results, a total of 8 candidate genes (including *flaE*, *flaG*, *cheA*, *fliN*, *fliS*, *kdsA*, *minD* and *cysN*) were analyzed by qRT-PCR. qRT-PCR assay displayed that the changes in mRNA expression of Δ*exsA* were consistent with those of RNA-Seq (Figure 5). These results further validate the reliability of the transcriptome data.

hop gene expression analysis

The results of qRT-PCR showed that compared with HY9901, Δ*exsA* decreased the expression of *hop* at 18, 24, 36, 48 and 72 h ($p < 0.01$) (Figure 6A). Besides, expression of the LacZ reporter gene was measured with a β-galactosidase enzymatic assay. As shown in Figure 6B, HY9901 wild type strain exhibited high β-galactosidase activity, and Δ*exsA* produced low β-galactosidase activity ($p < 0.05$). These results suggested that *exsA* gene could facilitate the expression of *hop* gene.

HY9901Δ*exsA* doesn't colonize stably *in vivo*

As shown in Figure 7, Δ*exsA* could survive momently in fish liver and spleen then was progressively excreted from the host body. The highest bacterial number was detected in spleen on day 2, followed by the liver.

HY9901Δ*exsA* has immune protective effects on zebrafish

Zebrafish were vaccinated with PBS and Δ*exsA* by intramuscular injection for 28 days, challenged with the wild type HY9901. As shown in Figure 8, the mortality rate in the control group injected with sterile PBS was 90%, the mortality rate in the injection immunization group was 30%, and the relative percentage survival was 66.7%.

HY9901Δ*exsA* can upregulate the expression of immune genes in zebrafish after vaccination

qRT-PCR was used to analyze the expression of proinflammation and anti-inflammation genes. The results indicated that compared to PBS group, vaccination with Δ*exsA*

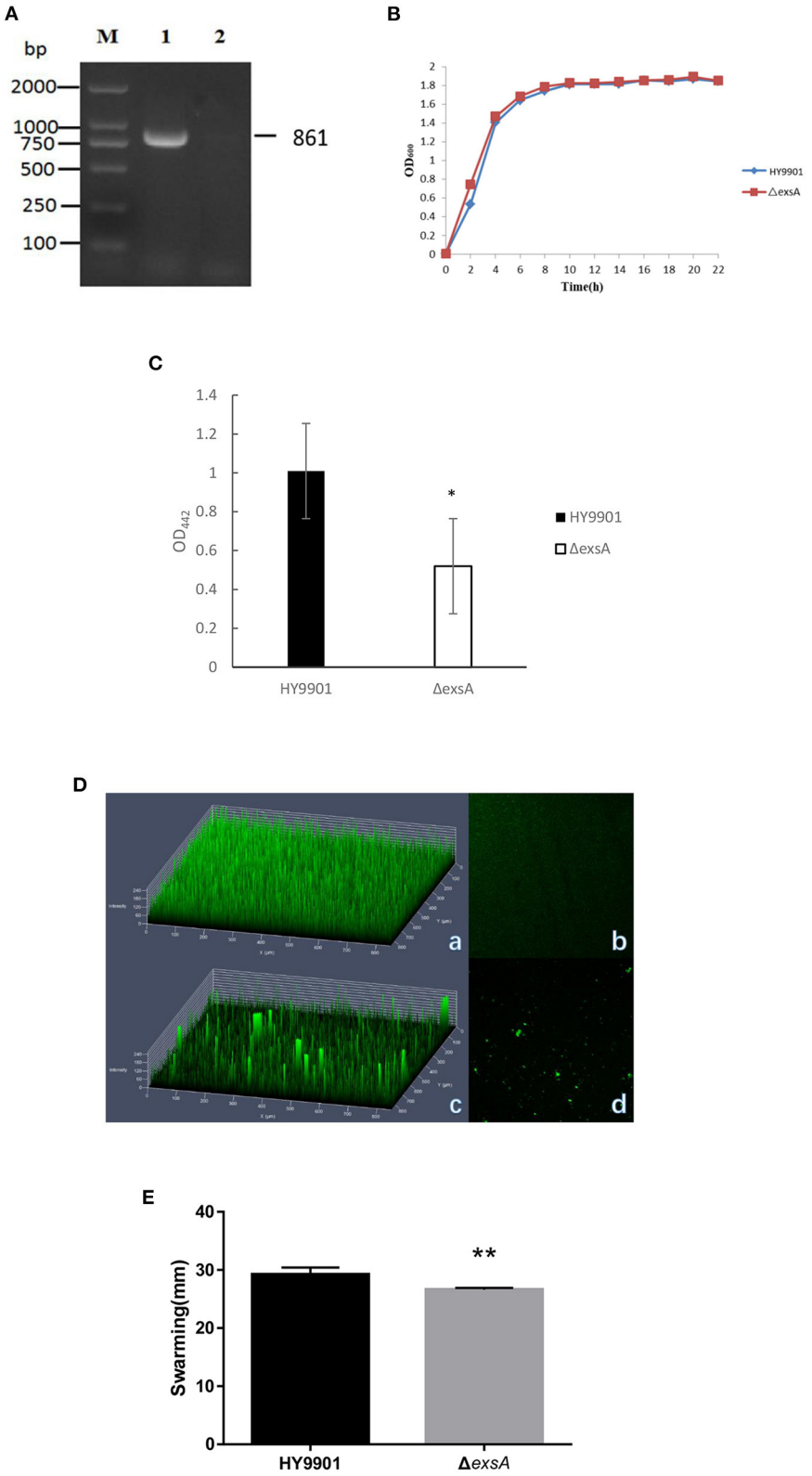

FIGURE 3
Characteristics of different strains. **(A)** Genetic stability detection of HY9901Δ*exsA* deletion mutantt. M: DL2000 marker; Lane 1. The 861 bp fragment amplified from genomic DNAs of HY9901 using primer pairs of ExsA-F/ExsA-R; Lane 2. The negative result amplified from genomic DNAs of Δ*exsA* using primer pairs of ExsA-F/ExsA-R. **(B)** Growth rates of HY9901Δ*exsA* and wild-type strain HY9901 (wt). Aliquots of cell culture

(Continued)

FIGURE 3
were obtained at various time points and measured for cell density at OD_{600}. **(C)** Activity of extracellaluar proteases. The extracellular protease activity was measured at OD_{442}. **(D)** Measurement of biofilm by LSCM. (a) HY9901 2.5d diagram. (b)HY9901Δ*exsA* 2.5d diagram. (c) HY9901 2d diagram. (d) HY9901Δ*exsA* 2d diagram; HY9901 Biofilm thickness: 60 ± 10 μm, HY9901Δ*exsA* Biofilm thickness:90 ± 20 μm. **(E)** Swarming diameters were measured after 24 h incubation on TSA containing 0.3% agar plates. $^{**}p < 0.01$.

TABLE 4 Characteristics of different strains.

Characteristics	HY9901	Δ*exsA*
Activity of ECPase (A_{442})[a]	1.01 ± 0.2	0.52 ± 0.2**
Swarming (mm)[b]	29.2 ± 1.2	26.6 ± 0.3**
Biofilm thickness (μm)	60 ± 10	30 ± 5**
LD_{50} (cfu/ml)[c]	5.8×10^5	6.3 × 107**

$^{**}p < 0.01$.
Values are mean ± standard deviation for three trials.
[a]Bacteria were incubated in TSB for 18 h at 28°C.
[b]Swarming diameters were measured after 8 h incubation on TSA containing 0.3% agar plates.
[c]LD_{50} was evaluated in zebrafish with an average weight of 0.11 ± 0.10 g.

had significantly increased expression of *IL6*, *IL8*, *IL-6R*, *IL-1β*, *TNF-α*, *tlr5*, *rag-1*, *gata-1*, *IgM*, genes in liver and *gata-1*, *IL6*, *IL-6R*, *IgM*, *TNF-α*, *rag-1*, *TNF-α* genes in spleen ($p < 0.01$) (Figure 9).

The HY9901Δ*exsA* vaccine had a favorable safety profile

As shown in Figure 10, pathological features, such as liver congestion and the boundaries between the lymphocytes in the spleen, were observed visually in the tissue sections of the zebrafish injected wild-type strain HY9901. There was a little number of bleeding spots and congestion in the zebrafish immunized by Δ*exsA* for 28 days, but not in PBS group.

Discussion

In recent years, vibriosis outbreaks in China have caused serious economic losses, and overuse of antibiotics has driven the emergence and spread of resistance. In this context, the development of a vibrio-based vaccine might be a valuable alternative. Live attenuated vaccines closely mimic natural infection and, *via* specific antibody and cell-mediated immune responses, usually provide excellent protection against infection (31). Recently, attenuated virus strains can be constructed by knockout of the virulence genes. In this study, we knocked out the T3SS gene *exsA* of *V. alginolyticus*, probed into its biology and pathogenicity, and evaluated its effect as a live attenuated vaccine. And the genetic stability result indicated that the genetic information of the Δ*exsA* was stably inherited to offspring after 30 generations.

Biofilms are an important protective mechanism in which microbes form a strong shield against several antimicrobials (32). Vibrio polysaccharide (VPS) is critical for the formation of biofilm architecture in *Vibrio cholera* (33, 34). Flagella-mediated motility is required for the initial stages of biofilm formation (35), and deletion of *V. parahaemolyticus* polar flagellum genes leads to defective biofilm formation (36). Although there was no significant difference in growth between HY9901 and Δ*exsA*, the biofilm formation ability test showed that the mutant strain Δ*exsA* was significantly decreased compared to the wild-type strain HY9901. It is tempting *to* speculate that *exsA* may represses the expression of flagellum-related genes (*flaA* and *fliG*) or genes related to biofilm matrix polysaccharides, resulted in reduced ability to form mature biofilms. Extracellular products (ECP) are mainly thought to be characteristics of the virulent strain of *V. alginolyticus* (20). In this study, the extracellular protease activity of Δ*exsA* was decreased compared to the wild-type strain HY9901, which suggest *exsA* gene may be a positive contributor to activity of ECP in *V. alginolyticus*. ExsA may promote related gene expression of ECP such as *vhh* and *ptlh*, but this needs further investigation. Flagellar motility has long been recognized as a major colonization and virulence factor in many bacterial pathogens, including *Pseudomonas aeruginosa* (37) and *Vibrio cholera* (38). The flagella contribute to swarming motility and enable bacteria to invade into host cells to maintain their ecological niches *in vivo* (39). In this study, Δ*exsA* had suppressed swarming motility, which indicated that *exsA* was a positive contributor to swarming motility in *V. alginolyticus*. We could speculate that *exsA* might play an important role in regulating the expression level of flagella *via* an unclear mechanism. However, the regulatory mechanism is still unknown and also needs further investigation. Compared to HY9901, the LD_{50} of Δ*exsA* was decreased by 20 orders. From these results, we can find that *exsA* is related to the pathogenesis of *V. alginolyticus*.

The origin and molecular basis of bacterial resistance is the presence of antibiotic resistance genes (ARGs). An organism can acquire antibiotic resistance through mutation, horizontal gene transfer, or inheriting resistance genes from other organisms (40, 41). Besides, it is also possible to acquire antimicrobial resistance by mutation, for example changing the antimicrobial target site (42). *V. alginolyticus* has been reported to be resistant to ampicillin, vancomycin, and cephalothin (43). The results of Raissy et al. (44)

10.3389/fvets.2022.938822

TABLE 5 Drug sensitivity test results of the HY9901 and HY9901Δ*exsA*.

Antibiotic	Dose (μg)	Bacteriostatic circle diameter			
		HY9901	Sensitivity	Δ*exsA*	Sensitivity
Cefoperazone	75	0.00	R	0.00	R
Oxacillin	1	0.00	R	0.00	R
Clindamycin	2	0.00	R	0.00	R
Ceftazidime	30	0.00	R	0.00	R
Penicillin	10U	0.00	R	0.00	R
Ampicillin	100	0.00	R	0.00	R
Carbenicillin	100	0.00	R	0.00	R
Cefazolin	30	0.00	R	1.00	R
Ceftriaxone	30	0.00	R	0.00	R
Cefradine	30	0.00	R	0.00	R
Piperacillin	100	0.00	R	0.00	R
Cefuroxime	30	0.00	R	0.00	R
SMZ/TMP	23.75/1.25	0.00	R	0.00	R
Mideamycin	30	0.00	R	0.00	R
Vancomycin	30	0.00	R	0.00	R
Cephalexin	30	0.00	R	0.00	R
Polymyxin B	200IU	0.00	R	0.00	R
Norfloxacin	10	0.00	R	0.00	R
Ofloxacin	5	0.00	R	0.00	R
Ciprofloxacin	5	0.00	R	0.00	R
Amikacin	30	11.0	R	11.5	R
Minocycline	30	13.5	I	18.0	S
Tetracycline	30	12.1	R	15.0	I
Gentamicin	10	0.00	R	12.3	I
Furazolidone	300	7.1	R	8.0	R
Chloramphenicol	30	14.5	I	0.00	R
Kanamycin	30	0.0	R	11.0	R
Erythromycin	15	0.0	R	0.0	R
Doxycycline	30	10.5	R	15.0	I
Neomycin	30	0.0	R	11.0	R

S, susceptible; I, intermediate; R, resistance.

showed that *strB*, *tetS*, and *ermB* genes, which encode streptomycin, tetracycline and erythromycin, respectively, could be detected in several strains of *V. alginolyticus* from seafood in Persian Gulf. Further, the author found that some strain not containing *tesT* gene was resistant to tetracycline and induced that there were other genes causing tetracycline resistance (44). In this study, HY9901 was highly resistant to chloramphenicol, while Δ*exsA* was sensitive. Besides, the Δ*exsA* was more sensitive to kanamycin, minocycline, tetracycline, gentamicin, doxycycline and neomycin. It could be guessed that the *exsA* gene might be related to drug resistance genes and regulate the expression of drug resistance-related genes. Nevertheless, it needs to be further studied.

The transcriptome is a collection of all RNA molecules in a cell, which reflects the expression status of the entire genome. It is essential for deciphering the functional complexity of the genome and to obtain a better understanding of cellular activities in organisms, including growth, development, disease, and immune defense (45–47). In the present study, a total of 541 upregulated and 663 downregulated differentially expressed genes in Δ*exsA* compared to HY9901. The outcome of GO analysis revealed that these genes were mainly enriched in a number of GO terms, including locomotion process,

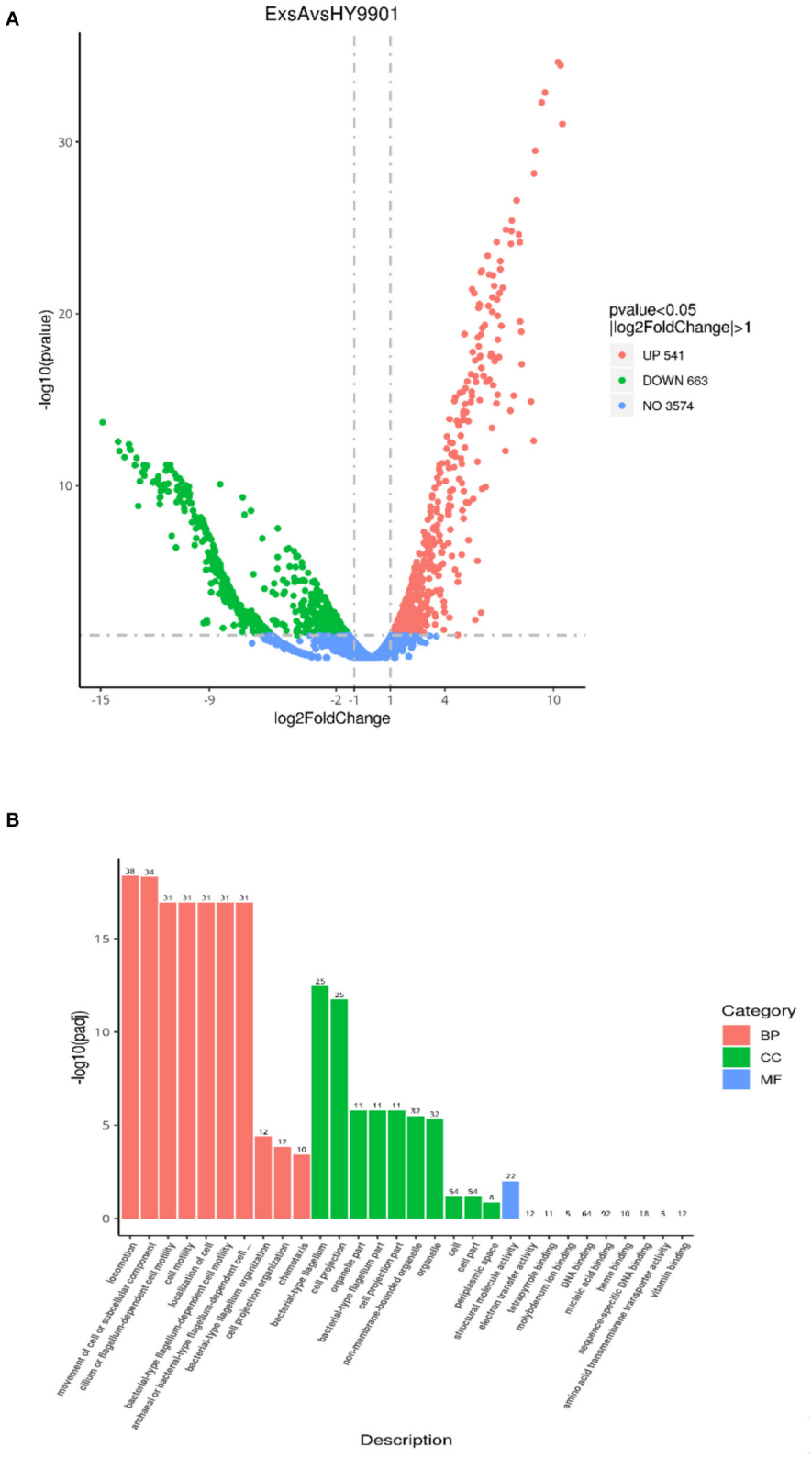

FIGURE 4
(A) Differential analysis volcano map. **(B)** The most enriched GO terms of differentially expressed genes.

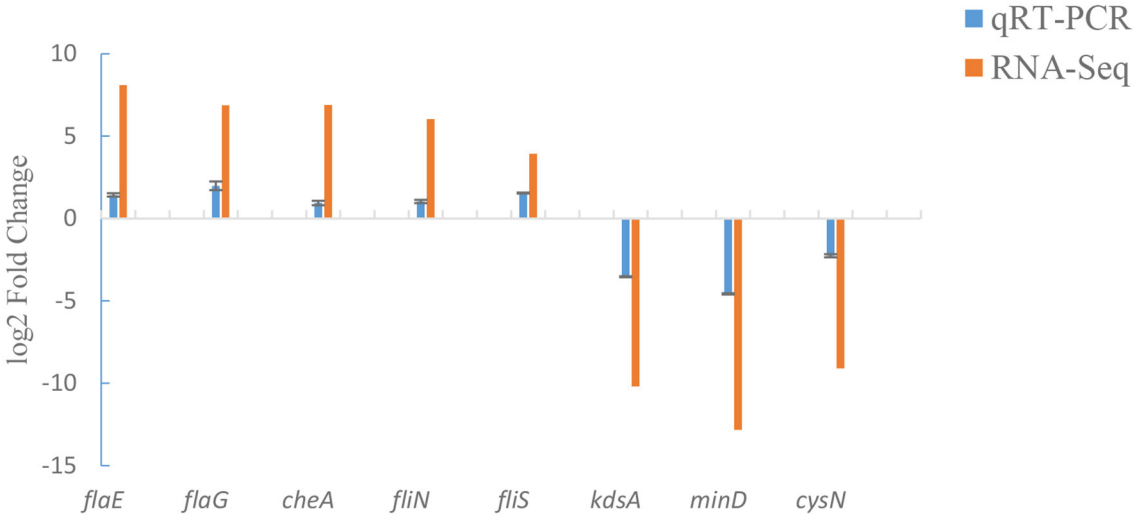

FIGURE 5
Comparison of qRT-PCR and RNA-Seq.

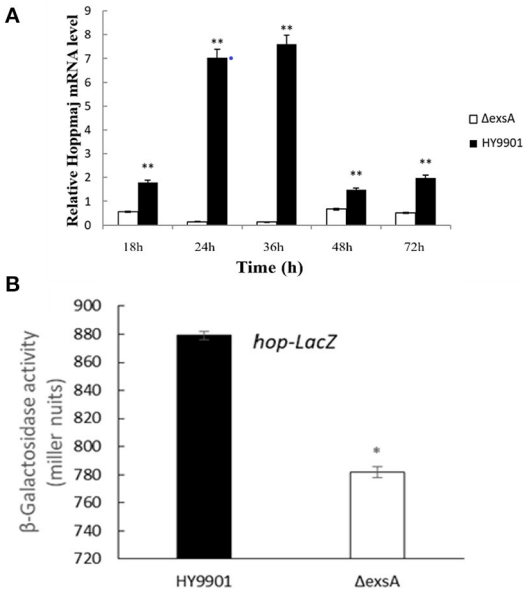

FIGURE 6
hop gene expression analysis. **(A)** Expression of *hop* genes by DMEM between HY9901 wild type and HY9901Δ*exsA*. **(B)** Expression of the LacZ reporter gene between HY9901 wild type and HY9901Δ*exsA*.

movement of cell or subcellular component process, non-membrane-bounded organelle process, organelle process, cilium or flagellum-dependent cell motility process and cell motility process. These results further suggest that exsA gene can regulate the expression of flagella related genes to affect the virulence of *V. alginolyticus*. Nonetheless, its specific regulatory mechanism needs further investigation.

The T3SS is a membrane-embedded nanomachine and it can deliver T3SEs from pathogen to host. The T3SS secretion *in vitro* and *in vivo* is complex, and its pathway is modulated by a single regulatory protein or several interacting regulatory proteins. For example, In *Pseudomonas savastanoi* HrpR and HrpS form a hetero-hexamer, which activates the expression of HrpL, inducing all T3SS genes by binding to a "hrp box" in promoters (48). ExsA is an activator of transcription in T3SS. A previous study indicates that in *P. aeruginosa impA* gene encoding an extracellular metalloprotease is under the regulation of ExsA, and ExsA can directly regulate the transcription of *impA* by binding to its upstream region, demonstrated in electrophoretic mobility shift assay (EMSA) (49). The results of Liu et al. (21) indicated that in *V. alginolyticus* ExsA was a positive regulator in effector proteins Va1686 and Va1687. HopPmaJ is one of the T3SEs from *V. alginolyticus*, which has been reported to attack the host efficiently (50). In this study, the deletion of *exsA* is responsible for the down-regulation of *hop* gene for various time periods, which was demonstrated in qRT-PCR assay. Furthermore, we also found that *exsA* gene could facilitate the expression of *hop* gene as well as acting as positive regulators. From these results, we can draw a conclusion that *exsA* can promote the expression of *hop* gene by binding the promoter regions, which may facilitate HopPmaJ protein secretion.

As a model of good vertebrate animals, zebrafish have been widely used for the study of immunity from a unique perspective. The low cost, rapid development and high fecundity of zebrafish makes it ideal as a vaccine-screening tool (24). It is reported that the *V. parahaemolyticus* can infect zebrafish larvae

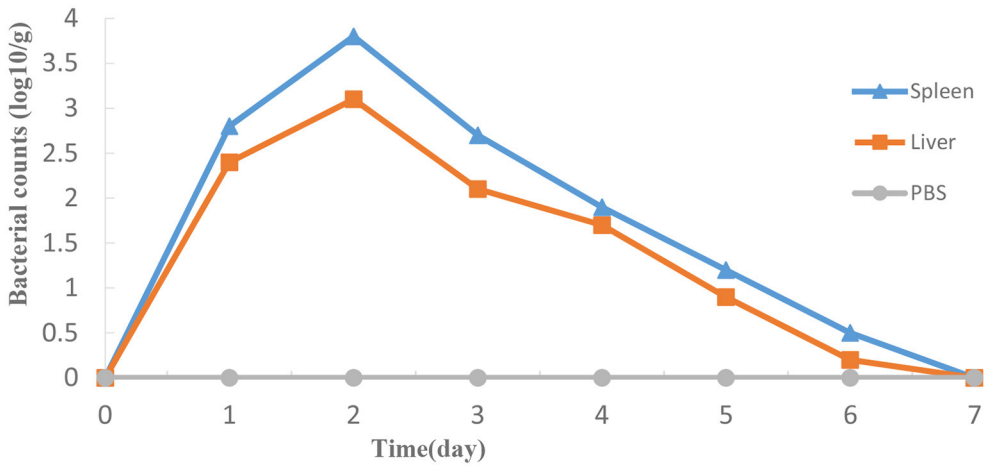

FIGURE 7
Propagation of HY9901Δ*exsA* in grouper liver **(A)** and spleen **(B)** following i.m. injection with 5 μL 1 × 10^5 cfu mL^{-1} Δ*exsA*. Control fish were i.m. injection with 5 μL sterile PBS. The number of viable bacteria was shown as the mean ± standard of three samples.

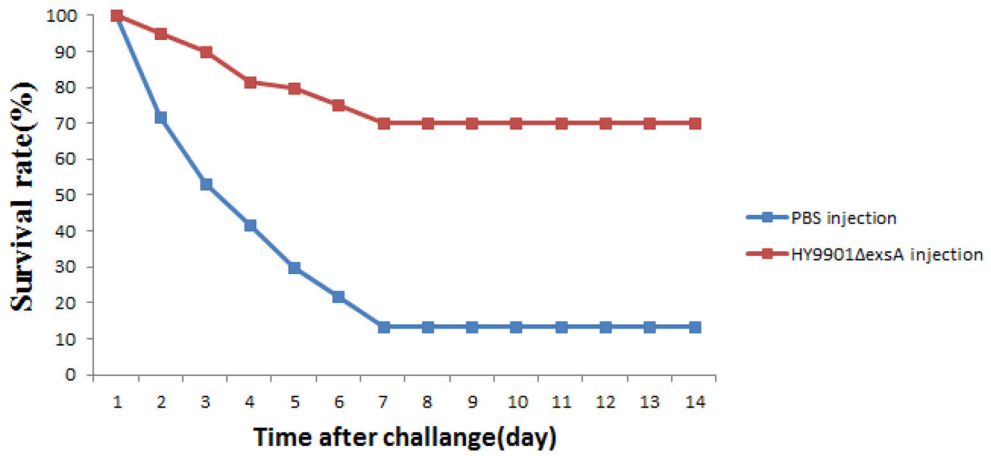

FIGURE 8
Survival in groups vaccinated with HY9901Δ*exsA* and PBS following challenge with *V. alginolyticus* HY9901.

and activate the innate immune response (51). A previous study indicated that Th17 cells were activated following vaccination of zebrafish (52). Therefore, it is achievable to use zebrafish to investigate the effectiveness of a Vibrio vaccine. In the present study, the RPS of zebrafish vaccinated with Δ*exsA* reached 77.6%, and it was significantly higher than that of the control group.

TLR5 can activate the innate immune system by recognition of bacterial flagellin (53). *IgM* of fish plays an important role in resisting diseases, similar function as *IgM* in mammals (54). *IgM* plays a vital role in immunity, driving direct antimicrobial functions including complement activation, opsonophagocytosis, and agglutination. *IL-1β* and *IL-6* are important cytokines involved in regulating inflammatory response (55, 56). *TNF-α* and *IL-8* are important inflammatory cytokines that mediate the body inflammatory responses and have important roles in the physiological functions and pathological processes (57). In the present study, the elevated expression of immune-related genes (*IgM*, *IL-1β*, *IL-6*, and *TNF-α*), confirmed that Δ*exsA* can effectively induce the protective immune response of zebrafish associated with proinflammatory and immunoglobulin activity. Tissue sections results indicated a favorable safety profile of Δ*exsA* vaccines. In summary, these results showed that the Δ*exsA* could provide protection against *V. alginolyticus* and has the potential as an attenuated live vaccine. In addition to antibiotics,

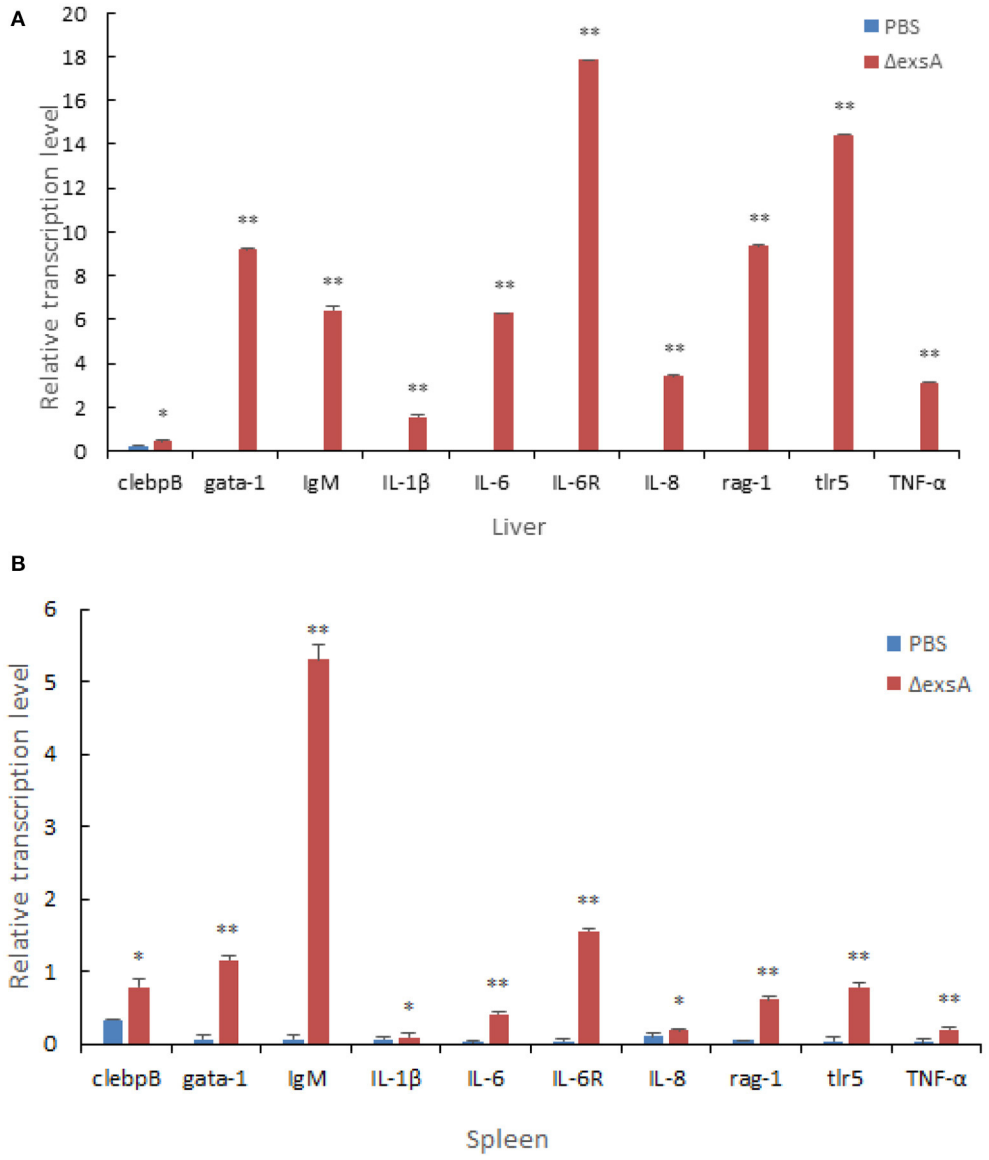

FIGURE 9
Comparative analysis of the expression of immune-related genes in liver **(A)** and spleen **(B)** of zebrafish given the live attenuated vaccine and unvaccinated zebrafish. The liver and spleen of zebrafish were sampled at 1 day before challenge, and the mRNA level of each immune-related gene was normalized to that of β-actin. Bars represent the mean relative expression of three biological replicates and error bars represent standard deviation.

vaccines are one of the most important means to prevent and control of *V. alginolyticus*, which has great significance for aquaculture industries.

Conclusions

Taken together, we have successfully constructed an in-frame deletion strain of Δ*exsA* and investigated its physiology and pathogenicity. We found that Δ*exsA* could decrease ECPase activity and swarming motility, and the *exsA* gene regulates *hop* genes expression. Moreover, Δ*exsA* exhibited a high level of protection against *V. alginolyticus* challenge, and could induce protective immune responses in zebrafish. These results may provide experimental evidence for the importance of *exsA* in *V. alginolyticus* and provide a reference for further study into this virulence and infection mechanism.

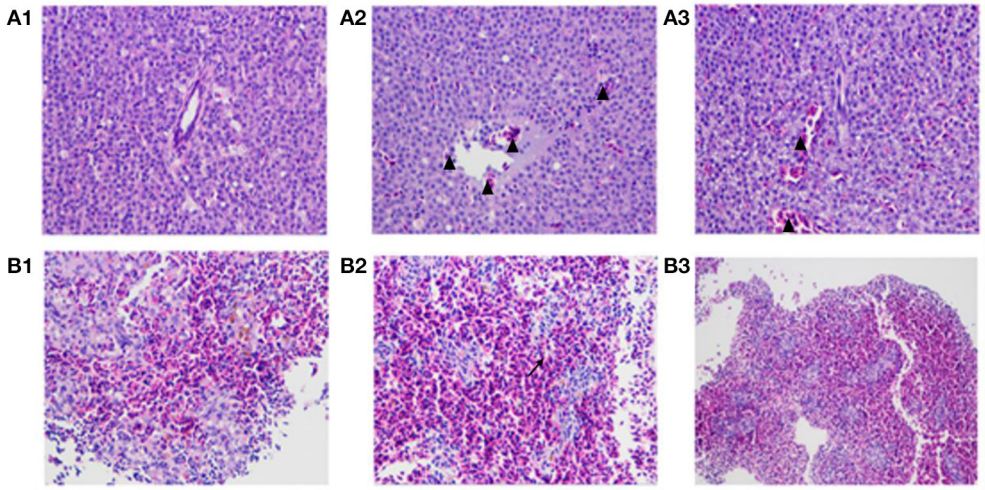

FIGURE 10
The pathological changes of vaccinated zebrafish. Zebrafish liver tissue section, 400×magnification (**A1**: injected with PBS **A2**: injected with HY9901 **A3**: injected with Δ*exsA*). Zebrafish spleen tissue section, 200 × magnification (**B1**: injected with PBS **B2**: injected with HY9901 **B3**: injected with Δ*exsA*). The triangle (▲) represents hyperemia, and the arrow (↗) represents the blurred boundary of lymphocytes in the figure.

Data availability statement

The datasets presented in this study can be found in online repositories. The names of the repository/repositories and accession number(s) can be found in the article/Supplementary material.

Ethics statement

The animal study was reviewed and approved by the Animal Ethics Committee of Guangdong Ocean University (Zhanjiang, China).

Author contributions

WZ and HP designed the experiment. FZ, HF, LC, and XX generated experimental data. WZ and JW wrote manuscripts. HP, JJ, and NW conceived the work and critically reviewed the manuscript. WZ, LC, HF, JW, FZ, XX, JJ, NW, and HP have made extensive contributions to the work in this manuscript. All authors contributed to the article and approved the submitted version.

Funding

This work was supported by the National Natural Science Foundation of China (No. 32073015), Natural Science Foundation of Guangdong Province (No. 2021A1515011078), Undergraduate Innovation Team of Guangdong Ocean University (No. CCTD201802), Innovation and Entrepreneurship Training Program for College Students (No. CXXL2022005), Science and Technology Innovation Cultivation Program for College Student (No. pdjh2021b0239), and Guangdong Postgraduate Education Innovation Project.

Conflict of interest

The authors declare that the research was conducted in the absence of any commercial or financial relationships that could be construed as a potential conflict of interest.

Publisher's note

Supplementary material

The Supplementary Material for this article can be found online at: https://www.frontiersin.org/articles/10.3389/fvets.2022.938822/full#supplementary-material

References

1. Millikan DS, Ruby EG. Vibrio fischeri flagellin A is essential for normal motility and for symbiotic competence during initial squid light organ colonization. *J Bacteriol.* (2004) 186:4315–25. doi: 10.1128/JB.186.13.4315-4325.2004

2. Kitaoka M, Nishigaki T, Ihara K, Nishioka N, Kojima S, Homma M. A novel dnaJ family gene, sflA, encodes an inhibitor of flagellation in marine Vibrio species. *J Bacteriol.* (2013) 195:816–22. doi: 10.1128/JB.01850-12

3. Jun JW, Kim HJ, Yun SK, Chai JY, Park SC. Eating oysters without risk of vibriosis: application of a bacteriophage against *Vibrio parahaemolyticus* in oysters. *Int J Food Microbiol.* (2014) 188:31–45. doi: 10.1016/j.ijfoodmicro.2014.07.007

4. Letchumanan V, Yin WF, Lee LH, Chan KG. Prevalence and antimicrobial susceptibility of *Vibrio parahaemolyticus* isolated from retail shrimps in Malaysia. *Front Microbiol.* (2015) 6:33. doi: 10.3389/fmicb.2015.00033

5. Ahmed HA, El Bayomi RM, Hussein MA, Khedr MHE, Abo Remela EM, El-Ashram AMM. Molecular characterization, antibiotic resistance pattern and biofilm formation of *Vibrio parahaemolyticus* and *V. cholerae* isolated from crustaceans and humans. *Int J Food Microbiol.* (2018) 274:31–7. doi: 10.1016/j.ijfoodmicro.2018.03.013

6. Matamp N, Bhat SG. Phage endolysins as potential antimicrobials against multidrug resistant vibrio alginolyticus and vibrio parahaemolyticus: current status of research and challenges ahead. *Microorganisms.* (2019) 7:84. doi: 10.3390/microorganisms7030084

7. Cornelis GR. The type III secretion injectisome. *Nat Rev Microbiol.* (2006) 4:811–25. doi: 10.1038/nrmicro1526

8. Galán JE, Wolf-Watz H. Protein delivery into eukaryotic cells by type III secretion machines. *Nature.* (2006) 444:567–73. doi: 10.1038/nature05272

9. Büttner D. Protein export according to schedule: architecture, assembly, and regulation of type III secretion systems from plant- and animal-pathogenic bacteria. *Microbiol Mol Biol Rev.* (2012) 76:262–310. doi: 10.1128/MMBR.05017-11

10. Brutinel ED, King JM, Marsden AE, Yahr TL. The distal ExsA-binding site in *Pseudomonas aeruginosa* type III secretion system promoters is the primary determinant for promoter-specific properties. *J Bacteriol.* (2012) 194:2564–72. doi: 10.1128/JB.00106-12

11. Frank DW. The exoenzyme S regulon of *Pseudomonas aeruginosa*. *Mol Microbiol.* (1997) 26:621–9. doi: 10.1046/j.1365-2958.1997.6251991.x

12. Qu J, Prasad NK, Yu MA, Chen S, Lyden A, Herrera N, et al. Modulating pathogenesis with mobile-CRISPRi. *J Bacteriol.* (2019) 201:e00304–19. doi: 10.1128/JB.00304-19

13. Gu D, Zhang Y, Wang Q, Zhou X. S-nitrosylation-mediated activation of a histidine kinase represses the type 3 secretion system and promotes virulence of an enteric pathogen. *Nat Commun.* (2020) 11:5777. doi: 10.1038/s41467-020-19506-1

14. Zhou X, Konkel ME, Call DR. Regulation of type III secretion system 1 gene expression in *Vibrio parahaemolyticus* is dependent on interactions between ExsA, ExsC, and Exs D. *Virulence.* (2010) 1:260–72. doi: 10.4161/viru.1.4.12318

15. Zhou X, Shah DH, Konkel ME, Call DR. Type III secretion system 1 genes in *Vibrio parahaemolyticus* are positively regulated by ExsA and negatively regulated by ExsD. *Mol Microbiol.* (2008) 69:747–764. doi: 10.1111/j.1365-2958.2008.06326.x

16. Darwinata AE, Gotoh K, Mima T, Yamamoto Y, Yokota K, Matsushita O. Vibrio alginolyticus VepA induces lysosomal membrane permeability and cathepsin-independent cell death. *Acta Med Okayama.* (2018) 72:231–9. doi: 10.18926/AMO/56068

17. Pang H, Qiu M, Zhao J, Hoare R, Monaghan SJ, Song D, et al. Construction of a *Vibrio alginolyticus* hopPmaJ (hop) mutant and evaluation of its potential as a live attenuated vaccine in orange-spotted grouper (*Epinephelus coioides*). *Fish Shellfish Immunol.* (2018) 76:93–100. doi: 10.1016/j.fsi.2018.02.012

18. Zhou S, Tu X, Pang H, Hoare R, Monaghan SJ, Luo J, et al. A T3SS regulator mutant of *Vibrio alginolyticus* affects antibiotic susceptibilities and provides significant protection to *Danio rerio* as a live attenuated vaccine. *Front Cell Infect Microbiol.* (2020) 10:183. doi: 10.3389/fcimb.2020.00183

19. Wu C, Zhao Z, Liu Y, Zhu X, Liu M, Luo P, et al. Type III secretion 1 effector gene diversity among vibrio isolates from coastal areas in China. *Front Cell Infect Microbiol.* (2020) 10:301. doi: 10.3389/fcimb.2020.00301

20. Cai SH, Wu ZH, Jian JC, Lu YS. Cloning and expression of the gene encoding an extracellular alkaline serine protease from *Vibrio alginolyticus* strain HY9901, the causative agent of vibriosis in *Lutjanus erythopterus* (Bloch). *J Fish Dis.* (2007) 30:493–500. doi: 10.1111/j.1365-2761.2007.00835.x

21. Liu J, Lu SY, Orfe LH, Ren CH, Hu CQ, Call DR, et al. ExsE is a negative regulator for T3SS gene expression in *Vibrio alginolyticus*. *Front Cell Infect Microbiol.* (2016) 6:177. doi: 10.3389/fcimb.2016.00177

22. Pang H, Chang Y, Zheng H, Tan H, Zhou S, Zeng F, et al. A live attenuated strain of HY9901Δ*vscB* provides protection against *Vibrio alginolyticus* in pearl gentian grouper (♀Epinephelus fuscoguttatus x ♂Epinephelus lanceolatu). *Aquaculture.* (2022) 546:737353. doi: 10.1016/j.aquaculture.2021.737353

23. Luo P, He X, Liu Q, Hu C. Developing universal genetic tools for rapid and efficient deletion mutation in vibrio species based on suicide T-vectors carrying a novel counterselectable marker, vmi480. *PLoS ONE.* (2015) 10:e0144465. doi: 10.1371/journal.pone.0144465

24. Wu P, Zhou S, Su Z, Liu C, Zeng F, Pang H, et al. Functional characterization of T3SS C-ring component VscQ and evaluation of its mutant as a live attenuated vaccine in zebrafish (*Danio rerio*) model. *Fish Shellfish Immunol.* (2020) 104:123–32. doi: 10.1016/j.fsi.2020.05.063

25. Windle HJ, Kelleher D. Identification and characterization of a metalloprotease activity from *Helicobacter pylori*. *Infect Immun.* (1997) 65:3132–237. doi: 10.1128/iai.65.8.3132-3137.1997

26. Mathew JA, Tan YP, Srinivasa Rao PS, Lim TM, Leung KY. Edwardsiella tarda mutants defective in siderophore production, motility, serum resistance and catalase activity. *Microbiology.* (2001) 147:449–57. doi: 10.1099/00221287-147-2-449

27. Chen Y, Cai S, Jian J. Protection against *Vibrio alginolyticus* in pearl gentian grouper (♀Epinephelus fuscoguttatus × ♂Epinephelus lanceolatu) immunized with an acfA-deletion live attenuated vaccine. *Fish Shellfish Immunol.* (2019) 86:875–81. doi: 10.1016/j.fsi.2018.12.030

28. Li W, Yao Z, Sun L, Hu W, Cao J, Lin W, et al. Proteomics analysis reveals a potential antibiotic cocktail therapy strategy for *Aeromonas hydrophila* infection in biofilm. *J Proteome Res.* (2016) 15:1810–20. doi: 10.1021/acs.jproteome.5b01127

29. Thibault G, Ismail N, Ng DT. The unfolded protein response supports cellular robustness as a broad-spectrum compensatory pathway. *Proc Natl Acad Sci USA.* (2011) 108:20597–602. doi: 10.1073/pnas.1117184109

30. Joseph J, Ametepe ES, Haribabu N, Agbayani G, Krishnan L, Blais A, et al. Inhibition of ROS and upregulation of inflammatory cytokines by FoxO3a promotes survival against *Salmonella typhimurium*. *Nat Commun.* (2016) 7:12748. doi: 10.1038/ncomms12748

31. Jang YH, Byun YH, Lee KH, Park ES, Lee YH, Lee YJ, et al. Host defense mechanism-based rational design of live vaccine. *PLoS ONE.* (2013) 8:e75043. doi: 10.1371/journal.pone.0075043

32. Wang Y, Wang Y, Liu B, Wang S, Li J, Gong S, et al. pdh modulate virulence through reducing stress tolerance and biofilm formation of *Streptococcus suis* serotype 2. *Virulence.* (2019) 10:588–99. doi: 10.1080/21505594.2019.1631661

33. Absalon C, Van Dellen K, Watnick PI. A communal bacterial adhesin anchors biofilm and bystander cells to surfaces. *PLoS Pathog.* (2011) 7:e1002210. doi: 10.1371/journal.ppat.1002210

34. Berk V, Fong JC, Dempsey GT, Develioglu ON, Zhuang X, Liphardt J, et al. Molecular architecture and assembly principles of *Vibrio cholerae* biofilms. *Science.* (2012) 337:236–9. doi: 10.1126/science.1222981

35. Yildiz FH, Visick KL. Vibrio biofilms: so much the same yet so different. *Trends Microbiol.* (2009) 17:109–18. doi: 10.1016/j.tim.2008.12.004

36. Enos-Berlage JL, Guvener ZT, Keenan CE, McCarter LL. Genetic determinants of biofilm development of opaque and translucent *Vibrio parahaemolyticus*. *Mol Microbiol.* (2005) 55:1160–82. doi: 10.1111/j.1365-2958.2004.04453.x

37. Demirdjian S, Hopkins D, Sanchez H, Libre M, Gerber SA, Berwin B. Phosphatidylinositol-(3,4,5)-trisphosphate induces phagocytosis of nonmotile *Pseudomonas aeruginosa*. *Infect Immun.* (2018) 86:e00215–18. doi: 10.1128/IAI.00215-18

38. Correa NE, Lauriano CM, McGee R, Klose KE. Phosphorylation of the flagellar regulatory protein FlrC is necessary for *Vibrio cholerae* motility and enhanced colonization. *Mol Microbiol.* (2000) 35:743–55. doi: 10.1046/j.1365-2958.2000.01745.x

39. Echazarreta MA, Klose KE. Vibrio flagellar synthesis. *Front Cell Infect Microbiol.* (2019) 9:131. doi: 10.3389/fcimb.2019.00131

40. Davies J, Davies D. Origins and evolution of antibiotic resistance. *Microbiol Mol Biol Rev.* (2010) 74:417–33. doi: 10.1128/MMBR.00016-10

41. Cox G, Wright GD. Intrinsic antibiotic resistance: mechanisms, origins, challenges and solutions. *Int J Med Microbiol.* (2013) 303:287–92. doi: 10.1016/j.ijmm.2013.02.009

42. Agersø Y, Bjerre K, Brockmann E, Johansen E, Nielsen B, Siezen R, et al. Putative antibiotic resistance genes present in extant *Bacillus licheniformis* and *Bacillus paralicheniformis* strains are probably intrinsic and part of the ancient resistome. *PLoS ONE.* (2019) 14:e0210363. doi: 10.1371/journal.pone.0210363

43. Kang CH, Shin Y, Jang S, Jung Y, So JS. Antimicrobial susceptibility of *Vibrio alginolyticus* isolated from oyster in Korea. *Environ Sci Pollut Res Int.* (2016) 23:21106–12. doi: 10.1007/s11356-016-7426-2

44. Raissy M, Moumeni M, Ansari M, Rahimi E. Antibiotic resistance pattern of some Vibrio strains isolated from seafood. *Iranian J Fish Sci.* (2012) 11:618–26. doi: 10.4103/0972-124X.99267

45. Xiang LX, He D, Dong WR, Zhang YW, Shao JZ. Deep sequencing-based transcriptome profiling analysis of bacteria-challenged *Lateolabrax japonicus* reveals insight into the immune-relevant genes in marine fish. *BMC Genomics.* (2010) 11:472. doi: 10.1186/1471-2164-11-472

46. Zhang B, Luo G, Zhao L, Huang L, Qin Y, Su Y, et al. Integration of RNAi and RNA-seq uncovers the immune responses of *Epinephelus coioides* to L321_RS19110 gene of *Pseudomonas plecoglossicida*. *Fish Shellfish Immunol.* (2018) 81:121–129. doi: 10.1016/j.fsi.2018.06.051

47. Tang Y, Xin G, Zhao LM, Huang LX, Qin YX, Su YQ, et al. Novel insights into host-pathogen interactions of large yellow croakers (*Larimichthys crocea*) and pathogenic bacterium *Pseudomonas plecoglossicida* using time-resolved dual RNA-seq of infected spleens. *Zool Res.* (2020) 41:314–27. doi: 10.24272/j.issn.2095-8137.2020.035

48. Wang J, Shao X, Zhang Y, Zhu Y, Yang P, Yuan J, et al. HrpS is a global regulator on type III secretion system (T3SS) and non-T3SS genes in *Pseudomonas savastanoi* pv. phaseolicola. *Mol Plant Microbe Interact.* (2018) 31:1232–43. doi: 10.1094/MPMI-02-18-0035-R

49. Tian Z, Cheng S, Xia B, Jin Y, Bai F, Cheng Z, et al. *Pseudomonas aeruginosa* ExsA regulates a metalloprotease, ImpA, that inhibits phagocytosis of macrophages. *Infect Immun.* (2019) 87:e00695–19. doi: 10.1128/IAI.00695-19

50. Zhuang Q, Dai F, Zhao X, Shao Y, Guo M, Lv Z, et al. Cloning and characterization of the virulence factor Hop from *Vibrio splendidus*. *Microb Pathog.* (2020) 139:103900. doi: 10.1016/j.micpath.2019.103900

51. Ji C, Guo X, Dong X, Ren J, Zu Y, Li W, et al. Notch1a can widely mediate innate immune responses in zebrafish larvae infected with *Vibrio parahaemolyticus*. *Fish Shellfish Immunol.* (2019) 92:680–689. doi: 10.1016/j.fsi.2019.06.058

52. Zhang H, Fei C, Wu H, Yang M, Liu Q, Wang Q, et al. Transcriptome profiling reveals Th17-like immune responses induced in zebrafish bath-vaccinated with a live attenuated *Vibrio anguillarum*. *PLoS ONE.* (2013) 8:e73871. doi: 10.1371/journal.pone.0073871

53. Voogdt CGP, Wagenaar JA, van Putten MJP. Duplicated TLR5 of zebrafish functions as a heterodimeric receptor. *Proc Natl Acad Sci USA.* (2018) 115:E3221–9. doi: 10.1073/pnas.1719245115

54. Solem ST, Stenvik J. Antibody repertoire development in teleosts–a review with emphasis on salmonids and *Gadus morhua* L. *Dev Comp Immunol.* (2006) 30:57–76. doi: 10.1016/j.dci.2005.06.007

55. Lin H, Gao D, Hu MM, Zhang M, Wu XX, Feng L, et al. MARCH3 attenuates IL-1β-triggered inflammation by mediating K48-linked polyubiquitination and degradation of IL-1RI. *Proc Natl Acad Sci USA.* (2018) 115:12483–12488. doi: 10.1073/pnas.1806217115

56. Alaridah N, Lutay N, Tenland E, Rönnholm A, Hallgren O, Puthia M, et al. Mycobacteria manipulate G-protein-coupled receptors to increase mucosal Rac1 expression in the lungs. *J Innate Immun.* (2017) 9:318–29. doi: 10.1159/000453454

57. Liang XT, Wang YY, Hu XY, Wang SB. The protective effects of water extracts of compound turmeric recipe on acute alcoholism: an experimental research using a mouse model. *Evid Based Complement Alternat Med.* (2021) 2021:6641919. doi: 10.1155/2021/6641919

frontiers | Frontiers in Veterinary Science

ORIGINAL RESEARCH
published: 11 August 2022
doi: 10.3389/fvets.2022.857064

Nano-Microemulsions of $CaCO_3$-Encapsulated Curcumin Ester Derivatives With High Antioxidant and Antimicrobial Activities and pH Sensitivity

Lian Wang[1,2†], Xuefei Wang[2†], Zhiwei Guo[3], Yajuan Xia[3], Minjie Geng[4], Dan Liu[5], Zhiqiang Zhang[2] and Ying Yang[1*]*

[1] College of Veterinary Medicine, Inner Mongolia Agricultural University, Hohhot, China, [2] College of Veterinary Medicine, Henan University of Animal Husbandry and Economy, Zhengzhou, China, [3] Inner Mongolia Autonomous Region Comprehensive Centre for Disease Control and Prevention, Hohhot, China, [4] Baotou City Primary Health Service Guidance Centre, Baotou, China, [5] Bayannaoer City Centre for Disease Control and Prevention, Bayannaoer, China

OPEN ACCESS

Edited by:
Kun Li,
Nanjing Agricultural University, China

Reviewed by:
Khalid Mehmood,
Islamia University of Bahawalpur, Pakistan
Qiqi Liu,
Academy of Military Medical Sciences (AMMS), China

***Correspondence:**
Ying Yang
yangyingzsy@126.com
Zhiqiang Zhang
392073683@qq.com

[†]These authors have contributed equally to this work

Specialty section:
This article was submitted to Veterinary Infectious Diseases, a section of the journal Frontiers in Veterinary Science

Received: 18 January 2022
Accepted: 31 January 2022
Published: 11 August 2022

Citation:
Wang L, Wang X, Guo Z, Xia Y, Geng M, Liu D, Zhang Z and Yang Y (2022) Nano-Microemulsions of $CaCO_3$-Encapsulated Curcumin Ester Derivatives With High Antioxidant and Antimicrobial Activities and pH Sensitivity. Front. Vet. Sci. 9:857064. doi: 10.3389/fvets.2022.857064

In this study, we synthesized nano-microemulsions of calcium carbonate ($CaCO_3$)-encapsulated curcumin (Cur)-Ferulic acid (FA) ester derivatives of diverse mass ratios by using the solution casting approach. The structures, antioxidant and antimicrobial activities, physical properties, and potential of hydrogen (pH) sensitivity of these products were examined. Compared with microparticles of $CaCO_3$, those of $CaCO_3$@Cur-FA exhibited excellent antimicrobial and antioxidant properties. Response to pH was indicated through the release of Cur-FA from $CaCO_3$@Cur-FA in solutions having different pH values. The results demonstrated that Cur-FA was released more quickly from $CaCO_3$@Cur-FA at pH 5.5 than at pH 7.4. $CaCO_3$@Cur-FA demonstrated good antioxidant capacities through its ability to scavenge 2,2′-amino-di(2-ethyl-benzothiazoline sulphonic acid-6)ammonium salt ($ABTS^+$) and 1,1-diphenyl-2-picrylhydrazyl (DPPH). These activities were three-fold more than those observed in $CaCO_3$ microparticle control groups; additionally, the antimicrobial activity against *Aspergillus niger* and *Escherichia coli* increased by 40.5 and 54.6%, respectively. Overall, the microparticles of $CaCO_3$@Cur-FA outperformed Cur-FA in terms of antimicrobial properties by inhibiting the growth of certain zoonotic pathogens.

Keywords: antioxidant activity, pH response, antimicrobial property, $CaCO_3$@Cur-FA, biological activity

HIGHLIGHTS

- $CaCO_3$@Cur-FA microspheres showed spherical morphology with uniform size.
- $CaCO_3$@Cur-FA exhibited excellently antioxidant activity.
- $CaCO_3$@Cur-FA exhibited excellently antibacterial activity.
- $CaCO_3$@Cur-FA exhibited excellently pH responsivity activity.
- $CaCO_3$@Cur-FA could as a new food additive, which applicated in the food industry,

INTRODUCTION

Curcumin (diferuloylmethane; Cur) is a leading curcuminoid extracted from the rhizome of *Curcuma longa* plant (1) and has been used as a traditional herbal medicine across Asian countries. This is because it has antioxidant, anticancer (2), antiviral (3), anti-inflammatory, and antimicrobial properties that help in controlling chronic disorders (4). In addition, curcumin, as a common natural pigment, is extensively used in various food industries such as those of canned food, sauces, and brine products. Cur has high solubility in solvents with lower polarity (for example, ethanol and propylene glycol), and it is deemed to be a lipophilic substance (4). Ferulic acid (FA) is suggested to markedly modulate the incidences of inflammation, oxidation, and metabolic syndrome (5). FA is easily soluble in solvents with high polarity (such as ethanol, water, and methanol) and is deemed to be a hydrophilic substance (6). Lipophilic and hydrophilic phytochemicals are extensively distributed in daily foods (such as plants, fruits, herbs, grains, and vegetables) and exhibit antiviral, antimicrobial, and antioxidant activities when used in combination (7). Based on this interesting finding, we designed a molecule in which Cur and FA were connected via an esterification reaction; this molecule was designated as Cur-FA and could be used as a novel food additive.

At present, nanotechnology has offered measures to cope with diverse technical challenges in various fields such as the food industry (8, 9). Calcium carbonate ($CaCO_3$) delivery systems (10) play an important role in various fields including biomedicine, healthcare, and industrial manufacturing (11). They can be used easily and extensively because of their high yield, cost-effectiveness, non-toxicity, biodegradability, biocompatibility, and appropriate decomposition efficiency, apart from their stability even in a basic environment (12). Therefore, $CaCO_3$ together with its modified substances could be used as a delivery vehicle and immobilizing carrier for food research, thus reducing the effective dose required (13). Besides, these materials have small droplet sizes, which enhances their antimicrobial bioactivity by allowing their penetration into the cell membrane, resulting in lipid bilayer destabilization.

In the present study, we hypothesized that the nano-microemulsion of $CaCO_3$-encapsulated curcumin ester derivatives would have a higher antimicrobial activity against pathogens. This may be because the nano-microemulsion has a small droplet size, which can facilitate its penetration into the microbial cell membrane for destroying its activity and inducing death. This study characterized the nano-microemulsion by using various approaches. Additionally, the nano-microemulsion was examined for its antimicrobial ability against seven zoonotic pathogens (*Escherichia coli*, *Staphylococcus aureus*, *Rhizopus*, and *Aspergillus niger*).

MATERIALS AND METHODS

Sodium carbonate (Na_2CO_3) and calcium chloride ($CaCl_2$) were provided by Xiqiao Science Co., Ltd. (Shantou, China). Cur-FA: ^{1}HNMR ($CDCl_3$, 400 MHz) δ:3.83 (s, 6H), 3.85 (s, 3H), 3.87 (s, 3H), 4.59 (s, 2H), 5.59(s, 2H), 6.31 (d, 1H), 6.79 (d, 2H), 6.91 (d, 3H), 6.93 (d, 1H), 6.99 (d, 2H), 7.06 (d, 1H), 7.10 (d, 1H), 7.11 (d, 2H), 7.20 (s, 1H), 7.23 (s, 1H), 7.27 (d, 1H), 7.48 (d, 1H), 7.60 (d, 3H), 9.5 (s, 2H). HRMS (ESI) calculated for [M + H]+$C_{42}H_{38}O_{12}$: 734.75 found 734.69.

Microbial Cultures

Four foodborne pathogenic strains were provided by the Microbiology Laboratory of the National Research Centre (Egypt), which included *E. coli, S. aureus, Rhizopus, A. niger*. Microbial cultures were maintained in a suitable agar medium inclined at an angle of at 4°C (slant culture), which served as the stock cultures. The pathogens were grown in Mueller–Hinton agar (MHA) or Mueller–Hinton broth (MHB).

$CaCO_3$ and $CaCO_3$@Cur-FA Microparticle Preparation

In this study, $CaCO_3$@Cur-FA microparticles were prepared by a method described previously. Briefly, water: acetone (3:1) solution was mixed with Na_2CO_3 (0.5 M) and $CaCl_2$ (0.5 M) with Cur-FA1 (0.1 M), Cur-FA2 (0.2 M), or Cur-FA3 (0.3 M) to prepare the stock solutions. The $CaCl_2$ solution was mixed with Cur-FA (Cur-FA1, Cur-FA2, or Cur-FA3) in a 50-mL beaker, followed by 10 min of stirring with the 85-1 constant temperature magnetic stirrer (Shanghai Zhiwei Electric Appliance Co., Ltd) to prepare $CaCO_3$@Cur-FA microparticles. After the rapid addition of Na_2CO_3 solution to the aforementioned mixture, the obtained solution was subjected to 5 min of stirring at 500 rpm at 40°C, followed by centrifugation to collect the products. $CaCO_3$ microparticles were synthesized using a similar method without adding Cur-FA solution.

Characterization of $CaCO_3$@Cur-FA Microparticles

The Zetasizer Nano-Zeta potentiometer (Nano ZS90, Malvern, UK) was used to measure zeta-potential and particle size of the $CaCO_3$@Cur-FA microparticles. The scanning electron microscope (SEM, Model S-4800 II FESEM, Hitachi, High-Technologies Co., Ltd., Japan) was used to observe the particle morphology.

pH Sensitivity of $CaCO_3$@Cur-FA Microparticles

To assess the pH sensitivity of $CaCO_3$@Cur-FA microparticles in a food microenvironment, the $CaCO_3$@Cur-FA samples (0.2 mg, 2 mL) were dissolved in phosphate buffered saline (PBS) of various pH (5.5, 6.8, and 7.4) and added into dialysis tubes (MWCO 3500). Thereafter, these tubes were soaked in 10 mL of PBS with corresponding pH (within the centrifuge tube) by constant shaking below 37°C. We took out 1 mL dialysate at pre-determined time intervals to measure the absorption, thereby assessing the amount of released Cur-FA. Then, 1 mL fresh PBS was added to the centrifuge tube.

Antioxidant Activity Assay

The antioxidant activity of $CaCO_3$@Cur-FA was assessed by measuring its ability to scavenge 2,2′-azino-bis (3-ethylbenzothiazoline-6 sulfonic acid; $ABTS^+$) and 1,

1-diphenyl-2-picrylhydrazyl (DPPH) free radicals. In brief, 0.2 g $CaCO_3$@Cur-FA was dissolved in 2 mL distilled water before the test. Further, 2 mL of the $CaCO_3$@Cur-FA supernatant was added into ∼2 mL of DPPH methanol solution (0.1 mM) to react for 30 min in dark. Subsequently, the ultraviolet spectrophotometer (Shimadzu, UV-2007, Japan) was used to measure the absorbance (optical density; OD) at 517 nm. The test tube was shaken for ensuring solution uniformity prior to measurements. For the composite film, its ability to scavenge $ABTS^+$ free radicals were determined using the modified approach.

The $ABTS^+$ or DPPH scavenging ability [R (%)] was determined through (Eq. 1)

$$R(\%) = (A2 - A1)/A0 \quad (1)$$

A0 is the OD value of DPPH ($ABTS^+$/PBS) in distilled water;

A1 is the OD value of $CaCO_3$@Cur-FA solution in distilled water mixed with the DPPH methanol solution (ABTS+/PBS mixed solution), and

A2 indicates the OD value of DPPH methanol solution ($ABTS^+$/PBS mixed solution).

Antimicrobial Assays

In this study, we adopted agar–well diffusion approach to perform antimicrobial studies. In brief, 1 mL of active strain culture (10^5 cells /mL) was added to 20 mL MHB (Becton Dickinson, USA) and poured into petri dishes containing MHA. When the agar solidified, wells (diameter, 5 mm) were cut using a sterile borer. Further, 50 μL of the nano-microemulsion or bulk extract was added to each well. The plates were incubated for 2 h under ambient temperature, so that the solutions in the wells diffused into the agar. Moreover, the plates were incubated for 24 h at 37°C. Afterwards, we determined the microbial growth inhibition rate and inhibition zone diameters. Every sample was measured thrice (penicillin G, bulk extract, and nano-microemulsion), and the experiment was performed in triplicates.

Discs containing penicillin G (10 U) and ethanol were used as the positive and negative controls, respectively.

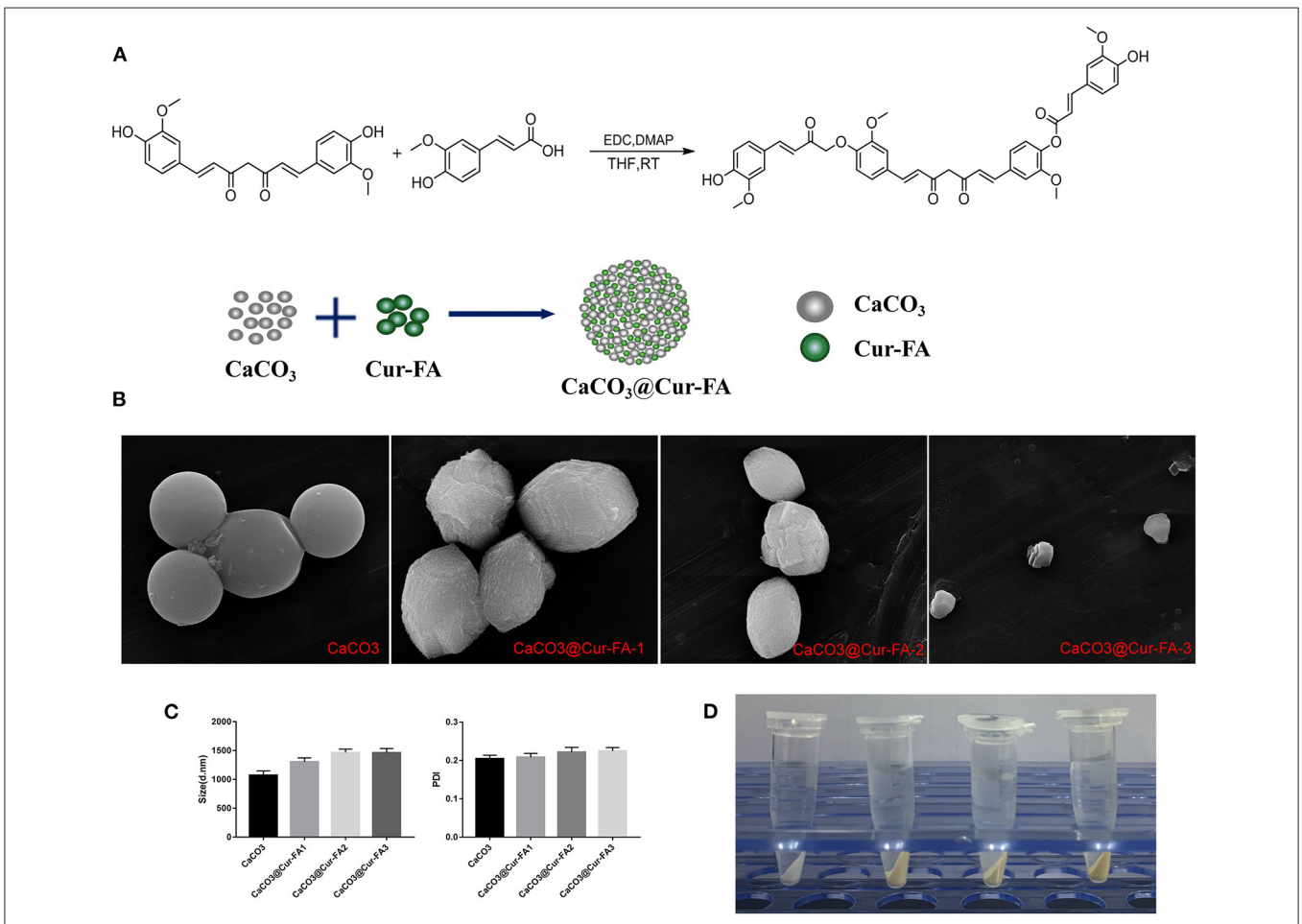

FIGURE 1 | Characterization of $CaCO_3$ and $CaCO_3$@Cur-FA. **(A)** Synthesis of Cur-FA and $CaCO_3$@Cur-FA. **(B)** SEM images of $CaCO_3$ and $CaCO_3$@Cur-FA. Scale bar = 5 μm. **(C)** Particle size and PDI for $CaCO_3$ and $CaCO_3$@Cur-FA. **(D)** The images of $CaCO_3$ and $CaCO_3$@Cur-FA.

Statistical Analysis

The differences among the samples were analyzed using ANOVA. Statistical analysis was performed using SPSS software. The significance of difference ($P < 0.05$) was compared by Duncan's multiple range tests.

RESULTS AND DISCUSSION

Characterization of $CaCO_3$ and $CaCO_3$@Cur-FA Microparticles

This study successfully prepared $CaCO_3$ microparticles using the mineralisation approach (**Figure 1A**). As shown in **Figure 1B**, the SEM data of $CaCO_3$ and $CaCO_3$@Cur-FA microparticles clearly revealed the spherical morphology as well as the almost even size distribution. The sample particle size is given in **Figure 1C**. **Table 1** displays the sample zeta potential. The average hydrodynamic sizes of the microparticles of $CaCO_3$, $CaCO_3$@Cur-FA1, $CaCO_3$@Cur-FA2, and $CaCO_3$@Cur-FA3 were 1070.1 ± 76 nm, 1303.5 ± 66 nm, 1464.8 ± 58 nm, and 1460.7 ±72 nm, respectively. Thus, the optimal concentration of Cur-FA required for preparing uniform-sized $CaCO_3$@Cur-FA microparticles was 0.2 M. The mean size of $CaCO_3$@Cur-FA mildly increased relative to that of the unmodified $CaCO_3$ microparticles, indicating the successful encapsulation of Cur-FA into the microemulsion. In addition, no droplet aggregation was observed, which indicated that $CaCO_3$@Cur-FA maintained its identity in the process of drying. The image of $CaCO_3$@Cur-FA microparticles is shown in **Figure 1D**.

TABLE 1 | Characterization of $CaCO_3$, $CaCO_3$@Cur-FA-1, $CaCO_3$@Cur-FA-2, $CaCO_3$@Cur-FA-3.

Nanoparticles	Size	PDI	Zeta (mV)
$CaCO_3$	1070.1 ± 76	0.205 ± 0.009	4.75 ± 0.34
$CaCO_3$@Cur-FA-1	1303.5 ± 66	0.208 ± 0.010	−12.34 ± 1.23
$CaCO_3$@Cur-FA-2	1464.8 ± 58	0.222 ± 0.012	−13.45 ± 3.08
$CaCO_3$@Cur-FA-3	1460.7 ± 72	0.225 ± 0.010	−12.14 ± 1.19

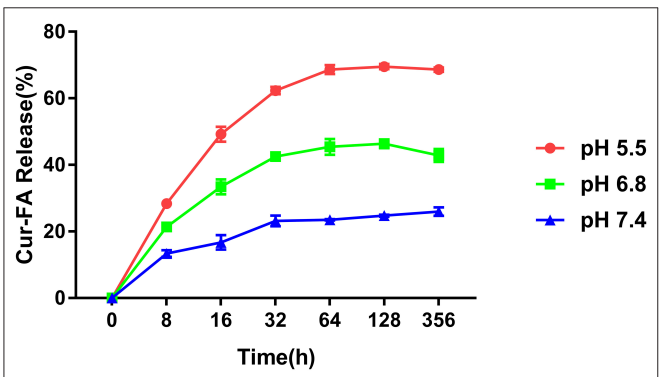

FIGURE 2 | pH sensitivity of CaCO3@Cur-FA. Cur-FA was released from $CaCO_3$@Cur-FA at pH 7.4, 6.8, and 5.5.

pH Sensitivity of $CaCO_3$@Cur-FA2 Microparticles

The pH sensitivity of $CaCO_3$@Cur-FA2 microparticles was evaluated in PBS of pH 7.4, 6.8, and 5.5. As shown in **Figure 2**, $CaCO_3$@Cur-FA2 released only 24.5% of loaded Cur-FA2 at pH 7.4 after 128 h. On the contrary, 70.1 and 45.6% of Cur-FA2 was released from $CaCO_3$@Cur-FA2 at pH 5.5 and 6.8, respectively, which was associated with $CaCO_3$ decomposition under the acidic condition. The results demonstrated that $CaCO_3$@Cur-FA could be used as a food additive with a visible pH sensitivity.

Antioxidant Activity of $CaCO_3$@Cur-FA2 Microparticles

Antioxidant activity plays a vital role in the food industry. It is the ability of inhibiting or delaying additional molecular oxidation (14). Previous results have demonstrated that Cur

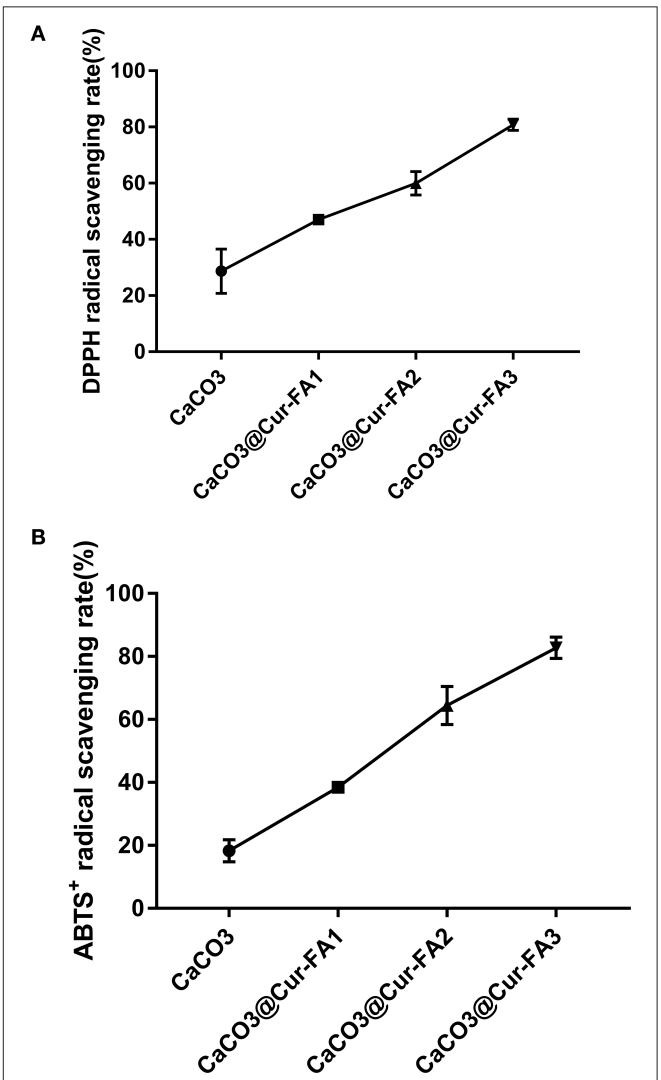

FIGURE 3 | Abilities of $CaCO_3$ and $CaCO_3$@Cur-FA to scavenge DPPH **(A)** and $ABTS^+$ **(B)** radicals.

TABLE 2 | Bacteriostatic activity of films.

Items	*Escherichia coli*	*Escherichia coli*	*Aspergillus niger*	*Rhizopus*
$CaCO_3$	8.2 ± 0.2^{d}	7.1 ± 0.3^{c}	10.5 ± 0.4^{d}	4.2 ± 0.1^{d}
$CaCO_3$@Cur-FA1	13.2 ± 0.3^{a}	8.3 ± 0.2^{b}	12.5 ± 0.6^{cd}	4.3 ± 0.5^{b}
$CaCO_3$@Cur-FA2	14.3 ± 0.4^{a}	9.1 ± 0.3^{b}	13.1 ± 0.4^{b}	5.1 ± 0.4^{bc}
$CaCO_3$@Cur-FA3	14.6 ± 0.2^{a}	9.3 ± 0.4^{a}	13.6 ± 0.3^{a}	5.6 ± 0.3^{a}

Comparison of differences between groups (a, b, c, and d).

(15) and FA (16) have very high antioxidant activity because of phenolic hydroxyl groups in their molecular structure. In our previous study, the antioxidant activity of Cur ester derivatives was shown to be significantly increased. A higher Cur-FA level resulted in the higher antioxidant activity of the Cur-FA film. The DPPH scavenging activity of $CaCO_3$@Cur-FA1 microparticles was increased three times compared with that of $CaCO_3$ microparticles (**Figure 3A**). The $ABTS^{+}$ scavenging ability of CaCO3@Cur-FA was similar to the DPPH scavenging ability (**Figure 3B**). The free radical scavenging ability of $CaCO_3$@Cur-FA microparticles was increased by 40% compared with that of $CaCO_3$ microparticles. Thus, $CaCO_3$@Cur-FA exhibited good antioxidant ability.

Antimicrobial Activity

$CaCO_3$@Cur-FA exhibited antimicrobial activity, which is significant for its application as a food additive (16). In the present work, we adopted the agar–well diffusion method to detect the ability of $CaCO_3$@Cur-FA to inhibit *Rhizopus*, *A. niger*, *E. coli*, *and S. aureus*, and the inhibition zones were found to be 5.6 ± 0.3, 13.6 ± 0.3, 14.6 ± 0.2, and 9.3 ± 0.4 mm, respectively (**Table 2**). Thus, $CaCO_3$@Cur-FA inhibited the growth of these pathogens. $CaCO_3$@Cur-FA microparticles demonstrated superior antimicrobial activity than $CaCO_3$ microparticles, indicating that adding $CaCO_3$ promoted the antimicrobial activity of Cur-FA.

CONCLUSION

A novel food additive comprising Cur-FA was designed and synthesized in this study. Herein, we successfully engineered a simple, efficient, well-characterized, and stable $CaCO_3$@Cur-FA nano-microemulsion as a food additive. The results demonstrated that $CaCO_3$@Cur-FA is a natural antimicrobial food additive with excellent antioxidant effects. The antimicrobial activity of $CaCO_3$@Cur-FA was irreversibly changed with the change in the environmental pH, and our results demonstrated that CaCO3@Cur-FA could be used as a food additive with a visible pH sensitivity, therefore, it could be used as an antibacterial preservative, or as a protective agent for some drugs that are easy to be damaged by gastric acid. Additionally, $CaCO_3$ enhanced the antimicrobial and antioxidant activities of Cur-FA. In conclusion, $CaCO_3$@Cur-FA is a natural material with high safety and degradability and may be extensively used as a food additive.

DATA AVAILABILITY STATEMENT

The original contributions presented in the study are included in the article/supplementary material, further inquiries can be directed to the corresponding authors.

AUTHOR CONTRIBUTIONS

LW and ZZ: research concept, methodology, data extraction, analysis, and draft writing. YY: resource searching, verification, formal analysis, supervision, and manuscript reviewing and editing. XW and DL: resources, methodology, project administration, supervision, and manuscript reviewing and editing. ZG: resource searching and manuscript reviewing and editing. Mengying Xia: methodology and manuscript reviewing and editing. All authors reviewed and approved the final manuscript.

FUNDING

The present work was funded by the National Natural Science Foundation of China (Grant Nos. 31602098 and 32072906), the Scientific and Technological Project of Henan Province (Grant Nos. 192102110188 and 192102110184), the Postgraduate Research and Practice Innovation Program of Jiangsu Province (Grant No. KYCX20-1494), the Veterinary Drugs Science Subject in Henan University of Animal Husbandry and Economy (Grant No. 41000003), the Scientific Research and Innovation Team in Henan University of Animal Husbandary and Economy (Grant No. 2018KYTD18), and the Science and Technology Major project of Prevention and Treatment of Major Infectious Diseases such as AIDS and Viral Hepatitis: Research on new technology of integrated field rapid detection of important viruses (Grant No. ZX10711001-003-003).

REFERENCES

1. Wang Y, Pan M, Cheng A, Lin L, Ho Y, Hsieh C, et al. Stability of curcumin in buffer solutions and characterization of its degradation products. *J Pharm Biomed Anal.* (1997) 15:1867–76. doi: 10.1016/S0731-7085(96)02024-9

2. Ashrafizadeh M, Zarrabi A, Hashemi F, Zabolian A, Saleki H, Bagherian M, et al. Polychemotherapy with curcumin and doxorubicin via biological nanoplatforms: enhancing antitumor activity. *Pharmaceutics.* (2020). 12:1084. doi: 10.3390/pharmaceutics1211 1084

3. Jennings M, Parks R. Curcumin as an antiviral agent. *Viruses.* (2020) 12:1242. doi: 10.3390/v12111242
4. Kunnumakkara A, Bordoloi D, Padmavathi G, Monisha J, Roy N, Prasad S, et al. Curcumin, the golden nutraceutical: multitargeting for multiple chronic diseases. *Br J Pharmacol.* (2017) 174:1325–48. doi: 10.1111/bph.13621
5. Seczyk Ł, Sugier D, Swieca M, Gawlik-Dziki U. The effect of *in vitro* digestion, food matrix, and hydrothermal treatment on the potential bioaccessibility of selected phenolic compounds. *Food Chem.* (2020) 344:128581. doi: 10.1016/j.foodchem.2020.128581
6. Dhayanandamoorthy Y, Antoniraj M, Kandregula C, Kandasamy R. Aerosolized hyaluronic acid decorated, ferulic acid loaded chitosan nanoparticle: a promising asthma control strategy. *Int J Pharm.* (2020) 591:119958. doi: 10.1016/j.ijpharm.2020.119958
7. Houghton C. Sulforaphane: its "coming of age" as a clinically relevant nutraceutical in the prevention and treatment of chronic disease. *Oxid Med Cell Longev.* (2019) 2019:2716870. doi: 10.1155/2019/2716870
8. Kah M, Tufenkji N, White J. Nano-enabled strategies to enhance crop nutrition and protection. *Nat Nanotechnol.* (2019) 14:532–40. doi: 10.1038/s41565-019-0439-5
9. Kranjc E, Drobne D. Nanomaterials in plants: a review of hazard and applications in the agri-food sector. *Nanomaterials (Basel, Switzerland).* (2019) 9:1094. doi: 10.3390/nano9081094
10. C, Jin E, Lee J, Hwang E. Immobilization and stabilization of enzyme in biomineralized calcium carbonate microspheres. *Front Bioeng Biotechnol.* (2020) 8:553591. doi: 10.3389/fbioe.2020.553591
11. Lee D, Oh J, Uhm J, Kim I, Park M, Moon S, et al. Impact of acidity regulator and excipient nutrients on digestive solubility and intestinal transport of calcium from calcium phosphate and carbonate. *Food Funct.* (2020) 11:10655–64. doi: 10.1039/D0FO02035D
12. Binevski P, Balabushevich N, Uvarova V, Vikulina A, Volodkin D. Bio-friendly encapsulation of superoxide dismutase into vaterite CaCO crystals. Enzyme activity, release mechanism, and perspectives for ophthalmology. *Colloids Surf B Biointerfaces.* (2019) 181:437–49. doi: 10.1016/j.colsurfb.2019.05.077
13. Hwang Y, Ramalingam K, Bienek D, Lee V, You T, Alvarez R. Antimicrobial activity of nanoemulsion in combination with cetylpyridinium chloride in multidrug-resistant Acinetobacter baumannii. *Antimicrob Agents Chemother 57.* (2013) 3568–75. doi: 10.1128/AAC.02109-12
14. Yadav S, Mehrotra G, Dutta P. Chitosan based ZnO nanoparticles loaded gallic-acid films for active food packaging. *Food Chem.* (2021) 334:127605. doi: 10.1016/j.foodchem.2020.127605
15. Wang Y, Zhang L, Wang P, Xu X, Zhou G. pH-shifting encapsulation of curcumin in egg white protein isolate for improved dispersity, antioxidant capacity and thermal stability. *Food Res Int (Ottawa, Ont).* (2020) 137:109366. doi: 10.1016/j.foodres.2020.109366
16. Zhang L, Zhang Z, Chen Y, Ma X, Xia M. Chitosan and procyanidin composite films with high antioxidant activity and pH responsivity for cheese packaging. *Food Chem.* (2021) 338:128013. doi: 10.1016/j.foodchem.2020.128013

Conflict of Interest: The authors declare that the research was conducted in the absence of any commercial or financial relationships that could be construed as a potential conflict of interest.

Publisher's Note: All claims expressed in this article are solely those of the authors and do not necessarily represent those of their affiliated organizations, or those of the publisher, the editors and the reviewers. Any product that may be evaluated in this article, or claim that may be made by its manufacturer, is not guaranteed or endorsed by the publisher.

frontiers | Frontiers in Veterinary Science

ORIGINAL RESEARCH
published: 15 September 2022
doi: 10.3389/fvets.2022.891157

Glycerol Monolaurate to Ameliorate Efficacy of Inactivated Pseudorabies Vaccine

Qinghai Ren[1,2,3,4], *Xiaobo Wang*[2,3,4], *Qingqing Gao*[2,3,4], *Gaiqin Wang*[5], *Xiaochen Chen*[5], *Chunxue Liu*[5], *Song Gao*[2,3,4] *and Yubao Li*[1]*

[1] College of Agronomy and Agricultural Engineering, Liaocheng University, Liaocheng, China, [2] Key Laboratory of Avian Bioproducts Development, Ministry of Agriculture, Yangzhou, China, [3] Jiangsu Co-innovation Center for Prevention and Control of Important Animal Infectious Diseases and Zoonoses, Yangzhou, China, [4] Institutes of Agricultural Science and Technology Development, College of Veterinary Medicine, Yangzhou University, Yangzhou, China, [5] Anyou Biotechnology Group Co., Ltd., Taicang, China

The present study is aimed to evaluate the effect of glycerol monolaurate (GML) on the growth performance and immune enhancement of pseudorabies virus (PRV)-inactivated vaccine in the early-weaned piglets. One hundred and twenty-five 28-day-old weaned piglets were randomly assigned to a control group (CON, no vaccine and no challenge), challenge control group (C-CON), inactivated PRV vaccine group (IPV), IPV + 500 mg/kg GML group (L-GML), and IPV + 1,000 mg/kg GML group (H-GML) during the entire 28-day experimental period. All the data analyses were performed by one-way analysis of variance (ANOVA) and multiple comparisons. Our results showed that the final weight, average daily gain (ADG), and average daily feed intake (ADFI) of H-GML were the highest in each group, and F/G of H-GML was increased but there was no significant difference with CON ($p > 0.05$). Levels of PRV glycoprotein B (gB) antibody and immunoglobulin in serum of L-GML and H-GML were higher than those of IPV, but only gB antibody levels and immunoglobulin G (IgG) in H-GML were significantly increased ($p < 0.05$). Compared with IPV, the contents of tumor necrosis factor-α (TNF-α), interleukin-6 (IL-6), and interleukin-1β (IL-1β) in serum of L-GML (TNF-α and IL-1β: $p > 0.05$, IL-6: $p < 0.05$, respectively) and H-GML ($p < 0.01$, both) were all decreased, and the content of interleukin-10 (IL-10) in H-GML was increased ($p > 0.05$). Furthermore, reverse transcription-polymerase chain reaction (RT-PCR) experiments proved that L-GML and H-GML were both superior to IPV in inhibiting the expression of TNF-α ($p < 0.01$), IL-6 ($p > 0.05$), and IL-1β ($p < 0.01$) mRNAs and promoting the expression of IL-10 mRNA (L-GML: $p > 0.05$, H-GML: $p < 0.05$, respectively) in the superficial inguinal lymph nodes. Histopathological examination found mild congestion in the lung and inguinal lymph nodes of IPV, while the tissues (brain, lung, and inguinal lymph nodes) of L-GML and H-GML were the same as CON with no obvious lesions. The above results indicate that GML may improve the growth performance of weaned piglets and enhance the immunity of PRV-inactivated vaccine by increasing the levels of PRV gB antibody and immunoglobulin and regulating cytokine levels.

Keywords: glycerol monolaurate, pseudorabies virus, inactivated vaccine, immune enhancement, weaned piglets

OPEN ACCESS

Edited by:
Ambreen Ashar, University of Agriculture, Faisalabad, Pakistan

Reviewed by:
Muhammad Akbar Shahid, Bahauddin Zakariya University, Pakistan
Amjad Islam Aqib, Cholistan University of Veterinary and Animal Sciences, Pakistan

***Correspondence:**
Yubao Li
liyubao@lcu.edu.cn

Specialty section:
This article was submitted to Veterinary Infectious Diseases, a section of the journal Frontiers in Veterinary Science

Received: *07 March 2022*
Accepted: *06 May 2022*
Published: *15 September 2022*

Citation:
Ren Q, Wang X, Gao Q, Wang G, Chen X, Liu C, Gao S and Li Y (2022) Glycerol Monolaurate to Ameliorate Efficacy of Inactivated Pseudorabies Vaccine. Front. Vet. Sci. 9:891157. doi: 10.3389/fvets.2022.891157

INTRODUCTION

Pseudorabies (PR), also called Aujeszky's disease (AD), is a highly contagious porcine infectious disease caused by pseudorabies virus (PRV), which causes substantial economic losses to the swine agriculture worldwide (1, 2). PRV is a linear double-stranded DNA virus that belongs to the family *Herpesviridae*, subfamily *Alphaherpesvirinae*, and genus *Varicellovirus* (3). Swine are the natural host and reservoir of PRV (4). PRV-infected pigs excreted large amounts of viruses in bodily secretions and excreta (5). Morbidity, mortality, and clinical symptoms of PRV infection in pigs vary with the age (3). For example, neurological signs and high mortality in piglets, respiratory illness, and growth retardation in growing-finishing pigs, as well as abortions or stillbirths in pregnant sows caused by PRV infection (3, 5, 6). At present, the prevention of PRV in China is mainly *via* immunization of gE-deleted live-attenuated vaccines (Bartha-K61 vaccine), which were imported from Hungary in the 1970s (7). Since the widespread application of the vaccine, the morbidity and mortality of newborn piglets in the infected herd have been significantly reduced (8). However, in late 2011, variant PRV strains that appeared in pig farms were vaccinated with Bartha-K61 in China (9, 10). Variant PRV showed strong pathogenicity to pigs of all ages, the Bartha-K61 vaccine did not provide effective protection in the swine industry (7, 11). Studies have shown that the cross-protection ability of the classical live-attenuated vaccines to the variant PRV strains is limited due to the change of antigenicity (7). It is necessary to develop an inactivated vaccine that can effectively resist the variant strain of PRV. Compared with live-attenuated vaccines, inactivated vaccines are safer but cannot induce cellular immune responses, and cellular immunity played a crucial role in PRV protective immunity (12). Therefore, it is of great clinical significance to study methods to improve the immune effect of inactivated vaccines and enhance the disease resistance of swine.

Glycerol monolaurate (GML), which is the monoglyceride derivative of lauric acid that is generally considered to be more biologically potent than medium-chain fatty acid (MCFA) *in vitro*, naturally existed in the breast milk and coconut oil (13, 14). It not only has excellent emulsification properties but also has a strong ability to inhibit the growth and proliferation of gram-positive bacteria and enveloped viruses *in vitro*, as well as the production of bacterial virulence factors (15–17). The results of Thomas et al. showed that adding GML and 1.0% 1:1:1 MCFA had the same effect, which could significantly improve the average daily gain (ADG), average daily feed intake (ADFI), and gain to feed ratio (G:F) of nursery pigs, when compared with pigs fed a control diet (18). Ghalib found that 4 g/kg of GML significantly increases body weight gain (BWG) and food conversion ratio, improvement of pro-inflammatory cytokines (tumor necrosis factor-α [TNF-α] and interleukin [IL]-12), and total antioxidant capacity (TAC) (19). Liu et al. demonstrated that dietary GML improved performance, intestinal morphology, and muscle amino acids in broilers *via* manipulating community, function, and metabolites of gut microbiota (20).

Currently, there were a few studies on GML as an immune enhancer to improve the effect of inactivated vaccines. The purpose of this experiment was to study the enhancement effect of oral GML in weaned piglets on the immunity of PRV-inactivated vaccine and provide a reference for using MCFAs and derivatives to improve the immune effect of inactivated vaccine in the clinic.

MATERIALS AND METHODS

Ethics Statement

All animal procedures related to experiment were carried out in strict accordance with the animal care and ethical standards, approved by the ethics committee of Yangzhou University (Jiangsu province, China). All efforts were made to reduce the suffering of animal.

Animal Experiment Design

One hundred and twenty-five weaned piglets (D × L × Y, 28-day old) were randomly distributed to 5 treatment groups: the control group (CON, no vaccine and no challenge), challenge control group (C-CON), inactivated PRV vaccine group (IPV), IPV + 500 mg/kg GML group (L-GML), and IPV + 1,000 mg/kg GML group (H-GML). Each group consisted of 5 replications per group, 5 piglets per replication. Entire experimental period lasted for 28 days, feed and water were available *ad libitum*. All piglets were adapted to the environment for 1 week. Except for CON and C-CON, the other groups were immunized with PRV-inactivated vaccine on the 7 day of the experiment. On the 14th day, a challenge test was conducted (except CON), and the challenge dose was 1×10^6 Median Tissue Culture Infectious Dose ($TCID_{50}$; vPRV/XJ5 strain from our laboratory). The animal experiment design of this article is presented in **Table 1**. The basic diet was prepared according to the National Research Council (21) without antibiotics or medicine. The feeding conditions, management, and sanitary environment of all experimental piglets are the same. Daily temperature measurement and clinical symptom observation were performed after the challenge. On the 28th day of the test, blood was collected from the anterior vena cava. After clotting, the blood was centrifuged at 3,500 r/min for 20 min to separate the serum. At the same time, the piglets were dissected, the corresponding tissues were taken out, and stored at −80°C together with the serum until use.

TABLE 1 | Animal experimental design.

Group	Diet	Vaccine	Challenge
CON	basic diet	unvaccinated	unchallenged
C-CON	basic diet	unvaccinated	challenged vPRV/XJ5 strain (day 14)
IPV	basic diet	PRV inactivated vaccine (day 7)	challenged vPRV/XJ5 strain (day 14)
L-GML	basic diet+ 500 mg/kg GML	PRV inactivated vaccine (day 7)	challenged vPRV/XJ5 strain (day 14)
H-GML	basic diet+ 1000 mg/kg GML	PRV inactivated vaccine (day 7)	challenged vPRV/XJ5 strain (day 14)

Measurement on Growth Performance

The piglets were weighed at the beginning and end of the experiment and fasted for 8 h before weighing. BWG and feed intake (FI) were recorded weekly for the piglets in each group. Calculated the ADG according to the initial weight and final weight of the piglets, calculated the ADFI according to the feed consumption, and finally the ratio of feeds to weight (F/G) was calculated.

Blood Analysis

According to the manufacturer's instructions of PRV glycoprotein B (gB) antibody detection kit (IEDXX, USA), the level of specific PRV gB antibody in serum was detected by blocking enzyme linked immunosorbent assay (ELISA). Blocking rate of PRV gB antibody = [1 – S (value of sample D_{450nm})/N (value of negative control D_{450nm})] × 100%. The serum levels of immunoglobulin [immunoglobulin G (IgG), immunoglobulin A (IgA), and immunoglobulin M (IgM)] were determined using ELISA kits that were purchased from Shanghai Fusheng Industrial Co., Ltd. (Shanghai, China). Serum cytokines (TNF-α, IL-6, IL-1β, and IL-10) were measured using the double antibody sandwich method of ELISA, according to the instructions (Abcam, United Kingdom).

Fluorescence Quantitative RT-PCR Analysis

According to the manufacturer's instructions, the total RNA in the inguinal lymph nodes was extracted using RNAprep Pure Tissue Kit (Tiangen Biotech Co., Ltd., China). Then, 1 μg of RNA was reverse transcribed into cDNA from total RNA using a PrimeScript™ RT Master Mix (Perfect Real Time) Kit (Takara Biomedical Technology Co., Ltd., China). The primer sequences for TNF-α, IL-6, IL-1β, IL-10, and glyceraldehyde-3-phosphate dehydrogenase (GAPDH) are represented in **Table 2**. Reactions of qRT-PCR were run with the AceQ® qPCR SYBR® Green Master Mix Kit (Vazyme Biotech Co., Ltd., China), according to the instructions of the manufacturer. The PCR amplification parameters were 95°C for 5 min followed by 40 cycles of 95°C for 10 s and 60°C for 30 s. GAPDH gene was served as the internal reference to normalize target gene expression levels. The relative fold-change in the expression of target genes was calculated by the 2–ΔΔCt (Ct: cycle threshold) method. The abundance of mRNA transcripts per sample was evaluated three times.

Histopathological Analysis

Tissues of brain, lung, and superficial inguinal lymph nodes were fixed in 4% paraformaldehyde for 24 h and embedded in paraffin (22). The paraffin section was cut into slices of 5 μm, stained with hematoxylin and eosin (H&E). Histopathological examination of the piglet tissues was performed using light microscope (OLYMPUS, Japan).

Statistical Analysis

All data are expressed as mean ± standard deviation (mean ± SD). The data were analyzed by one-way analysis of variance (one-way ANOVA), followed by least significant difference (LSD) multiple comparison tests with SPSS version 21.0 (SPSS Inc., Chicago, IL, USA) (23). Difference between samples was considered to be significant when $p < 0.05$. GraphPad Prism 8 (GraphPad Software Inc. San Diego, CA, USA) was used for statistical analysis (22).

TABLE 2 | Primer sequences used for the reverse transcription-polymerase chain reaction (RT-PCR) analysis.

Primer name	Sequence (5′-3′)	Product size (bp)	Genbank accession number
TNF-α	F: AGACACCATGAGCACTGAGAGCAT R: GAAGTGCAGTAGGCAGAAGAGCGT	166	X 57321.1
IL-6	F: CAGGAACGAAAGAGAGCTCCATCT R: TCACCTTTGGCATCTTCTTCCAG	159	NM 214399.1
IL-1β	F: CTACCCTCTCCAGCCAGTCTTCATT R: GCCATCAGCCTCAAATAACAGGTC	130	NM 214055.1
IL-10	F: GAAGCTCACAACTCCGAAGGAATC R: ATCGAGGGAGCCAGAATTGGTC	132	JQ 687536.1
GAPDH	F: TCAAGATCGTCAGCAATGCCTC R: GGTAGAAGCAGGGATGATGTTCTG	203	NM 001206359.1

RESULTS

Growth Performance

As shown in **Table 3**, there is no significant difference in the initial weight of each group ($p > 0.05$). In C-CON, IPV, and L-GML, the final weight was lower than CON, but only C-CON had a significant difference ($p < 0.05$). The final weight of H-GML was the highest in each group, there was no significant difference with CON ($p > 0.05$). In terms of weight gain, both H-GML and L-GML were significantly higher than C-CON and IPV ($p < 0.05$), and HGML was even higher than CON, but the difference was not significant ($p > 0.05$). Compared with CON, ADG and ADFI in C-CON and IPV were decreased significantly ($p < 0.05$). In addition, ADG and ADFI of L-GML were reduced but the differences were not significant ($p > 0.05$), while H-GML was increased instead ($p > 0.05$). An increase in F/G was found ($p < 0.05$) in C-CON when compared with CON piglets, whereas there was no significant effect on the F/G of piglets from IPV, L-GML, and H-GML ($p > 0.05$).

PRV gB Antibody Levels

Figure 1 shows that there is no significant difference in PRV gB antibody levels of each group at the first week ($p > 0.05$). Compared with CON, the levels of PRV gB antibody in IPV, L-GML, and H-GML were extremely significantly higher than those in C-CON ($p < 0.001$) from the second week to the end of the experiment. Moreover, the antibody levels of L-GML and H-GML were both higher than IPV, but only H-GML had a significant difference ($p < 0.05$).

Serum Levels of Immunoglobulin

As shown in **Figure 2**, the serum IgG content of C-CON is extremely significantly higher than CON ($p < 0.001$). Except that the serum IgG content of IPV was significantly higher than

TABLE 3 | The effects of different treatments on growth performance of weaned piglets.

Item	CON	C-CON	IPV	L-GML	H-GML
Initial weight (kg)	7.65 ± 0.37	7.73 ± 0.40	7.82 ± 0.44	7.67 ± 0.42	7.62 ± 0.39
Final weight (kg)	21.69 ± 3.09^{a}	18.91 ± 2.44^{b}	19.81 ± 2.90^{ab}	20.59 ± 3.63^{ab}	22.07 ± 3.21^{a}
Weight gain (kg)	14.04 ± 2.08^{a}	11.18 ± 2.46^{b}	11.99 ± 2.93^{b}	12.92 ± 3.77^{ab}	14.45 ± 3.18^{a}
ADG (kg)	0.50 ± 0.11^{a}	0.40 ± 0.09^{b}	0.43 ± 0.10^{b}	0.46 ± 0.13^{ab}	0.52 ± 0.11^{a}
ADFI (kg)	0.88 ± 0.22^{a}	0.78 ± 0.18^{b}	0.80 ± 0.19^{b}	0.84 ± 0.23^{ab}	0.92 ± 0.23^{ab}
F/G	1.76 ± 0.11^{a}	1.94 ± 0.12^{b}	1.88 ± 0.10^{ab}	1.83 ± 0.12^{ab}	1.78 ± 0.13^{a}

Values with different letter superscripts mean significant difference ($p < 0.05$). No letter or the same letter superscripts represent no significant difference ($p > 0.05$).

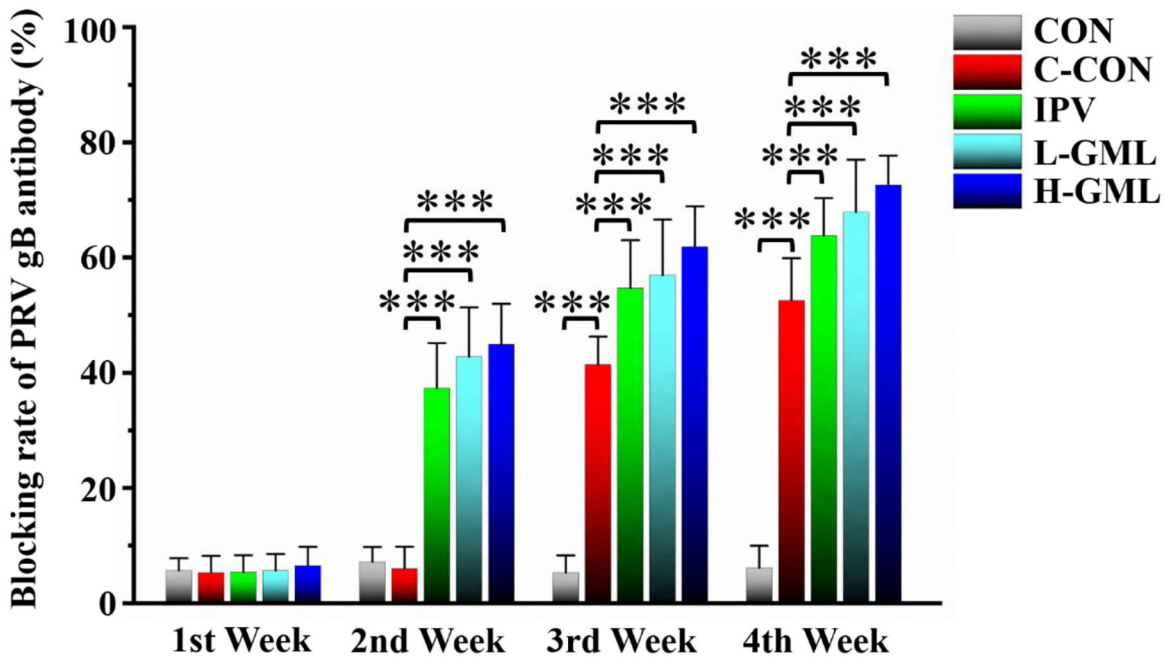

FIGURE 1 | Pseudorabies virus glycoprotein B (PRV gB) antibody levels in serum of experimental pigs. The results are presented as mean ± SD. Dissimilar numbers of stars represent significant differences (*: $p < 0.05$, **: $p < 0.01$, ***: $p < 0.001$).

C-CON ($p < 0.05$), both L-GML and H-GML were extremely significantly higher than C-CON ($p < 0.001$). Although the levels of IgA and IgM in the serum of IPV, L-GML, and H-GML were higher than those of C-CON, there was no obvious difference among the groups ($p > 0.05$).

Serum Levels of Cytokines

The results showed that TNF-α level in serum of the piglets from CON was significantly reduced ($p < 0.05$) and the other groups were extremely significantly decreased ($p < 0.001$), when compared with the C-CON (**Figure 3A**). At the levels of IL-6 and IL-1β, no differences between IPV and C-CON were observed ($p > 0.05$) but the other groups were extremely significantly lower than C-CON ($p < 0.01$, **Figures 3B,C**). Except for IL-10 level of H-GML was significantly higher than that of C-CON ($p < 0.05$), there was no difference in the other groups ($p > 0.05$, **Figure 3D**).

Gene Expression of Cytokines

As presented in **Figure 4**, piglets from C-CON have obvious significantly increased TNF-α, IL-6, and IL-1β mRNAs in the superficial inguinal lymph nodes ($p < 0.001$), when compared with other groups. Although there was no statistical significant in the mRNA expression level of IL-6 ($p > 0.05$), the mRNAs of TNF-α and IL-1β in L-GML and H-GML were extremely significantly higher than those of IPV ($p < 0.001$, **Figures 4A–C**). Compared with C-CON, IL-10 mRNAs in IPV, L-GML, and H-GML were increased, and the differences were all significant ($p < 0.05$), but a significant decrease in CON was found ($p < 0.01$, **Figure 4D**).

Histopathological Analysis

As shown in **Figure 5**, the brain is congested, and there is mild-to-moderate lymphocyte infiltration around the blood vessels, forming a lymphocytic vascular cuff in C-CON. In addition, the pulmonary veins from the tissues of C-CON were congested

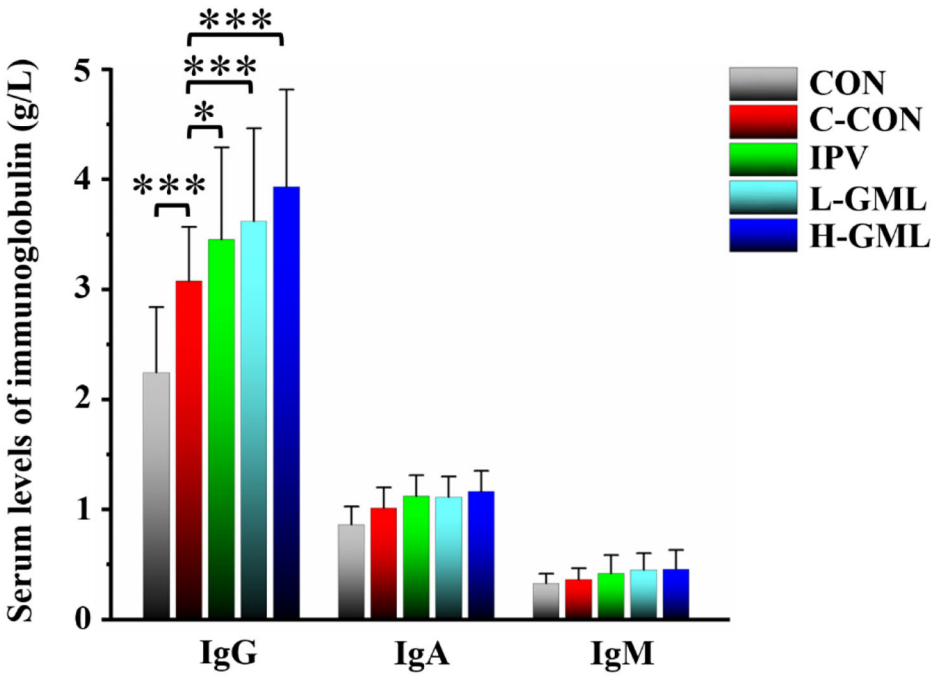

FIGURE 2 | Levels of immunoglobulin G (IgG), immunoglobulin G (IgA), and immunoglobulin G (IgM) in serum of experimental pigs. The results are presented as mean ± SD. Dissimilar numbers of stars represent significant differences (*: $p < 0.05$, **: $p < 0.01$, ***: $p < 0.001$).

extensively, and there was bleeding into the inguinal lymph nodes. In IPV, no lesions were observed in the brain, but there was mild congestion in the lungs and inguinal lymph nodes, and a few lymphocytes in the lymph nodes were necrotic. The tissues of CON, L-GML, and H-GML showed no obvious pathological changes.

DISCUSSION

Pseudorabies virus is prevented and controlled by the use of vaccination with attenuated live and inactivated vaccines (24). Attenuated live vaccine played a key role in the attempt to control or even eradicate PR (25–28). However, safety is one of the most important indicators for evaluating qualified vaccines. Kong et al. found that attenuated live vaccine (Bartha-K16) caused an outbreak of PR in sheep (29). Attenuated live vaccine, because of incomplete attenuation and reversion to pathogenic virus, would lead to disease outbreaks in severe cases (30, 31). Unfortunately, severe PR outbreaks took place in pigs vaccinated with Bartha-K61 vaccine in China, indicating that the PRV variant has proved to be more virulent (32–35). Therefore, inactivated vaccines were widely used in China, which can generate strong and durable specific antibodies in serum, and were safer than attenuated live vaccines (36, 37). However, inactivated vaccine had little ability to induce a cellular immune response in animals (38). This results in live vaccines often being more effective than inactivated preparations, especially when they contain high viral titers and are adjuvant (39). Thus, it is necessary to develop new methods to enhance the efficacy of inactivated vaccines against PRV, and it has become a trend of current research.

Combination of GML and Inactivated Vaccine Could Improve the Reduction of Piglet Growth Performance Caused by PRV

Recently, it has been reported that using inactivated vaccines, supplemented with adjuvants, can effectively enhance the immune effect of vaccines (38, 40). Yoo et al. found that muramyl dipeptide derivatives enhance immunogenicity of a hantavirus-inactivated vaccine (41). Rivera et al. reported that adding ginseng to the inactivated antigen of porcine parvovirus (PPV) could significantly increase amount of cytokines, specific antibody titers, and elicited a balanced Th1 and Th2 immune response in the serum of Balb/c mice (42). Sun et al. evaluated the immune-enhancing activity of polysaccharides from the Rhizoma of Atractylodis Macrocephalae Koidz (RAMPS), and the results showed that RAMPS could significantly enhance T lymphocyte proliferation (43). GML is not only an excellent food emulsifier but also a safe, efficient, and broad-spectrum bacteriostatic agent and has excellent antiviral function, which makes it a potential vaccine immune enhancer (17, 44–46). Therefore, the purpose of this experiment was to evaluate the immune-enhancing function of oral GML in weaned piglets on PRV-inactivated vaccine.

Studies have shown that MCFAs are more easily absorbed by newborn piglets than long-chain fatty acids (LCFAs) (47). MCFAs could directly supply energy for piglets and affect the composition of the gut microbiota through antibacterial

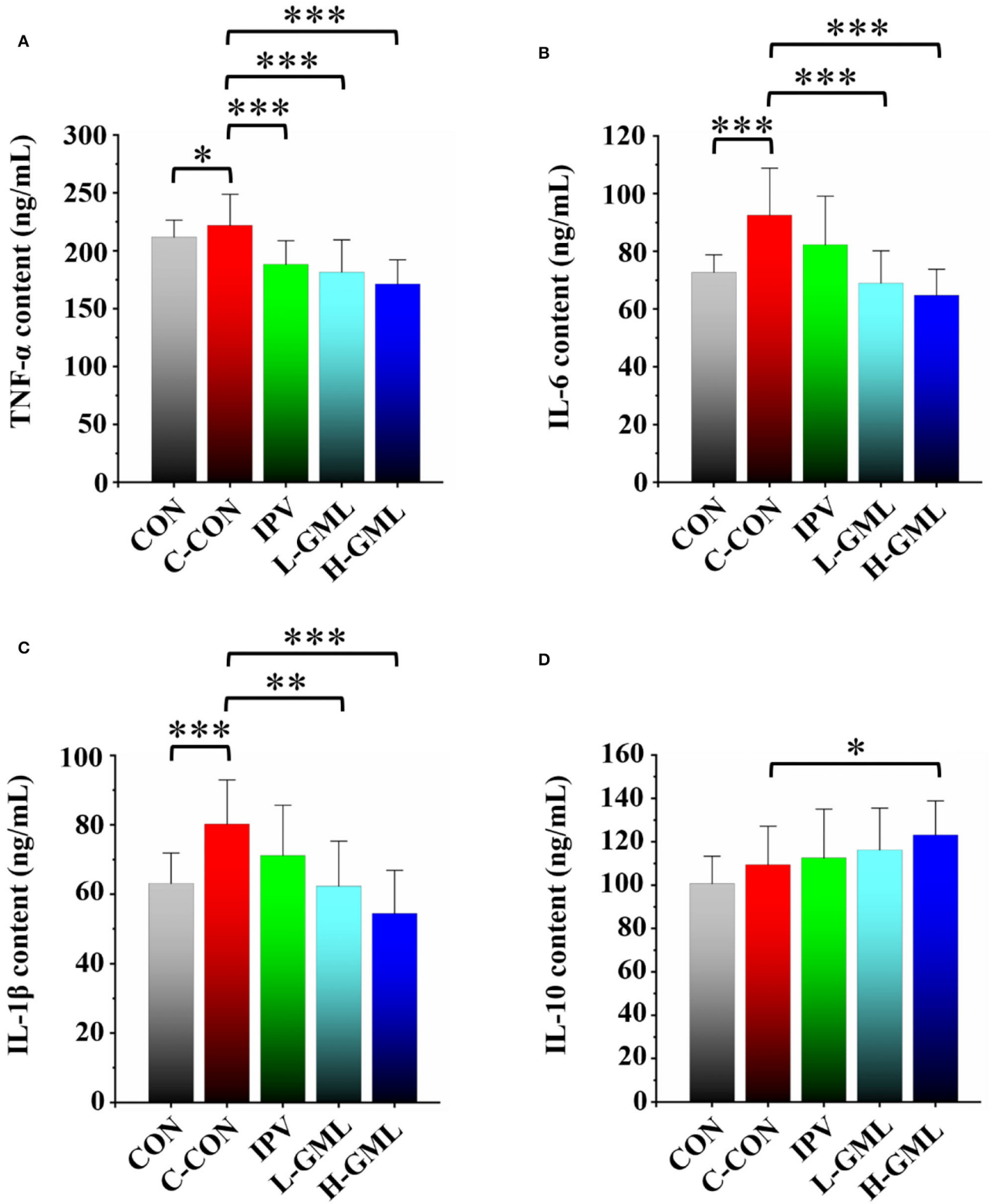

FIGURE 3 | Levels of cytokines **(A)** TNF-α, **(B)** IL-6, **(C)** IL-1β, and **(D)** IL-10 in serum of experimental pigs. Dissimilar numbers of stars represent significant differences (*: $p < 0.05$, **: $p < 0.01$, ***: $p < 0.001$).

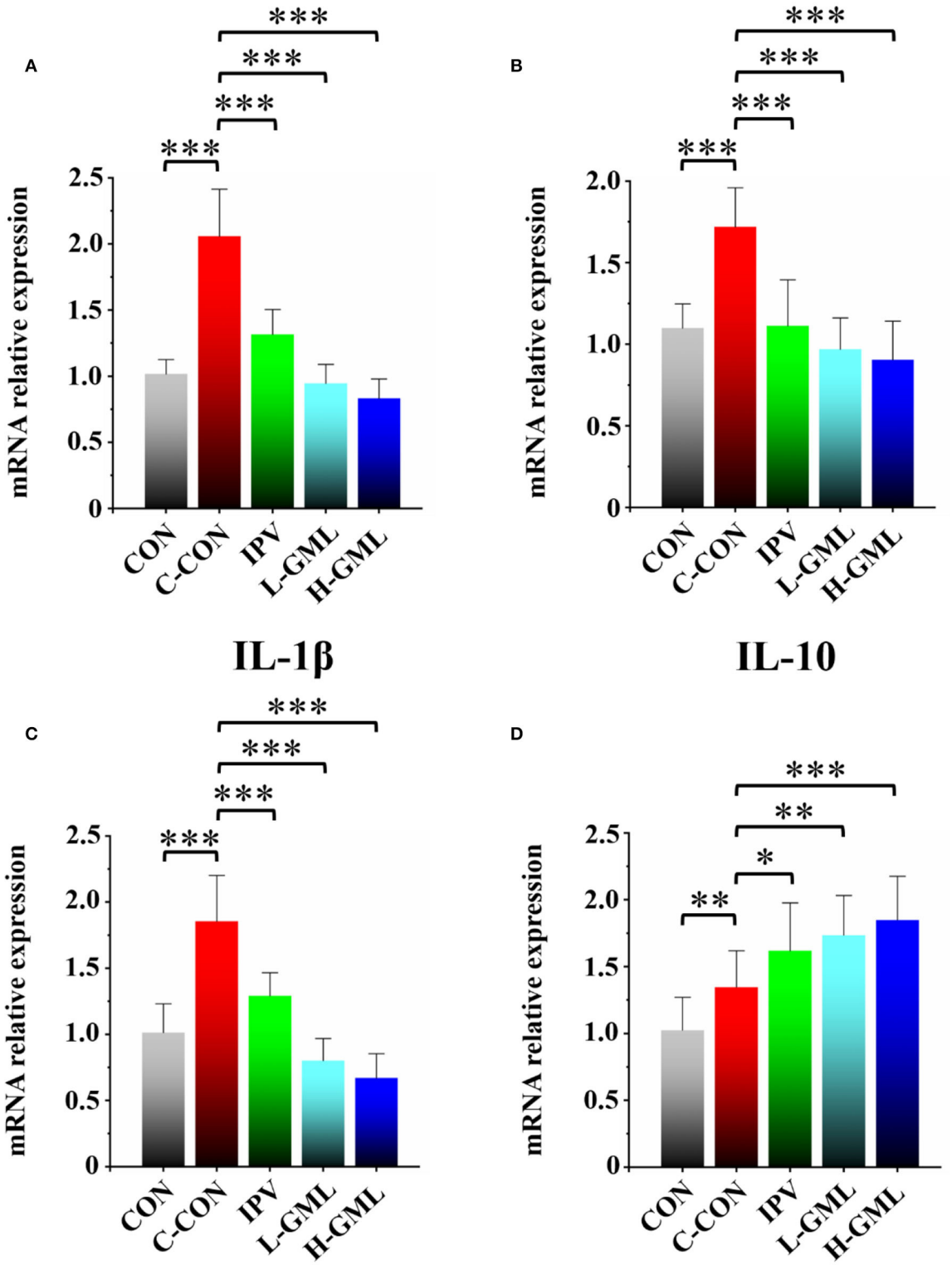

FIGURE 4 | Cytokine **(A)** TNF-α, **(B)** IL-6, **(C)** IL-1β, and **(D)** IL-10 level of the superficial inguinal lymph nodes of experimental pigs. Dissimilar numbers of stars represent significant differences (*: $p < 0.05$, **: $p < 0.01$, ***: $p < 0.001$).

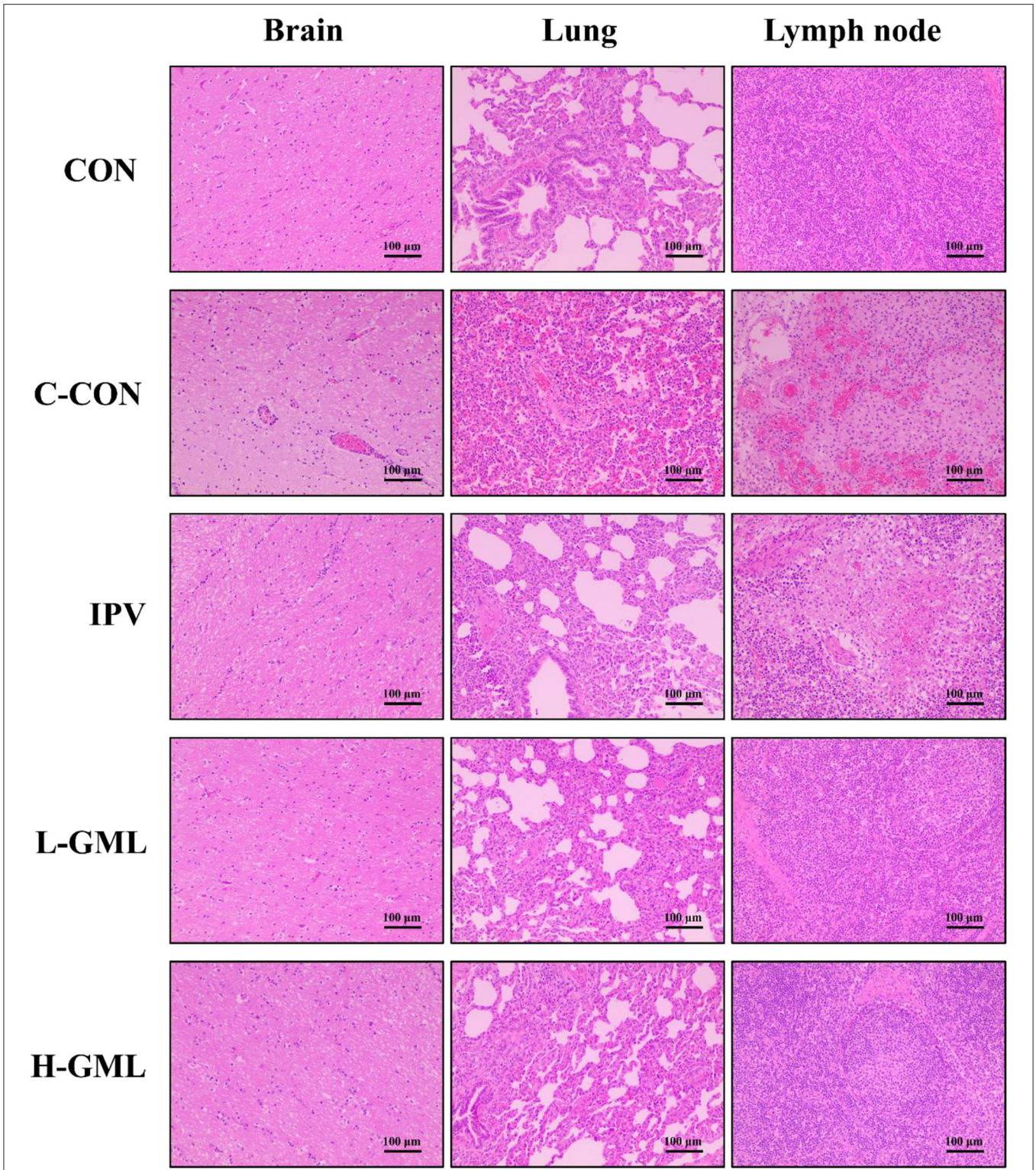

FIGURE 5 | Histopathological observations in the brain, lung, and superficial inguinal lymph nodes of experimental pigs.

properties, thereby improving the survival rate of weaned piglets and improving growth performance (48, 49). As a representative of MCFAs, GML could not only significantly improve the ADG, ADFI, and G:F of weaned piglets but could also increase the weight gain and food conversion ratio in chicks (18, 19). Our results showed that ADG of IPV ($p > 0.05$), L-GML ($p > 0.05$),

and H-GML ($p < 0.001$) was increased and F/G was decreased (IPV and L-GML: $p > 0.05$, H-GML $p < 0.001$, respectively), when compared with C-CON. Furthermore, the ADG of H-GML was the highest in each group. Although the F/G of H-GML was higher than that of CON, there was no significant difference ($p > 0.05$). Therefore, the above results showed that the combination of GML- and PRV-inactivated vaccine could significantly improve the reduction of piglet growth performance caused by PRV when compared with the single use of the vaccine.

GML Could Increase PRV gB Antibody Levels, the Immunoglobulin Content in Serum, and Regulate Cytokines in Serum and Lymph Nodes

Central to the membrane fusion event is gB, which is the most conserved envelope protein across the herpesvirus family (50). Previous studies showed that PRV gB was a major target of host immune defense due to its involvement in virus infection of cells (51, 52). Detection of PRV gB antibody levels in serum by ELISA could evaluate the overall immunity level of pigs and then guide vaccine immunization. In this study, we found that GML could enhance the immune effect of inactivated vaccines by increasing PRV gB antibody levels in serum. Ig is one of the major anti-infective components in blood, colostrum, and breast milk, protecting the body from harmful bacteria, viruses, and other environmental pathogens by either binding to them or forming an encapsulating barrier (53). Gomez et al. found that feeding porcine immunoglobulin could improve growth performance and survival in colostrum-deficient piglets (54). It could be seen that immunoglobulins were of great significance to enhance the immune ability and resistance to infection of piglets (55). Our results showed that levels of immunoglobulins in serum of L-GML and H-GML were higher than those of IPV, especially the levels of IgG in H-GML were significantly increased ($p < 0.05$). This study indicated that GML might assist the vaccine by increasing the immunoglobulin content in piglets to enhance humoral immunity, thereby improve the ability of piglets to resist PRV infection.

Cytokines as immunomodulatory proteins are secreted by a variety of cells, especially those involved in immune response, such as macrophages and T cells (56, 57). Researchers found that co-administrating of recombinant porcine interleukin-2 (IL-2) could enhance protective immune responses to PRV-inactivated vaccine in pigs (12). GML could modulate T-cell proliferation by affecting the cell signal cascade leading to the regulation of IL-2 production (15). In this study, our results showed that the addition of GML reduced the expression of pro-inflammatory cytokines (TNF-α, IL-6, and IL-1β) and increased the secretion of anti-inflammatory cytokine (IL-10) in piglet serum, when compared with the single use of inactivated vaccine. The lymphatic system plays an important role in host immune defense and body metabolism [57, 58]. Therefore, we collected the superficial inguinal lymph nodes of piglets to detect the differences in mRNA expression of cytokines. Our RT-PCR experiments demonstrated that the differences of cytokine mRNA expression in lymph nodes were similar to those of serum cytokines. The results suggested that GML could selectively regulate cytokine expression in serum and lymph nodes to improve the cellular immune function of piglets and the immune effect of the PRV-inactivated vaccine.

GML Could Cooperate With an Inactivated Vaccine to Prevent and Improve Histopathological Changes Caused by PRV

According to the previous research in our laboratory, the pathological lesions in challenge only pigs included dilated and congested blood vessels in the brain, a large number of eosinophils infiltrating the superficial inguinal lymph nodes and edema, congestion, hemorrhaging, and massive neutrophil infiltration in the alveolar space (22). Thus, in order to observe histopathological changes in piglet tissues under different treatment conditions, we performed pathological analysis of brain, lung, and superficial inguinal lymph nodes. Our results of this study observed that mild congestion in the lungs and inguinal lymph nodes of IPV and a small number of lymphocytes in the lymph nodes were necrotic. The tissues (brain, lung, and inguinal lymph nodes) of GML adding group were the same as CON with no obvious lesions. This indicated that GML could cooperate with inactivated vaccine to prevent and improve histopathological changes caused by PRV.

CONCLUSION

Our study demonstrated that GML might improve growth performance of weaned piglets and enhance the immunity of PRV-inactivated vaccine by increasing the levels of PRV gB antibody and immunoglobulin, as well as selectively regulating cytokine levels. The above findings laid a solid foundation for future studies on the effect of MCFAs and derivatives to improve the immune effect of PRV-inactivated vaccine in the clinics.

DATA AVAILABILITY STATEMENT

The original contributions presented in the study are included in the article/supplementary material, further inquiries can be directed to the corresponding author.

ETHICS STATEMENT

The animal study was reviewed and approved by Yangzhou University (Jiangsu Province, China). Written informed consent was obtained from the owners for the participation of their animals in this study.

AUTHOR CONTRIBUTIONS

QR designed experiments and wrote the manuscript. XW, QG, GW, XC, CL, SG, and YL were involved in discussing data and modifying the manuscript. All authors read and agreed to the published manuscript.

FUNDING

This study was funded by grants from the Key R&D Program of Jiangsu Province (BE2020320), the National Key R&D Program (2016YFD0500704-2), the Novel Agricultural Research Program of Jiangsu Province (SXGC [2017] 231), funding from the Priority Academic Program Development of Jiangsu Higher Education Institutions (PAPD) and Science and Technology Support Program of Jiangsu Province (BE2014355), and the earmarked fund for Jiangsu Agricultural Industry Technology System (JATS [2018]221).

REFERENCES

1. Zhang T, Liu Y, Chen Y, Wang A, Feng H, Wei Q, et al. A single dose glycoprotein D-based subunit vaccine against pseudorabies virus infection. *Vaccine.* (2020) 38:6153–61. doi: 10.1016/j.vaccine.2020.07.025
2. He W, Auclert LZ, Zhai X, Wong G, Zhang C, Zhu H, et al. Interspecies transmission, genetic diversity, and evolutionary dynamics of pseudorabies virus. *J Infect Dis.* (2019) 219:1705–15. doi: 10.1093/infdis/jiy731
3. Pomeranz LE, Reynolds AE, Hengartner CJ. Molecular biology of pseudorabies virus: impact on neurovirology and veterinary medicine. *Microbiol Mol Biol Rev.* (2005) 69:462–500. doi: 10.1128/MMBR.69.3.462-500.2005
4. Müller T, Hahn EC, Tottewitz F, Kramer M, Klupp BG, Mettenleiter TC, et al. Pseudorabies virus in wild swine: a global perspective. *Arch Virol.* (2011) 156:1691–705. doi: 10.1007/s00705-011-1080-2
5. Wong G, Lu J, Zhang W, Gao GF. Pseudorabies virus: a neglected zoonotic pathogen in humans? *Emerg Microbes Infect.* (2019) 8:150–4. doi: 10.1080/22221751.2018.1563459
6. Zhang C, Liu Y, Chen S, Qiao Y, Guo M, Zheng Y, et al. A gD&gC-substituted pseudorabies virus vaccine strain provides complete clinical protection and is helpful to prevent virus shedding against challenge by a Chinese pseudorabies variant. *BMC Vet Res.* (2019) 15:2. doi: 10.1186/s12917-018-1766-8
7. An TQ, Peng JM, Tian ZJ, Zhao HY Li N, Liu YM, et al. Pseudorabies virus variant in Bartha-K61-vaccinated pigs, China, 2012. *Emerg Infect Dis.* (2013) 19:1749–55. doi: 10.3201/eid1911.130177
8. Gu Z, Hou C, Sun H, Yang W, Dong J, Bai J, et al. Emergence of highly virulent pseudorabies virus in southern China. *Can J Vet Res.* (2015) 79:221–8.
9. Wu R, Bai C, Sun J, Chang S, Zhang X. Emergence of virulent pseudorabies virus infection in northern China. *J Vet Sci.* (2013) 14:363–5. doi: 10.4142/jvs.2013.14.3.363
10. Yu X, Zhou Z, Hu D, Zhang Q, Han T, Li X, et al. Pathogenic pseudorabies virus, China, 2012. *Emerg Infect Dis.* (2014) 20:102–4. doi: 10.3201/eid2001.130531
11. Wang CH, Yuan J, Qin HY, Luo Y, Cong X, Li Y, et al. A novel gE-deleted pseudorabies virus (PRV) provides rapid and complete protection from lethal challenge with the PRV variant emerging in Bartha-K61-vaccinated swine population in China. *Vaccine.* (2014) 32:3379–85. doi: 10.1016/j.vaccine.2014.04.035
12. Lin Y, Qigai H, Xiaolan Y, Weicheng B, Huanchun C. The co-administrating of recombinant porcine IL-2 could enhance protective immune responses to PRV inactivated vaccine in pigs. *Vaccine.* (2005) 23:4436–41. doi: 10.1016/j.vaccine.2005.03.034
13. Mo Q, Liu T, Fu A, Ruan S, Zhong H, Tang J, et al. Novel gut microbiota patterns involved in the attenuation of dextran sodium sulfate-induced mouse colitis mediated by glycerol monolaurate via inducing anti-inflammatory responses. *MBio.* (2021) 12:e0214821. doi: 10.1128/mBio.02148-21
14. Jackman JA, Hakobyan A, Zakaryan H, Elrod CC. Inhibition of African swine fever virus in liquid and feed by medium-chain fatty acids and glycerol monolaurate. *J Anim Sci Biotechnol.* (2020) 11:114. doi: 10.1186/s40104-020-00517-3
15. Witcher KJ, Novick RP, Schlievert PM. Modulation of immune cell proliferation by glycerol monolaurate. *Clin Diagn Lab Immunol.* (1996) 3:10–3. doi: 10.1128/cdli.3.1.10-13.1996
16. Peterson ML, Schlievert PM. Glycerol monolaurate inhibits the effects of Gram-positive select agents on eukaryotic cells. *Biochemistry.* (2006) 45:2387–97. doi: 10.1021/bi051992u
17. Schlievert PM, Peterson ML. Glycerol monolaurate antibacterial activity in broth and biofilm cultures. *PLoS ONE.* (2012) 7:e40350. doi: 10.1371/journal.pone.0040350
18. Thomas LL, Hartman AR, Woodworth JC, Tokach MD, Jones AM. Evaluation of different combinations of medium chain fatty acids and monolaurin as a dietary additive for nursery pigs. *Kansas Agric Exper Station Res Rep.* (2018) 4:12. doi: 10.4148/2378-5977.7660
19. Ghalib N. Biochemical trails associated with different doses of alpha- monolaurin in chicks. *Adv Anim Vet Sci.* (2018) 7:187–92. doi: 10.17582/journal.aavs/2019/7.3.187.192
20. Liu T, Tang J, Feng F. Glycerol monolaurate improves performance, intestinal development, and muscle amino acids in yellow-feathered broilers via manipulating gut microbiota. *Appl Microbiol Biotechnol.* (2020) 104:10279–91. doi: 10.1007/s00253-020-10919-y
21. National Research Council. *Nutrient Requirements of Swine.* Washington, DC: National Academies Press (2012).
22. Wang J, Cui X, Wang X, Wang W, Gao S, Liu X, et al. Efficacy of the Bartha-K61 vaccine and a $gE^{-}/gI^{-}/TK^{-}$ prototype vaccine against variant porcine pseudorabies virus (vPRV) in piglets with sublethal challenge of vPRV. *Res Vet Sci.* (2020) 128:16–23. doi: 10.1016/j.rvsc.2019.10.005
23. Wu QJ, Jiao C, Liu ZH, Cheng BY, Liao JH, Zhu DD, et al. Effect of glutamine on the growth performance, digestive enzyme activity, absorption function, and mRNA expression of intestinal transporters in heat-stressed chickens. *Res Vet Sci.* (2021) 134:51–7. doi: 10.1016/j.rvsc.2020.12.002
24. Freuling CM, Müller TF, Mettenleiter TC. Vaccines against pseudorabies virus (PrV). *Vet Microbiol.* (2017) 206:3–9. doi: 10.1016/j.vetmic.2016.11.019
25. Mettenleiter TC. Aujeszky's disease and the development of the Marker/DIVA vaccination concept. *Pathogens.* (2020) 9:563. doi: 10.3390/pathogens 9070563
26. Forsythe KW, Corso B. Welfare effects of the national pseudorabies eradication program: comment. *Am J Agr Econ.* (1994) 76:968–71. doi: 10.2307/1243760
27. Mayr T, Claes L. *Pseudorabies (Aujeszky's Disease) and its Eradication.* United States Department of Agriculture Animal and Plant Health Inspection Service Technical Bulletin No. 1923. (2010).
28. Delva JL, Nauwynck HJ, Mettenleiter TC, Favoreel HW. The attenuated pseudorabies virus vaccine strain Bartha K61: a brief review on the knowledge gathered during 60 years of research. *Pathogens.* (2020) 9:897. doi: 10.3390/pathogens9110897
29. Kong H, Zhang K, Liu Y, Shang Y, Wu B, Liu X. Attenuated live vaccine (Bartha-K16) caused pseudorabies (Aujeszky's disease) in sheep. *Vet Res Commun.* (2013) 37:329–32. doi: 10.1007/s11259-013-9568-8
30. Dong B, Zarlenga DS, Ren X. An overview of live attenuated recombinant pseudorabies viruses for use as novel vaccines. *J Immunol Res.* (2014) 2014:824630. doi: 10.1155/2014/824630
31. Takashima Y, Tsukamoto M, Ota H, Matsumoto Y, Hayashi Y, Otsuka H. Immunization with pseudorabies virus harboring Fc domain of IgG makes a contribution to protection of mice from lethal challenge. *Vaccine.* (2005) 23:3775–82. doi: 10.1016/j.vaccine.2005.02.031
32. Hu D, Zhang Z, Lv L, Xiao Y, Qu Y, Ma H, et al. Outbreak of variant pseudorabies virus in Bartha-K61-vaccinated piglets in central Shandong Province, China. *J Vet Diagn Invest.* (2015) 27:600–5. doi: 10.1177/1040638715593599
33. Yin Y, Xu Z, Liu X, Li P, Yang F, Zhao J, et al. A live gI/gE-deleted pseudorabies virus (PRV) protects weaned piglets against lethal variant PRV challenge. *Virus Genes.* (2017) 53:565–72. doi: 10.1007/s11262-017-1454-y

34. Luo Y, Li N, Cong X, Wang CH, Du M, Li L, et al. Pathogenicity and genomic characterization of a pseudorabies virus variant isolated from Bartha-K61-vaccinated swine population in China. *Vet Microbiol.* (2014) 174:107–15. doi: 10.1016/j.vetmic.2014.09.003
35. Andries K, Pensaert MB, Vandeputte J. Effect of experimental infection with pseudorabies (Aujeszky's disease) virus on pigs with maternal immunity from vaccinated sows. *Am J Vet Res.* (1978) 39:1282–5.
36. Ben-Porat T, DeMarchi JM, Lomniczi B, Kaplan AS. Role of glycoproteins of pseudorabies virus in eliciting neutralizing antibodies. *Virology.* (1986) 154:325–34. doi: 10.1016/0042-6822(86)90458-7
37. Rooij B, Visser Boersma W, Bianchi ATJ. Analysis of protective immunity against PRV infection in pigs using attenuated and inactivated PRV vaccines. *Vet Res.* (2000) 31:135. doi: 10.1051/vetres:2000063
38. Guimarães LE, Baker B, Perricone C, Shoenfeld Y. Vaccines, adjuvants and autoimmunity. *Pharmacol Res.* (2015) 100:190–209. doi: 10.1016/j.phrs.2015.08.003
39. Yoo YC, Yoshimatsu K, Koike Y, Hatsuse R, Yamanishi K, Tanishita O, et al. Adjuvant activity of muramyl dipeptide derivatives to enhance immunogenicity of a hantavirus-inactivated vaccine. *Vaccine.* (1998) 16:216–24. doi: 10.1016/S0264-410X(97)00188-6
40. Rivera E, Ekholm Pettersson F, Inganäs M, Paulie S, Grönvik KO. The Rb1 fraction of ginseng elicits a balanced Th1 and Th2 immune response. *Vaccine.* (2005) 23:5411–9. doi: 10.1016/j.vaccine.2005.04.007
41. Sun W, Meng K, Qi C, Yang X, Wang Y, Fan W, et al. Immune-enhancing activity of polysaccharides isolated from Atractylodis macrocephalae Koidz. *Carbohydr Polym.* (2015) 126:91–6. doi: 10.1016/j.carbpol.2015.03.034
42. Lopes LQ, Santos CG, de Almeida Vaucher R, Gende L, Raffin RP, Santos RC. Evaluation of antimicrobial activity of glycerol monolaurate nanocapsules against American foulbrood disease agent and toxicity on bees. *Microb Pathog.* (2016) 97:183–8. doi: 10.1016/j.micpath.2016.05.014
43. Hess DJ, Henry-Stanley MJ, Wells CL. Antibacterial synergy of glycerol monolaurate and aminoglycosides in Staphylococcus aureus biofilms. *Antimicrob Agents Chemother.* (2014) 58:6970–3. doi: 10.1128/AAC.03672-14
44. Sun CQ, O'Connor CJ, Roberton AM. Antibacterial actions of fatty acids and monoglycerides against Helicobacter pylori. *FEMS Immunol Med Microbiol.* (2003) 36:9–17. doi: 10.1016/S0928-8244(03)00008-7
45. Zentek J, Buchheit-Renko S, Ferrara F, Vahjen W, Van Kessel AG, Pieper R. Nutritional and physiological role of medium-chain triglycerides and medium-chain fatty acids in piglets. *Anim Health Res Rev.* (2011) 12:83–93. doi: 10.1017/S1466252311000089
46. Dierick NA, Decuypere JA, Degeyter I. The combined use of whole Cuphea seeds containing medium chain fatty acids and an exogenous lipase in piglet nutrition. *Arch Tierernahr.* (2003) 57:49–63. doi: 10.1080/0003942031000086626
47. Decuypere JA, Dierick NA. The combined use of triacylglycerols containing medium-chain fatty acids and exogenous lipolytic enzymes as an alternative to in-feed antibiotics in piglets: concept, possibilities and limitations. An overview. *Nutr Res Rev.* (2003) 16:193–210. doi: 10.1079/NRR200369
48. Vallbracht M, Brun D, Tassinari M, Vaney MC, Pehau-Arnaudet G, Guardado-Calvo P, et al. Structure-Function Dissection of Pseudorabies Virus Glycoprotein B Fusion Loops. *J Virol.* (2017) 92:e01203–17. doi: 10.1128/JVI.01203-17
49. Mettenleiter TC. Immunobiology of pseudorabies (Aujeszky's disease). *Vet Immunol Immunopathol.* (1996) 54:221–9. doi: 10.1016/S0165-2427(96)05695-4
50. Curanovic D, Enquist LW. Virion-incorporated glycoprotein B mediates transneuronal spread of pseudorabies virus. *J Virol.* (2009) 83:7796–804. doi: 10.1128/JVI.00745-09
51. Balan P, Sik-Han K, Moughan PJ. Impact of oral immunoglobulins on animal health-A review. *Anim Sci J.* (2019) 90:1099–110. doi: 10.1111/asj.13258
52. Gomez GG, Phillips O, Goforth RA. Effect of immunoglobulin source on survival, growth, and hematological and immunological variables in pigs. *J Anim Sci.* (1998) 76:1–7. doi: 10.2527/1998.7611
53. Miller I, Cerná J, Trávnícek J, Rejnek J, Kruml J. The role of immune pig colostrum, serum and immunoglobulins IgG, IgM, and IgA, in local intestinal immunity against enterotoxic strain in Escherichia coli O55 in germfree piglets. *Folia Microbiol.* (1975) 20:433–8. doi: 10.1007/BF02877048
54. Rizza P, Ferrantini M, Capone I, Belardelli F. Cytokines as natural adjuvants for vaccines: where are we now? *Trends Immunol.* (2002) 23:381–3. doi: 10.1016/S1471-4906(02)02276-7
55. Rook GA. New meanings for an old word: adjuvanticity, cytokines and T cells. *Immunol Today.* (1993) 14:95–6. doi: 10.1016/0167-5699(93)90072-S
56. McLafferty E, Hendry C, Farley A. The lymphatic system. *Nurs Stand.* (2012) 27:37–42. doi: 10.7748/ns2012.12.27.15.37.c9482
57. von der Weid PY, Rainey KJ. Review article: lymphatic system and associated adipose tissue in the development of inflammatory bowel disease. *Aliment Pharmacol Ther.* (2010) 32:697–711. doi: 10.1111/j.1365-2036.2010.04407.x

Conflict of Interest: Authors GW, XC, and CL were employed by Anyou Biotechnology Group Co., Ltd.

The remaining authors declare that the research was conducted in the absence of any commercial or financial relationships that could be construed as a potential conflict of interest.

frontiers | Frontiers in Veterinary Science

ORIGINAL RESEARCH
published: 24 November 2022
doi: 10.3389/fvets.2022.879478

Reproductive Performance of Zi-Goose Promoted by Red Color Illumination

Manyu Li[1], Chen Liang[1], Xiuhua Zhao[1], Guojun Liu[1], Yuanliang Zhang[1], Shan Yue[1] and Zhiqiang Zhang[2]**

[1] *Institute of Animal Husbandry, Heilongjiang Academy of Agricultural Sciences, Harbin, China,* [2] *College of Pharmacy, Henan University of Traditional Chinese Medicine, Zhengzhou, China*

The color of light affects the reproductive performance of poultry, but it is not clear what efficient illumination strategy could be adopted to improve the reproductive performance of Zi-goose. Red light can increase the average weekly egg production rate, egg production, and qualified production. It can increase the serum GnRH level and decrease the serum PRL, MT, and T4 levels. In our study, red light for 12 h increased the average weekly laying rate, average qualified egg production, and hatching rate of Zi-goose eggs, and increased the serum levels of FSH, LH, P4, E2, MT, T3, and T4. Blue light at 14 h improved the average weekly egg production rate, average egg production, and average qualified egg production, and reduce serum PRL and MT levels to ensure the improvement of reproductive performance of goose. A total of 705,714 overlapping group sequences, 471,145 transcript sequences, and 268,609 single gene sequences were obtained from 18 sequencing samples, with a total length of 323.04, 668.53, and 247.88 M, respectively. About 176,416 unigenes were annotated successfully in six databases, accounting for 65.68% of the total unigenes obtained. 2,106, 2,142, and 8,892 unigenes were identified in the hypothalamus, pituitary gland, and ovary of the birds respectively, with different expressions of light regulation. The hypothalamus, ovary, and pituitary were involved in 279, 327, and 275 KEGG (Kyoto Encyclopedia of Genes and Genomes) metabolic pathways in response to light, respectively. Through further significance analysis and differential discovery rate control, a total of five metabolic pathways were obtained which were closely related to the reproductive hormones of goose. Ten candidate genes related to the reproductive performance of goslings were selected according to the identification results of differentially expressed genes of goslings under red light and white light conditions and the genes involved in metabolic pathways significantly related to the reproductive hormones of goslings. The expression levels of *GnRh-1* in the hypothalamus, *GnRH-R*, *FSH* β and *LH* β in the pituitary gland, and *FSH-R* and *LH-R* candidate genes in the ovary were higher under the 12 h red light treatment than white light. However, the expression levels of *VIP*, *PRL,* and *PRL-R* candidate genes in the hypothalamus, pituitary and ovary were lower under 12 h red light than under 12 h white light.

Keywords: red light, reproductive, transcriptome, Zi-goose, hypothalamus

Edited by:
Kun Li,
Nanjing Agricultural University, China

Reviewed by:
Huanxi Zhu,
Jiangsu Academy of Agricultural Sciences (JAAS), China
Qigui Wang,
Chongqing Academy of Animal Science, China

****Correspondence:***
Manyu Li
380755361@qq.com
Zhiqiang Zhang
392073683@qq.com

Specialty section:
This article was submitted to Veterinary Infectious Diseases, a section of the journal Frontiers in Veterinary Science

Received: *19 February 2022*
Accepted: *06 June 2022*
Published: *24 November 2022*

Citation:
Li M, Liang C, Zhao X, Liu G, Zhang Y, Yue S and Zhang Z (2022) Reproductive Performance of Zi-Goose Promoted by Red Color Illumination. Front. Vet. Sci. 9:879478. doi: 10.3389/fvets.2022.879478

INTRODUCTION

Lighting is essential in avian species, such as manipulating reproductive performance and sexual maturity (1). Currently, artificial light supplements have become a major measure to improve the reproductive performance of poultry in modern domestic fowl production (2). It is known that different colors of light have different wavelengths and long wavelength lights are perceived more easily by birds than the short wavelength lights, though the light intensities remain the same (3). Generally, red light of long wavelength has a favorable effect on egg production and the onset of laying, while blue or green light of short wavelength had a negative effect on egg production but had an accelerating effect on growth (4, 5). To our knowledge, a majority of research on this aspect was focused on hens, ducks, and turkeys along with rabbits, sheep, camels, and so on (6). However, scarce information is available on the impact of light color on the reproductive performance of goose. Moreover, it is also not clear how the endocrine hormones and their gene affect the reproductive performance of goose exposed to different color light sources. As for changes in the transcriptomic profile of goose gonads in response to different color lighting, we can hardly find any literature.

As a result of photostimulation, hypothalamic photoreceptors in avian species initiate a photo-sexual response that controls their reproductive performance through the hypothalamic-pituitary-ovarian gonadal axis. Longer wavelengths of light (such as red) penetrate through the feathers, skull, and cranial tissues to the hypothalamus more efficiently than lights of shorter wavelengths (such as blue), and have a great influence on the reproductive performance of birds (7, 8). Building on the findings of Baxter et al. (9) that the reproductive axis in chickens was activated by red light and this phenomenon occurred independent of the involvement of the hen's retina, we hypothesized that red light will greatly affect the reproductive performance of goose by regulating the secretion of their reproductive hormones and the expression of reproduction-related genes (8, 9).

This research aims at assessing the efficacy of colored lighting that improves the reproductive performance of goose, uncovering the responses of the reproductive hormones and expression of reproduction-related genes to different color lighting conditions. Our study also looks at differentiating the changes in the transcriptomic profile of the hypothalamic gonad of goose.

MATERIALS AND METHODS

Ethics Statement

This study was conducted in strict accordance with the guidelines of the Animal Ethical Welfare Committee. The research protocol was reviewed and approved by the Animal Care and Use Committee of Northeast Agricultural University.

Animals and Experiment Design

A total of 450 Zi-goose (1 year old) were randomly distributed into three groups with three replicates per group and 10 males and 40 females per replicate. The grouping was based on the color of the light: blue LED group, red LED group, and white LED group, which served as the control. The birds were housed inside the chambers that provided a stocking density of 5.0 birds/m^2 and exposed to different color LED illumination for 12 h lighting per day from 1 March to 30 June 2018. Routine feeding and management were adopted during the whole experiment. The diet compositions of the experiment are shown in **Table 1**.

TABLE 1 | The diet composition of experiment.

Diet composition	Contents (%)	Nutrient components[b]	Content
Corn	3.00	Metabolizable energy (MJ/kg)	10.21
Maize starch	39.00	Crude protein (CP) (g/kg)	15.60
Corn germ meal	18.00	Total Calcium (g/kg)	1.72
Soybean oil	0.50	Total phosphorus (g/kg)	0.85
Rice bran meal	16.00	Total lysine (g/kg)	0.70
Soybean meal	12.00	Total methionine (g/kg)	0.50
Chili meal	3.00	Crude fiber (g/kg)	4.81
DDG distillers dried grains	0.50		
Salt	0.35		
Dicalcium phosphate	1.10		
Limestone	3.50		
Methionine	0.35		
Choline	0.30		
Chinese herbal medicine	1.00		
Premix[a]	2.00		

[a] *Premix can provide 10 mg of copper, 90 mg of zinc, 0.1 mg of selenium, 15 mg of manganese, 60 mg of iron, 0.1 mg of iodine, 4000 IU of vitamin A, 600 IU of vitamin D3, 0.1 mg of vitamin K, 0.6 mg of vitamin B2, 0.4 mg of pantothenic acid, 0.6 mg of nicotinic acid, 2.6 mg of vitamin C, 0.04 mg of folic acid, 60.06 mg of vitamin B and 0.06 mg of vitamin B1 for 1 kg diet;* [b] *Values of nutrient components are gained by calculation.*

Determination of Reproductive Performance Indexes

The eggs were collected every day from each group and sorted into qualified and unqualified eggs, which were then used for calculating weekly averages of egg-laying, qualified egg-laying, and egg-laying rates. In May, qualified eggs within a week of their incubation were tested to determine the weekly average fertilization and hatching rates.

Weekly egg-laying numbers = Egg-laying numbers in seven consecutive days/seven.

Weekly qualified egg-laying numbers = Qualified egg-laying numbers in seven consecutive days/seven.

Weekly average egg-laying rate (%) = Egg-laying numbers in a week/average female goose numbers × 100%.

Average fertilization rate (%) = Number of fertilized eggs/hatching eggs in a week × 100%.

Average hatching rate (%) = Number of hatchlings/Number of fertilized eggs in a week × 100%.

Three birds in each treatment were slaughtered randomly and the hypothalamus, ovary, and pituitary gland tissues were taken

and frozen immediately in liquid nitrogen and stored at −80°C for quantitative real-time PCR analysis of the reproduction-related genes. Simultaneously, the hypothalamus tissues treated with red LED and white LED were also used for transcriptome sequencing analysis.

Determination of Reproductive Hormone Levels in Serum

The blood samples from the pterygoid vein of four female birds for each replicate were collected to measure the reproductive hormone levels in serum on 20 March and 28 May 2018 respectively. After coagulation, the blood samples were centrifuged at 3,000 rpm for 10 min, and the serums were collected respectively. The levels of Gonadotropin-Releasing Hormone (GnRH), Prolactin (PRL), Follicle-Stimulating Hormone (FSH), Luteinizing Hormone (LH), Estradiol (E2), Progesterone (P4), Melatonin (MT), Triiodothyronine (T3), and Thyroxine (T4) in serum were determined by ELISA assay according to the quantitative diagnostic kit of estradiol produced by North Institute of Biotechnology (Beijing).The assay sensitivity were 0.1 mIU/ml, 1.0 ng/ml, 1.0 pg/ml, 0.1 ng/ml, 1.0 ng/ml, 1.0 mIU/L, 0.1 nmol/L, and 1.0 nmol/L, respectively. The coefficient of variation among individuals and replicates was <15%. The serum samples were continuously diluted to obtain the inhibition curve parallel to the standard curve. The R-value of the measurement curve and the standard curve was more than 0.99.

The Expression Levels of Reproduction-Related Genes Detected by RT-PCR

In this study, the expression levels of reproduction-related genes in the hypothalamus, pituitary, and ovary gland tissues, such as GnRH Receptor (GnRH-R), GnRH Inhibitor (GnRH-I), Gonadotropin-Inhibiting Hormone Receptor (GnIH-R), VIP, FSH beta, LH beta, FSH Receptor (FSH-R), LH Receptor (LH-R), PRL, and PRL Receptor (PRL-*R),* were detected by RT-qPCR using *β-actin* as an internal standard gene. The RT-qPCR was conducted in 20 μl reactions that each contained 10 μl 2× SYBR Premix Ex Taq, 1 μl cDNA, 0.5 μl upstream primer (10 μM), 0.5 μl downstream primer (10 μM), and 8 μl sterile distilled H_2O. An ABI PRISM-7500 sequence detection system was used to detect the amplified products. Gene expression levels were expressed using the $2^{-\Delta\Delta CT}$ method (10) and were normalized to the expression levels of *β-actin*, an internal housekeeping gene.

Transcriptome Sequencing Analysis

RNA Extraction and Detection

Total RNA was extracted by Trizol one-step extraction method, and the samples were treated with DNase I to remove DNA contamination. The integrity of RNA was detected by 1% agarose gel electrophoresis. RNA purity and concentration were detected by NanoDrop 1000.

Construction and Library Inspection of CDNA Library

The mRNA with polyA structure in total RNA was enriched by Oligo (dT) magnetic beads, and the RNA was interrupted to about 300 bp in length by ion interruption. The fragment with a length of 300 bp was selected because the length of the joint was fixed. Using RNA as a template, the first cDNA strand was synthesized with 6-base random primers and reverse transcriptase, and the second cDNA strand was synthesized with the first cDNA strand as a template.

After the library was constructed, the library fragments were enriched using PCR amplification. Then, the total concentration and effective concentration of the library were detected through Agilent 2100 Bioanalyzer. According to the effective concentration of the library and the amount of data required by the library, the library containing different index sequences was mixed in proportion. The mixed library was uniformly diluted to 2 nM, and a single strand library was formed by alkali denaturation.

Quality Control of Sequencing Data

The short sequences obtained by sequencing are generally raw data. Because redundant or low-quality data, such as low base recognition, specific sequence interference, PCR non-specific amplification, and sequencing joint contamination often occur in RNA extraction, during library preparation and sequencing, the reads with these quality problems get filtered out through quality assessment and control to ensure the normal conduct of subsequent bioinformatics analysis.

Quality Control Data Splicing

Clean Reads were spliced with Trinity software to obtain transcripts and then analyzed. Trinity is a *de novo* assembly software for transcriptome splicing, which splices high-quality sequences based on DBG (De Bruijn Graph) splicing principle. The software is composed of three independent software modules, and the workflow of these three modules is as follows:

1) Inchworm: constructs a short sequence library of k-mer length by using high-quality sequences, and extends the short sequence by k-mer-1 length. It then overlaps between short sequences to obtain a preliminary contig sequence.
2) Chrysalis: clusters them through overlap between contig sequences, and then constructs Bruijn graph for each class.
3) Butterfly: processes these Bruijn diagrams, finding pathways according to Reads and paired Reads in the diagram, and obtains transcripts.

   After stitching, transcript sequence files in FASTA format can be obtained. The longest transcript under each gene is extracted as the representative sequence of the gene, called unigene.

Functional Annotation and Classification of Unigene

In order to clarify the biological functions of unigene, Blast analysis was performed on the unigene obtained from different databases, following which gene function annotation was performed.

Screening and Analysis of Differential Expression of Unigene

Of the gene expressed by DESeq variance analysis, screening of differentially expressed gene conditions were: multiple expression differences|$\log_2$FoldChange|>1, significance $P < 0.05$. In order to explore the differentially expressed genes between unknown biological contact, we used R language Pheatmap packages to compare the difference between the set of genes and sets and two-way clustering analysis samples, according to the same gene expression level in different samples and different gene expression patterns in the same sample clustering, using the method of Euclidean distance. Complete Linkage was used for clustering.

Gene Ontology Enrichment Analysis of Differentially Expressed Genes

TopGO was used for Gene Ontology (GO) enrichment analysis. During the analysis, the gene list and gene number of each term were calculated using the differential genes annotated by GO term. The *P*-value was calculated by the hypergeometric distribution method to find out the GO terms with significant enrichment of differential genes compared with the whole genome background. Thus the main biological functions performed by the differential genes were determined.

KEGG Enrichment Analysis and KEGG Orthology (KO) Analysis of Differentially Expressed Genes

According to KEGG enrichment results, the enrichment degree was measured by Rich Factor, FDR value, and the number of genes enriched into this pathway. Rich factor refers to the ratio of the number of differential genes enriched and annotated in this pathway. The greater the Rich factor, the greater the degree of enrichment. KO and Pathway annotations mainly use the KEGG KAAS (KEGG Automatic Annotation Server) (http://www.genome.jp/tools/kaas/). Related species were selected for gene sets, and Bi-directional Best Hit (BBH) was used for gene KO identification.

RNA-Seq Data Validation

Candidate genes were screened from reproductive hormone-related metabolic pathways in goose, and *β-actin* was used as an internal reference gene to verify transcriptome data by RT-qPCR. Primer Premier 5.0 software was used to design target gene primers, and practical target gene primers were screened by Real-time PCR (**Table 2**).

TABLE 2 | Primers corresponding to the purpose genes used in the real-time quantitative PCR assay.

Gene name	Primer sequence(5′-3′)	Annealing temperature (°C)	PCR product (bp)
β-actin	F: CCA AAG CCA ACA GAG AGA AG	60	159
	R: TCA CCA GAG TCC ATC ACA ATA C		
GnRH-I	F: CTG GGA CTT CAC AGA CCT AAC	60	232
	R: GGA CTT CCA ACC ATC ACT G		
VIP	F: GGG CTA AAC TTG CTG TGA	58	204
	R: GAA AGC GGC TGT AGT TGT C		
GnRH-R	F: GGT CAT CGT CTC CTC CTT CAT C	60	232
	R: CCA GGC AGG CAT TGA AGA G		
GnIH-R	F: GCC CTC ATC GTC GTC ATG TA	58	186
	R: AGA CAC CTT CCT CCC CTC AG		
PRL	F: CAG CAG ATT CAC CAT GAA GAC	56	218
	R: CAA TGT CGC CAG AAT GAA C		
FSH beta	F: AGC AGT GGA AAG AGA AGA ATG TG	60	209
	R: ACC GTT CAG ACT GTC AAT GTA TCTA		
LH beta	F: CCC CAA TGT ATG GCT GTG	58	90
	R: CAA AGG GCT GCG ATA CAC		
LH-R	F: TCT GAA GGA CAA CAG AAA CCT C	58	179
	R: CCA GTG CCG TTG AAG AAA TA		
FSH-R	F: AAA CTG GAA AAG ACA AAA CAC TG	60	228
	R: GGT CAA AAC CAA TGC CAT AG		
PRL-R	F: TCT GAA AGA TGC CAG GTA CAC	56	206
	R: TGC CCA GTC ATT TAT TGA CA		

Data Analysis and Statistics Method

The test data were analyzed by SAS software (8.1), ANOVA by one-way and two-way ANOVA, and the differences were compared using the Duncan method. The test results were expressed as mean ± standard error, and $P < 0.05$ was used as the criterion to judge the difference.

RESULTS

Reproductive Performance

There were no significant differences on day of first egg for Zi-goose reared with different color LED lighting. But day of first egg for Zi-goose provided with red LED lighting advanced 1 day more than those provided with blue and white LED lighting. Particularly, significant differences were found in the egg-laying peak duration, total egg number, total qualified egg number, and total average egg-laying rate for Zi-goose reared with different color LED lighting. The reproductive performance of Zi-goose treated with red LED lighting was higher than those treated with blue and white LED lighting (**Table 3**). There were no

TABLE 3 | Egg-laying peak duration, total egg number, total qualified egg number and total average egg-laying rate for Zi-geese under different color LED treatments.

LED color	Day of first egg	Egg-laying peak duration (week)*	Total egg number	Total qualified egg number	Total average egg-laying rate
Red	Mar.2	12a*	1,531a	1,373a	32.16a
White	Mar.3	9b	1,417b	1,236b	29.77b
Blue	Mar.3	9b	1,424b	1,250b	29.93b

**Here egg-laying peak duration represented week numbers when weekly average egg-laying rate was more than 30%. *Different letters in the same column represented significant differences at 0.05 level.*

significant differences in these reproductive indexes between blue LED treatment and white LED treatment.

The weekly average egg-laying numbers, qualified egg-laying numbers, egg-laying rate, fertilization rates, and hatching rates were used to explore the reproductive performance of Zi-goose under different treatments. Under different color LED treatments, the reproductive performance indexes of Zi-goose are shown in **Figure 1**. The weekly average egg-laying numbers, qualified egg-laying numbers, and egg-laying rate of Zi-goose under red LED treatment were 90.06, 80.76, and 32.16%, respectively, which were significantly higher than those under white LED and blue LED treatments ($P < 0.05$). However, there were no significant differences in weekly average egg-laying numbers, qualified egg-laying numbers, and egg-laying rate of Zi-goose between blue LED treatment and white LED treatment ($P > 0.05$). The weekly average egg-laying numbers and egg-laying rate under blue LED treatment were subtly higher than those under white LED from week 15 to week 17, and the qualified egg-laying numbers under blue LED treatment were subtly higher than those under white LED light from week 11 to week 17. According to the data on the weekly average fertilization rate and hatching rate of Zi-goose (**Figure 1**), there were no significant differences in the weekly average fertilization rate and hatching rate of Zi-goose among different treatments ($P > 0.05$). These results indicated that red LED treatment was beneficial to improve the reproductive performance of Zi-goose, as evidenced by the increase in weekly average egg-laying numbers, qualified egg-laying numbers, and egg-laying rates.

Effects of Different Color Illumination on Egg Quality of Zi-Goose

There was no significant difference in average egg weight, egg white ratio, egg yolk ratio, and eggshell ratio under different illumination (**Table 4**) ($P > 0.05$). However, different treatments had significant effects on yolk color and Haugh unit ($P < 0.05$). Also, there were no significant effects on egg shape index, eggshell strength, and eggshell thickness ($P > 0.05$). The yolk color of blue light treated birds was significantly darker than that of white light ($P < 0.05$), while the yolk color of red light treated birds were somewhere in between. The Haugh units of birds under blue light treatment were significantly lower than that of white light ($P < 0.05$), and the Haugh units of red light treated birds were still in the middle level (**Table 5**).

Effects of Different Color Illumination on Reproductive Hormone Levels in Zi-Goose

The changes in reproductive hormone levels in serum under different color LED treatments are shown in **Figure 2**. It is evident that the serum GnRH, FSH, LH, and E2 levels under red LED treatment were significantly higher than those under blue LED treatments ($P < 0.05$), while these serum hormone levels under blue LED treatment were significantly higher than those under white LED treatments ($P < 0.05$). However, the serum PRL, T3, and T4 levels under red LED treatment were significantly lower than those under blue LED treatment ($P < 0.05$), while these serum hormone levels under blue LED treatment were significantly lower than those under white LED treatments ($P < 0.05$). Although the serum MT and P4 levels under red LED treatment were slightly higher than those under blue LED treatment while lower than those under white LED treatment ($P > 0.05$), these hormone levels under blue LED treatment were significantly lower than those under white LED treatment ($P < 0.05$). Meanwhile, there was no significant difference in serum PRL level between white LED treatment and blue LED treatment ($P > 0.05$). It could be concluded that red LED illumination was more effective to improve the serum GnRH, FSH, LH, and E2 levels and decrease serum PRL, T3, and T4 levels of Zi-goose, which were the main reasons for improving its reproductive performances. Although blue LED lighting could also promote the synthesis and secretion of GnRH, FSH, LH, and E2, the synthesis and secretion of PRL, T3, T4, P4, and MT were significantly decreased ($P < 0.05$), which resulted in the nearly similar egg laying performance between blue LED and white LED lighting, but slightly improved in the later laying period.

Transcriptome Sequencing Analysis

Screening of Differentially Expressed Unigene

After the samples underwent RNA extraction, purification, library construction, and sequencing, the original sequencing data were formed, and then the unigenes were obtained through quality control and splicing. The functional annotation and classification of unigenes and screening of differentially expressed unigenes were carried out. The results of screening differentially expressed unigenes are shown in **Figure 3**. We noticed 2,106 unigenes (in the hypothalamus of Zi-goose) which showed differences in expression due to different color LED treatments. Of these, 1,229 unigenes were down-regulated and 877, up-regulated.

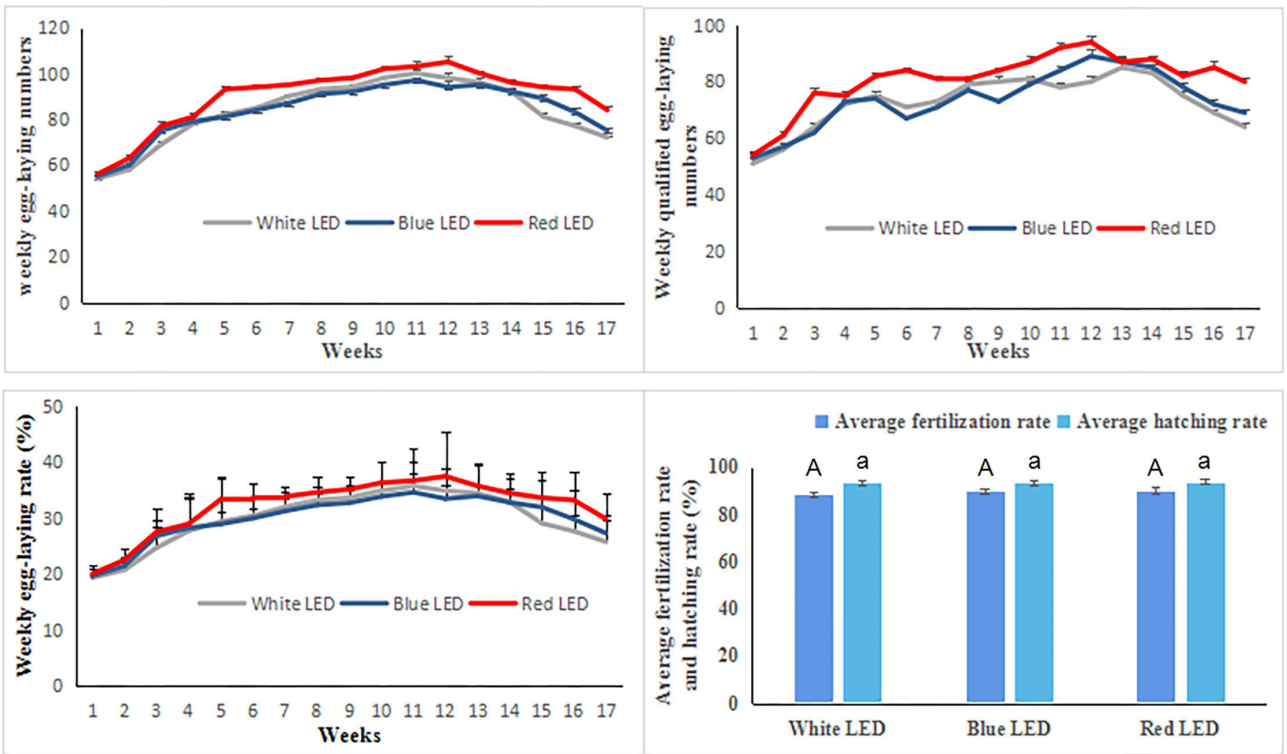

FIGURE 1 | The weekly average egg-laying numbers, qualified egg-laying numbers, egg-laying rate, fertilization rates, and hatching rates of Zi-goose under different color LED treatments. The uppercase letter A indicates the difference significance of average fertilization rate while the lowercase letter a indicates for the difference significance of average hatching rate under different color LED illumination.

TABLE 4 | Effects of different color light on egg weight and its composition of Zi-goose.

Light type	Egg weight (g)	Ratio of egg white to egg weight	Ratio of yolk to egg weight	Ratio of eggshell to egg weight
White light	119.85 ± 9.51[a]	0.53 ± 0.05[a]	0.33 ± 0.05[a]	0.14 ± 0.01[a]
Blue light	121.43 ± 8.14[a]	0.53 ± 0.03[a]	0.33 ± 0.03[a]	0.14 ± 0.01[a]
Red light	119.30 ± 9.81[a]	0.52 ± 0.03[a]	0.33 ± 0.03[a]	0.14 ± 0.01[a]

That there are different alphabets at the same columns indicate significant differences at 0.05 level.

Enrichment Analysis of Differentially Expressed Genes by GO Analysis

The differentially expressed genes screened from the hypothalamus of Zi-goose were taken for the GO enrichment analysis. The top ten differentially expressed genes were associated with signal receptor activity, molecular sensor activity, receptor activity, transmembrane signal receptor activity, transmembrane receptor activity, signal receptor activity, G-protein coupling receptor activity, peptide antigen binding, antigen binding, and transporter activity, respectively. The top ten differentially expressed genes in BP classification were related to stimulus-response, multicellular biological process, signal transduction, cell communication, biological regulation, signal sending, cell response to stimulus, biological process regulation, external stimulus-response, and multi-organism process. The top ten differentially expressed genes with the most significant enrichment in cell component (CC) classification were classified as the overall component of plasma membrane, inherent component of plasma membrane, plasma membrane, cell periphery, MHC protein complex, level 1 MHC protein complex, overall component of membrane, inherent component of membrane, plasma membrane part, and membrane part respectively (**Figure 4A**). In Zi-goose pituitary screened for differentially expressed genes, the molecular functions (MF) classification enrichment of the most significant top ten differentially expressed genes and hormone activity respectively were: receptor activity, receptor ligands activity, peptide antigen, antigen, extracellular matrix structure composition, platelet-derived growth factor binding, peptide receptor, the receptor activity, and combining with related. The top ten differentially expressed genes were associated with multicellular biological processes, JAK-STAT cascade regulation, STAT cascade regulation, JAK-STAT cascade positive regulation, STAT cascade positive regulation, neuronal fate

TABLE 5 | Effects of different color light on egg quality of Zi-goose.

Light type	Egg shape index	Yolk color	Eggshell strength (N)	Eggshell thickness (mm)	Harge unit
White light	1.44 ± 0.10^{a}	6.44 ± 0.92^{b}	80.23 ± 15.34^{a}	0.60 ± 0.05^{a}	52.51 ± 8.45^{a}
Blue light	1.45 ± 0.06^{a}	6.93 ± 1.08^{a}	81.13 ± 15.10^{a}	0.61 ± 0.06^{a}	48.63 ± 9.48^{b}
Red light	1.46 ± 0.06^{a}	6.78 ± 0.98^{ab}	80.70 ± 13.78^{a}	0.60 ± 0.05^{a}	50.84 ± 5.92^{ab}

That there are different alphabets at the same columns indicate significant differences at 0.05 level.

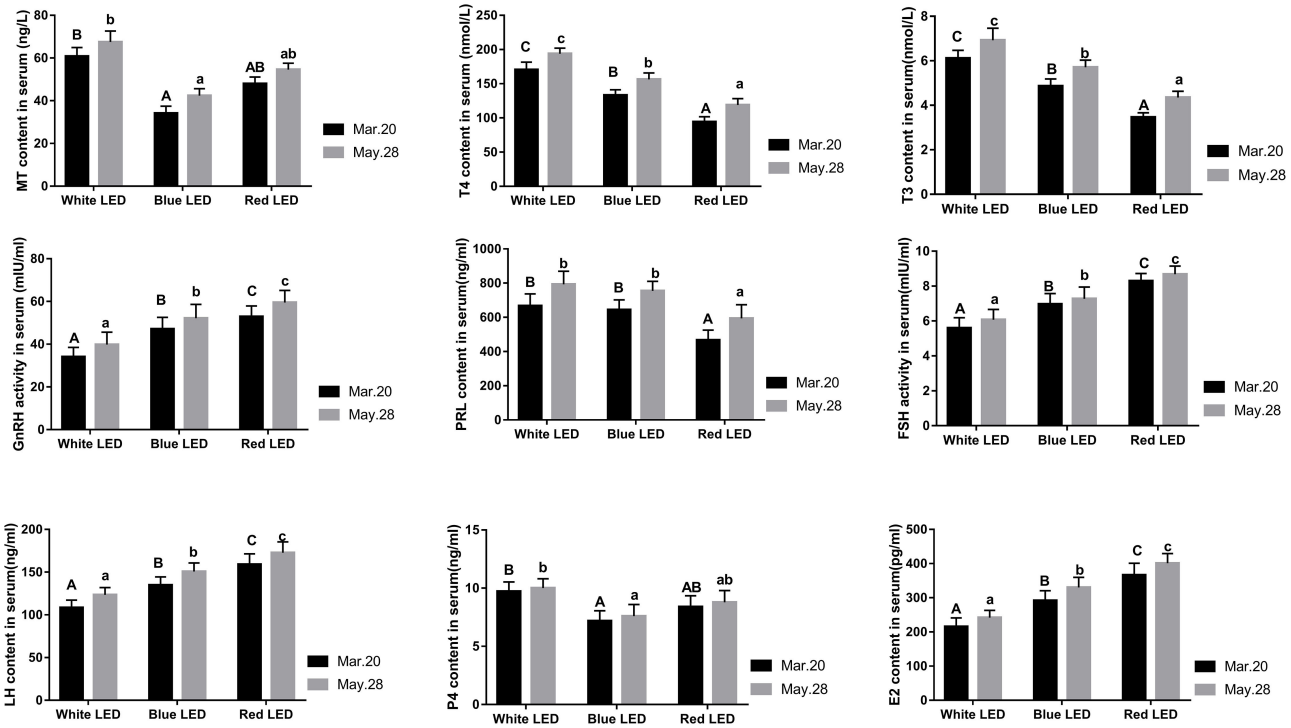

FIGURE 2 | Effects of different color LED illumination on serum hormone levels of Zi-goose. The columns containing different letters in the figure represent significant differences at 0.05 level. Capital letters indicate significant differences among the average egg-laying number, and small letters indicate significant differences among the average eligible egg-laying number.

determination, developmental process, and animal organ development, respectively. The top ten differentially expressed genes with the most significant enrichment in CC classification belonged to extracellular matrix, level 1 MHC protein complex, extracellular region, MHC protein complex, extracellular region part, protein extracellular matrix, extracellular space, collagen trimer complex, and high-density lipoprotein particles (**Figure 4B**). Among the differentially expressed genes screened in Zi-goose nests, the MF classification enrichment of the most significant top ten differentially expressed genes was transporter activity, transmembrane transporter activity, auxiliary factor, secondary active transmembrane transporter activity, the substrate specificity of transmembrane transporter activity, REDOX enzyme activity, receptor activity, transporter substrate specificity, single oxygenase activity, and ion transmembrane transporter activity, The top ten differentially expressed genes were associated with transmembrane transport, multicellular biological process, localization, establishment of localization, ion transport, small molecule biosynthesis, carboxylic acid metabolism, organic acid metabolism, and oxyacid metabolism. The top ten differentially expressed genes with the most significant enrichment in CC classification belonged to the inherent component of membrane, whole component of membrane, membrane part, plasma membrane, plasma membrane part, cell periphery, inherent component of plasma membrane, whole component of plasma membrane, extracellular region, and the membrane category (**Figure 4C**).

Enrichment Analysis of Differentially Expressed Genes by KEGG Analysis

KEGG pathway enrichment analysis showed that the hypothalamus, ovary, and pituitary were involved in 279, 327, and 275 KEGG metabolic pathways in light response, respectively. Through further screening, the same eight

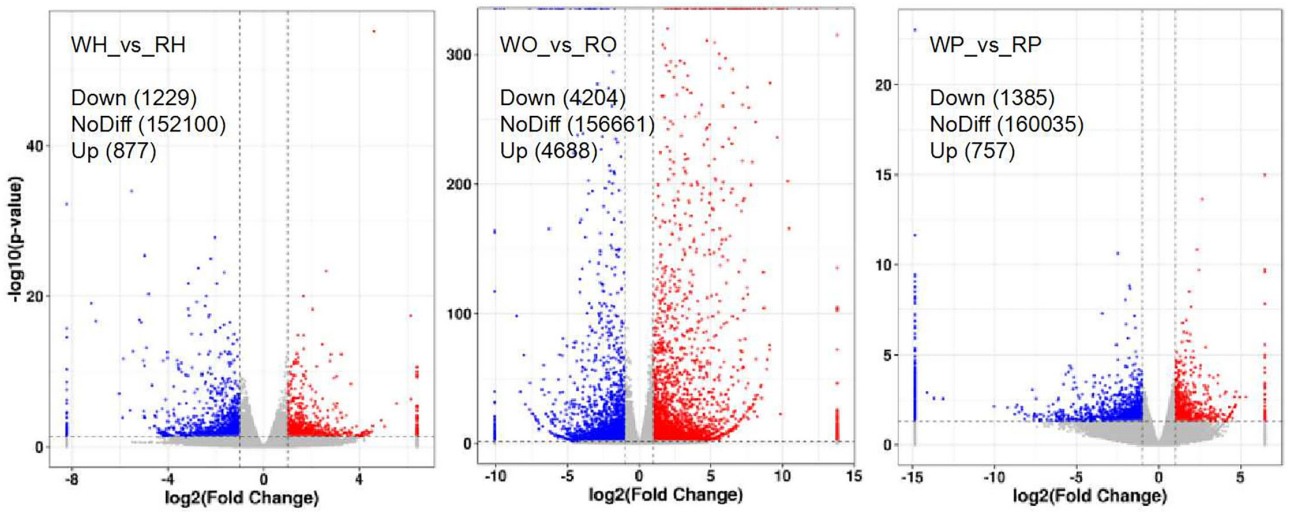

FIGURE 3 | Volcanic map of differentially expressed genes. The abscissa is $\log_2$ (Fold Change) and the ordinate is $-\log_{10}$ (*P*-value). In the figure, the two vertical dashed lines are twice the threshold of expression difference. The horizontal dashed line is the threshold of $P = 0.05$. Red dots indicate up-regulated genes in this group, blue dots indicate down-regulated genes in this group, and gray dots indicate genes that are not significantly differentially expressed.

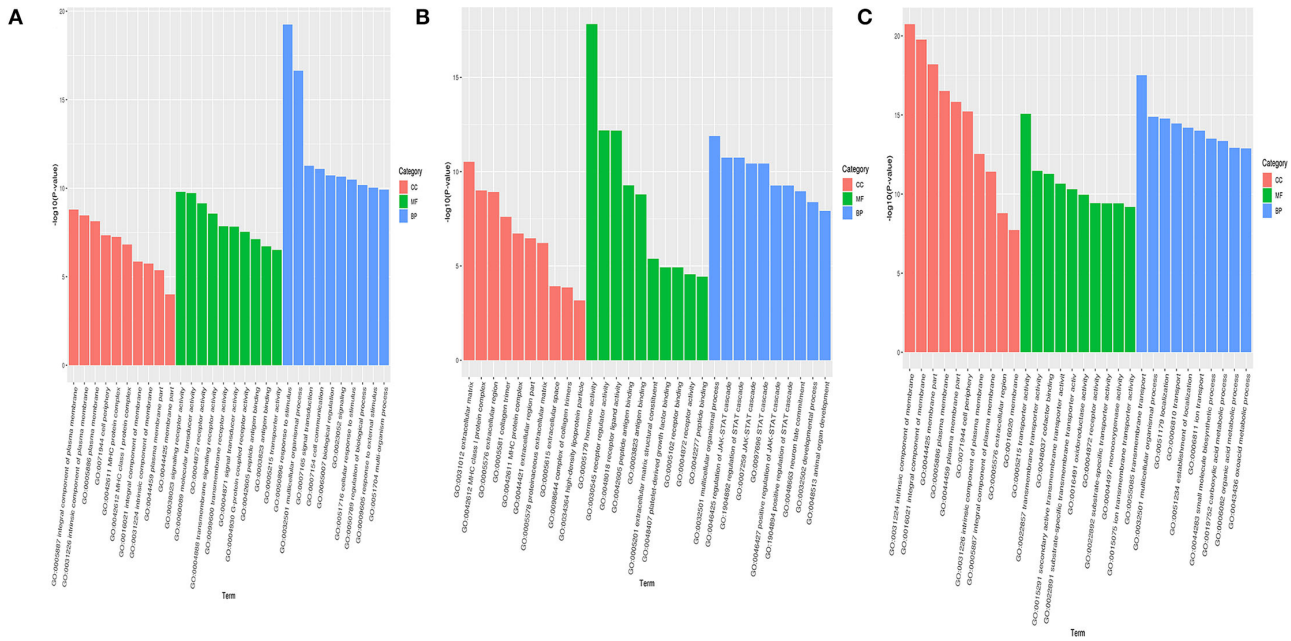

FIGURE 4 | Hypothalamus, pituitary, ovary of GO enrichment analysis of differentially expressed genes in Zi-goose. Note: the abscissa is the term of Go level 2 grade, and the ordinate is the $-\log_{10}$ (*P*-value) enriched for each term. **(A–C)** represent the results of GO enrichment analysis of differentially expressed genes in hypothalamus, pituitary, ovary of Zi-goose.

metabolic pathways closely related to reproductive hormones were obtained in the hypothalamus, pituitary gland, and ovary (**Tables 6–8**).

Expression of Reproduction-Related Genes

The reproductive genes in the hypothalamus, pituitary, and ovary of Zi-goose were heavily affected by the light color (**Figure 5**). The expression of *GnRH-I*, *GnIH*, *TRH*, *LH* beta, *FSH* beta, *GnRH-R*, *PRL*, *LH-R*, *FSH-R*, and *PRL-R* mRNA of Zi-goose under red light treatment and the expression of *GnIH*, *VIP*, *LH* beta, *FSH* beta, *GnRH-R*, *PRL*, *LH-R*, *FSH-R*, and *PRL-R* mRNA of Zi-goose under blue light treatment were significantly up-regulated in comparison with those under white light treatment ($P < 0.05$). Compared with blue light treatment, the expression of *GnRH-I*, *TRH*, *LH* beta, *FSH* beta, and *GnRH-R* mRNA

TABLE 6 | Metabolic pathways related to reproductive hormones in hypothalamus of Zi-geese.

Pathway ID	Pathway name	Up DEGs	Down DEGs	DEGs no.	*P*-value	FDR
ko04912	GnRH signaling pathway	9	6	15	0.00	0.00
ko04913	Ovarian sterogenesis	0	1	1	0.88	1.00
ko04914	Oocyte maturation mediated by progesterone	1	0	1	0.99	1.00
ko04915	Estrogen signaling pathway	2	4	6	0.71	1.00
ko04916	Melanin formation	2	7	9	0.06	0.23
ko04917	Prolactin signaling pathway	1	3	4	0.59	0.93
ko04918	Thyroid hormone synthesis	2	5	7	0.05	0.21
ko04919	Thyroid hormone signaling pathway	1	8	9	0.28	0.65

TABLE 7 | Metabolic pathways related to reproductive hormones in pituitary of Zi-geese.

Pathway ID	Pathway name	Up DEGs	Down DEGs	DEGs No.	*P*-value	FDR
ko04912	GnRH signaling pathway	8	5	13	0.00	0.01
ko04913	Ovarian sterogenesis	2	3	5	0.04	0.21
ko04914	Oocyte maturation mediated by progesterone	0	3	3	0.81	1.00
ko04915	Estrogen signaling pathway	2	7	9	0.18	0.57
ko04916	Melanin formation	1	1	2	0.94	1.00
ko04917	Prolactin signaling pathway	1	18	19	0.00	0.00
ko04918	Thyroid hormone synthesis	0	3	3	0.58	1.00
ko04919	Thyroid hormone signaling pathway	0	3	3	0.95	1.00

of goose treated with red LED lighting were significantly up-regulated while the expression of *GnIH*, *VIP*, *PRL*, *LH-R*, *FSH-R* and *PRL-R* of goose treated with red LED lighting were significantly down-regulated ($P < 0.05$). However, the light color had no obvious impact on the expression of *GnIH-R* mRNA of Zi-goose ($P > 0.05$).

DISCUSSION

Light wavelengths (light color) have an important impact on the reproductive performance of birds. When the light intensity and lighting time are accurately controlled, the effect of the light treatment on the reproductive performance of birds can be identified concisely (11, 12). In our experiment, the lighting time was set at 12 h/Day from 6:00 AM to 6:00 PM and the light intensity constantly remained at 10 Lux measured from one meter above the ground in the chamber, which proved to be the most effective for improving the reproductive performance of the goose in our preliminary experiment. The results indicated that the day of first egg for Zi-goose provided with red LED lighting advanced one day more than those provided with blue and white LED lighting. Despite no significant acceleration in sex maturity of Zi-goose, the red LED lighting showed a certain promotive role in the sex maturity of Zi-goose, which was in accordance with the results of Zhu et al. (13) and Hassan et al. (14). Our results confirmed that the red LED lighting could improve the egg-laying performances, showing longer egg-laying peak duration, higher total egg number, higher total qualified egg number, and higher total average egg-laying rate than those provided with blue LED and white LED lighting. Comparatively, the weekly average egg-laying numbers, qualified egg-laying numbers, and egg-laying rate of Zi-goose with red LED lighting were obviously higher than those treated with white LED and blue LED lighting. These results indicated that it was effective to improve egg-laying performances of Zi-goose by treating them with red LED lighting, which not only confirmed our hypothesis, but also corroborated the results of Gongruttananun et al. (15), Reddy et al. (16), and Zhu et al. (13). As for the favorable effects of red light on the reproductive performance of Zi-goose, we deemed that Zi-goose had a preferable perception and uptake on red light (long-wavelength Spectra), which are more efficient to penetrate and enter the brain and produce more intense stimulation to photoreceptors than blue light (short-wavelength Spectra), eventually enhancing reproductive function and increasing egg production in poultry.

It is known that photo simulation impacts the reproductive performances of birds by regulating the synthesis and secretion of reproductive hormones of the gonadal axis. Our results showed that red LED illumination was more effective to improve the serum GnRH (17), FSH (18), LH, and E2 (9) levels and decrease serum PRL, T3, and T4 levels of Zi-goose, which were the main reasons for improving its reproductive performances of

TABLE 8 | Metabolic pathways related to reproductive hormones in ovary of Zi-geese.

Pathway ID	Pathway name	Up DEGs	Down DEGs	DEGs No.	*P*-value	FDR
ko04912	GnRH signaling pathway	10	12	22	0.52	0.94
ko04913	Ovarian sterogenesis	9	13	22	0.00	0.00
ko04914	Oocyte maturation mediated by progesterone	9	8	17	0.74	1.00
ko04915	Estrogen signaling pathway	15	20	35	0.10	0.33
ko04916	Melanin formation	14	12	26	0.09	0.33
ko04917	Prolactin signaling pathway	10	7	17	0.47	0.89
ko04918	Thyroid hormone synthesis	13	10	23	0.01	0.04
ko04919	Thyroid hormone signaling pathway	15	8	23	0.88	1.00

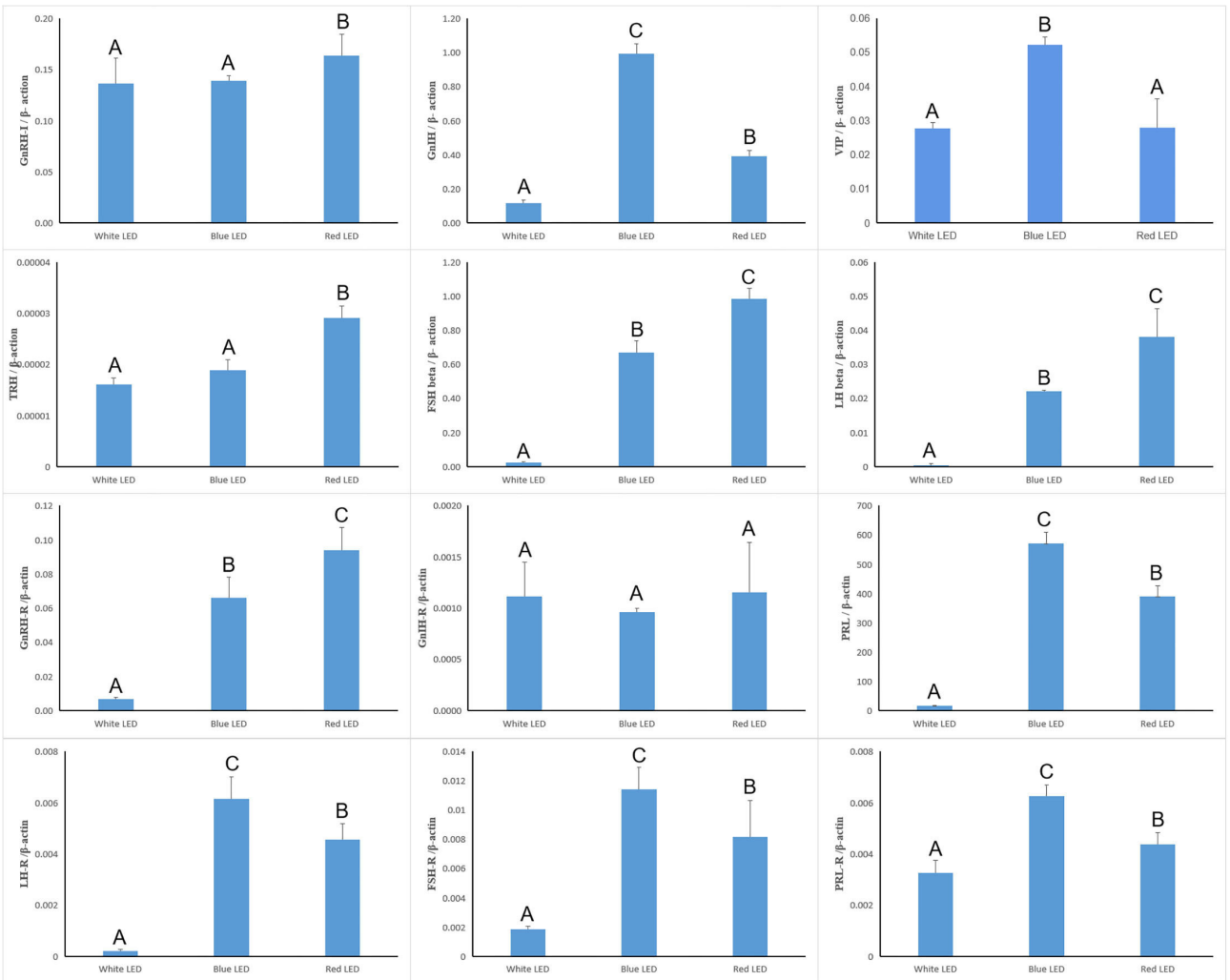

FIGURE 5 | Real-time quantitative PCR of reproduction-related genes. The A–C letters indicate significant differences at 0.05 level.

Zi-goose (19, 20). Reddy et al. also found that when treated with red light, group laying performance was the highest, and the LH and GnRH concentration of laying hens was higher than in the blue light group (21). The results showed that blue light could stimulate the secretion of FSH and LH, improve the secretion in the Fallopian tube, and prolong the peak time of laying. Wang (22) points out that blue and green light promotes the secretion of the thyroid hormone and testosterone more than other monochromatic light. When Reddy et al. (23) treated leghorn chickens at the end of laying period (72–82 weeks)

with red light, the concentrations of serum LH and E2 were significantly increased. Baxter et al. also found that egg-laying hens treated with red light for 6 weeks had significantly increased peripheral blood E2 levels at 20 weeks of age (9).

RNA sequencing can not only sort and classify gene expressions but also compare them (24). Previous studies have suggested that all cells of an individual of any species should contain the same DNA, but each organ, tissue, and even cell has a slightly different RNA expression, which allows different organs, tissues, and cells to perform different functions (25). Therefore, to explain these differences, we need to study RNA in these different organs, tissues, and cells, which requires RNA sequencing, or transcriptomics. In this study, to understand the impact of photo simulation on the reproductive performance of Zi-goose, transcriptomic research techniques were used to analyze the reproductive organ samples of Zi-goose during the peak laying period, so as to identify the possible genes and regulation mode of red light for 12 h to improve the reproductive performance of Zi-goose. Transcriptome research methods mainly include hybridization technology represented by cDNA chip and oligonucleotide chip, sequencing technology represented by SAGE, MPSS, and RNA-seq high throughput sequencing technology. Transcriptome research based on hybridization technology has disadvantages such as low sensitivity and difficult detection of microarray technology. While it is suitable for the detection of known sequences, it cannot capture new mRNA. SAGE and MPSS based on sequencing technology also have problems of long analysis time, relatively low throughput, and high cost, and are gradually getting replaced by RNA-seq based on high-throughput sequencing technology. RNA-seq research technology has the advantages of fast analysis, high throughput, low cost, and direct transcriptome analysis without understanding the genetic information of species, which is particularly important for the study of non-model organisms (26). In this study, we used Next-Generation Sequencing (NGS) for parametric transcriptome analysis based on the Illumina Sequencing platform. According to the raw data obtained, the base quality of the $5'$ and $3'$ ends of all Reads was low, and the base quality of the middle part was high. The base mass of most sequences was more than 20, indicating good sequencing quality. The average quality distribution of Reads also showed a high peak tip corresponding value and no trailing peak, indicating good overall sequencing quality, which not only proved that the sequencing technology we adopted was reasonable and effective but also provided the necessary basic guarantee for differential gene screening and functional analysis.

This study showed that red light for 12 h could significantly improve the reproductive performance of goose, which was manifested by the improvement of serum GnRH, FSH, LH, P4, E2, MT, T3, and T4 levels of female goose. Transcriptomic analysis showed that 2,106 unigenes were differentially expressed in the hypothalamus of birds under 12 h red light and 12 h white light, among which 1,229 unigenes were down-expressed and 877 were up-expressed. There were 8,892 unigenes differentially expressed in light color in Zi-goose egg nests, including 4,204 down-expressed and 4,688 up-expressed. There were 2,142 unigenes differentially expressed in the hypophysis of goose, including 1,385 down-expressed and 757 up-expressed. These differentially expressed genes involved 279, 275, and 327 KEGG metabolic pathways in the hypothalamus, pituitary, and ovary, respectively. Further screening showed the presence of GnRH signaling pathways in the Zi-goose hypothalamus, GnRH signaling pathways and PRL signaling pathways in the Zi-goose pituitary, and ovarian steroidogenesis and thyroid hormone synthesis pathways in the Zi-goose egg nest. These are closely related to the goose's reproductive hormones and genes and regulatory factors involved in these pathways are an important factor to improve the performance of breeding Zi goose.

Also, ten candidate genes related to reproductive performance were identified. Two candidate genes were from the hypothalamus (*VIP* and *GnRH-1*), five candidate genes were from the pituitary (*GnIH*, *PRL*, *GnRH-R*, *FSH β*, and *LH β*), and three candidate genes were from the ovary (*PRL-R*, *FSH-R*, and *LH-R*). The expression levels of *GnRH-1* in the hypothalamus, *GnRH-R*, *FSH β*, and *LH β* in the pituitary, FSH-R and LH-R in the ovary under red light for 12 h were higher than those under white light for 12 h. On the other hand, the expressions of hypothalamus *VIP*, pituitary PRL, and ovary PRL-R candidate genes were lower under red light 12 h than those under white light 12 h. These results showed that the expression of *GnRH-1*, *GnRH-R*, *FSH β*, *LH β*, *FSH-R*, and *LH-R* were up-regulated, and *VIP*, *PRL*, and *PRL-R* were down-regulated by red light 12 h. The secretion and activity of reproductive hormones were also regulated, which led to the improvement of reproductive performance. These results were consistent with the findings of Mobarkey et al. (27) and Reddy et al. (21).

DATA AVAILABILITY STATEMENT

The original contributions presented in the study are publicly available. This data can be found here: https://www.ncbi.nlm.nih.gov/sra/PRJNA902280.

AUTHOR CONTRIBUTIONS

ML: research concept, methodology, data extraction, analysis, and writing the draft. CL: resource searching, verification, formal analysis, supervision, and manuscript reviewing and editing. XZ: resources, methodology, project administration, supervision, and manuscript reviewing and editing. GL, YZ, and SY: resource searching and manuscript reviewing and editing. ML and ZZ: methodology and manuscript reviewing and editing. All authors contributed to the article and approved the submitted version.

FUNDING

This research study was supported by the research business expenses of the scientific research institutes of Heilongjiang Province (No. CZKYF2021B003?, National Modern Waterfowl Industry Technical System Special Project (No. CARS-42-24).

REFERENCES

1. Mauch C, Bilkei G. Strategic application of oregano feed supplements reduces sow mortality and improves reproductive performance: a case study. *Vet Pharmacol Ther.* (2004) 27:61–3. doi: 10.1046/j.0140-7783.2003.00531.x
2. Stevenson JS. Late-gestation ear-surface temperatures and subsequent postpartum health, activity, milk yield, and reproductive performance of dairy cows. *Theriogenology.* (2022) 181:170–9. doi: 10.1016/j.theriogenology.2022.01.022
3. Parsons CT, Dafoe JM, Wyffels SA, Delcurto T, Boss DL. Impacts of heifer postweaning residual feed intake classification on reproductive and performance measurements of first, second, and third parity angus beef females. *Trans Anim Sci.* (2019) 3:1782–5. doi: 10.1093/tas/txz095
4. Li X, Zheng Z, Pan J, Jiang D, Huang Y. Impacts of colored light-emitting diode illumination on the growth performance and fecal microbiota in goose. *Poult Sci.* (2020) 99:1805–12. doi: 10.1016/j.psj.2019.12.034
5. Chiu TL, Hsiao YP, Chuang YT, Lai CM, Ho HC. Colored reflective organic light-emitting device without bias. *Org Elect.* (2014) 15:785–91. doi: 10.1016/j.orgel.2013.12.031
6. Leike I. Optimized additive mixing of colored light-emitting diode sources. *Opt Eng.* (2004) 43:1531. doi: 10.1117/1.1753273
7. Larsen PM, Wüstenhagen S, Terney D, Gardella E, Alving J, Aurlien H, et al. Photoparoxysmal response and its characteristics in a large EEG database using the SCORE system. *Clin Neurophysiol.* (2021) 132:365–71. doi: 10.1016/j.clinph.2020.10.029
8. Wirbisky SE, Freeman JL. Atrazine exposure and reproductive dysfunction through the hypothalamus-pituitary-gonadal (HPG) axis. *Toxics.* (2015) 3:414–50. doi: 10.3390/toxics3040414
9. Baxter M, Joseph N, Osborne VR, Bédécarrats GY. Red light is necessary to activate the reproductive axis in chickens independently of the retina of the eye. *Poultry Sci.* (2014) 93:1289–97. doi: 10.3382/ps.2013-03799
10. Livak KJ, Schmittgen TD. Analysis of relative gene expression data using real-time quantitative pcr and the 2(-delta delta c (t)) method. *Methods.* (2001) 25:402–8. doi: 10.1006/meth.2001.1262
11. Ocon-Grove OM, Poole DH, Johnson AL. Bone morphogenetic protein 6 promotes FSH receptor and anti-Müllerian hormone mRNA expression in granulosa cells from hen prehierarchal follicles. *Reproduction.* (2012) 143:825. doi: 10.1530/REP-11-0271
12. Wang Y, Chen Q, Liu Z, Guo X, Du Y, Yuan Z, et al. Transcriptome analysis on single small yellow follicles reveals that Wnt4 is involved in chicken follicle selection. *Front Endocrinol.* (2017) 8:317. doi: 10.3389/fendo.2017.00317
13. Zhu HX, Hu MD, Guo BB, Qu XL, Lei CR, et al. Effect and molecular regulatory mechanism of monochromatic light colors on the egg-laying performance of yangzhou geese. *Anim Reprod Sci.* (2019) 204:131–9. doi: 10.1016/j.anireprosci.2019.03.015
14. Hassan MR, Sultana S, Choe HS, Ryu KR. Effect of monochromatic and combined light colour on performance, blood parameters, ovarian morphology and reproductive hormones in laying hens. *Ital J Anim Sci.* (2013) 12:272–7. doi: 10.4081/ijas.2013.e56
15. Gongruttananun N. Influence of red light on reproductive performance, eggshell utrastructure, and eye morphology in thai-native hens. *Poult Sci.* (2011) 90:2855–63. doi: 10.3382/ps.2011-01652
16. Reddy IJ, David CG, Kiran GR, Mondal S. Pulsatile secretion of luteinizing hormone and gnrh and its relation to pause days and egg production in hens exposed to different wavelengths of light. *Indian J Anim Sci.* (2011) 81:919–23. doi: 10.1177/147323000903700413
17. Zhang K, Huyan J, Han X, Gao G, Zhong H, Wang Q. Analysis of the serum concentrations and mRNA expression levels of GnRH and GnIH in goose during different reproductive periods. *Acta Vet Zootech Sin.* (2016) 47:1720–172. doi: 10.11843/j.issn.0366-6964.2016.08.025
18. Wang Z, Xu J, Peng L. Construction and expression of eukaryotic expression vector on Zi goose FSH. *J Heilongjiang Bayi Agri Univ.* (2015) 4:39–41. doi: 10.3969/j.issn.1002-2090.2015.04.009
19. Yang C, Li Z, Bai H, Mao H, Li J, Wu H, et al. Long-term efficacy of T3 versus T3+T4 thoracoscopic sympathectomy for concurrent palmar and plantar hyperhidrosis. *J Surg Res.* (2021) 263:224–9. doi: 10.1016/j.jss.2020.11.064
20. Aruna V. Correlation of T3, T4 and TSH with lipid indices in obesity. *Int J Res Med Sci.* (2021) 9:2078. doi: 10.18203/2320-6012.ijrms20212527
21. Reddy IJ, David CG, Selvaraju S, Mondal S, Kiran GR. GnRH-I mRNA, LHSurges, steroid hormones, egg production, and intersequence pause days alter in birds exposed to longer wavelength of light in the later stages of production in *Gallus gallus domesticus*. *Trop Anim Health Prod.* (2012) 44:1311–17. doi: 10.1007/s11250-012-0073-9
22. Wang HY. Research progress on the effect of light color on poultry. *Modern Livestock Poult Breed Indust*. (2012) 1:16–8.
23. Reddy IJ, Mishra A, Mondal S. GnRH-I, GnIH mRNA and luteinizing hormone in domestic hens (*Gallus gallus* domesticus) exposed to different wavelengths of light. *Int J Bioassays.* (2017) 6:5446–5446. doi: 10.21746/ijbio.2017.08.001
24. Wali N, Merteroglu M, White RJ, Busch-Nentwich EM. Total nucleic acid extraction from single zebra fish embryos for genotyping and RNA-seq. *Bio Protocol.* (2022) 12:e4284. doi: 10.21769/BioProtoc.4284
25. Kang M, Choi Y, Kim H, Kim SG. Single-cell RNA-sequencing of *Nicotiana attenuata* corolla cells reveals the biosynthetic pathway of a floral scent. *New Phytol.* (2022) 234:527–44. doi: 10.1111/nph.17992
26. Schulze B R, Lukas T, Schulz M H, Stefanie D, David J. Comparative analysis of common alignment tools for single-cell RNA sequencing. *GigaScience*. (2022) 11:giac001. doi: 10.1093/gigascience/giac001
27. Mobarkey N, Avital N, Heiblum R, Rozenboim I. The role of retinal and extra-retinla photostimulation in reproductive activity in broiler breeder hens. *Domest Anim Endocrinol.* (2010) 38:235–43. doi: 10.1016/j.domaniend.2009.11.002

Conflict of Interest: The authors declare that the research was conducted in the absence of any commercial or financial relationships that could be construed as a potential conflict of interest.

Frontiers in Veterinary Science

Transforms how we investigate and improve animal health

The third most-cited veterinary science journal, bridging animal and human health with a comparative approach to medical challenges. It explores innovative biotechnology and therapy for improved health outcomes.

Discover the latest Research Topics

See more →

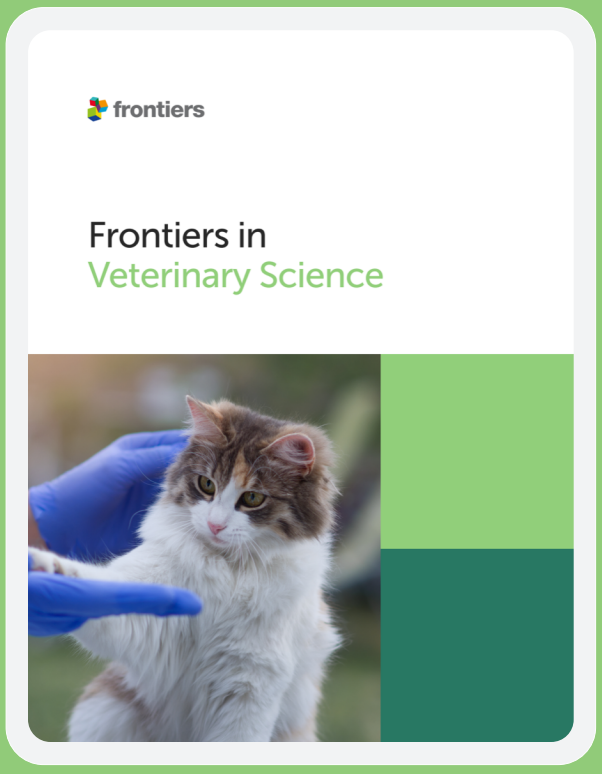

Frontiers

Avenue du Tribunal-Fédéral 34
1005 Lausanne, Switzerland
frontiersin.org

Contact us

+41 (0)21 510 17 00
frontiersin.org/about/contact